The role of plant-parasitic nematodes in modulating plant symbioses with arbuscular mycorrhizal fungal networks

Emily Magkourilou

PhD

University of Sheffield

School of Biosciences

September 2025

Supervisors:

Prof. K. J. Field, Prof. P. E. Urwin, Prof. T. J. Daniell

Declaration of Authorship

As the author of this thesis, I declare that all the material contained within is a result of my own work. Where others have contributed to the work, this is stated in the Acknowledgements section. All sources are acknowledged as references. This work has not previously been presented for an award at this, or any other, University.

Chapters 1 and 2 are largely based on already published material –

Magkourilou, E., Bell, C. A., Daniell, T. J., & Field, K. J. (2025). The functionality of arbuscular mycorrhizal networks across scales of experimental complexity and ecological relevance. *Functional Ecology*, 39, 1384–1399. https://doi.org/10.1111/1365-2435.14618

Magkourilou, E., Durant, E. K., Bell, C. A., Daniell, T. J., Urwin, P. E., & Field, K. J. (2025). Plant pests influence the movement of plant-fixed carbon and fungal-acquired nutrients through arbuscular mycorrhizal networks. *Functional Ecology*, 39, 1400–1410. https://doi.org/10.1111/1365-2435.14693

Acknowledgements

Although I had the privilege of being in the driver's seat for this PhD journey, I couldn't have done it without the help of many others. First, I'd like to thank my supervisors, **Katie**, **Urwin**, and **Tim**. Each offered their own expertise and guided me throughout the process. Katie and Urwin, in particular, for introducing me to the world of mycorrhizal fungi-root feeding nematode interactions when I was a Research Technician at Leeds and then offering to take me on for the PhD. Katie again, who as my primary supervisor lifted the main load, and was encouraging and understanding throughout. Finally, Tim, for offering valuable insights, particularly into the use of metabarcoding for mycorrhizal research and for questioning some of my assumptions.

Then, I'd like to thank a lot of other people for offering specific help. **Dr Chris Bell** for contributing to making my time at Leeds productive and enjoyable at the same time, and for his continued support once I moved to Sheffield. **Dr Besiana Sinanaj**, and **Dr Alex Williams** for their assistance in harvesting the experiments described in Chapters 2 and 3, and **Emily Durant** for helping harvest and process some of the same samples. **Professor Dylan Childs** for feedback on the initial statistical analyses performed in Chapter 2. The **NERC Environmental Omics Facility: NEOF** for providing training and funding the sequencing required for Chapter 3, and the whole team at Sheffield and Liverpool, in particular, **Tom Holden**, **Dr Gavin Horsburgh** and **Lucy Knowles** for providing advice on the wet-lab procedures. **Dr Sara Moeskjaer** for advice on the data analysis required for Chapter 3. **Jennie Hibbard**, **Dr Mirela Coke**, and **Dr Catherine Lilley** for advice and help in setting up trials for Chapter 4. **Dr Peter Daniels** and **Professor Stuart Wilson** for advice and for lending some of the imaging equipment used in Chapter 4. **David Pardo** for his help in processing some of the samples used in Chapter 4 and for his assistance in harvesting the VOC experiment described in Chapter 5. **Dr Stuart Campbell** for his help in designing and collecting the VOCs samples used in Chapter 5, and **Dr Upuli Wickramaarachchi** for advice on the processing of these same samples. **Dr Heather Walker**, **Rachel George**, and **James Prout** for their help in using the MALDI-TOF and GS-MS instruments required for Chapter 5, and **Dr Alex Williams** and **Dr James Pitman** for advice on the analysis of the same metabolomic data**.**

Although doing a PhD is a real privilege, it is fair to say that I'd prefer not to have done it amidst rising global conflicts, UK-wide fearmongering targeting the most dispossessed and a

somewhat collapsing UK academic and Higher Education sector. That said, sharing this journey with colleagues with similar values made it easier. I am also just simply grateful to these people for having a laugh or a good chat over lunch. Big Alex, Emily, little Alex, James, Miles, Pedzi, Jacob, Nathan and Besiana, and to the other frequent guests of the Alfred Denny Common Room, you've all been great company.

Next, I'd like to thank my family, particularly my parents, my brother, Jenny and my nieces. For their love and support throughout my educational journey, and for instilling in me the belief that although education and the pursuit of knowledge are important, other things remain more important. To my partner, Yiorgos, thank you endlessly, and hopefully one day you'll know as much about my PhD as I know about yours. :P

Finally, I want to thank Scotland for offering tuition-free undergraduate education, without which I might never have been able to consider applying to university in the first place. For the PhD per se, I'd also like to acknowledge funding support from the UKRI-funded BBSRC White Rose DTP studentship (BB/T007222/1). Although the level of funding doesn't reflect the contributions of PhDs to research, it allowed me to complete my PhD whilst somehow keeping on top of my bills. May future PhDs get rewarded more fairly!

To our dog Meg

Who I lost halfway through this PhD, and who, if still around, would surely have been the creature closest to my heart to care the least about the contents of this Thesis

Contents

Abstract

Arbuscular mycorrhizal (AM) fungi form widespread symbioses with plants, exchanging soil nutrients for carbon (C) fixed through photosynthesis. While this bidirectional exchange is thought to be regulated by both partners, natural interactions involve multiple co-occurring organisms and complex mycorrhizal networks (MNs) linking neighbouring plants, complicating resource distribution.

This thesis investigated the relationship between AM networks, potato plants, and potato cyst nematodes (PCN). First, using multi-plant systems likely connected to the same MN and isotope tracing, I quantified the movement of fungal-acquired phosphorus (P) and plant-derived C under herbivory by PCN. Fungal-acquired P was preferentially allocated to uninfected plants relative to their infected neighbours, while plant-fixed C was consistently redistributed within the MNs *away* from infected hosts.

To assess the influence of the wider microbial environment, I characterised root and soil communities using metabarcoding. PCN infection reduced fungal diversity, including AM fungal richness, and altered community composition, whereas bacterial communities remained largely unchanged. This suggests fungal communities are sensitive to PCN infection, with associated shifts potentially influencing C-for-P exchange. However, using simplified microcosms stripped of microbial complexity, I found that AM networks redirected C towards non-infected plants, confirming the MNs capacity to regulate allocation independent of other microbes.

Finally, I explored plant metabolic responses. Non-volatile metabolites in leaves were overall unaffected by PCN infection, with only infected plants showing elevated defence-related compounds relative to their uninfected neighbours, indicating limited below-ground signalling. In contrast, volatile metabolites emitted from PCN-free plants were subtly altered by neighbouring PCN infection, suggesting MN-mediated below-ground signalling can influence some above-ground plant responses.

Collectively, these results show that AM networks can, at least partly, regulate both resource exchange and plant volatile metabolite responses, and that these dynamics are modified by herbivory. This highlights the ecological importance of AM networks and their role in shaping plant–microbe–herbivore interactions.

List of Figures

List of Abbreviations

AM	Arbuscular mycorrhizal
ASV	Amplicon Sequence Variant
BMT	Biological Market Theory
C	Carbon
CAZyme	Carbohydrate-active enzyme
CMN	Common mycorrhizal network
EcM	Ectomycorrhizal
GC-MS	Gas Chromatography–Mass Spectrometry
GLMM	Generalised Linear Mixed-effects Model
GLV	Green leaf volatiles
HIPV	Herbivore-induced plant volatile
HPLC	High-Performance Liquid Chromatography
ISR	Induced systemic resistance
JA	Jasmonic acid
LC-MS	Liquid Chromatography–Mass Spectrometry
LMM	Linear Mixed-effects Model
MALDI-TOF MS	Matrix-Assisted Laser Desorption/Ionisation Time-of-Flight Mass Spectrometry
MN	Mycorrhizal network
N	Nitrogen
P	Phosphorus
PSB	Phosphate-solubilising bacteria
PPN	Plant parasitic nematode
PCN	Potato cyst nematode
RKN	Root-knot nematode
SA	Salicylic acid
SAR	Systemic acquired resistance
VOC	Volatile organic compound
Zn	Zinc

Chapter 1. General Introduction: The functionality of arbuscular mycorrhizal networks across scales of experimental complexity and ecological relevance

1.1 ABSTRACT

One of the most prevalent symbioses on Earth is that formed between the majority of land plants and arbuscular mycorrhizal (AM) fungi. Through these intimate associations, AM fungi transfer soil nutrients to their plant hosts in exchange for photosynthetically fixed carbon resources. It has been hypothesised that this nutritional mutualism is evolutionarily stable because both partners are in control of the exchange of resources and can discriminate between partners according to whichever offers the highest returns. However, in nature, plant–AM symbioses are exposed to a wealth of additional biotic and abiotic interactions which can affect the regulation of carbon-for-nutrient exchange between symbionts. Moreover, the extraradical hyphae of AM fungi make up underground networks that may be interactive or physically connected, known as common mycorrhizal networks (CMNs). These can link neighbouring plants, potentially further influencing resource distribution across the network. How these layers of complexity interact to influence resource regulation and allocation between plants and AM fungi is not often considered by experimental designs. Here, I focus on resource allocation in AM symbioses, scaling up from evidence from reductionist experimental systems using axenic root organ cultures to complex systems incorporating multiple neighbouring plants dealing with other, co-occurring symbionts. I note biotic factors which might influence the carbon-for-nutrient exchange in plant-AM symbioses via direct or indirect mechanisms. As experimental designs increase in scale and ecologically relevant complexity, the carbon-for-nutrient exchange between plants and their AM symbionts is increasingly subject to disruption associated with the wider ecological context, such as the intricacies of the plant-fungal interactions in a CMN or the presence of co-occurring organisms.

1.2 ARBUSCULAR MYCORRHIZAL SYMBIOSES: AN OVERVIEW

One of the oldest (Redecker et al., 2000) and most widespread (Brundrett and Tedersoo, 2018) symbiotic associations on Earth is that which occurs between the roots (or rhizoids) of nearly all plants and mycorrhizal fungi. The most common type is formed between arbuscular mycorrhizal (AM) fungi of the Glomeromycotina subphylum (Spatafora et al., 2017) and 72% of vascular plant species (Brundrett and Tedersoo, 2018). AM fungi are obligate biotrophs, relying on their plant hosts for their entire carbon (C) nutrition (Bago and Bécard, 2002; Figure 1.1). In exchange, through their extraradical mycelium, AM fungi forage for and supply their hosts with critical soil nutrients such as phosphorus (P) and nitrogen (N; Smith and Read, 2010; Figure 1.1).

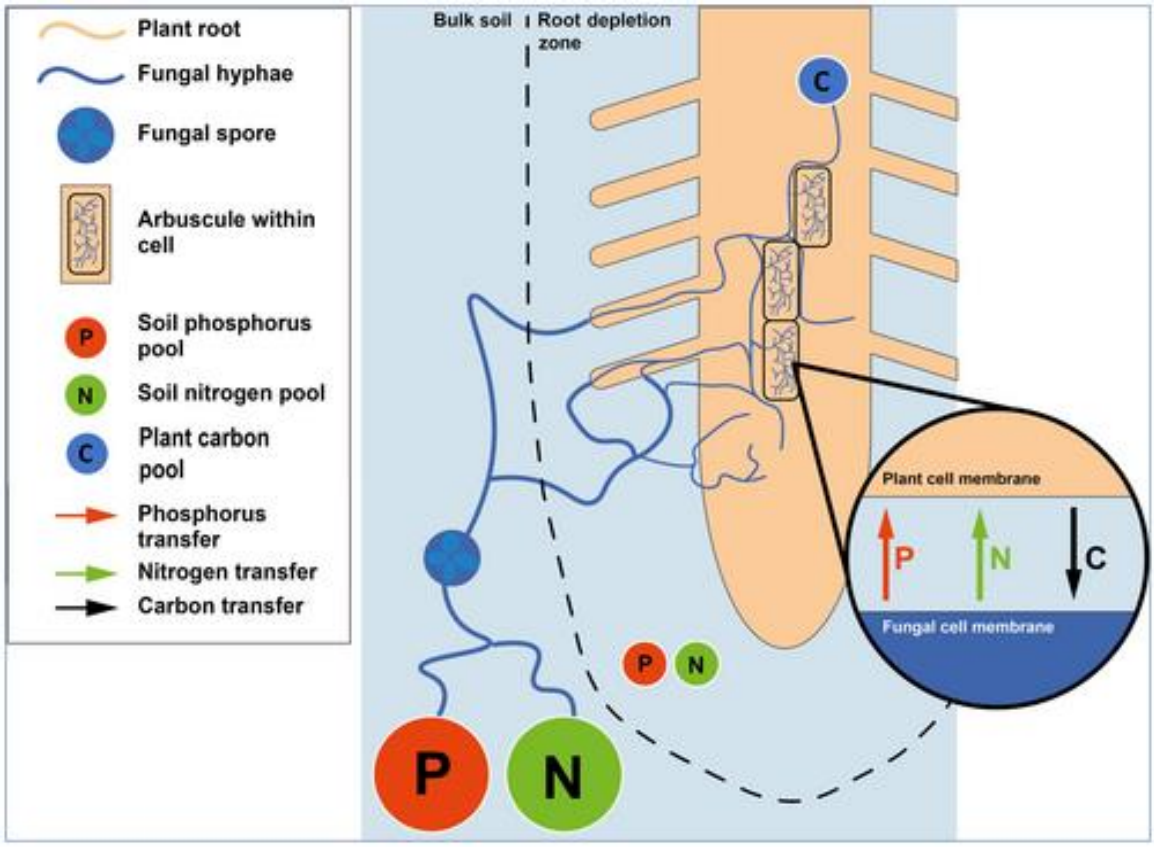

Figure 1.1 Schematic representation of arbuscular mycorrhizal hyphae extending from the root depletion zone to the inside of the plant host roots, where C-for-nutrient exchange occurs between the two partners (adapted from Watts et al., 2023).

Increased access and assimilation of soil nutrients are considered the primary benefits of associating with AM fungi for plants, especially in nutrient-poor soils where P and N are the main growth-limiting factors (Mosse & Phillips, 1971; Smith & Read, 2010). Plant responses to AM colonisation range from positive to negative, varying substantially within (Ellouze et al., 2015; Sawers et al., 2017; Watts-Williams, 2022) and between species and often depending on the combination of plant-fungal species involved (Hoeksema et al., 2010; Klironomos, 2003). However, the extent and mechanisms, as well as the external influences, that govern the exchange of resources and the outcomes of the symbiosis remain unresolved in the vast majority of instances. Evidence suggests that nutritional outcomes and plant growth responses driven by mycorrhizal relationships are very context-dependent (Bennett & Groten, 2022), with biotic factors such as cultivar (Elliott et al., 2021; Ellouze et al., 2015; Sawers et al., 2017; Thirkell et al., 2016; Watts-Williams, 2022), species or functional group of both plant host and AM fungi (Klironomos, 2003), as well as abiotic factors such as CO_2 concentration (Field et al., 2012; Thirkell et al., 2020) influencing the mycorrhizal receptivity of host plants and the functioning of the symbiosis (Caris et al., 1998; Thirkell et al., 2021; Treseder, 2004).

In addition to positive growth responses, plant benefits derived from associating with AM fungi may also include enhanced responses to abiotic constraints such as drought (Ruiz-Lozano et al., 2016; Symanczik et al., 2018) and protection against biotic pressures, including pests and diseases (Berdeni et al., 2018; Cameron et al., 2013; Jung et al., 2012; Koricheva et al., 2009; Sikes et al., 2009). Although it is theoretically and technically challenging to decouple the nutritional from the non-nutritional benefits provided to plants by AM fungi (Delavaux et al., 2017), it does appear that host mycorrhiza-induced resistance and tolerance against pathogens are not necessarily related to AM-mediated nutrient provision (De Kesel et al., 2021; Fritz et al., 2006; Jung et al., 2012; Liu et al., 2007; Schouteden et al., 2015; Vos et al., 2012). In any case, the overall costs and benefits of AM symbioses appear very context-dependent (Bennett & Groten, 2022), despite studies often measuring only a single trait (e.g. plant growth promotion) and rarely considering the implications for AM fungi themselves.

AM fungal hyphae grow outwards from colonised roots into the surrounding soil, forming a mycelial web known as a ‘mycorrhizal network’ (MN). In some cases, hyphae meet and fuse via anastomosis (de Novais et al., 2017). The MN of one AM genotype or the anastomosis of

separate mycelia can reach and colonise neighbouring plants of the same or different species, forming what is then described as a 'common mycorrhizal network' (CMN; Giovannetti et al., 2004; Mikkelsen et al., 2008). Studies on the capacity of such networks to facilitate the transfer of C between plants first appeared in the 1980s (e.g., Francis & Read, 1984). The implications that such interplant C transfer could have on plant diversity were also addressed using *in vitro* microcosms (Grime et al., 1987), with debate soon arising as to the mechanisms involved (Grime et al., 1988). Further debate about the ecological relevance of CMNs, especially in terms of the impact on plant hosts (Fitter et al., 1998), began almost as soon as the idea of ectomycorrhizal (ECM) CMNs facilitating net C transfer between forest trees started to gain traction (Robinson & Fitter, 1999; Simard et al., 1997). Recently, this debate has resurfaced (Henriksson et al., 2023; Karst et al., 2023; Robinson et al., 2023), raising important questions about the suitability of experimental designs employed to study ECM CMNs in forests and highlighting how findings from relevant studies have been extrapolated or miscited to support claims that are not unequivocally supported by the underlying data.

Despite the ongoing debate, it is clear that CMNs exist across mycorrhizal types, including AMs, and that they play a potentially important role in plant community composition and ecosystem function (Tedersoo et al., 2020). In ECM systems, C movement from host trees to a MN (potentially a CMN) and then further to neighbouring trees of similar and distinct phylogenies has been detected (Cahanovitc et al., 2022). Similarly, in microcosms including both ECM and AM trees, C transfer between individuals has also been detected (Avital et al., 2022); however, in this case, the proportion of transfer occurring via a CMN versus alternative means such as by diffusion through the soil could not be determined. In AM systems, experimental evidence supports a role for CMNs in modulating resource allocation below-ground (Mikkelsen et al., 2008) and allowing for the transmission of signals (e.g., for defence) between neighbouring plants (Alaux et al., 2020; Babikova et al., 2013; 2013a; Barto et al., 2012; Song et al., 2010, 2014, 2015, 2019).

1.3 REGULATION OF RESOURCE ALLOCATION IN AM SYMBIOSES

The evolution and dynamics behind the bidirectional resource exchange between AM fungi and their host plants are often described using Biological Market Theory (BMT; Noë & Kiers, 2018; Werner et al., 2014; Werner & Kiers, 2015; Wyatt et al., 2014). One interpretation of

this model suggests that nutrients supplied by AM fungi and plants are 'commodities' to be traded, and both 'partners' perceive the cost and benefits of the symbiosis, discriminating among alternative partners according to who offers the best 'exchange rate' (Werner et al., 2014). Theoretical models have proposed this is underpinned by a tightly coupled C-for-P exchange (Fitter, 2006); however, the exact principles of BMT and how it applies in the context of plants and AM fungi remain a topic of debate (Kiers et al., 2016; van der Heijden & Walder, 2016; Walder & van der Heijden, 2015; Bunn et al., 2024). For example, access to alternative partners is a prerequisite for partner discrimination, and in the case of AM fungi, MNs and CMNs allow this to occur. However, although MNs are an integral part of AM fungal community structure and function, it is unclear how the presence of a CMN influences resource regulation and, specifically, whether they provide a route by which sanctions and preferential resource allocation in plant-mycorrhizal symbioses can be undermined (Kiers & Denison, 2008). It is possible that the effectiveness of host-imposed punishment could be altered, as fungi denied resources by one host plant may receive resources from another plant connected to the same CMN (Kiers & Denison, 2008).

Most research conducted to assess mycorrhizal resource exchange employs experimental designs based either on monoxenic culture of AM fungi with a plant, usually a root organ culture on sucrose-rich media, or pots filled with either sterilised or natural soil, as well as with non-soil mixes such as sand and perlite. All approaches have yielded important and interesting findings; however, each has constraints. As such, the appropriate caveats must be applied when interpreting data and generalisations on the regulation of resource allocation in AM symbioses should be made with caution. The renewed debate around the functionality of CMNs is raising the bar on how research on CMNs is conducted and reported, which is timely considering the number of critical research questions that remain unresolved.

This introductory literature review aims to assess the extent to which AM symbioses, and CMNs in particular, operate via a tightly-regulated C-for-nutrient exchange. More specifically, I explore under which scenarios plant and AM fungal partners appear to be able to control the C-for-nutrient exchange for their own benefit (e.g., as per a 'reciprocal rewards' type of regulation suggested by Kiers et al., 2011) or, equally, what are the conditions that can disrupt such an exchange. To do so, I categorise evidence gathered across a gradient of ecological complexity and relevance, from simple monoxenic experimental systems involving single

plant–AM interactions to more complex (and ecologically relevant) soil-based systems sometimes involving multiple plant hosts, AM fungi and other co-occurring symbionts. This allows us to reflect on the strengths and weaknesses of each experimental approach, but also, as we critically evaluate findings from different approaches, we can provide alternative or additional mechanisms for the allocation of resources. Although there is some evidence for a coupled C-for-nutrient exchange in simple AM–plant symbioses, new patterns emerge as the scale of observation expands from simplified axenic systems to soil systems incorporating communities of plants coexisting with other non-mycorrhizal symbionts. By revealing the caveats and context dependencies of past findings, and by linking them to more recent studies, I aim to inform the continued debate on the regulation of resources across AM–plant symbioses (Noë, 2021; Prescott et al., 2020, 2021; Bunn et al., 2024) and to help strengthen future experiments.

1.4 EXPERIMENTAL APPROACHES FOR INVESTIGATING RESOURCE ALLOCATION IN AM SYMBIOSES

1.4.1 Compartmentalised monoxenic microcosms

Using compartmentalised Petri dishes containing root organ cultures and AM fungi, it has been shown that the AM fungal uptake and supply of P (Bücking & Shachar-Hill, 2005) and N (Fellbaum et al., 2012) to roots is triggered by increased C supply via a plant host, in line with a 'reciprocal rewards' mode of regulation. Further evidence from monoxenic microcosms supports this, suggesting that roots preferentially allocate more C to AM compartments that offer a more generous supply of fungal-acquired nutrients (Kiers et al., 2011). While a 'reciprocal rewards'-based mechanism could explain the evolutionary stabilisation of the AM–plant symbioses (Kiers & van der Heijden, 2006), it is important to note that in some cases (e.g. Kiers et al., 2011) the C movement from root to fungus and the P movement from fungus to root have been tested on separate plate systems, and thus, a direct link between the two flows within each system cannot be drawn.

Using an in-vitro system with a plant 'donor' and plant 'receiver' compartment, zinc (Zn) has also been shown to be transferred between plants via a presumed CMN, and this evidence was supported by changes in the expression of Zn transport-related genes in fungi and plants (Cardini et al., 2021). By tagging rock phosphate apatite with fluorescent quantum-dot

nanoparticles and tracking its movement, it has also been shown that AM fungi can transfer P from 'rich' to 'poor' patches of the same MN (van 't Padje, Bonfante, et al., 2021; van 't Padje, Werner, et al., 2021; Whiteside et al., 2019) or across a CMN linking two separate root compartments (van 't Padje et al., 2020). Consequently, in the latter case, roots growing in these 'poorer' P patches were found to acquire more P transferred from the other 'richer' side of the CMN, although this effect was not instantaneous (van 't Padje et al., 2020). Taken together, this evidence suggests that, at least *in vitro*, when patches of a CMN have restricted access to nutrients, the entire MN might be supported (in terms of C) by a single host, while the least contributing host might benefit directly through nutrient acquisition from the CMN without giving much in return. However, when P concentration is high or when it does not vary greatly between different parts of a MN, transport of P might be compromised as, rather than distributing P across the network where it can be taken up by roots, the fungus might increase the allocation of P to its storage structures (van 't Padje, Bonfante, et al., 2021; van 't Padje, Werner, et al., 2021; Whiteside et al., 2019). That said, this hypothesis contrasts with findings from a visual assessment of fungal structures, where high P availability increased the formation of branched absorbing structures at the expense of storage structures (Olsson et al., 2014).

Under conditions of limited C availability, AM fungi accumulate more P in their spores and hyphae (Hammer et al., 2011), likely because C provision to hyphae, and especially to spores, becomes reduced (Olsson et al., 2014). Potentially, this is a strategy that the fungus has evolved to supply nutrients with a better exchange rate if either root demand for nutrients or plant C supply increase at a later stage (van 't Padje, Bonfante, et al., 2021; van 't Padje, Werner, et al., 2021; Whiteside et al., 2019). Although the exact mechanisms behind such a strategy remain unresolved, a level of detection of the changing conditions by the MN would appear necessary, as would the capacity of this signal to then be transferred to arbuscules where the fungus would be able to control the rate of nutrient exchange through changes in nutrient transporters for C-based sugars (Doidy et al., 2012) and/or lipids (Jiang et al., 2017; Keymer et al., 2017) as well as fungal-acquired N (Koegel et al., 2013, 2017) and P (Walder et al., 2015; Xie et al., 2013). That said, it has been argued that plant C does not represent a significant cost to the plant as it is typically fixed surplus to requirements and that other, more parsimonious explanations such as source-sink dynamics regulate, or at least influence,

resource allocation among plants and AM fungi (Corrêa et al., 2023; Prescott et al., 2020, 2021; van der Heijden & Walder, 2016).

An additional pattern of increased AM fungal allocation of P to roots with a higher C root status has been shown using a four-compartment Petri dish system where 'donor' roots were connected via a CMN to two 'receiver' roots of varying C status (Lekberg et al., 2010). It was also suggested that C was transported from one root section to the other via AM fungi, with the strength being stronger in the direction from C-rich to C-limited roots (Lekberg et al., 2010). However, in either case, the transferred C remained in the fungal tissue of both the C-rich and the C-limited roots (Lekberg et al., 2010). This distinction is important as it adds to the evidence contradicting the significance of plant-to-plant C transfer (e.g. Pfeffer et al., 2004; Voets et al., 2008) and suggests that any fungal-mediated C movement likely primarily benefits the fungus.

From experiments involving compartmentalised monoxenic microcosms, it appears overall that both AM and plant partners can control the bidirectional C-for-nutrient exchange characteristic of AM symbioses, although the level of control seems to be impacted by abiotic conditions. The exact mechanisms underpinning this remain unresolved and could be equally attributed (at least partly) to other drivers such as sink-source dynamics. The monoxenic approach to investigating dynamics and regulation of mycorrhizal function, whether as one-on-one or CMN-wide interactions between plants and fungi, has a number of strengths and weaknesses. Monoxenic systems are simpler and more easily manipulated or controlled than those that include soil and other microbes. As such, causation can be attributed with more confidence and more mechanistic insights revealed. On the other hand, their artificial nature (notably the absence of soil and the lack of photosynthetic plant materials through use of root organ culture), lack of ecological complexity as well as the potentially altered AM fungal evolution stemming from the continuous *in vitro* propagation (Kokkoris & Hart, 2019) limit our ability to draw conclusions on what really governs resource allocation in natural AM ecosystems.

1.4.2 Soil-based microcosms with a single plant host

Despite the mechanistic insights that monoxenic systems can potentially provide, an important consideration with any such reductionist approach is that the results might not be representative of what occurs in more natural, complex settings. Reciprocal allocation of

resources between symbionts in monoxenic experiments involving root organ culture might not be representative of effects observed where whole plants in soil-based experiments are used as, among other things, the lack of a photosynthetic plant shoot is likely to influence nutrient demand and thus sink strength dynamics between host plant and AM fungi (Smith & Smith, 2011). Another consideration relates directly to the challenge of transferring experimental techniques and conclusions from tightly controlled and highly simplified plate systems to more complex soil-based systems. For example, AM fungal-mediated increases in the uptake of quantum-dot apatite were not detected in either root or shoot in a soil-based experiment (van ’t Padje, Bonfante, et al., 2021; van ’t Padje, Werner, et al., 2021), although they were detected in similar monoxenic experiments (e.g., van ’t Padje, Bonfante, et al., 2021; van ’t Padje, et al., 2021; Whiteside et al., 2019).

Experiments conducted in soil-based experiments have also shown how the functional significance of mycorrhizal symbioses, and even the partner selection process, can be strongly influenced by environmental conditions, which typically (and necessarily) remain constant in axenic systems. For example, the preferential allocation of plant-fixed C to the more beneficial fungal partner has been shown to decrease with increasing soil P availability (Ji & Bever, 2016). This is likely because under high P availability (e.g., fertilisation), the C allocation to AM fungi by host plants sometimes decreases considerably as the mycorrhizal-derived benefits are also reduced (Olsson et al., 2010). Similarly, in high or low P soils, plants might favour the direct over the mycorrhizal P uptake pathway, while under intermediate, suboptimal conditions, the mycorrhizal pathway may become preferred (Zhang et al., 2021). This suggests that the dynamics of resource regulation of a single plant species might change as its ‘fungal collaboration gradient’ (Bergmann et al., 2020) changes from a ‘do-it-yourself’ resource uptake to a ‘mycorrhizal outsourcing’ of resource uptake according to external conditions.

Ultimately, although environmental conditions (e.g., elevated atmospheric CO_2 concentrations) do not always influence the levels of mycorrhizal colonisation or the total amount of plant C that AM fungi receive (e.g. Thirkell et al., 2021), changes in environmental conditions can still influence how plants associate with AM fungi species and vice versa (Forczek et al., 2022). For example, the level of CO_2 in the atmosphere has been found to influence plant-to-AM fungi C dynamics, with shifts in the AM taxa that received most of the plant C at ambient or elevated CO_2 levels correlating with niche and life history strategies

(Drigo et al., 2010). This could have knock-on effects on plant–AM symbioses and the distribution of resources if fungal species that receive most of the plant C became dominant over time. In a different case, the preferential allocation of plant C to the more beneficial AM fungi and a reciprocal differential P uptake decreased with shading (Zheng et al., 2015). A similar pattern was observed in a separate experiment, where even though *Medicago trunculata* preferentially allocated C to *Funneliformis mosseae* over *Claroideoglomus claroideum* under simulated drought conditions, this was not the case under a shading treatment (Forczek et al., 2022). The lack of a shading-induced preferential allocation of resources could be explained by the reduction in the availability of above-ground resources caused by the shading treatment, which, as previously described, can lead plants to reduce their overall C allocation to AM fungi (Olsson et al., 2010). But even if it does not translate to a detectable change in how a plant allocates C to AM fungi, shading can still lead to a rapid shift in the mycorrhizal community composition (Forczek et al., 2022). Ultimately, all of these examples point to the importance of considering the longer-term implications relating to the regulation of C-for-nutrient exchange, such as the potential longer-term benefits of maintaining simultaneous root colonisation by different AM fungi ('evolutionary bet-hedging'; Lekberg and Koide, 2014; Veresoglou et al., 2022), even in the absence of consistent synergistic effects of inoculations with multiple AM species (e.g. Jansa et al., 2008; Martina et al., 2013). Although relevant data are scarce, incorporating some longer-term cost–benefit calculations into BMT models would greatly benefit their predictive capacity for understanding how the C-for-nutrient exchange is regulated under different scenarios.

Using a split-root experimental system, where each fungal partner is inoculated separately in different parts of the root, Bever et al. (2009) demonstrated increased plant C delivery to the more beneficial (i.e., growth-promoting) of two AM fungal symbionts tested. A similar pattern was later confirmed, where the preferential allocation of C from a plant to two AM fungi separated by a split-root system was matched by a differential P uptake by the two AM fungi (Zheng et al., 2015). It is important to note that split-root designs might introduce positive bias, as it has been evidenced that spatial separation of fungal partners might be required for partner discrimination, and thus, the preferential allocation of C by plants to the more mutualistic AM fungi (Ji & Bever, 2016). That said, in other cases, reducing spatial structure by mixing soil has increased the abundance of the more 'cooperative' AM fungal symbionts

(Verbruggen et al., 2012), suggesting that plants preferentially associate with more mutualistic species, even under mixed species conditions. It might well be that in split-root systems, plants favour different parts of their root system rather than specifically different AM fungi.

1.4.3 Single plant hosts with AM fungi and other interacting symbionts

Despite these caveats and context dependencies, there is evidence from soil-based experiments that plant hosts can preferentially allocate more C to AM fungal partners that provide a greater return of nutrients (Bever et al., 2009; Kiers et al., 2011; Lendenmann et al., 2011; Zheng et al., 2015). However, our understanding of how resources are regulated and allocated within AM–plant symbioses is still limited by the frequent oversight of other co-occurring organisms that may compete for plant and/or fungal resources. This is particularly relevant given that AM colonisation has been shown to increase the attractiveness and consumption of plants by above-ground insect herbivores, possibly due to mycorrhizal-mediated increases in plant size and nutrient content (Koricheva et al., 2009). In turn, above-ground herbivores can themselves influence these same plant traits and consequently affect AM fungi—either by altering mycorrhizal community composition or by reducing (Gehring & Whitham, 2002) or increasing (Frew et al., 2023) mycorrhizal colonisation (Figure 1.2a). In other cases, above-ground herbivory does not appear to affect colonisation levels (Charters et al., 2020; Zhao et al., 2024), although abiotic factors such as atmospheric CO_2 concentration can (Charters et al., 2020; Figure 1.2a).

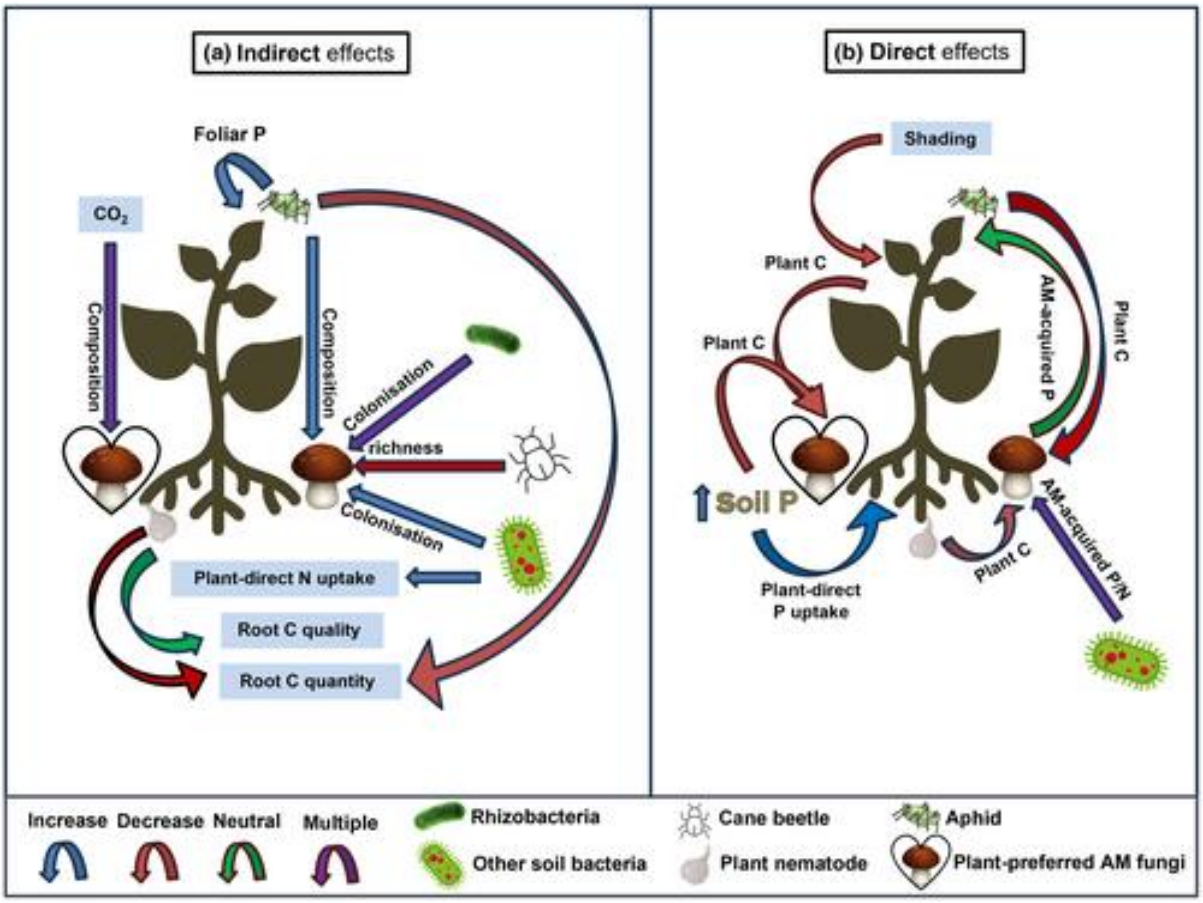

Figure 1.2 Illustrative summary of how above and below-ground complexity might have **(a)** indirect and **(b)** more direct effects on the C-for-nutrient exchange in plant-arbuscular mycorrhizal (AM) symbioses (Bell et al., 2022, 2024; Charters et al., 2020; Frew, 2022; Jiang et al., 2021; Larimer et al., 2014; Rozmoš et al., 2021; Svenningsen et al., 2018; Zhang et al., 2016, 2024). The direction and colour of the arrows illustrate the direction of influence as per the legend.

More specifically, above-ground herbivory can also reduce root C concentrations and increase foliar P of mycorrhizal plants (Frew et al., 2023; Figure 1.2b). Frew et al. (2024) hypothesised that when above-ground herbivores or pathogens infect a mycorrhizal plant host, the AM fungal communities in the roots might be shaped by the capacity of the AM species to either (i) tolerate the herbivore/pathogen-induced constraints on plant C or (ii) enhance plant defences against the same herbivores/pathogens. Additionally, as well as the amount of C, the shift in the type of C provided to AM fungi in response to plant herbivory is likely to also be an important factor in determining the community composition (Bell et al., 2024). For example, some plant pests might induce plant limitation of certain C compounds to AM fungi

more than others, thereby indirectly selecting AM species that may themselves have a preferential C usage or an ability to cope with less of a certain resource (i.e., fatty acids or hexose sugars). Below-ground, root-herbivory by cane beetle larvae (*Dermolepida alborhirum*) changes the community structure of AM fungi and reduces AM fungal species richness in roots (Frew, 2022; Figure 1.2a). Plant P concentration also becomes reduced (Frew, 2022), although it remains unclear whether this is due to a reduction in fungal-acquired P or an impact on the plant's own capacity to acquire P directly.

Other than root herbivory, below-ground, mycorrhizal symbioses are also modulated by interactions with bacteria, most notably phosphate-solubilising bacteria (PSB; Jiang et al., 2021; Wang et al., 2023; Duan et al., 2024; Duan et al., 2025). Due to the absence of most carbohydrate-active enzyme (CAZyme) genes, AM fungi are limited in their ability to utilise polymeric organic matter in soil (Miyauchi et al., 2020). As such, the AM fungal-bacterial symbiosis is based on the premise that hyphospheric bacteria feed on fungal metabolites containing plant-derived C, and in return, the bacteria use extracellular enzymes to decompose organic compounds into mineral forms that AM fungi can then access (Zhang et al., 2018). As a result, AM fungi do not associate with soil bacteria randomly; instead, they appear to 'cooperate' preferentially with bacteria that possess a large repertoire of CAZymes (Nuccio et al., 2022), potentially reflecting an evolutionary strategy to avoid C limitation.

In fact, by varying the composition of their hyphal exudates (Zhou et al., 2020), AM fungi seem to be able to select for a specific microbiome, which often has AM-beneficial properties (Emmett et al., 2021). For example, bacteria from the family Oxalobacteraceae are thought to be preferentially promoted by AM fungi (Offre et al., 2007; Scheublin et al., 2010), and more recently, certain bacterial genera—such as *Halangium*, *Pseudomonas*, *Devosia*, and *Sulfurifustis*—have also been identified as commonly associating with AM fungi and even stimulating AM fungal colonisation (Zhang et al., 2024; Figure 1.2a). Plant inoculation with the bacterial genus *Devosia* was specifically found to lead to enhanced direct N uptake by the plant (Zhang et al., 2024; Figure 1.2a), which could mean that these plants become less reliant on AM fungi for their N nutrition. In some cases, soil biota (including bacteria) act antagonistically to AM fungi and have been found to inhibit their ability to colonise plant roots (Cruz-Paredes et al., 2019; Svenningsen et al., 2018). This context dependency is also observed in the interactions between AM fungi and rhizobacteria, where, although they often

act synergistically on plant growth, in some cases, rhizobia inoculation can also lead to neutral (Pérez-De-Luque et al., 2017) or even negative effects on AM colonisation (Larimer et al., 2014; Figure 1.2a).

Finally, other than interactions with hyphospheric or soil bacteria, AM fungi harbour endobacteria, notably *Burkholderia*-related (Bianciotto et al., 1996) and *Mycoplasma*-related endobacteria (Naumann, Schüßler, and Bonfante, 2010), which depend on the AM fungi for their C (Lumini et al., 2007) and nutrient demands (Ghignone et al., 2012) and can thus indirectly drive the C-for-nutrient exchange between AM fungi and their plant hosts. *Mycoplasma*-related endobacteria in particular seem to rely more on the fungus for their C demands (Kuga et al., 2021), and it has thus been speculated that they might be weak parasites (Duan et al., 2024). Moreover, these endobacteria can influence the fungus's gene expression and also remarkably, the gene expression of the fungus's plant host (Venice et al., 2021), revealing a complex network of direct AM fungal-bacterial-plant interactions.

Regardless of whether they might be synergistic or not, interactions between AM fungi and other organisms are typically not captured by most studies focusing on C-for-nutrient exchange in plant-mycorrhizal symbioses. However, this is important because any indirect impact on AM fungi (e.g., degree of colonisation) or the plant (e.g., uptake of N via non-mycorrhizal means) might influence the extent to which each can control the C-for-nutrient exchange. The presence of multiple, simultaneous and diverse symbionts on the plants can also have other, more direct impacts on the C-for-nutrient exchange between AM fungi and their plant hosts. For example, other than only influencing levels of AM colonisation, certain soil bacteria appear to directly suppress (Cruz-Paredes et al., 2019; Svenningsen et al., 2018) or enhance (Jiang et al., 2021; Zhang et al., 2016) the P-delivery capacity of AM fungi (Figure 1.2b). *In vitro*, it has been demonstrated that the AM fungus's capacity to obtain N from an organic source can increase in the presence of the soil bacterium *Paenibacillus sp.* and the protist *Polysphondylium pallidum*, but other chitinolytic bacteria, such as *Janthinobacterium sp.*, did not have an effect (Rozmoš et al., 2021; Figure 1.2b).

Also, in soil-based systems, the allocation of plant C to AM fungi decreases dramatically following plant exposure to aphids (Charters et al., 2020) or PCN (Bell et al., 2022), although in both cases the supply of fungal-acquired nutrients to the plants was largely maintained (Figure 1.2b). A split-root experiment found that roots colonised by AM fungi and/or PCN

accumulate more plant C than asymbiotic roots (per gram of root), possibly because roots with symbionts represent a greater sink for plant C than those without (Bell et al., 2024). Furthermore, in a split-root experiment, roots colonised by AM fungi have been found to contain more recently-fixed plant C than roots of the same host that are infected with PCN, which, again, could simply suggest that AM fungi represent a larger C sink than PCN (Bell et al., 2024). An alternative, not mutually exclusive hypothesis, is that plants may preferentially allocate C to AM-hosting roots rather than those hosting PCN to selectively enhance mutualistic interactions and limit the effects of parasitic infection (Bell et al., 2024). It could also be true, however, that plants simply have a greater degree of control over the plant–AM fungi flow rather than the plant–parasite flow, or that the supply of resources towards AM fungi is simply an indirect consequence of the plant trying to shuttle resources away from PCN (Bell et al., 2024).

In any case, contrary to expectations based on a 'reciprocal rewards' mode of regulation, it appears that above- or below-ground herbivory drives asymmetry in the C-for-nutrient exchange between plants and AM symbionts. Another consideration for the theoretical framework of the interactions between AM fungi and other co-occurring symbionts is that individual organisms, such as aphids or PCN, function as distinct entities with the aim of acquiring resources to produce a second generation. In contrast, due to their coenocytic hyphae and spores, heterokaryotic nuclear organisation, and ability to fuse to form vast networks (Kokkoris et al., 2020), AM fungi cannot be easily classified as distinct, singular entities. This, in turn, might have implications for the evolution of the dynamics of inter- and intra-species competition between mycorrhizal fungi and result in the acquisition of C for the benefit of the entire MN rather than a single part of it consisting of a single genet. Moreover, the lifetime and cycle of co-occurring symbionts are likely to influence the C-for-nutrient exchange between hosts and their mycorrhizal symbionts. For example, aphids are seasonal, and one generation of PCN feeding lasts around 6 weeks, whereas, despite the patchy and ephemeral nature of the fungal colonisation and fungal intracellular structures (Friese & Allen, 1991) which could mean that individual hyphae live on average only 5 to 6 days (Staddon et al., 2003), AM associations may last the entirety of a plant's lifetime. This could mean that in nature, AM fungi might have evolved to endure relatively short periods of a pathogen/parasite-constrained C flow before supply returns to pre-stress levels. As such,

given the impacts of plant and fungal phenologies as well as the impacts of any additional biotic and abiotic interactions, considerations and extrapolations of AM functionality to an ecosystem or even global scale should be undertaken with careful thought.

Overall, while some evidence of the ability of plant and AM fungal partners to each control the C-for-nutrient exchange also stems from soil-based experiments, this is increasingly influenced or disrupted by various factors such as environmental conditions, the presence of additional/multiple symbionts, and the specific experimental design used. More research is needed on the varied ways that biotic and abiotic factors influence the C-for-nutrient exchange, and the longer implications of such factors need to be understood and incorporated into relevant models. Moreover, understanding complex processes influencing AM fungi is important in order to harness the benefits of AM fungal associations, but also to understand any unintended consequences. For example, the results from a combination of greenhouse and field experiments suggest that, although inoculation with AM fungi increases host tolerance to PCN, this also leads to a build-up of PCN in the soil, which can in turn start eradicating the benefits that AM provided their plant hosts in the first place (Bell et al., 2022; Bell et al., 2023).

As with monoxenic approaches, soil-based experimental systems have strengths and weaknesses. Soil-based experiments add some necessary ecological complexity, and their findings are likely to be more realistic than those stemming from monoxenic plate-based systems. However, increased ecological complexity (e.g., a more diverse soil microbial community) can lead to additional, interactive indirect or direct consequences on both plant and fungal partners, which in turn makes it more challenging to decipher the mechanism behind resource allocation between symbionts. One such limitation is the difficulty of accounting for AM fungal C respiration, especially in a complex soil system with a diverse microbial community. Additionally, when soil-based systems involve only one plant, it is vital to consider that plant–plant interactions and the ability of AM fungi to form below-ground networks are lacking; and, as such, specific hypotheses such as the ability of AM fungi to associate with more beneficial plant hosts within a CMN cannot be tested.

1.4.4 Common mycorrhizal networks and multi-species interactions in soil-based experiments

Although MNs and CMNs are an integral part of AM fungal functioning, it is unclear how the presence of a CMN influences resource regulation and to what extent it can facilitate resource

transfer between plants. Early evidence from soil-based systems suggests that resources such as C (e.g., Graves et al., 1997) and P (e.g., Mikkelsen et al., 2008) are transferred across a MN. However, it is not always clear whether this transfer tends to be bidirectional between plants (Lerat et al., 2002) or unidirectional (Pfeffer et al., 2004) based on the unique characteristics of a 'donor' and a 'receiver' plant (Selosse et al., 2006). The physiological significance of interplant C transfer between host plants is also unclear, with a more mycocentric view of the transfer being required (Fitter et al., 1998).

In line with the 'reciprocal rewards' hypothesis for regulation of symbiotic C-for-nutrient exchange, experiments using two CMN-connected plants, one shaded and one non-shaded, suggest that AM fungi retain their 'bargaining power' and provide the plant assumed to supply more C to the CMN (i.e., the non-shaded plant) with more nutrients (Faghihinia & Jansa, 2022; Fellbaum et al., 2014; Weremijewicz et al., 2016). However, it is important to consider these results in the context of the experimental design since shading does not always lead to a reduction in plant C flow (Faghihinia & Jansa, 2022; Olsson et al., 2010) and in other cases (e.g., Fellbaum et al., 2014) the strength of the plant C-source is assumed rather than experimentally quantified. Other potentially confounding impacts implicit in treatments such as shading include those on plant growth or metabolism (altering sink strength of the host plant for nutrients), or even the variability of plant species responses to shading (e.g., Semchenko et al., 2010), which could substantially influence the results.

C-for-nutrient exchange across a CMN depends on the AM fungal and plant species involved in forming a network. In one experiment consisting of flax (*Linum usitatissimum*) and sorghum (*Sorghum bicolor*) linked to the same CMN, sorghum contributed more C to the AM network despite receiving fewer nutrient returns (Walder et al., 2012). Interestingly, this type of asymmetry was only observed when the CMN comprised a single AM fungal species *Rhizophagus irregularis* (formerly *Glomus intraradices*); when the CMN consisted of another AM fungal species, *Funneliformis mosseae* (formerly *Glomus mosseae*), both plants received similar amounts of nutrients from the CMN, although plant C inputs remained uneven (Walder et al., 2012). The functioning of a CMN in terms of nutrient allocation to plants could not be explained by the expression of genes that regulate orthophosphate (Pi) transporters (Walder et al., 2015), suggesting that another regulatory mechanism must be at play. The consequences of varied plant benefits derived from CMNs can be important in understanding

wider plant community structure and function. Invasive plant species, for instance, may receive a greater nutritional benefit from incorporation into CMNs than native plant species, but again, the exact patterns of AM fungal-mediated nutrient transfers to different plant hosts depend on the fungal species comprising the CMN (Awaydul et al., 2019).

Plant community diversity can have impacts on the C inputs into a CMN, with more diverse plant communities associated with greater movement of C into CMNs than those comprising fewer species (Řezáčová et al., 2018). Similarly, more diverse plant communities are associated with greater benefits in terms of fungal-derived N, although the direction and strength of the transfer appear to be species-specific (Ingraffia et al., 2021). Such species specificity was also reflected in terms of mycorrhizal-growth responses by plant hosts, and this was attributed to the higher amounts of N transferred by the AM fungi (Ingraffia et al., 2021). In a different example, no differences in C investment to the CMN were found between a C3 and a C4 plant at either low or elevated temperatures (Řezáčová et al., 2018). In fact, C_3 plants were found to supply the CMN with similar amounts of C at both temperatures, despite their growth being negatively affected, AM root abundance being suppressed, and also the C_3 hosts receiving less fungal-acquired N compared with the C_4 hosts at the elevated temperature (Řezáčová et al., 2018).

Despite increasing attention and experiments involving CMNs, relatively little is known about the distance over which nutrients and C can be conveyed by extraradical mycorrhizal hyphae (Werner et al., 2014) and how this might be influenced by the varied abiotic and biotic factors. For instance, N can be transported between plants across a distance of 12 cm (the maximum distance tested), presumably via mycorrhizal hyphal connections; however, this again appears to be species-specific, with no significant transfer being detected when the CMN was comprised by the AM fungal species *Rhizophagus irregularis* (Schütz et al., 2022). CMN-mediated N transfer between plants also appears to be influenced by the levels of N availability in the soil as well as the source-sink strength dynamics of the plant hosts (e.g. C_3 vs C_4 physiology; Muneer et al., 2023). In a pot-intercropping experiment, N was also found to be transferred from soybean (*Glycine max*) to maize (*Zea mays*), presumably via a CMN; with this transfer increasing when plants were also inoculated with rhizobia (Meng et al., 2015). Overall, the diversity in CMN functionality is likely due to a combination of biotic and abiotic factors such as variation in sink-source strengths of plant hosts and fungal symbionts (Walder

& van der Heijden, 2015), potentially partly driven by differences in plant physiologies (Muneer et al., 2023; Řezáčová et al., 2018), and indeed the capacity of individuals within the network to control the C-for-nutrient exchange (Werner & Kiers, 2015).

When considering the significance of CMNs in wider ecosystems, it is important to note that any impact of CMN function on inter-specific plant and/or fungal competition could indirectly generate further feedbacks on mycorrhizal resource exchange across the network (Bücking et al., 2016; Figure 1.3). By influencing below-ground resource transfer and competition, CMNs can enhance plant growth (Muneer et al., 2023), sometimes promoting and perpetuating size inequality and resource sink strengths among neighbouring plants (Merrild et al., 2013; Weremijewicz et al., 2016; Weremijewicz & Janos, 2013; Figure 1.3). Plant-fungal interactions, the importance of symbiont compatibility, and the high variability in plant growth responses (e.g., Castelli & Casper, 2003; Klironomos, 2003) allow CMNs to play a role in fungal-mediated soil feedbacks, where one plant species promotes or discourages AM fungal species so that it enhances its performance relative to other, co-occurring plant species (Selosse et al., 2006; Figure 1.3).

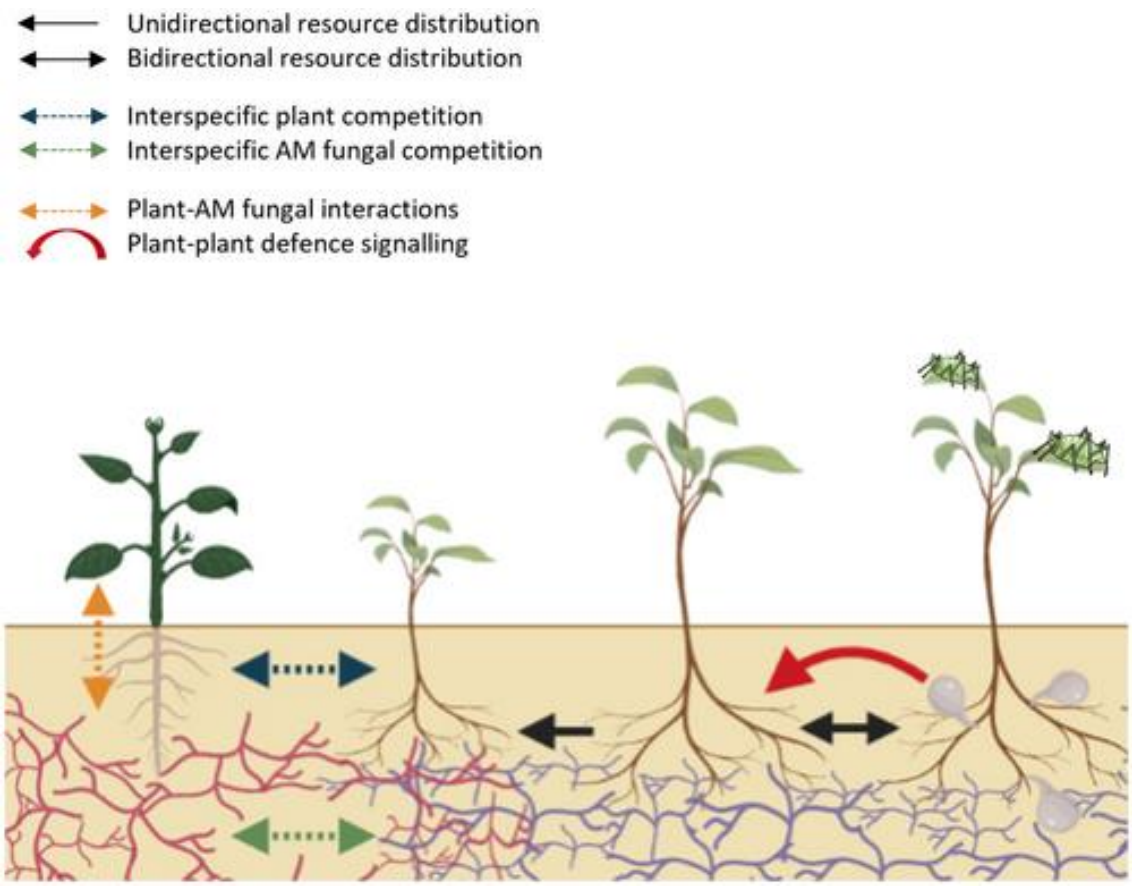

Figure 1.3 Summary of the various possible ecological implications of common mycorrhizal networks (CMNs). The black arrows show the movement of resources (e.g. carbon and phosphorus) across the network. This can be bidirectional between plants or unidirectional from a 'donor' plant to a 'receiver' plant. Blue and green arrows illustrate how CMNs can influence interspecific plant and fungal competition respectively. This below-ground resource competition can promote size inequality among neighbouring plants. The orange arrow illustrates plant-fungal interactions. Symbiont compatibility and the high variability in plant growth responses mean that CMNs can play a role in fungal-mediated soil feedbacks and plant-fungal community structure. The red arrow from a plant attacked above-ground by aphids and below-ground by plant-parasitic nematodes to a healthy plant refers to the ability of CMNs to facilitate plant–plant communication by transfer of phytohormones and defence signals.

The role of CMNs is not limited to modulating resource allocation below-ground or enhancing plant nutrient uptake (Mikkelsen et al., 2008); their role in mediating plant–plant interactions appears to also be important, particularly where plants linked to a CMN are affected by other co-occurring organisms. CMNs can serve as pathways for plant–plant communication, including phytohormones, disease resistance and induced defence signals (Alaux et al., 2020; Babikova et al., 2013, 2013a; Barto et al., 2012; Song et al., 2010, 2014, 2015, 2019; Figure 1.3), influencing wider environmentally relevant characteristics such as plant competition dynamics (Tedersoo et al., 2020). In some cases, allelochemicals produced by certain plant species can be transported via CMNs and inhibit the growth of neighbouring plants (Barto et al., 2012). In other cases, it has been suggested that interplant communication occurring via CMNs can increase disease resistance as signals induced by pathogenic fungi are transmitted from diseased plants to healthy neighbours (Song et al., 2010). The induction of herbivore-repellent VOCs and the elicitation of defence genes have also been observed in healthy plants sharing a MN with plants attacked by above-ground herbivores, whilst importantly, plant-plant communication via aerial VOCs and root exudates was controlled for (Song et al., 2014; Babikova et al., 2013).

Co-occurring organisms that compete for plant C resources can lead to asymmetry in C-for-nutrient exchange between the plant and AM fungi (Bell et al., 2022; Charters et al., 2020). In these scenarios, the pest-infested plant reduces the movement of C via the export of hexose sugars from root to AM fungi but maintains the flow of fatty acids, presumably thereby providing enough C to AM fungal partners to maintain the symbiosis (Bell et al., 2024). Such regulatory mechanisms are likely further modulated across multiple hosts that are linked by a CMN (Bell et al., 2021; Figure 1.4). It is also an interesting observation that under increasing PCN densities in the soil, levels of AM fungal colonisation decrease, whereas soil hyphal densities increase, potentially suggesting a mechanism whereby AM fungi invest more in expanding their mycelium network to reach neighbouring plant hosts of better quality (Bell et al., 2022).

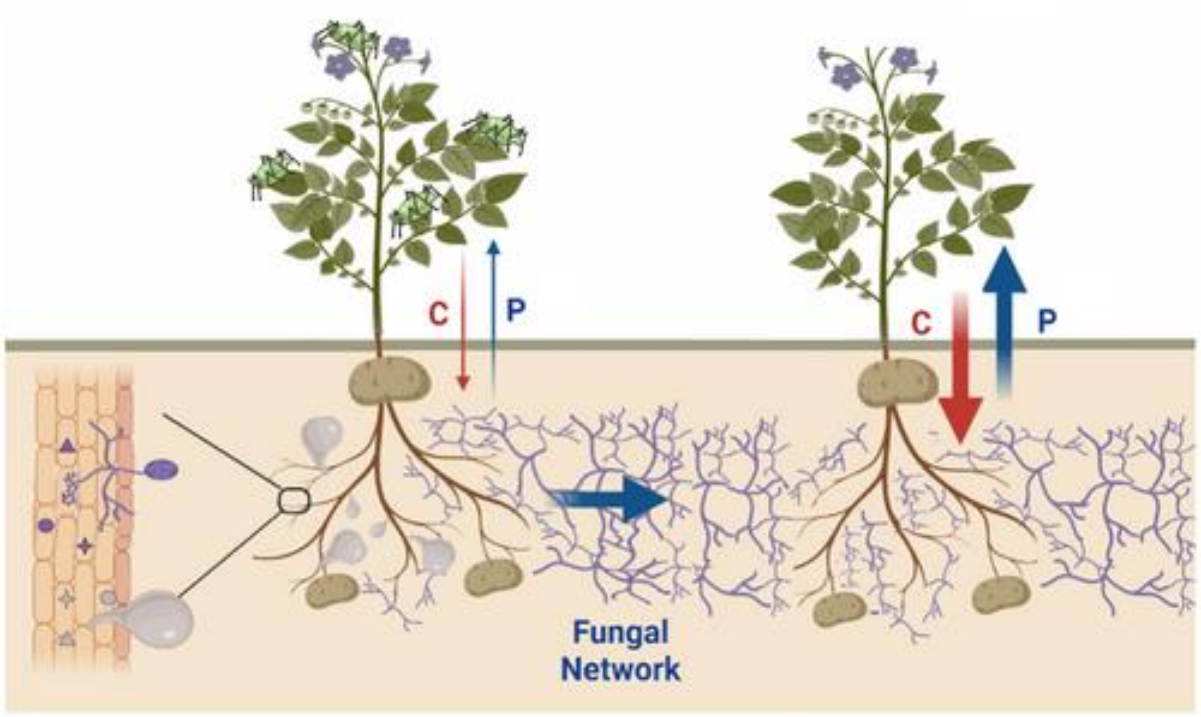

Figure 1.4 Potential scenario for the allocation of resources between a CMN and its plant hosts in the presence of competing above- and below-ground herbivores (i.e., aphids and plant-parasitic nematodes, respectively). The strain imposed on plant C supply by herbivores leads to a reduced allocation of C to the CMN by the plants. In turn, the CMN reduces the allocation of P to the infected plant host and directs resources towards a non-infected plant host that is offering more C in return. Red arrows—plant-to-symbionts C flow; Blue arrows—AM fungi to host P flow; width of arrows—flow strength (adapted from Bell et al., 2021).

For example, in the presence of an assumed CMN, parasitism of *Trifolium pratense* by the stem holoparasite *Cuscuta australis* reduced the acquisition of AM fungal-mediated N of the parasitised plant relative to its non-parasitised neighbour (Yuan et al., 2021). In this case, the non-parasitised plant also grew larger, which in turn supports the hypothesis that CMNs preferentially transport nutrients to larger plants or that differential nutrient supply from a CMN to plants amplifies plant size inequality (Awaydul et al., 2019; Merrild et al., 2013; Weremijewicz et al., 2016). Additionally, it is plausible in this case that the CMN provided more N to the non-parasitised plant, as that plant was providing more C in return. Durant et al. (2023) found that plants with aphids reduced the amount of C supplied to MN(s) (potentially a CMN) while uninfested neighbouring plants likely maintained C flow into the

MN(s), helping to support the wider MN(s). In this case, AM fungi maintained P transfer to both infested and non-infested plants (Durant et al., 2023), suggesting that the net C inputs into a MN are more important than one-on-one interactions in maintaining MN functionality. This also supports the idea that the presence of a CMN potentially undermines the capacity of the plant hosts to control AM fungi by denying them resources (Kiers & Denison, 2008). As in previous studies that created C sinks across a CMN, either by shading (Fellbaum et al., 2012) or by chemically altering nutrient gradients in vitro (Lekberg et al., 2010; van ’t Padje, Bonfante, et al., 2021; van ’t Padje, Werner, et al., 2021; Whiteside et al., 2019), these results demonstrate how CMNs are responsive and resilient and potentially have an important role to play in ameliorating the impacts of plant stresses.

Overall, experiments involving multiple symbionts have shown that CMNs can play a role in facilitating resource transfer between plants and influencing plant–plant interactions within an ecosystem. However, CMNs can also play other roles, such as in plant–plant communication through the transfer of phytohormones and defence signals. Moreover, their overall functioning is highly context-dependent, influenced by both biotic and abiotic factors (e.g., the number or identity of plant and fungal species involved). All these factors appear to then feed into (and often compromise) the ability of plants, and especially that of AM fungi, to control the C-for-nutrient exchange for their own benefit. While soil-based experimental systems that incorporate multiple plants and other non-mycorrhizal symbionts are more ecologically relevant than the other experimental systems reviewed here, this increased complexity compromises our ability to draw clear causal links and to get a more detailed mechanistic understanding of the relationships occurring .

1.5 CONCLUSIONS

Although there is some evidence for a preferential allocation of resources to more beneficial partners and for a tight link between plant-mediated and AM fungal-mediated resource flows, there is also growing evidence that the dynamics behind the partner selection process and the characteristic bidirectional nutrient exchange are context-dependent. Factors such as resource abundance, soil microbial composition, the presence of other symbionts, and the compatibility between plant and AM species are all likely to play an important role in the strength and direction of resource allocation in AM symbioses.

Overall, it appears that the extent of a tightly coupled C-for-nutrient exchange in AM symbioses (in particular one that resembles a 'reciprocal rewards' type of regulation) might decrease with increasing experimental system complexity. At the CMN scale, nutrient exchange is not always balanced, and one plant host might maintain the CMN while neighbouring plant hosts benefit from the fungal-mediated nutrient allocation without providing much in return. Strict regulation of C-for-nutrient exchange by both a plant host and its AM symbionts might be less evident under increased ecological complexity, as other drivers such as source-sink dynamics (Walder & van der Heijden, 2015) and a C-for-defence exchange (Frew et al., 2024) become increasingly important. Moreover, the ability of both plant hosts and AM fungi to govern the exchange of resources is likely also compromised by the variation of limiting factors across space and time (e.g., how does plant physiology change when the plant moves from P limitation to water limitation to a pest infection, and how do plant 'choices' to associate with certain AM fungi are made when many of these limiting factors co-occur?).

To improve the capacity of BMT to describe the C-for-nutrient exchange, 'service' provision (such as defence enhancement) should be incorporated alongside 'goods' provision (such as C or P acquisition). More research using varied biological systems across multiple scales is also needed to fully comprehend the role of CMNs in modulating the C-for-nutrient exchange and to test hypotheses quantitatively (e.g., using meta-analyses) while ensuring the inclusion of mechanisms or outcomes commonly overlooked by one plant × one fungus experiments. Techniques such as next-generation sequencing can be incorporated into C-for-nutrient experiments to increase the resolution of our results and test alternative hypotheses. Apart from increasing our fundamental understanding of how AM fungi might utilise CMNs, how they interact with other co-occurring organisms, and how this then influences the C-for-nutrient exchange, it is also vital that experimental designs include CMNs so we can better address the plethora of unresolved questions, including pertinent topics such as the role of CMNs in enhancing ecosystem functionality, and specifically their role in sustainable farming practices (Alaux et al., 2021; Wipf et al., 2019).

1.6 PROJECT OVERVIEW

The overall aim of this thesis is to understand how the presence of plant pests influences the functionality of mixed-species AM fungal networks connecting neighbouring potato (*Solanum tuberosum*) plants. I predominantly employ the potato cyst nematode (PCN) *Globodera pallida* as a below-ground pest, but in Chapter 4, I also introduce aphids (*Myzus persicae*) as a simultaneous above-ground pest. Across the thesis, the primary focus is on resource allocation, but I also explore PCN-induced changes in above-ground metabolites and volatile organic compounds (VOCs) as well as changes in the root and soil microbiome. This is imperative to understand the wider context that might be influencing any PCN-induced changes in the C-for-nutrient exchange between plants and the AM networks.

PCN (*Globodera pallida* and *G. rostochiensis)* are obligate biotrophic plant-parasitic nematodes (PPN) which invade host roots, inducing syncytial feeding structures that siphon C and essential nutrients from the plant, ultimately undermining both growth and yield (Price et al., 2021). Together with other PPN, they amount to more than US$80 billion annual market losses worldwide (Nicol et al., 2011), whereas in the United Kingdom, PCN infestation alone is responsible for losses of approximately £31 million (Price et al., 2021). PCN are responsible for around 9-10% of potato yield losses worldwide (Turner & Rowe, 2006; Kantor et al., 2022), although, in some cases, losses can be up to 70% (Turner and Subbotin, 2013). They are among the most serious and strictly regulated quarantine pests, partly due to the limited control methods that are commercially and environmentally viable (Whitehead and Turner, 1998).

After hatching, infective juveniles must locate a host root, penetrate the cell wall at a suitable site, and migrate towards the vascular cylinder, where a feeding site is initiated (Wyss, 2002). PCN rely on cues received from the environment and their potential host plants (e.g., semiochemicals that function as attractants, repellents, hatching stimulants or hatching inhibitors) to synchronise their life cycle with that of their potential host plant (Ochola et al., 2020; Rasmann et al., 2012; Kihika et al., 2017). There is evidence to show that plants can control the release of root metabolites (Sikder and Vestergård, 2020), including VOCs (Kihika et al., 2017) and root exudates (Ochola et al., 2020), in order to influence PPN behaviour. Information related to changes in above-ground VOCs in response to root herbivory is limited; however, it could be possible that, similar to herbivory of foliar tissue (Brosset and Blande,

2022), PCN induce changes in above-ground VOCs. Indeed, although no study has directly measured headspace VOCs after infection by PCN, the cyst nematode (*Heterodera glycines*) has been shown to alter foliar VOC emissions of soybean (*Glycine max*; Constantino et al., 2021) and the PPN *Xiphinema index* to alter the VOC emissions of grapevines (*Vitis vinifera* L.; Castorina et al., 2020).

Similar PCN-induced changes in VOCs could have important implications for plant–plant communication and the induction of defence responses in 'receiver' plants naïve to infection. Monitoring the effects of PCN infection on the VOC profiles of both infected plants and their uninfected neighbours is particularly valuable for assessing the role of the MN, as it can reveal the extent to which plant–plant communication occurs below-ground (via the MN) and above-ground (via headspace VOCs). Other than influencing plant-defence responses, evidence of either form of signalling could also represent a mechanism by which plants regulate C distribution within the MN. For example, if PCN-infected plants alter their metabolic profiles and these changes are transmitted to neighbouring plants, those neighbours may, in turn, adjust their own C allocation to the fungi.

The plant host responses to PCN invasion have long been a subject of discussion (Bleve-Zacheo and Melillo, 1997). However, there is no information on how PCN-induced changes to the host might influence the soil and root microbiome. However, this is also an important consideration when wanting to understand how PCN might influence the movement of P and C within a plant-mycorrhizal system, as PCN might indirectly influence C-for-P dynamics via changes in the microbiome. Overall, other PPN have been found to influence the microbiome either by increasing (e.g., Yeates et al. 1998; Denton et al., 1998) or decreasing species richness (Wurst et al., 2009; Zhou et al., 2019). Similarly, the community structure of both fungi and bacteria can be influenced by PPN (e.g., Kudjordjie et al., 2024).

Primary objectives and associated research questions:

Objective 1/Chapter 2: To track resource exchange in a system of two neighbouring plants potentially connected via one or more MNs and identify how infection with PCN influences the C-for-nutrient exchange.

- What is the role of the MN in modulating resource allocation and regulation within AM-plant symbiosis?

- Do AM fungi provide plants with similar amounts of P regardless of their PCN status, and how does the PCN status of their neighbouring plants affect this?
- Do PCN-infected plants, potentially linked to a common AM fungal network, continue to supply C to AM fungi?
- How does the PCN status of the plants influence the movement of plant-derived C within the system?

Main hypothesis: AM fungal networks will provide uninfected plant hosts with increased P provision because those hosts will be providing increased C provision in return.

Objective 2/Chapter 3: To explore whether, in addition to or in contrast to what is predicted from BMT, any impact of plant PCN infection on the movement of P and C within the system can be explained indirectly via PCN-associated changes in the soil and root microbiome.

- Does PCN infection influence the root and/or soil microbiome?
- If so, does the PCN infection status of the neighbouring plant also affect microbial communities?
- Ultimately, how might PCN-associated shifts in fungal and/or bacterial communities alter C-for-nutrient exchange between plants and AM fungi?
- Do results from ITS- and 18S-based sequencing of the AM fungal community lead to consistent conclusions regarding these effects?

Main hypothesis: PCN infection will shape the root microbiome. Specifically, PCN infection will lead to decreases (e.g., in richness and abundance) in AM fungi and AM-associated bacteria, but root pathogenic fungi will increase under PCN infection.

Objective 3/Chapter 4: To track plant-derived C in a system of three neighbouring plants connected via an MN and identify how infection with plant pests influences the movement of C in a compartmentalised *in vitro* microcosm.

- Do the results from soil-based mesocosms with multiple fungal and bacterial species agree with those of *in vitro* microcosms with limited microbial diversity?
- Does the MN distribute plant-derived C in a similar way when there is the option of two 'receiver' plants of contrasting plant pest-infection status in the same system rather than just one?

- Can the distribution of plant-derived C within a compartmentalised *in vitro* microcosm be visually assessed?

Main hypothesis: Plant-derived C will be preferentially distributed in parts of the MN surrounding pest-free hosts. This pattern will be more pronounced when the ^{14}C-labelled host is pest-infected.

Objective 4/Chapter 5: To collect above-ground leaf metabolites (non-volatile and volatile) to establish the extent to which these are influenced by PCN infection of the plant in question, as well as the infection of its neighbour.

- What in-leaf non-volatile metabolites and headspace VOCs might be influenced by PCN infection?
- To what extent do above-ground (e.g., VOCs) and below-ground (e.g., CMNs) pathways mediate defence signalling from PCN-infected plants to neighbouring uninfected plants?

Main hypothesis: Leaf metabolites, in particular ones related to defence, will be shaped by PCN infection. Below-ground signalling processes will result in this PCN impact also being manifested in neighbouring PCN-free plants.

Chapter 2. Plant-parasitic nematodes influence the movement of plant-fixed carbon and fungal-acquired nutrients through arbuscular mycorrhizal networks

2.1 ABSTRACT

Plants typically interact with multiple, co-occurring symbionts, including arbuscular mycorrhizal (AM) fungi, which can form networks, connecting neighbouring plants. A characteristic aspect of mycorrhizal symbioses is the bidirectional exchange of resources between host plants and fungal partners. Concurrent interactions with competing organisms, such as aphids or potato cyst nematodes (PCN), can disrupt the carbon-for-nutrient exchange between plants and AM fungi. However, the role of mycorrhizal networks (MNs) in mediating these interactions remains unclear. Using isotope tracing in multi-plant experimental systems, I investigated the movement of plant photosynthates and fungal-acquired soil phosphorus through MNs and the interactive effects of PCN infection on this. I found evidence of preferential allocation of fungal-acquired phosphorus to plants that were not infected by PCN compared with infected neighbours. Contrary to previous findings using single plants, I did not detect a PCN-induced reduction in the amounts of plant carbon delivered to AM fungi in multi-plant systems. However, the MN(s) moved plant-fixed carbon *away* from PCN-infected host plants, regardless of the PCN infection status of the neighbouring plant host. This work highlights the responsiveness of MNs to interactions with below-ground organisms. It also strengthens the argument for a more mycocentric view of AM–plant symbioses. Experimental designs of increasing ecological complexity are needed for a more comprehensive understanding of the carbon-for-nutrient dynamics in AM fungi–plant networks. This will, in turn, help to elucidate the role of AM fungi in terrestrial carbon cycling and their function in agricultural systems.

2.2 INTRODUCTION

The intimate associations formed between the roots (or rhizoids) of plants and symbiotic soil fungi, together known as mycorrhizas, evolved at the dawn of plant terrestrialisation >450 million years ago (Redecker et al., 2000). Today, mycorrhizal symbioses are formed by the vast majority of land plants across nearly all terrestrial ecosystems (Tedersoo and Brundrett, 2017). At least 72% of vascular plant species (Brundrett and Tedersoo, 2018), including many crops (Wang & Qiu, 2006), form mycorrhizal symbioses with arbuscular mycorrhizal (AM) fungi of the subphylum Glomeromycotina (Spatafora et al., 2016). AM fungal hyphae extend beyond the roots of host plants into the surrounding soil to form a complex web of extraradical mycelium, also known as a 'mycorrhizal network' (MN). These MNs can reach and colonise additional neighbouring plants, sometimes involving the fusion of separate fungal hyphae of the same species by anastomosis (de Novais et al., 2017; Giovannetti et al., 2004; Mikkelsen et al., 2008), forming what is then often referred to as a 'common mycorrhizal network' (CMN; Wipf et al., 2019).

Through their MNs, AM fungi supply up to 80% of phosphorus (P; Bago & Bécard, 2002) and ~30% of nitrogen (N; Govindarajulu et al., 2005) of their host plants' requirements alongside other micronutrients (Hamilton & Smith, 2000; Lehmann et al., 2014), offering a vital ecosystem service to plant communities. AM fungi are obligate biotrophs, unable to produce and exude the necessary degradative enzymes for the decomposition of complex soil organic materials (Tisserant et al., 2012, 2013), relying entirely on their plant hosts for their carbon (C) nutrition (Bago & Bécard, 2002). Up to 30% of a plant host's photosynthetically fixed C can be allocated to AM fungi (Drigo et al., 2010). As such, together with other types of mycorrhizal fungi, AM fungi are important regulators of global C dynamics (Averill et al., 2014; van der Heijden et al., 2015; Wurzburger et al., 2017). According to recent estimates, plants allocate 13.12 Gt of CO_2e to mycorrhizal fungi globally, an amount equivalent to around 36% of current annual CO_2 emissions from fossil fuels (Hawkins et al., 2023).

The evolutionary drivers and mechanisms that underpin bidirectional nutrient exchange between AM fungi and their host plants are often discussed using Biological Markets Theory (BMT; e.g., Noë & Kiers, 2018; Werner et al., 2014; Werner & Kiers, 2015; Wyatt et al., 2014). According to one version of this, plant C is preferentially allocated to AM fungal partners that offer the most 'generous' supply of fungal-acquired nutrients (Kiers et al., 2011). In return, it

is hypothesised that AM fungi also discriminate between alternative partners, 'rewarding' more 'generous' hosts by supplying them with more nutrients (Bücking & Shachar-Hill, 2005; Fellbaum et al., 2012; Kiers et al., 2011). However, the regulation and control of mycorrhizal resource exchange remain a topic of hot debate, with source–sink regulation presented as an alternative or complementary mechanism (Kiers et al., 2016; van der Heijden & Walder, 2016; Walder & van der Heijden, 2015; Corrêa et al., 2023; Bunn et al., 2024). An important, yet often overlooked, factor in mycorrhizal resource exchange is that plants rarely interact only with mutualistic symbionts (Chapter 1; Magkourilou et al., 2024). Instead, they exist as part of complex, multi-kingdom ecosystems, interacting with a myriad of co-occurring organisms and with neighbouring plants usually interconnected underground by one or more MNs. When these complex symbiotic scenarios are considered, the evidence suggests that co-occurring, competing organisms such as aphids (Charters et al., 2020) and plant-parasitic nematodes (Bell et al., 2022) drive asymmetry in C-for-nutrient exchange, where infected plants reduce the allocation of C to their AM fungal symbionts, but nutrient supplies from AM fungi to plants are maintained. However, these studies still do not reflect ecologically relevant scenarios in which the regulation of plant C and soil nutrient flows is modulated across multiple hosts of various infection statuses by CMNs (Bell et al., 2021).

Experiments assessing the impacts of changing C source–sink strengths across a CMN, either by shading (Fellbaum et al., 2012; Weremijewicz et al., 2016) or by altering nutrient gradients *in vitro* (Lekberg et al., 2010; van't Padje et al., 2021; Whiteside et al., 2019) suggest that CMN can modulate resource regulation. Moreover, results from experiments employing multitrophic interactions (e.g., Alaux et al., 2020; Babikova et al., 2013; Durant et al., 2023; Song et al., 2014) point to the responsiveness and resilience of CMNs and their ability to potentially ameliorate some plant stresses. Despite these advances in understanding nutrient dynamics in plant–AM fungal networks, the relative C contribution of each plant partner into the MN(s) remains unclear. An important consideration should be the spatial distribution and movement of C by AM fungal hyphae through the soil. An aspect of the responsiveness of MNs is likely their ability to move resources away from 'poor' hosts, increasing AM hyphal proliferation and subsequent exploration of the soil profile; potentially in search of alternative, more 'generous' hosts.

Aims

To address these important knowledge gaps, I investigated the movement of fungal-acquired P from the soil and plant-fixed C across MNs formed between two neighbouring plants. I specifically manipulated the resource dynamics of the symbioses using the potato cyst nematode (PCN), a common pest that feeds on potato roots and is responsible for 9% of yield losses worldwide (Turner & Rowe, 2006). I tested the hypothesis that AM fungi provide more P to host plants not infected with PCN because uninfected plants would provide the MN with more photosynthetically fixed C (Kiers et al., 2011; Werner & Kiers, 2015).

2.3 MATERIALS AND METHODS

2.3.1 Mesocosm design and plant growth

Plants were grown in mesocosms (37 cm length × 26 cm width × 22 cm height) that were divided into two equal compartments by a 35 µm pore nylon mesh barrier (no air gap) affixed centrally using hot glue. This mesh excluded plant roots but allowed mycorrhizal hyphae to cross (Johnson et al., 2001). A single, non-sterile tuber from *Solanum tuberosum* cv. Désirée (Denholm Seed Potatoes, UK) was planted in the middle of each compartment within each mesocosm, containing a total of ~10 kg of non-sterile coarse sand: topsoil (50:50) mix (sand acquired from RHS Enterprise Ltd., UK for coarse sand and topsoil from East Riding Horticulture Ltd., UK). The distance between the two plant stems was ~18 cm.

Both compartments of all mesocosms received 100 g of a commercially available mixed species mycorrhizal fungal inoculum (*Funneliformis mosseae*, *Funneliformis geosporus*, *Claroideoglomus clarodeum*, *Rhizophagus intraradices*, *Glomus aggregatum*, *Diversispora* spp. and *Scleroderma citrinum*; PlantWorks Limited, UK). Three treatment combinations were established based on the presence or absence of the PCN *Globodera pallida* (population Lindley) in each compartment of the mesocosms (Figure 2.1). The PCN-containing compartments were established by mixing in stock soil of known PCN density to achieve a final density of ~10 eggs per gram of substrate. These relatively low levels of infection reflected the conditions of most infected fields in England (Minnis et al., 2002) and ensured that plants would not be severely damaged by PCN. Mesocosms were established in a randomised block layout, in the same controlled environment glasshouse (16°C night–18°C day, 16 h day length, 60% humidity) and grown for a total of 7 weeks. Plants

were watered with tap water three times a week, taking care not to flush too much water down the ^{33}P-labelled cores which had been inserted in the middle (see details below).

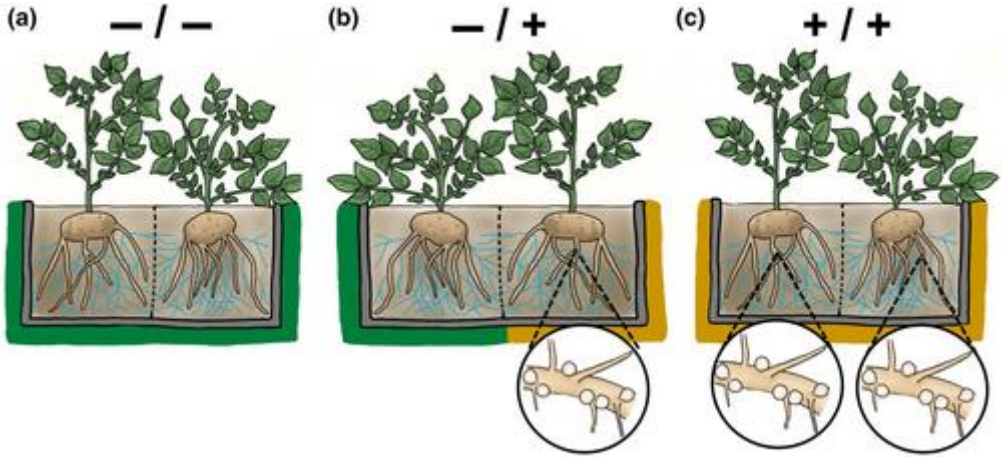

Figure 2.1 Treatment combinations were used to test the effect of potato cyst nematodes (PCN; illustrated by the beige shapes on the magnified portions of the roots) on the carbon-for-phosphorus exchange between plants and arbuscular mycorrhizal fungi. All plants were connected by one or more mycorrhizal networks (illustrated by the blue lines) across a root-excluding 35 µm pore mesh. Plants without PCN are indicated by '–' and green borders, whereas plants with PCN are indicated by '+' and orange borders. Three treatment combinations were deployed: **(a)** –/–; **(b)** –/+; **(c)** +/+.

2.3.2 Tracing fungus-to-plant ^{33}P transfer

Mesocosms (*n* = 12 per treatment combination shown in Figure 2.1) were established in three identical blocks across subsequent weeks. Two soil-filled PVC cores (18 mm diameter × 130 mm length; Barkston Ltd., UK) with 35 µm pore nylon mesh-lined windows (70 mm × 16 mm) affixed using Tensol 12 acrylic adhesive (Bostik Ltd., Stafford, UK) were positioned in the middle of each mesocosm (Figure S2.1). A 1 mm diameter silicone capillary tube (Smiths Medical Ltd., Ashford, UK), perforated every 0.5 cm using a mounted needle, was also fixed centrally in each core to allow for the distribution of ^{33}P through one core in each mesocosm, with water added to the control cores. Specifically, 5 weeks after planting, 150 µL of ^{33}P-orthophosphate (1.5 MBq; [^{33}P]-orthophosphate; Hartmann Analytic, Braunschweig, Germany) was supplied to one of the two cores in each mesocosm via the capillary tube. In half of the mesocosms per treatment combination (*n* = 6; Figure 2.1), the ^{33}P-labelled cores were rotated every other day to sever hyphal connections between the core

and plant roots (Figure 2.2). The non-labelled cores in these pots remained static to preserve the hyphal links between the core contents and the plant roots. In the remaining pots (n = 6 per treatment combination), ^{33}P-labelled cores remained static with non-labelled cores rotated (Figure 2.2). This allows fungal-acquired ^{33}P transfer to plants to be estimated by excluding the transfer of ^{33}P via alternative means, such as by diffusion or alternative microbial nutrient cycling processes (see below for more details; Johnson et al., 2001). The experiment was harvested 2 weeks following the application of ^{33}P (Figure S2.2A).

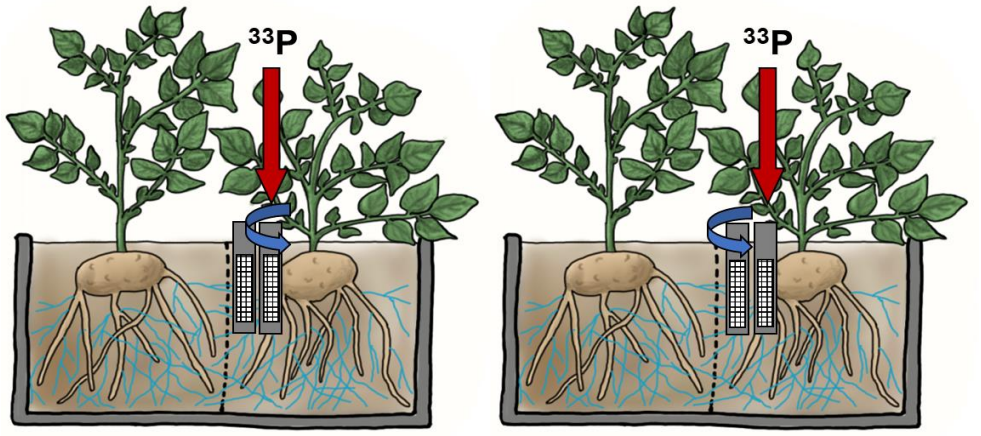

Figure 2.2 The experimental design used to test the effect of potato-cyst nematodes (PCN) on the transfer of fungal-acquired ^{33}P to pairs of potato plants. The treatment where neither plant had PCN is used as an example. Plants were connected by one or more mycorrhizal networks (illustrated by the blue lines) across a root-excluding 35 µm pore mesh. Two root-excluding mesh cores were inserted randomly at either side of the mesh. In half of the mesocosms, the labelled cores were rotated every other day to sever the hyphal connection between the core and plant roots (left-hand side example). The non-labelled cores in these pots were kept static to preserve the hyphal links. In the remaining half of the pots, the opposite was applied; ^{33}P-labelled cores were kept static, to preserve hyphal connections, and the non-labelled cores were rotated (right-hand side example).

2.3.3 Tracing plant-to-fungus C transfer

Mesocosms (n = 6 for each shown in Figure S2.2) were established in two identical blocks across subsequent weeks. Seven weeks after planting (Figure S2.1B), the above-ground tissue of all plants was enclosed within polythene bags (Polybags Ltd., London, UK), sealed airtight

using anhydrous lanolin and cable ties at the base of the plant stem. One plant per mesocosm was labelled with $^{14}CO_2$, with plants for labelling selected randomly where appropriate (Figure S2.3). At the beginning of the photoperiod, one of the two soil-filled, meshed-walled cores on each side of the mesh barrier separating the plants was rotated to sever the hyphal connection between the core and plant roots (Figure S2.2). $^{14}CO_2$ was liberated into the chamber by adding 2 mL 10% lactic acid to a cuvette containing 190 µL ^{14}C-sodium bicarbonate (specific activity: 1.62 GBq mmol^{-1}; total activity released: 1 MBq; Perkin Elmer, USA). Plants were left in situ for 24 h post-labelling (Figure S2.2b), at which point 2 mL of 2 M KOH was added to vials within each labelled chamber to capture any remaining gaseous $^{14}CO_2$. At the end of the experiment, soil sub-samples from within the cores were used to estimate the amount of recently-fixed plant C provided to the fungus (i.e., fungal C; see below for more details).

2.3.4 Preparation and harvest of plants and soils

The week of harvest, using leaves of similar size, the photochemical activity of photosystem II characterised by FvP/FmP and the relative chlorophyll content (SPAD; Photosynthesis RIDES protocol, MultispeQ 2.0, PhotosynQ; Kuhlgert et al., 2016) was recorded in a subset of plants as a functional indicator of plant photosynthetic efficiency and plant stress (Cessna et al., 2010). Two weeks after the introduction of ^{33}P tracer or 24 h after the release of $^{14}CO_2$, soil and plant material were separated into shoots, roots, and tubers, as well as the soil from each compartment and the soil from within each core. Roots were cleaned with tap water and sub-samples (~5–10 g) of a subset of plants were taken and stored in 50% ethanol (v/v) at 4°C for AM colonisation counts. All of the soil in each compartment was weighed fresh and the measurements were used to extrapolate the hyphal counts to the equivalent compartments. All other components (i.e., the above-ground portion of plants, tubers, remaining roots, and soil from within the cores) were stored at −20°C until they were freeze-dried (CoolSafe 55-4; LaboGene, Allerød, Denmark) and dry mass of each was recorded. All freeze-dried plant materials were then homogenised using a hand-blender and stored at room temperature until subsequent analysis.

2.3.5 Quantification of fungal-acquired ^{33}P and total P in plant shoots

To quantify ^{33}P in plant shoots, ~100–200 mg of the homogenised freeze-dried samples were processed as per Cameron et al. (2007). Briefly, samples were digested in duplicate in 2 mL

concentrated sulphuric acid (H_2SO_4) at 365°C for 15 min (Grant BT5D; Grant Instruments Ltd., St Ives, UK), cleared in hydrogen peroxide (H_2O_2; 300–600 µL), diluted to 10 mL with distilled water (dH_2O) and then a 2 mL sub-sample was added to 10 mL of the liquid scintillant (Emulsify-safe; PerkinElmer). Sample radioactivity was quantified through liquid scintillation counting (Tri-Carb 3100TR; PerkinElmer) and ^{33}P quantified using previously published equations (Cameron et al., 2007). ^{33}P budgets were calculated using established equations (see Durant et al., 2023 for detailed equations as adapted from Cameron et al., 2007). For each of the three experimental blocks, the mean ^{33}P content of plants with no direct hyphal access to the isotopes ('rotated' core pots) was subtracted from the individual measured ^{33}P content of each plant with hyphal access to the isotopes ('static' core pots). This accounts for the movement of isotopes out of the cores by diffusion or alternative microbial nutrient cycling processes. The total P content (i.e., plant and fungal-acquired) of plant shoot material from a subset of plants was also determined using an adapted method of Murphy and Riley (1962). Sample optical density was recorded at 822 nm using a spectrophotometer (Jenway 6300, Staffordshire, UK). A 10 mg/mL standard P solution was used to produce a standard curve against which total sample P was calculated.

2.3.6 Quantification of host-fixed C in fungi

About 100–250 mg of freeze-dried soil from within each core was weighed in duplicate into Combusto-cones (PerkinElmer, Beaconsfield, UK). ^{14}C was measured following sample oxidation (Model 307 Packard Sample Oxidiser; Isotech, Chesterfield, UK) with released $^{14}CO_2$ from burnt soil samples trapped in 10 mL of the liquid scintillant CarbonTrap and mixed with 10 mL CarbonCount (Meridian Biotechnologies Ltd., Tadworth, UK). Radioactivity was quantified by liquid scintillation counting (Packard Tri-Carb 4910TR; PerkinElmer). The total C (i.e., $^{12}CO_2$ and $^{14}CO_2$) contained in each soil sub-sample was calculated by quantifying the total CO_2 volume and content mass in the labelling chamber and the proportion of the supplied $^{14}CO_2$ that was photosynthetically fixed by the plant during the 24 h labelling period (see Durant et al., 2023 for detailed equations as adapted from Cameron et al., 2008).

To account for the movement of ^{14}C via diffusion and to estimate the amount of plant-fixed C transferred from the ^{14}C-labelled plants to the MN (i.e., fungal C), the rotated core C values (i.e., soil and severed hyphae) were subtracted from the static core (i.e., soil and intact

hyphae) for each mesocosm compartment. These values were then extrapolated to the entire compartment and expressed relative to the soil hyphal density measurements for each compartment. To calculate the percentage (%) of fungal C that moved from the ^{14}C-labelled plant compartment to the unlabelled plant compartment of the same mesocosm, the following equation was used:

$$\% \text{ of fungal C that moved} = \frac{\text{fungal C in the compartment of the unlabelled plant}}{\text{(fungal C in the compartment of the of the unlabelled plant + fungal C in the compartment of the } ^{14}C\text{-labelled plant)}} \times 100$$

2.3.7 Fungal colonisation of roots and soil

Root samples that had been stored for colonisation assessment were stained using the 'ink and vinegar' staining method (Vierheilig et al., 1998) at 70°C for 20 min. Roots were de-stained in 1% acetic acid at room temperature and mounted on microscope slides using polyvinyl lacto-glycerol (16.6 g polyvinyl alcohol powder, 10 mL glycerol, 100 mL lactic acid, 100 mL dH2O). Assessment of percentage root length colonisation (including intraradical hyphae, arbuscules, and vesicles) was made using the magnified intersection methodology (around 150 intersects per mesocosm, 100× magnification; McGonigle et al., 1990).

Fungal hyphae were extracted from soil from each of the two compartments of the mesocosms used for ^{33}P tracing and from within the static cores of each compartment for the mesocosms used for ^{14}C labelling. 4.5–5 g of dried soil sub-samples were first suspended in 500 mL H_2O. A 10 mL aliquot was filtered through a cellulose nitrate membrane filter (47 mm diameter, 0.45 µm pore size; CYTIVA, Whatman™, Germany) and stained with a few drops of ink and vinegar solution (Vierheilig et al., 1998). Filter papers were halved and mounted on microscope slides using polyvinyl lacto-glycerol and oven-dried at 65°C for an hour. Hyphal lengths (excluding only a few unstained, thick, and highly septate hyphae) per mesocosm were calculated using the gridline-intersection methodology (50 fields of view per half filter paper, 100× magnification; Tennant, 1975).

2.3.8 PCN infection

Upon harvest, PCN cysts were removed from the roots by vigorously shaking the roots. The cysts were then extracted from a sub-sample of soil (minimum 250 g) from each mesocosm compartment used for ^{33}P tracing using Fenwick's (1940) method. Briefly, soil was washed through a 1 mm mesh into the Fenwick can (i.e., a metal can with a sloped base at the top and a sloping collar below the rim). Heavy soil particles sink to the bottom of the water-filled can, whereas cysts and light soil debris float to the surface and are siphoned over the rim into a 250 mm sieve. The contents of the sieve were then washed through a filter paper, which was in turn examined under a dissecting microscope for the collected cysts to be counted and PCN infection to be expressed as cysts per gram of soil.

2.3.9 Statistical analysis

All statistical analyses and figure construction were performed in RStudio (RStudio Team, 2025) using the R programming language (R Core Team, 2023). For the ^{33}P tracing experiment, one or both plants did not grow sufficiently in two mesocosms, so these were removed from all analyses. For all comparisons, linear mixed-effects models were performed, including a block effect (i.e., week of planting) and the PCN infection treatment of a plant and/or the PCN infection treatment of its neighbouring plant as fixed effects. A random intercept for the mesocosm was included to account for non-independence among pairs of plants from the same mesocosm. After visual evaluation of the data for the fungal-acquired ^{33}P concentration in the shoots, a further mixed-effects model with the same parameters as explained above was performed on the mixed treatment combination (i.e., 'PCN−/PCN+'). The significance of all model parameters was assessed using the *anova* function in R and the `lmerTest` package (Kuznetsova et al., 2017). Assumptions for the use of general linear models were validated by plotting residuals versus fitted values, square root residuals versus fitted values, normal qq plot, and constant leverage using the *autoplot* function of the `ggplot2` package (Wickham, 2014). The data for soil hyphal counts did not satisfy assumptions so these were ($\log_{10} + 1$) transformed. Data for the percentage of fungal C that moved across the mesocosm showed an unequal variance, so a Welch two-sample *t*-test was performed to assess the effect of the PCN infection on the ^{14}C-labelled plant.

2.4 RESULTS

2.4.1 Impact of PCN infection on AM fungi and plant growth

The soil PCN population did not differ across PCN treatment combinations (Figure 2.3). AM fungal measures, including total root colonisation (Figure 2.4A), arbuscular and vesicular colonisation (Figure S2.3A and B), and soil hyphal length density (Figure 2.4B), were also unaffected by PCN infection of plants or that of their neighbours (Table S2.1). Similarly, shoot dry biomass (Figure S2.4A), FvP/FmP (Figure S2.5A), and SPAD (Figure S2.5B) showed no significant effects of PCN infection in either plants or their neighbours (Table S2.1).

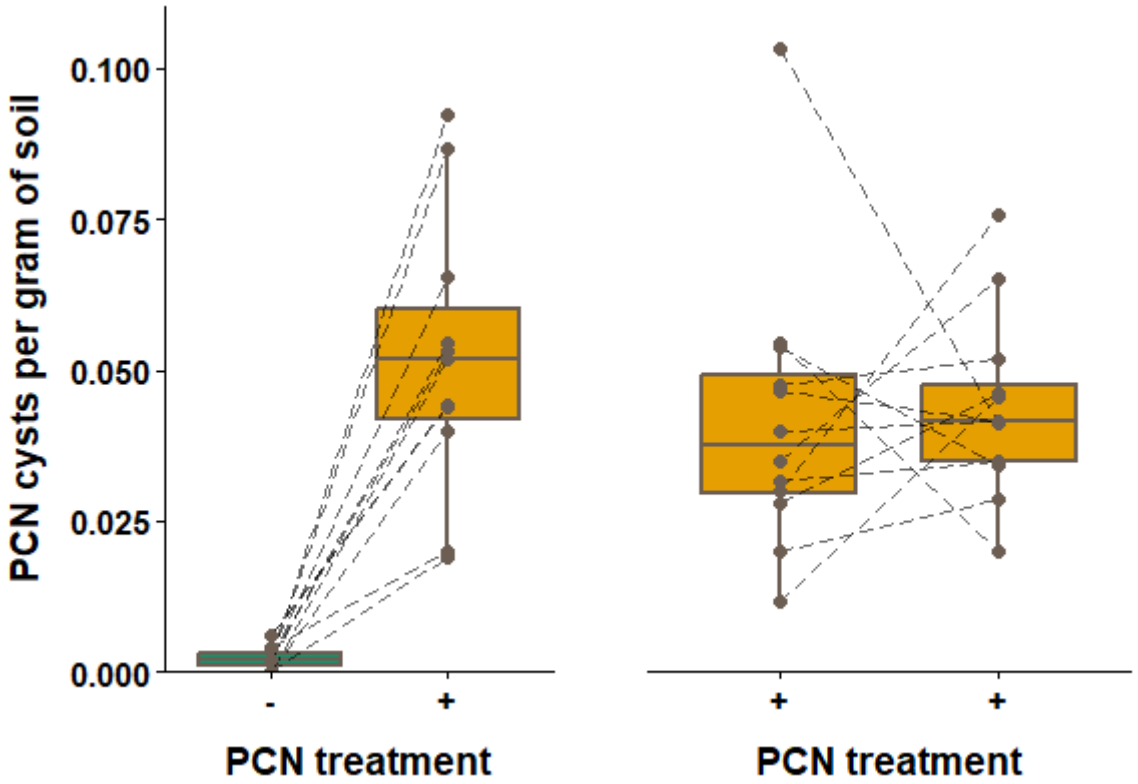

Figure 2.3 Soil PCN population at the end of the experiments expressed as the number of cysts per gram of soil. Dashed lines connect paired samples across each side of the same container. The centre line of the boxplot denotes the median, the box the interquartile range and the whiskers show no more than 1.5 times the distance between the 25th and 75th percentile. Data were extracted from pots used for ^{33}P tracing. Treatments without PCN are indicated by '–' and green bars, whereas treatments with PCN are indicated by '+' and orange bars.

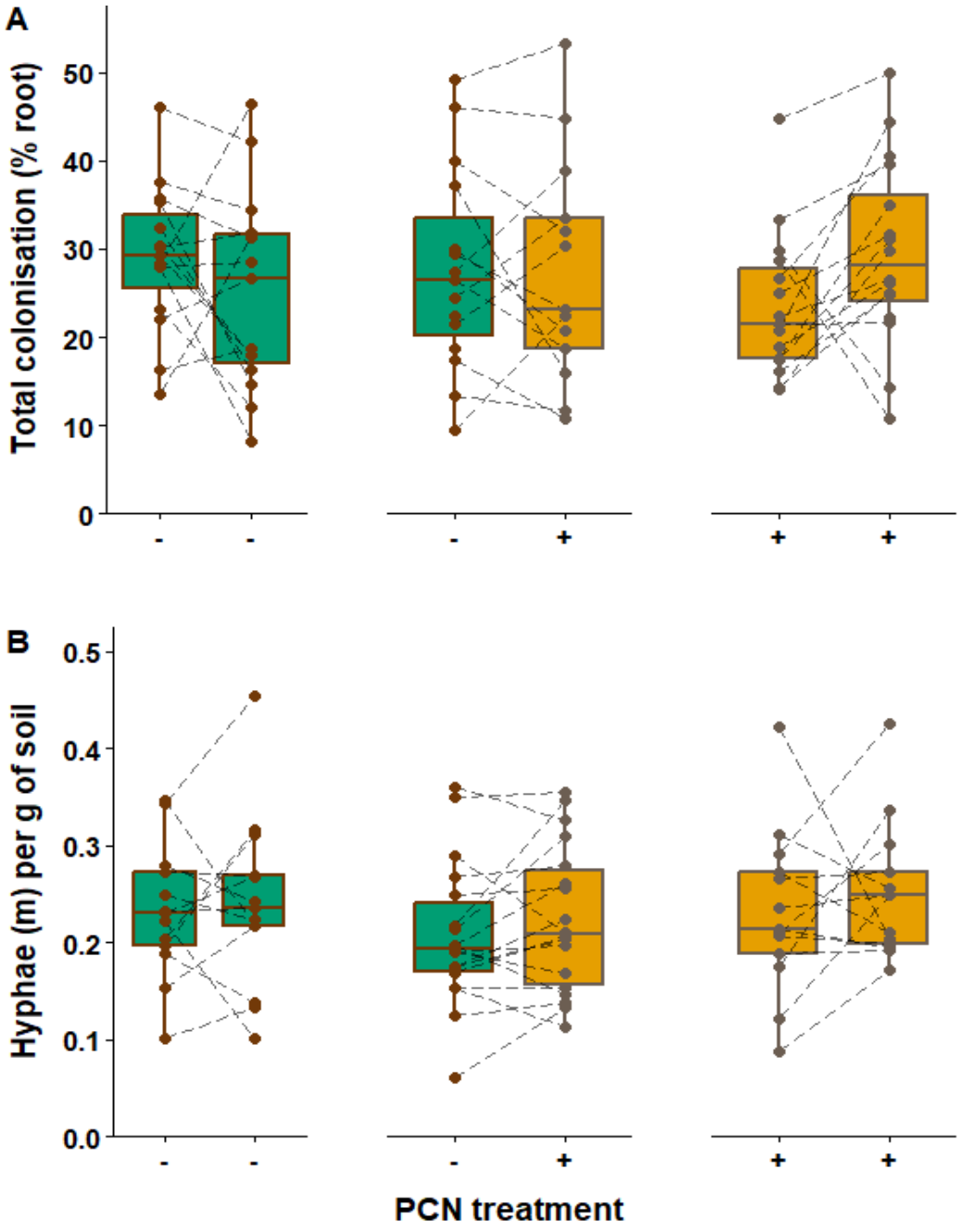

Figure 2.4 A. Percentage total root colonisation, **B.** Hyphal lengths expressed as metres in a gram of soil (log_{10}+1 transformed), for each PCN treatment. Dashed lines connect paired samples across each side of the same container. The centre line of the boxplot denotes the median, the box the interquartile range and the whiskers show no more than 1.5 times the distance between the 25th and 75th percentile. Data were extracted from a subset of mesocosms across both experiments. Treatments without PCN added to soil are indicated by '–' and green bars, whereas treatments with PCN are indicated by '+' and orange bars.

2.4.2 Total P in plant shoots and AM fungal-acquired ^{33}P

The total concentration of P (plant and AM fungal-acquired; Figure S2.6) in plant shoots did not differ overall based on the PCN infection of the plants ($F = 0.14$, $p = 0.71$) nor the PCN infection of their neighbours ($F = 1.82$, $p = 0.19$). The concentration of fungal-acquired ^{33}P in the shoots (Figure 2.5) was also not overall influenced by either the presence of PCN on the plants ($F = 0.03$, $p = 0.86$) or the presence of the PCN on their neighbours ($F = 0.32$, $p = 0.57$). However, within the same mesocosms, when an uninfected plant was grown next to a PCN-infected plant (i.e., '−/+'), the uninfected plants consistently acquired more fungal ^{33}P in the shoots relative to their PCN-infected neighbours ($F = 8.38$, $p = 0.03$; Figure 2.5).

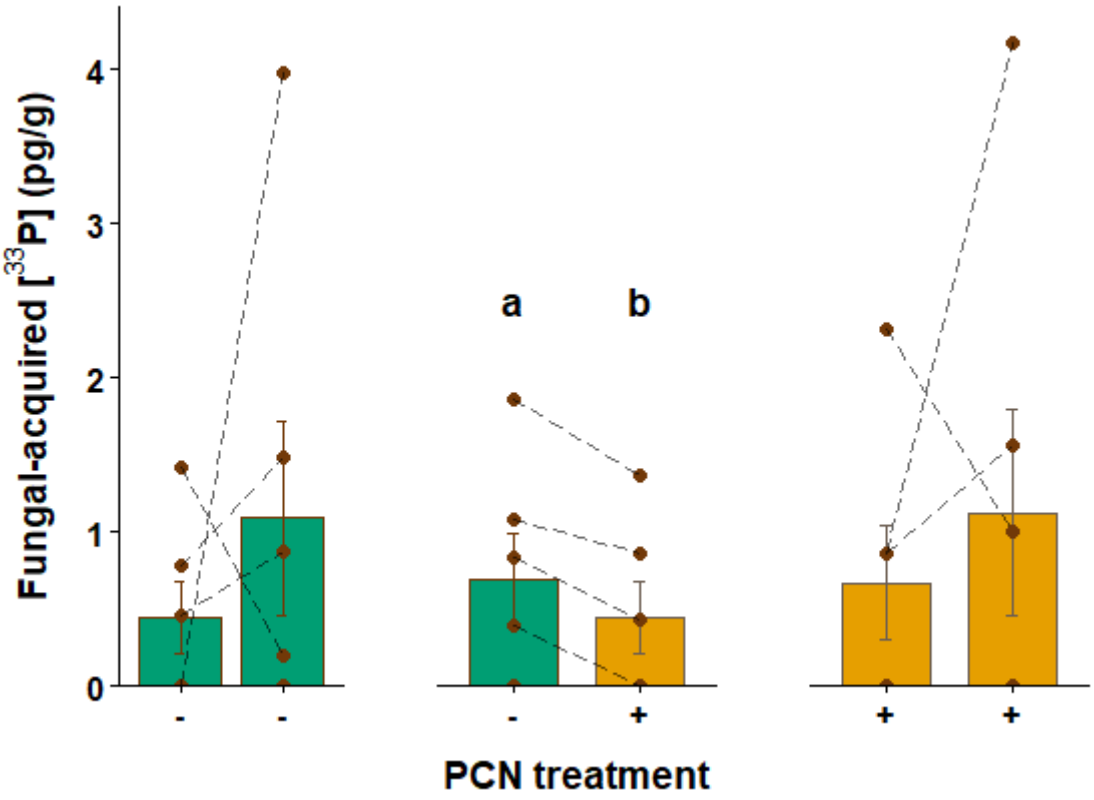

Figure 2.5 Concentration of AM fungal-acquired ^{33}P in plant shoots for each PCN treatment. Dashed lines connect paired samples across each side of the same container. Letters above barplots indicate paired plants within the same mesocosm when significant effects were observed ($p < 0.05$; Linear Mixed-Effects Model). Barplots denote mean ± SE. Plants without PCN are indicated by '−' and green bars, plants with PCN are indicated by '+' and orange bars.

2.4.3 Plant-fixed C transfer to AM fungal networks

The total recently-fixed plant-derived C in extraradical hyphae (i.e., fungal C) across the whole mesocosm (Figure 2.6) did not significantly differ based on the PCN infection of the ^{14}C-labelled plant ($F = 1.30$, $p = 0.27$) nor the infection of the neighbouring plant ($F = 0.68$, $p = 0.42$).

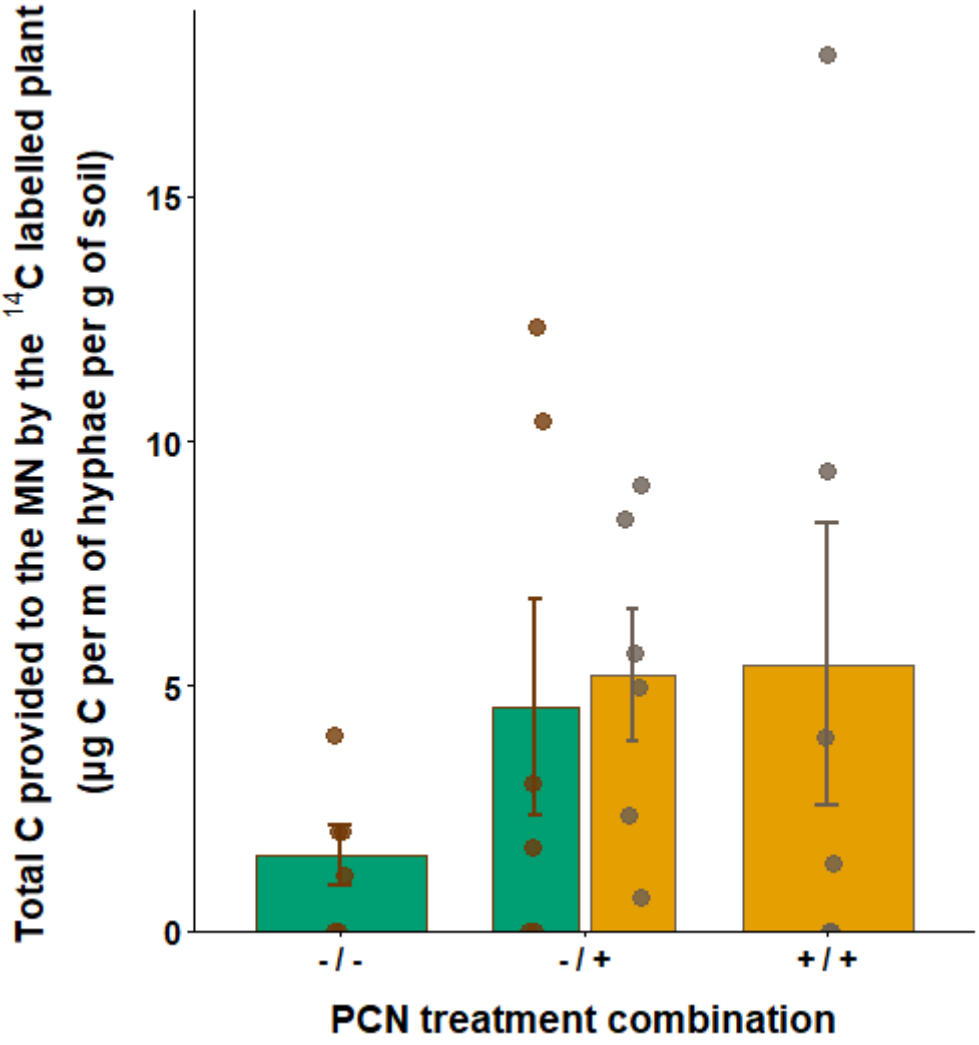

Figure 2.6 The total amount of recently-fixed plant-derived C detected in the mycorrhizal network (MN; µg C per metre of hyphae per gram of dry soil) across both compartments of the mesocosm based on the PCN treatment combination. Barplots denote mean ± SE. Treatments without PCN are indicated by '–' and green bars, treatments with PCN are indicated by '+' and orange bars.

However, the percentage of fungal C that moved across the mesocosms (i.e., from the ^{14}C-labelled to the unlabelled compartment; Figure 2.7) was significantly influenced by the PCN infection of the ^{14}C-labelled plant ($t = 2.74$, $p = 0.02$), with more C moving away from infected plants (i.e., 46% or 38% depending on whether the plant on the other side was also infected or uninfected) than from uninfected plants (0% or 6% depending on whether the plant on the other side was also uninfected or PCN-infected).

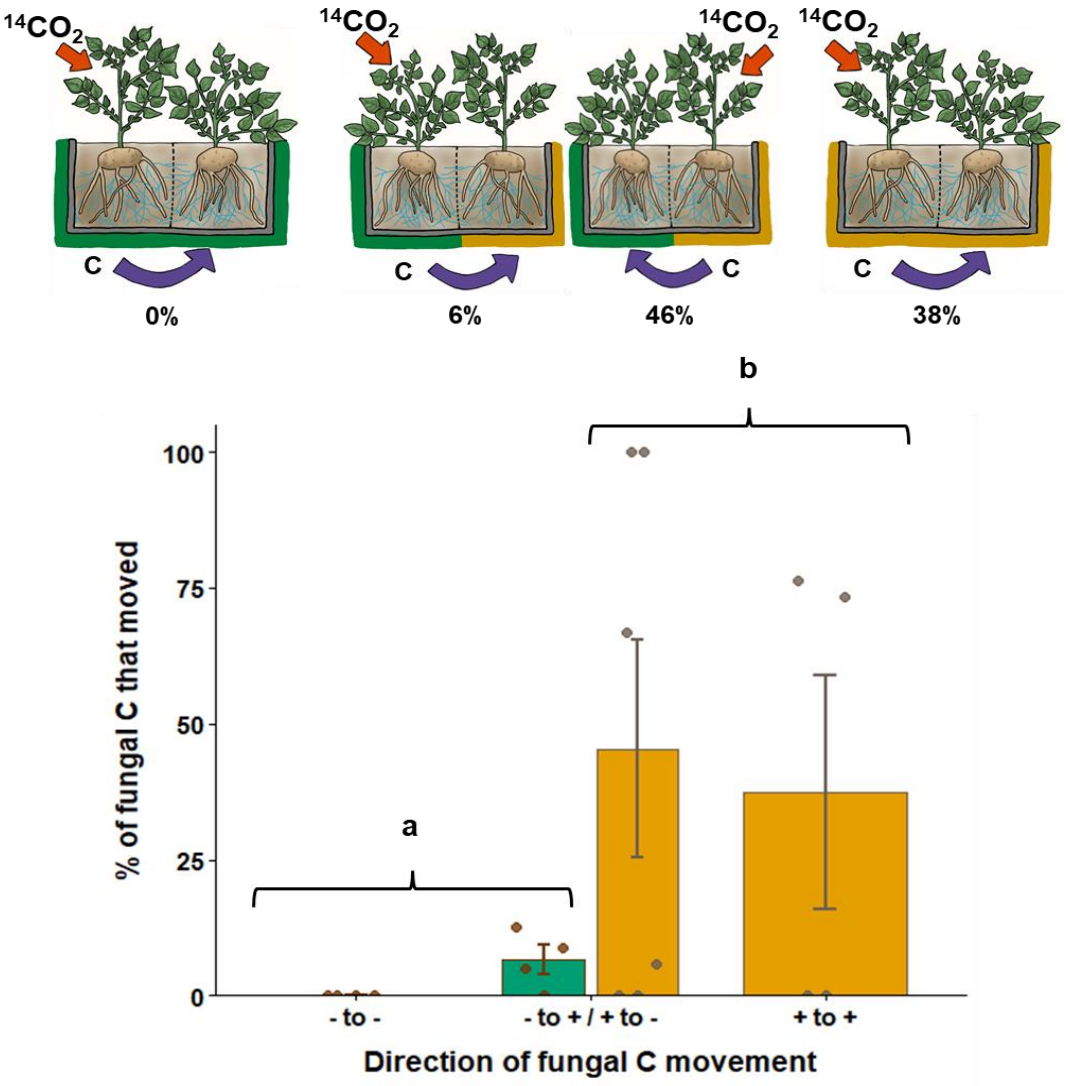

Figure 2.7 Percentage of fungal C (amount per metre of hyphae in a gram of dry soil) that moved from the ^{14}C-labelled compartment to the unlabelled compartment of the mesocosm according to the PCN treatment of both plants. Numbers underneath the visual schematics represent means. Brackets indicate the significantly different groups ($p < 0.05$). Barplots denote mean ± SE. Treatments without PCN are indicated by '–' and the green colour, treatments with PCN are indicated by '+' and the orange colour.

2.5 DISCUSSION

Despite the near ubiquity of plant symbioses with AM fungi, their function in complex, ecologically relevant scenarios is not often addressed experimentally. We do know that interacting or interconnected MNs can modulate resource allocation below-ground (Durant et al., 2023; Mikkelsen et al., 2008) and facilitate the transmission of defence signals between neighbouring plants (Alaux et al., 2020; Babikova et al., 2013, 2013a; Barto et al., 2012; Song et al., 2010, 2014, 2015, 2019). In this way, MNs influence wider ecological processes and dynamics, including plant competition and subsequent community structure and function (Tedersoo et al., 2020) as well as global C cycling (Hawkins et al., 2023). However, the function and responsiveness of MNs to biotic perturbation, such as that caused by a disruption of the C supply by pests or pathogens, which is common in natural ecosystems, remains largely unexplored. Here, using a dual tracer approach, I determined the allocation of P from the MN to plant hosts of contrasting PCN infection, as well as the relative contribution of C made by the two neighbouring plants and the movement of C through the MN.

Despite relatively low levels of PCN infection (Minnis et al., 2002) and no obvious PCN-induced physiological impact on the plants (Figures S2.4 and S2.5; Table S2.1), AM fungi in my experiments transferred more ^{33}P to uninfected plants compared with PCN-infected plant neighbours ('−/+'; Figure 2.5). However, in line with previous experiments using single plants (Bell et al., 2022), fungal-acquired P transfer to PCN-infected hosts was overall maintained, regardless of PCN treatment (Figure 2.5). Together, these findings suggest a degree of preference in the allocation of fungal-acquired resources towards non-infected plants, but only when the MN is linked to plant hosts of contrasting parasitism. However, this effect does not appear to be universal across plant and pest species, as another experiment that also used paired plants with interconnected or interacting MNs detected no differences (between or within treatments) in fungal-acquired P between aphid-infested and uninfested plants (Durant et al., 2023).

Although there were differences in the levels of fungal-acquired ^{33}P in shoots within the '−/+' PCN treatment combination (Figure 2.5), this was not matched by a PCN-induced difference in the total amount of C each plant contributed to the MN (Figure 2.6). Contrary to a previous experiment using single plants, where plant C provision to AM fungi decreased in the presence of PCN (Bell et al., 2022), a similar level of PCN infection in my experiment did not impact the

overall amount of plant C delivered to the MN. This difference may be driven by plant–plant interactions modifying the amounts of plant resources invested below-ground (Weiner & Thomas, 1992). CMNs can increase competition between plants (Merrild et al., 2013; Weremijewicz et al., 2016), and host plants connected to the same CMN, or even interacting MNs, may partially adjust C resource allocation below-ground according to each other's C provision (Wyatt et al., 2014). For example, in my '−/+' treatment combination, uninfected plants could have reduced their C allocation to the MN to mimic that of their infected neighbours. It is also worth noting that although we do not know the exact effect of the temporary pulse of $^{14}CO_2$ on the labelled plants, these results suggest that PCN-infected and uninfected plants reacted similarly in terms of total C provision below-ground.

The movement of P from 'rich' to 'poor' patches has been observed in *in vitro* experiments using AM root organ cultures (Whiteside et al., 2019). However, Whiteside et al. (2019) did not resolve how the AM fungus itself might redistribute C across the network. My experimental design allowed me to explore this in soil, where I detected below-ground movement of plant-fixed C resources *away* from plants infected with PCN (Figure 2.7). The movement of plant-derived C resources could have promoted AM fungal mycelium expansion and soil exploration, away from the 'drain' on plant C caused by PCN. However, this greater accumulation of plant C did not translate into increased fungal hyphal density in the soil (Figure 2.2B). This is somewhat surprising, as absorptive AM hyphal networks are typically ephemeral and highly responsive, with hyphae disintegrating 5–7 days after formation (Friese & Allen, 1991; Staddon et al., 2003), so differences might have been expected to manifest within the timescale of my experiments.

Another important consideration is that host plants may regulate not only the amount but also the form of C supplied to AM fungi. In split-root experiments, transcriptomic analyses showed that expression of mycorrhizal-induced hexose transporters is reduced when plants are co-infected with above- or below-ground parasites (Bell et al., 2024). Nevertheless, C transfer to AM fungi was maintained through sustained fatty acid biosynthesis and transport (Bell et al., 2024). These C sources have different fates in the fungus: hexoses are rapidly metabolised to support immediate hyphal growth, whereas fatty acids are preferentially stored in fungal structures (Salmeron-Santiago et al., 2022). If a similar mechanism operated in my system, AM fungi associated with PCN-infected roots may have received proportionally

more C as fatty acids. This C would be channelled into storage rather than supporting active hyphal growth, potentially explaining the absence of an increase in hyphal density. A further consideration is methodological: fatty acids may be underrepresented in the ^{14}C pool recovered after a 24 h labelling experiment, meaning that the apparent redistribution of C away from infected hosts could be an underestimate.

In any case, in my experiment, the capacity of the MN to detect parasitism of host plants and move C according to the C source–sink strength seems to be limited spatially. Specifically, although I detected an overall movement of C away from PCN-infected hosts, there was no clear indication that this movement was more pronounced when the plant in the other compartment was uninfected (+ to −) rather than infected (+ to +; Figure 2.7). Therefore, it appears that extraradical AM fungal hyphae may be able to 'perceive' parasitism of their proximal plant host and move C away if that host is infected, but the direction of C movement thereafter appears to be 'blind' to infection of the more distal plant host. Similarly to what has been suggested for plants (Veresoglou et al., 2022), AM fungi may thus be 'hedging their bets'; moving C away from infected hosts in case of a future physiological decline of those same hosts. In the field, PCN infection tends to be heterogeneous (Been & Schomaker, 2000), so any movement of C and mycelium growth away from infected plants would increase the chances of the MN associating with an uninfected host.

To date, many studies investigating the AM fungi–plant symbiosis have focused on plant benefits or conceptualise the C-for-nutrient regulation using a rigid 'reciprocal rewards' framework. Here, I have shown evidence of a fungal-mediated movement of C based on the pest-infection status of the host plants. From a fungal perspective, resources could be distributed evenly across MNs to compensate for C losses due to competing plant symbionts (Durant et al., 2023), or alternatively, resources could be invested more readily in parts of the networks that might be more 'profitable'. The data on C movement from this study support the latter hypothesis; however, any differences in perceived 'profitability' between PCN-infected and uninfected hosts by AM fungi remain to be determined, as a reduction in plant C delivery under PCN infection was not detected. A better understanding of the physiology and evolution of AM fungi, as well as the varied benefits they receive from their plant hosts, would help further elucidate these results.

In the long term, any fungal-mediated C movement is likely to influence plant hosts themselves via effects on the growth and functioning of MNs. As pointed out by Finlay and Söderström (1992) and later by Pfeffer et al. (2004), the distribution of C within MNs may be significant to plants even in the absence of net transfer of C from fungus to plants. This is because the C demand of the fungal mycelium would be reduced, and newly colonised plants would gain access to nutrients from the mycelium without contributing as much C in return. Overall, my findings reveal a new dimension which aligns with a more mycocentric view of MNs (Fitter et al., 1998), whereby fungi move C to satisfy their own needs as well as those of their plant hosts. A similar ability of fungi to be able to discriminate between hosts and supply the uninfected host with more nutrients is suggested by my ^{33}P-tracing experiment. However, alternative (or supplementary) explanations are also possible. For example, any PCN-induced change in the movement of P and C could also affect the composition of the AM fungal community, which in turn affects the movement of P and C back. Such changes in the AM fungal community can be induced by other root herbivores (e.g., Frew, 2022), and recently it has been suggested that, in addition to C availability driving changes in mycorrhizal species composition, the ability of mycorrhizal species to support the plant hosts' defence mechanisms might also act as a selection pressure (Frew et al., 2024). In other words, the impact of plants on AM fungi could be, at least partly, driven indirectly by PCN-induced differences in the composition and functionality of the AM fungal community, rather than directly by differences in plant C inputs. In addition to PCN-induced changes in P and C being mediated by changes in the AM mycorrhizal community, the wider fungal and bacterial microbiome might also be an explanatory factor. These alternative theories are the focus of the following chapter.

Chapter 3. Plant-parasitic nematodes suppress fungal diversity and alter community composition

3.1 ABSTRACT

In the previous chapter, I showed that in two-plant systems connected to the same arbuscular mycorrhizal (AM) fungal network (MN), plants without potato cyst nematodes (PCN) received more fungal-acquired phosphorus while carbon was redistributed *away* from PCN-infected hosts, indicating that MNs can mediate bidirectional nutrient exchange. Since plant-parasitic nematodes can also influence root and soil microbiota, PCN-induced changes in microbial communities could underlie these altered C–P dynamics. In this chapter, I used Illumina metabarcoding of root and soil samples from the same systems to test whether microbial communities differ between PCN-infected and PCN-free plants. Two primer sets (18S and ITS rRNA) were applied to specifically examine AM fungi. I found that PCN infection reduced fungal diversity and shifted community structure, with consistent reductions in root AM fungal richness across both primer datasets. All fungal phyla except Ascomycota declined in infected roots, including Mucoromycota (dominated by AM fungi). By contrast, bacterial communities showed few shifts, though some taxa (e.g., Pseudomonadales) declined under PCN. These results demonstrate the sensitivity of fungal communities to PCN infection, with possible consequences for nutrient cycling, but provide little evidence that PCN manipulate microbiota to their advantage or that their infection leads to an increase in pathogen loads. Future work should target functional profiling of responsive taxa to clarify their roles in PCN-affected systems and direct contributions to the dynamics of C-for-P exchange between plants and AM fungi.

3.2 INTRODUCTION

Despite the nutritional aspects of the plant-arbuscular mycorrhizal (AM) fungal symbiosis being one of the most studied aspects of the relationship (see Chapter 1), the regulatory mechanisms governing the carbon (C)-for-nutrient exchange and their context dependency remain unclear (Chapter 1; Magkourilou et al., 2024). However, despite the experimental caveats, there is evidence to show that both plant (Bever et al., 2009; Kiers et al., 2011; Lendenmann et al., 2011; Zheng et al., 2015) and AM fungi (Bücking & Shachar-Hill, 2005; Fellbaum et al., 2012; Kiers et al., 2011; van ’t Padje, Bonfante, et al., 2021; van ’t Padje, Werner, et al., 2021; Whiteside et al., 2019; van ’t Padje et al., 2020) can under some circumstances control the exchange of resources for their respective benefits. Using different combinations of potato cyst nematode (PCN) infection on two neighbouring plants, Chapter 2, showed how AM fungi allocate more phosphorus (P) to PCN-free plants relative to their PCN-infected neighbours (Magkourilou et al., 2024). In this scenario, according to the ‘reciprocal rewards’ hypothesis (e.g., Kiers et al., 2011) or source-sink strength dynamics (e.g., Corrêa et al., 2023), in line with the observed increased AM-acquired P provision, AM fungi could be expected to receive an increased C provision from the PCN-free plants relative to their infected neighbours. However, according to my observations, this was not the case, although it was observed that once plant-derived C was assimilated below-ground, it was consistently moved *away* from the PCN-infected plants through the mycorrhizal network (MN; Magkourilou et al., 2024).

In nature, plants and AM fungi form complex associations, whereby a single plant is often colonised simultaneously by multiple AM fungi, and the same MN can also simultaneously colonise multiple neighbouring plants (Smith and Read, 2010). Although a lot of AM fungal species are generalists, the plant response (e.g., plant growth promotion) varies based on the exact combination of plant and fungal species (Klironomos et al., 2003). Moreover, the effects of AM symbioses on plants typically span a continuum that ranges from mutualism, where both parties benefit from the association, to parasitism, where one party benefits from the association at the expense of the other (Johnson et al., 1997). This is exemplified by how abiotic and other biotic factors can influence plant responses to AM fungal colonisation (Hoeksema et al., 2010).

An alternative explanation for the differential provision of AM-fungal acquired P to the two plants that I discussed in Chapter 2 could be that the AM fungal community connected to each plant differed, possibly due to the influence of PCN. More specifically, it could be, for example, that PCN-free plants are colonised by AM fungi that are better at acquiring and delivering P to the plant, or that the fungi acquire similar amounts of P, but they are more 'generous' with this provision to the plants. Similar herbivore-induced changes in the AM fungal community have been observed under root herbivory by the cane beetle (*Dermolepida alborhirtum*; e.g., Frew, 2022). In fact, it has more recently been suggested that, in addition to C availability driving changes in AM species composition, the ability of AM species to support the plant hosts' defence mechanisms might also act as a selection pressure (Frew et al., 2024). Moreover, it has been shown that PCN infection reduces the amount of C in the form of sugars that the host provides to AM fungi, whereas the provision of fatty acids remains largely unimpacted (Bell et al., 2024). Such PCN-induced localised root conditions could be driving the loss of some fungal taxa. Moreover, any difference in the quality of plant-C delivered to the AM fungi could also shape the AM community if individual taxa show different preferences for a particular C type (i.e., sugar vs fatty acids).

Alternatively, PCN-infected plants might be actively selecting for a different microbial community that favours AM fungi or other beneficial species capable of mitigating the impact of PCN, as plants are known to be able, at least to some extent, to shape their microbiomes to enhance their own health (Berendsen et al., 2012). Finally, although not much is known specifically about PCN, it has been shown that other plant-parasitic nematodes (PPN) can also manipulate the rhizosphere microbiome to their advantage (Liu et al., 2023). And even when the microbiome is not explicitly engineered by PPN, it is well-known that PPN can be vectors of many bacterial and fungal plant pathogens (Moens and Perry, 2009), which again can cause shifts in the soil and/or microbial communities.

In short, if any of these scenarios occur in my experiments, rather than the same AM fungal isolate being able to discriminate between a PCN-infected and a PCN-free plant and provide differential amounts of P accordingly, it could be hypothesised that PCN-associated changes in microbial communities are indirectly driving the distribution of P. Similarly, the movement of plant-derived C could also influence or have been influenced by indirect changes to the microbial communities, as it has been previously shown that an increased plant C allocation

can correlate with changes in the soil microbial community (Huang et al., 2023). These changes in the microbial community could involve direct shifts in the AM fungal community, or shifts in other fungi (e.g., saprotrophs) and bacterial communities, which may in turn directly affect AM fungi or indirectly influence them through altered P and C cycling.

As introduced in Chapter 1, AM fungal-associated bacteria, most notably phosphate-solubilising bacteria (PSB), can modulate mycorrhizal symbioses in a number of ways (Jiang et al., 2021; Wang et al., 2023; Duan et al., 2024; Duan et al., 2025). For example, hyphospheric bacteria (i.e., bacteria associated with AM fungal hyphae) can make otherwise inaccessible nutrients available to AM fungi, as well as to their plant hosts (Duan et al., 2023; Hestrin et al., 2019). It has also been observed that AM fungi can use C sources to facilitate the movement of PSB to organic P patches along their hyphal networks, supporting the establishment of mutualistic relationships (Jiang et al., 2021). In other cases, competition for nitrogen (N; and possibly also P) has been suggested as a mechanism by which bacteria might limit AM fungal growth (Leigh et al., 2011) and vice versa (Nottingham et al., 2013). C metabolism in mycorrhizal roots is tightly linked to C flow towards bacteria, as hyphospheric bacteria (in particular, the Orders Solibacterales, Sphingobacteriales, Myxococcales and Nitrososphaerales) rely heavily on hyphal exudates as a C source (Kakouridis et al., 2024). Moreover, some bacteria also have preferences as to which C sources to metabolise (Zhang et al., 2018), which could consequently influence the C-for-nutrient dynamics in AM symbioses, especially when the plant host is experiencing herbivory, where it has been reported that C-flow is mainly disrupted in the form of hexoses rather than fatty acids (Bell et al., 2024).

Traditionally, bacteria were considered more efficient than fungi at exploiting labile C sources released in the rhizosphere (Moore et al., 1996). However, although saprotrophic fungi primarily fulfil their C demands by decomposing organic matter, evidence is accumulating that they can also utilise plant-derived C, such as root exudates (Hannula et al., 2012; Morriën, 2016; Hannula et al., 2017; Hannula et al., 2020). This has led to a growing appreciation of how saprotrophic fungi might, in this way, compete with AM fungi for plant-derived C, although in some cases, no competition is reported as both groups seem to be equally stimulated by plant-derived C (Clochiatti et al., 2021). In fact, it appears that plant-derived C reaching fungi might be mediated by exudation via AM fungi themselves rather than directly

consumed after being exuded by the plant (Drigo *et al*., 2010; Kaiser et al., 2014; Hünninghaus et al., 2019). As for nutrient flows going in the other direction, similar to what has been shown for bacteria, some saprotrophic fungi release extracellular enzymes that depolymerise organic P or N compounds into smaller, mineral forms (Sinsabaugh, 1994; Richardson and Simpson, 2011), which could then become accessible to plants and AM fungi. In fact, organic P mineralisation by microbes is thought to be stimulated by plants through root exudation (Spohn et al., 2013), which in turn can be modulated by AM fungi through changes in plant C allocation or P status (Ma et al., 2022).

AM fungi can also influence saprotrophs more directly, as they often enhance decomposition through a 'priming effect' (Frey, 2019; Choreño-Parra and Treseder, 2024). This is when they release plant-derived labile C into the soil, which—similar to the case with bacteria—alleviates C limitation and thereby stimulates saprotrophic activity (Cheng et al., 2012; Herman et al., 2012; Nottingham et al., 2013; Chowdhury et al., 2022). This microbial stimulation can increase AM fungal access to nutrients, particularly N released during organic matter breakdown (Hodge & Fitter, 2010; Posada et al., 2012). Ultimately, however, this can lead to a stabilisation effect, as AM fungi begin competing with saprotrophs for N, potentially reducing saprotrophic activity and slowing decomposition (Leifheit et al., 2015).

Aims

Because trait characterisation of AM fungi is still in its infancy (e.g., too few isolates have been characterised for their P-provision capabilities; Chaudhary et al., 2022; Antunes et al., 2025; Camenzind et al., 2024), in this study I used species richness, community composition, and the differential abundance of specific taxa as proxies for the functional capacities of the microbial communities. Specifically, to assess whether PCN-induced changes to fungal communities, including specific AM communities, and bacterial communities might have influenced the results discussed in Chapter 2, I performed Illumina metabarcoding of plant roots and soil samples collected from the same experiments described in Chapter 2, where neighbouring plants were inoculated with different combinations of PCN.

3.3 MATERIALS AND METHODS

3.3.1 Collection of samples

Samples from the experiments described in the two experiments described in Chapter 2 were used for this analysis. Specifically, relevant soil and root samples were taken from the systems upon harvest and snap-frozen in liquid nitrogen until subsequent storage at -80 °C. A detailed summary of the sample composition used in the final analysis is included in Table S3.1.

3.3.2 DNA extraction and PCR amplification

DNA was extracted from sub-samples of freeze-dried and homogenised roots (mean = 22.3 mg, SE = 2.0 mg) and soils (mean = 157.2 mg, SE = 4.4 mg) using the DNeasy PowerSoil Pro Kit (Qiagen, Germany) according to the manufacturer's protocol. For soils, the samples were first mixed with tweezers and any stones removed. The CD1 solution of the kit was then added directly to the weighed subsamples in the PowerPro tubes, followed by homogenisation in a FastPrep-24™ (MP Biomedicals, USA) at 5.5 m s^{-1} for two 30-s cycles with a 5-min incubation between runs. For roots, samples were first homogenised using the same FastPrep settings, but with the incubation performed on ice, after which the CD1 solution was added to the weighted subsamples before continuing with the extraction protocol.

DNA concentrations were measured on a subsample by fluorometric quantification (Qubit™ Flex 3.0 Fluorometer) using the Qubit™ dsDNA high-sensitivity assay kit (Invitrogen, USA) following the manufacturer's protocol. Amplicons were generated using three primer sets targeting: the 18S–5.8S rRNA region (including ITS1) for general fungi, the V4–V5 region of 18S rRNA for Glomeromycotan fungi, and the V4 region of 16S rRNA for bacteria (Table S3.2).

Primer pairs were applied in separate PCR reactions using an aliquot from the DNA extraction (2 µL of average concentration 3.7 ng µL-1 for soil and 1 µL of average concentration 13.27 ng µL-1 for roots) in a master mix containing 10 µl Taq PCR Master Mix Kit (Qiagen, Germany), 4 µl ddH_2O for soil samples or 5 µl for root samples, and 2 µl forward and reverse primers (5 µM each) respectively. The PCR programme for each primer pair is detailed in Table S3.2 and was run on a Mastercycler X50s machine (Eppendorf UK Limited, UK). The size of the amplicons was checked by gel electrophoresis on a 1% agarose gel. Following PCR, a magnetic bead purification method was employed to purify the DNA amplicons using the ProNex® Size-Selective Purification System (Promega, USA) according to the manufacturer's instructions. The purified amplicons were then modified by attaching unique identifier sequences (dual-

plexed: Fi5 and R17 primers in unique combinations) using 8 µl of template from PCR1, 10 µl MyTaq HS Mix (Meridian Bioscience, USA), 1 µl Fi5/Fi7 primers (10 µM), and 1 µl ddH_2O per reaction. The conditions for PCR2 were: 95°C for 15 min, followed by 10 cycles starting with polymerase activation at 98°C for 10 s. Annealing of primers was set at 65°C for 30 s and at 72°C for 30 s. Then, 72°C for 5 min.

A selection of pre- and post-PCR2 samples was run on a 4200 TapeStation System (Agilent Technologies, USA) according to the manufacturer's protocol to confirm the addition of PCR2 primers.

3.3.2 Library quantification and sequencing run

A 2 µl aliquot of each amplicon was quantified using the QuantiFluor® dsDNA System (Promega, USA) on a BioTek Synergy LX multi-mode reader (Agilent Technologies, USA). Samples were then normalised to a concentration of 35 ng µL-1 and pooled into primer-pair specific groups of 8 to 24 samples. The pools produced were each purified using ProNex® Size-Selective Purification System (Promega, USA). A subsample from each pool was run on a 4200 TapeStation System (Agilent Technologies, USA) to check for primer dimers and confirm the presence of the target peaks. A likely primer dimer was identified for the bacterial pools, so these were size-selected using a BluePippin (Sage Science, USA). Pools were quantified in a qPCR run using KAPA Library Quantification Kit (F. Hoffmann-La Roche Ltd, Switzerland). These results were used to further pool samples into two libraries at equimolar libraries, 3.4 nM for the bacteria and general fungi, and 8.4 nM for the Glomeromycotan fungi.

Libraries were sequenced on an Illumina MiSeq platform at the Centre for Genomic Research of the University of Liverpool using a 300 bp paired-end configuration. A 10% PhiX spike-in was included on both runs to increase the sequence complexity.

3.3.3 Bioinformatic analyses

Demultiplexed sequences with primer sequences removed using Cutadapt version 4.5 and -O 3 were processed using the *DADA2* pipeline (Callahan et al., 2016) on the High-Performance Computing Cluster at the University of Sheffield. In brief, primers were identified and subsequently removed using *cutadapt* (Martin, 2011), low-quality reads, chimeras and singletons were removed from the library using *filterAndTrim*. The sequence error rates were assessed, and dereplication was performed using the *learnErrors* and *derepFastq* functions; forward and reverse reads were subsequently merged to form Amplicon Sequence Variants

(ASVs). For the ITS and 18S primers, the ASVs were also curated using LULU, a method which identifies errors by combining sequence similarity and co-occurrence patterns (Frøslev et al., 2017).

For the fungal ITS and 18S primers, taxonomy was assigned using *assignTaxonomy* of *DADA2* (MacLaren and Callahan, 2021) to ASVs using the EUKARYOME reference database version 1.9.4 ('DADA2-EUK-long' and 'DADA2-EUK-SSU' versions, respectively for the ITS and 18S primers (Tedersoo et al., 2024). For this, only the fungal sequences trimmed for the respective primers were used and some taxonomy was manually updated as per http://www.amf-phylogeny.com/. . After cleaning and filtering the bacterial 16S sequences, a few samples retained only a low number of sequences. Taxonomy was therefore assigned only to ASVs present in samples with at least 1000 sequences, using the *assignTaxonomy* and *addSpecies* functions from *DADA2* (MacLaren and Callahan, 2021) against the bacterial sequences from the SILVA database release 138.2 (Quast et al., 2013). For all three primer pairs, ASVs were also assigned taxonomy using BLASTn (Camacho et al., 2009) as well as using Taxonomizr (Sherrill-Mix, 2025) and employing a Last Common Ancestor (LCA) method against the same respective databases. If a taxonomic level was missing in the first approach (DADA2), it was filled using the second approach (BLAST), provided the two methods agreed at the lowest taxonomic level already assigned. Six bacterial sequences were detected in the negative controls, and to reduce the impact of false positives, these ASVs were removed from the dataset. Moreover, sequences assigned to 'chloroplast' and 'mitochondria' were also removed from the bacterial dataset.

Following taxonomic assignment, additional filtering was applied across all datasets. First, ASVs represented by fewer than five total reads across all samples were removed. Next, ASVs assigned to the same species were aggregated, resulting in 2,985, 631, and 1,684 sequences for the ITS, 18S, and 16S datasets, respectively. Finally, only sequences assigned to at least the Phylum level and detected in either root or bulk soil samples were retained. This yielded final datasets of 1,862 ITS sequences, 369 18S sequences, and 1,062 16S sequences, which were used for all subsequent analyses and visualisations.

3.3.4 Statistical analyses and data visualisation

Statistical analysis and data visualisation were carried out in R (R Core Team, 2025) using R Studio (R Studio Team, 2025). Briefly, for each primer set, the ASV table, taxonomy table and

metadata were imported to create a phyloseq object using the R package `phyloseq` (McMurdie and Holmes, 2013). Ultimately, a phyloseq object containing filtered ASVs assigned to at least Phylum level and with a total abundance across all samples of at least five was used for each of the primer pairs. ASVs were also aggregated to species levels if relevant.

Three alpha diversity metrics—Observed ASV richness, Shannon diversity, and Simpson diversity—were analysed using mixed-effects models to account for the hierarchical experimental design. Observed richness, as count data, was modelled using a negative binomial GLMM (*glmer*) to account for overdispersion, with PCN treatment, sample type (roots vs. soil), and their interaction as fixed effects, and individual plants nested within containers and experimental replicate as random effects. Shannon diversity was modelled using linear mixed-effects models (*lmer*; LMMs) with heterogeneous variance structures to account for unequal variance between treatment × sample type groups. Simpson diversity was modelled using a beta GLMM (*glmmTMB*) with a logit link to account for the bounded nature of the metric (values between 0 and 1). In some cases, very small values were slightly adjusted to fall within the (0, 1) interval to allow use of the beta distribution. For all models, relevant assumptions were evaluated via residual diagnostics, including residuals versus fitted values, QQ-plots, and formal tests for overdispersion and zero-inflation where appropriate. Statistical significance of fixed effects was assessed using Type III Wald chi-square tests. Estimated marginal means (EMMs) were calculated for pairwise comparisons between treatments within each sample type, with Tukey-adjusted p-values to account for multiple testing where necessary.

Principal coordinate analysis (PCoA) based on Bray-Curtis dissimilarity was used to examine beta diversity differences for fungal and bacterial communities based on PCN treatment and sample type (roots or soil). The *stat_ellipse* function of the `ggplot2` R package was used to overlay 95% confidence ellipses for each treatment within each sample type, aiding visual assessment of group separation. Homogeneity of variances across groups was tested using the *betadisper* function from the `VEGAN` R package (Oksanen et al., 2020) was used to test for homogeneity of variances across comparison groups. Groups that met the assumption of homogeneity ($p \geq 0.05$) were analysed using permutational multivariate analysis of variance (PERMANOVA) with the *adonis2* function in `VEGAN`. For groups exhibiting overdispersion, the argument *by = "margin"* was included to weight contributions by variance. Pairwise

differences between groups were further assessed using PERMANOVA implemented in the `pairwiseAdonis` R package (Martinez Arbizu, 2020). To identify the taxa most strongly associated with community variation, the most influential ASVs (top 10 for fungi and top 8 for bacteria) were fitted to the ordination, indicating their contribution to the separation of samples along the PCoA axes.

Relative abundance was calculated as the number of sequences assigned to a given taxon divided by the total number of sequences in the same sample that were taxonomically assigned to at least the Phylum level. Differential abundance analyses at relevant taxonomic levels (e.g., Phylum or Genus) were performed using the `DESeq2` R package (Love et al., 2014) to compare taxonomic abundances between treatments or sample types. Count data were first normalised using the DESeq2 internal size-factor estimation, with the 'poscounts' method applied if any ASVs had zero counts. Pairwise contrasts (e.g., roots vs. bulk soil) were extracted from the shrunken results. Significance of differential abundance was assessed with the Wald test, and p-values were corrected for multiple testing using the Benjamini–Hochberg method (Benjamini & Hochberg, 1995), with a threshold of $p < 0.05$.

For ITS primers, the trophic mode of each ASV was determined using the FUNGuild database (Nguyen et al., 2016).

3.4 RESULTS

3.4.1 Fungi

3.4.1.1 Alpha diversity

Using the ITS primers, 1862 ASVs were successfully assigned to at least the Phylum level and retained for all subsequent analyses. Of these, 1573 ASVs were also assigned to a Class level, 1420 to an Order level, 1152 to a Family level, 1004 to a Genus level and 287 to a Species level.

Overall, roots showed lower Observed richness ($\chi^2 = 111.09$, $p < 0.01$) as well as lower diversity than soil across both metrics, Shannon ($\chi^2 = 94.76$, $p < 0.01$) and Simpson ($\chi^2 = 77.61$, $p < 0.01$; Table S3.3). Within roots, samples with PCN exhibited reduced richness (z-ratio = 3.90, $p < 0.01$) compared to those without, as well as reduced diversity for both Shannon (t-ratio = 4.62, $p < 0.01$) and Simpson (z-ratio = 6.35, $p < 0.01$) indices (Figure 3.1; Table S3.4).

No statistically significant differences were observed based on PCN treatment within soil (Figure 3.1; Table S3.4).

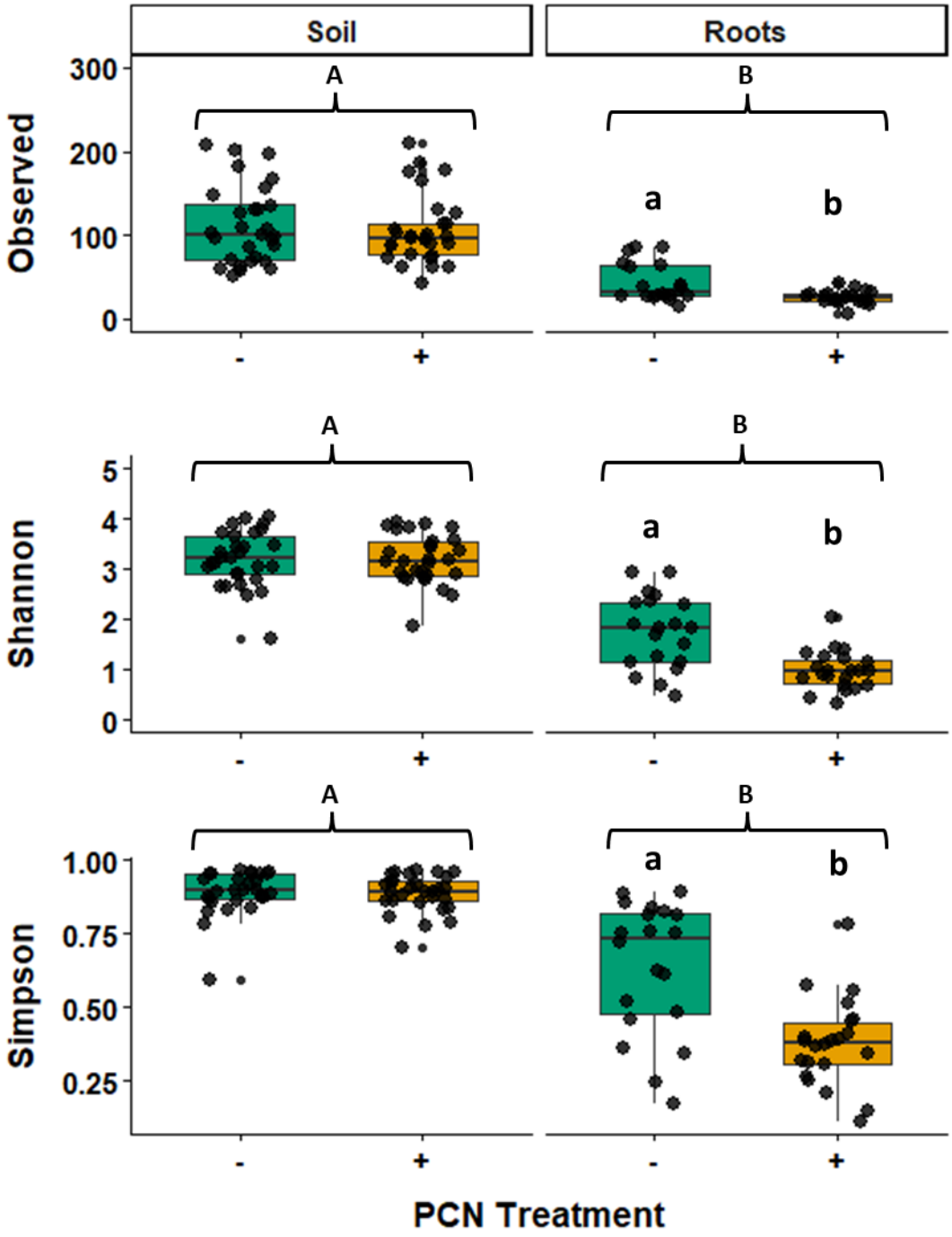

Figure 3.1 Observed richness and Alpha diversity (**ITS dataset; all fungi**) based on PCN treatment within soil and roots. Capital letters above grouped-boxplots indicate significant effects between soil and roots, whereas small letters above single boxplots indicate any PCN treatment differences within each sample type (Tables S3.3 and S3.2). Boxplots span the interquartile range (IQR), the line inside marks the median, and whiskers extend to 1.5 × IQR. Points outside are potential outliers. Plants without PCN are indicated by '–' and green bars, plants with PCN are indicated by '+' and orange bars.

Looking specifically at the roots of neighbouring plants with the mixed PCN treatment combination '−/+', those infected by PCN typically showed a lower fungal diversity than their uninfected neighbours across all indices (Observed: $\chi^2 = 11.84$, $p < 0.01$; Shannon: $\chi^2 = 18.99$, $p < 0.01$; Simpson: $\chi^2 = 16.44$, $p < 0.01$; Figure 3.2).

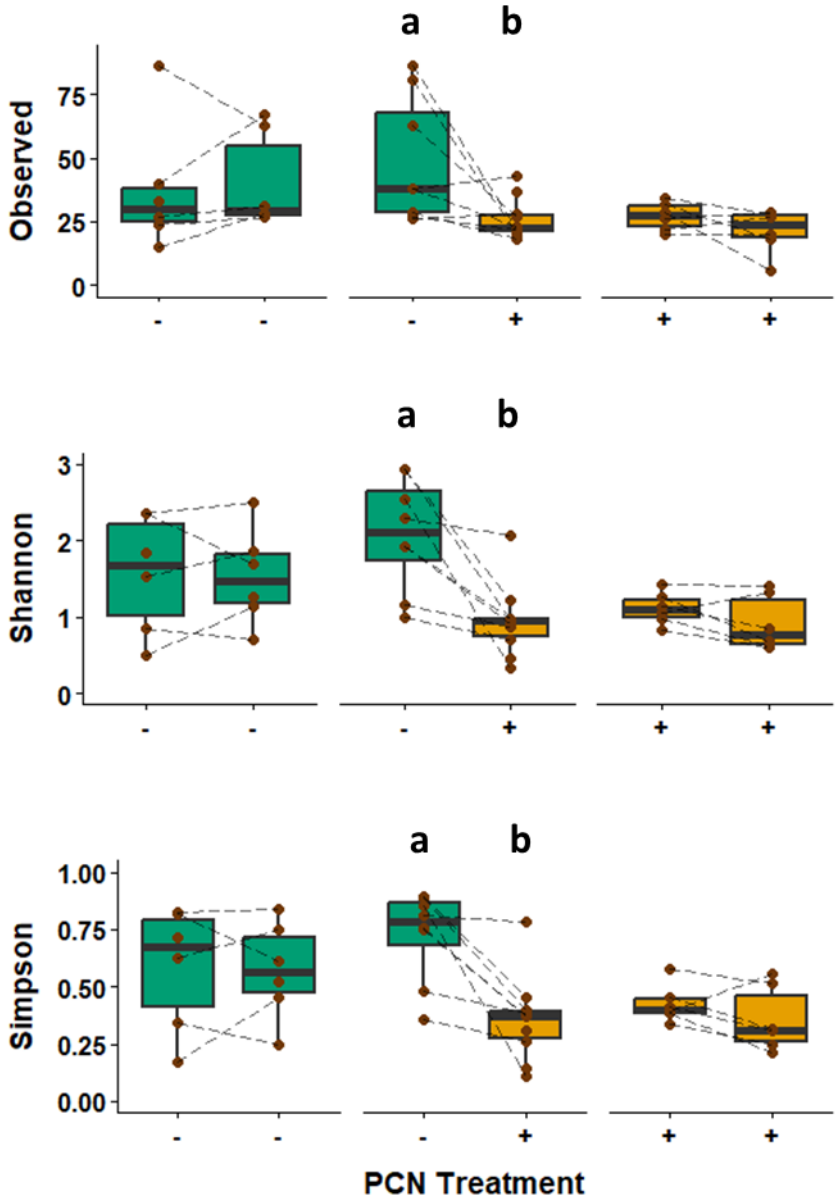

Figure 3.2 Observed richness and Alpha diversity (**ITS dataset; all fungi**) for roots, split per container. Dashed lines connect paired samples across each side of the same container. Letters above boxplots indicate significant PCN treatment effects within the '−/+' mesocosms ($p < 0.05$). Boxplots span the interquartile range (IQR), the line inside marks the median, and whiskers extend to 1.5 × IQR. Points outside are potential outliers. Plants without PCN are indicated by '−' and green bars, plants with PCN are indicated by '+' and orange bars.

Focusing on AM fungal groups within the total fungal ITS dataset, 156 ASVs (out of 1,862 ASVs that had been filtered, cleaned, and assigned to at least the Phylum level) were classified into one of the Glomeromycotan Classes containing AM fungi: Glomeromycetes, Paraglomeromycetes, Archaeosporomycetes, or Diversisporomycetes. Similarly, analysis of the 18S dataset revealed 177 ASVs (out of 369 phylum-level assigned ASVs) that were assigned to at least one of the Glomeromycotan Classes.

Although both the 18S and ITS primers captured a similar total number of Glomeromycotan ASVs, the 18S primers detected roughly four times higher Observed richness per sample, indicating that more taxa were captured consistently within individual samples. Shannon and Simpson diversity indices were also higher with the 18S primers, reflecting a more even distribution of taxa without any single taxon dominating abundance.

Overall, Glomeromycotan Observed richness was higher in roots than in soil for both the ITS ($\chi^2 = 25.10$, $p < 0.01$; Figure 3.3A) and 18S primers ($\chi^2 = 10.52$, $p < 0.01$; Figure 3.3B; Table S3.5), a pattern largely driven by increased richness in PCN-free roots. Pairwise comparisons within each sample type confirmed that PCN treatment significantly reduced richness in roots for both datasets (ITS: z-ratio = 3.12, $p < 0.01$; 18S: z-ratio = 2.32, $p = 0.02$), but a similar trend for reduced diversity under PCN, particularly pronounced for the ITS dataset, was not statistically confirmed (Table S3.6). In soil, richness was not significantly affected in the ITS dataset, but richness showed a marginal reduction under PCN treatment within the 18S dataset (z-ratio = 1.92, $p = 0.05$). This reduction in both roots and soil within the 18S dataset contributed to an overall effect of decreased Observed richness under PCN treatment ($\chi^2 = 3.70$, $p = 0.05$).

Finally, within the ITS dataset, similarly to richness, there was also a trend for diversity to be higher in roots than in soil, but this was marginally not statistically significant for both measures (Figure 3.3A; Table S.3.5)

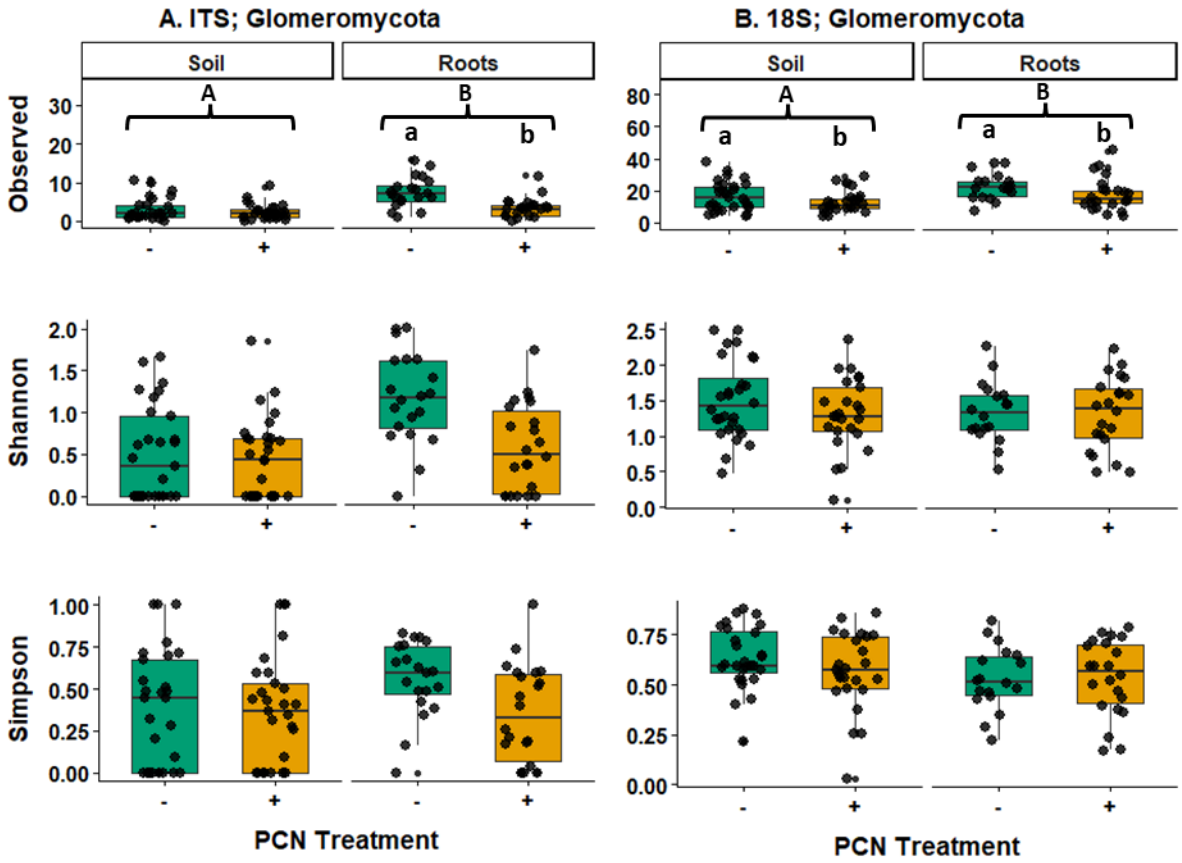

Figure 3.3 Observed richness and Alpha diversity for Glomeromycota identified using **A. ITS**, and **B. 18S** dataset. Capital letters above grouped-boxplots indicate significant effects between soil and roots, whereas small letters above single boxplots indicate any PCN treatment differences within each sample type (Tables S3.5 and S3.6). Boxplots span the interquartile range (IQR), the line inside marks the median, and whiskers extend to 1.5 × IQR. Points outside are potential outliers. Samples without PCN are indicated by '–' and green bars, whereas plants with PCN are indicated by '+' and orange bars.

Looking at all fungi using the ITS primers revealed that there was a trend for the proportion of ASVs shared across each side of the same mesocosm to be higher in soil than in roots (Figure 3.4A). Albeit the trend was overall statistically insignificant, likely due to the large variation between the '+/+' roots (Table S3.7). The proportion of shared ASVs across each side of the same mesocosm was, however, overall significantly affected by the PCN treatment combination (Figure 3.4A; Table 3.7), with roots within '+/+' containing a significantly higher

proportion of shared ASVs than '−/+' mesocosms (Table 3.8). For the 18S primers, the proportion of Glomeromycota ASVs shared showed a statistically insignificant trend to be slightly higher in roots compared to soil, whereas there was no difference based on the PCN treatment combination (Figure 3.4B; Tables S3.8 and S3.7).

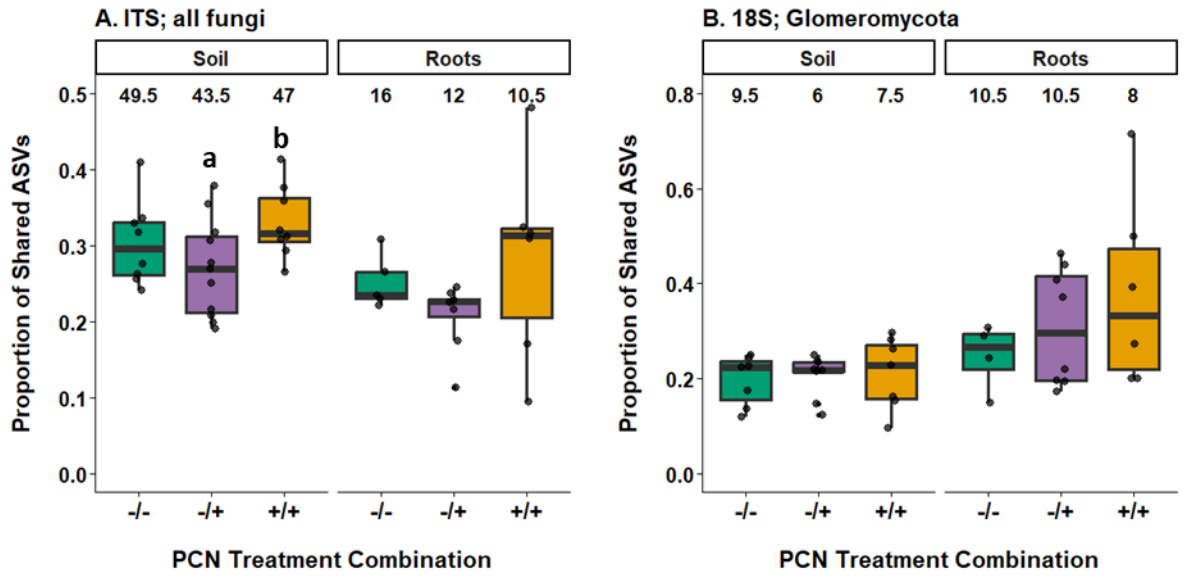

Figure 3.4 Proportion of shared ASVs across each side of the same mesocosm identified using the **A.** ITS dataset for all fungi, and the **B.** 18S dataset for Glomeromycotan fungi. The number above each boxplot represents the mean total number of ASVs detected for the respective category. Letters indicate any significant pairwise differences between PCN treatment combinations within each sample type (Table S3.x). Boxplots span the interquartile range (IQR), the line inside marks the median, and whiskers extend to 1.5 × IQR. Points outside are potential outliers. Mesocosms without PCN are indicated by '−/−' and green boxplots, whereas mesocosms with PCN are indicated by '+/+' and orange boxplots. Mesocosms with mixed PCN treatment combinations are indicated by '−/+' and purple boxplots.

3.4.1.2 Beta diversity

Fungal community composition was primarily shaped by sample type ($R^2 = 0.40$, $F = 75.93$, $p < 0.01$) and, to a smaller but still significant extent, by PCN treatment ($R^2 = 0.03$, $F = 4.70$, $p < 0.01$; Figure 3.5; Table S3.9). When examining the effect of PCN treatment further, comparisons performed separately within roots and soil revealed that only root communities were significantly influenced by PCN ($R^2 = 0.20$, $F = 9.89$, $p < 0.01$).

PCoA indicated that among the top 10 ASVs most strongly associated with community variation, the AM fungal species *Funneliformis mosseae* was linked to PCN-free roots, whereas the genus *Scutellinia* (Phylum: Ascomycota) was more associated with PCN-infected roots (Figure 3.5). Soil communities were characterised by associations with taxa from the Phyla Ascomycota (families Plectosphaerellaceae and Microascaceae), Basidiomycota (Piskurozymaceae and Trimorphomycetaceae), and Mortierellomycota (Mortierellaceae).

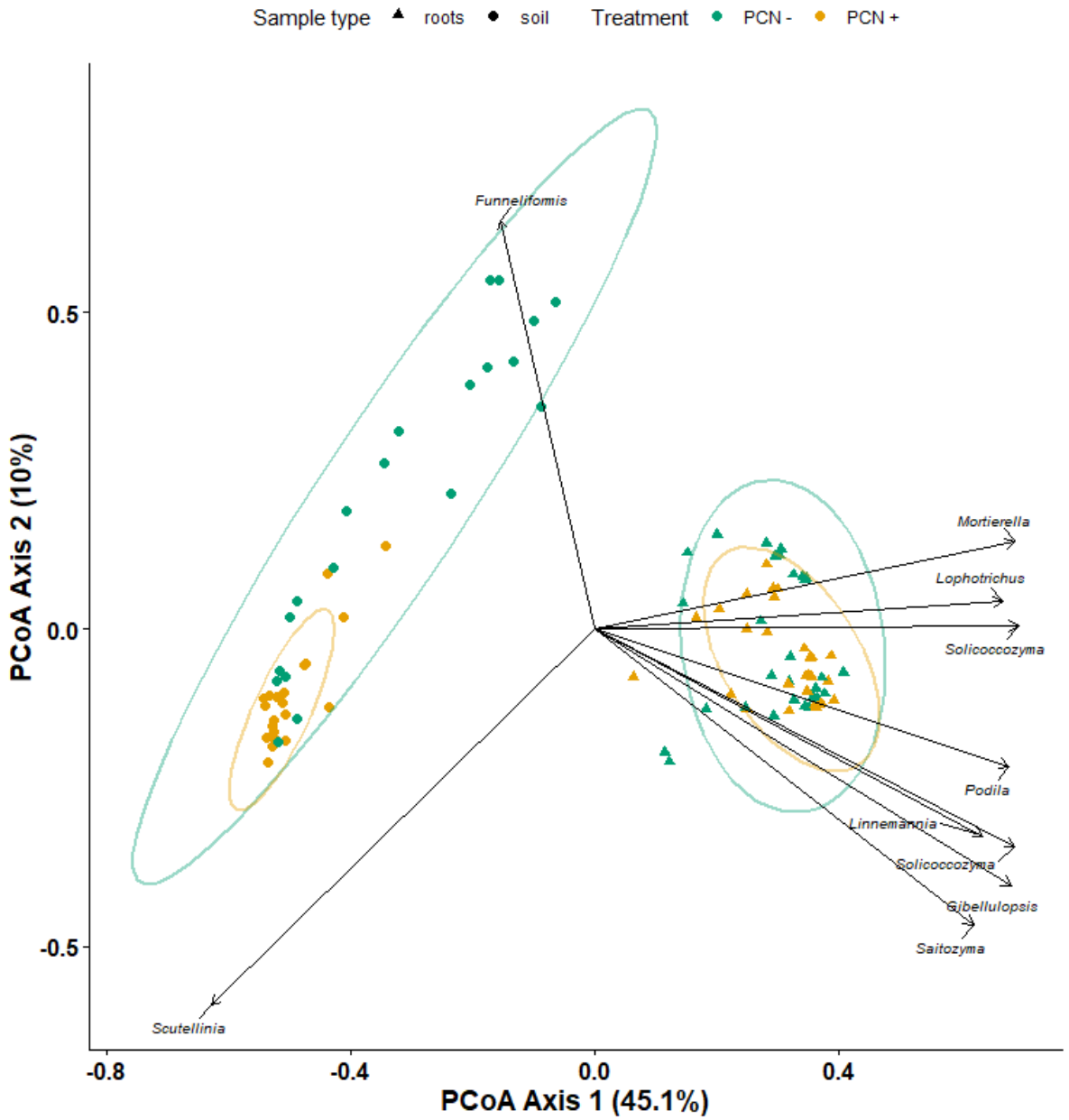

Figure 3.5 Principal Coordinates Analysis (PCoA) based on Bray-Curtis dissimilarity of fungal communities (**ITS dataset; all fungi**) from soil and root samples. Points represent individual samples, coloured by treatment group ('PCN –' or 'PCN +') and shaped by sample type (roots or bulk soil). Ellipses show 95% confidence intervals for each treatment within each sample type. Arrows indicate the top 10 most influential ASVs, with labels based on Genus assignment, highlighting the taxa most strongly associated with variation along the PCoA axes.

3.4.1.3 Relative and differential abundance

Overall, the relative abundance of fungal Phyla was influenced by sample type (i.e., roots vs soil). In particular, most fungal Phyla were more abundant in soil samples than in roots except for Olpidiomycota and Mucoromycota, which were more abundant in root samples (Figure 3.6A; B; Table S3.11).

Within sample type, PCN treatment effects were more pronounced in the roots (Figure 3.6A. Most prominently, Mucoromycota and Olpidiomycota were relatively more abundant in roots without PCN, at the expense of Ascomycota (Figure 3.6A). However, although differential abundance analysis confirmed that Mucoromycota and Olpidiomycota were negatively influenced by the presence of PCN, Ascomycota, a very prominent taxon, showed no significant fold change based on PCN treatment (Figure 3.6D; Table S3.11), suggesting that the apparent higher relative abundance of Ascomycota in PCN-infected roots was driven primarily by the depletion of Mucoromycota and Olpidiomycota, and to some extent also the reduction of Basidiomycota (Figure 3.6A; Figure 3.6D; Table S3.11).

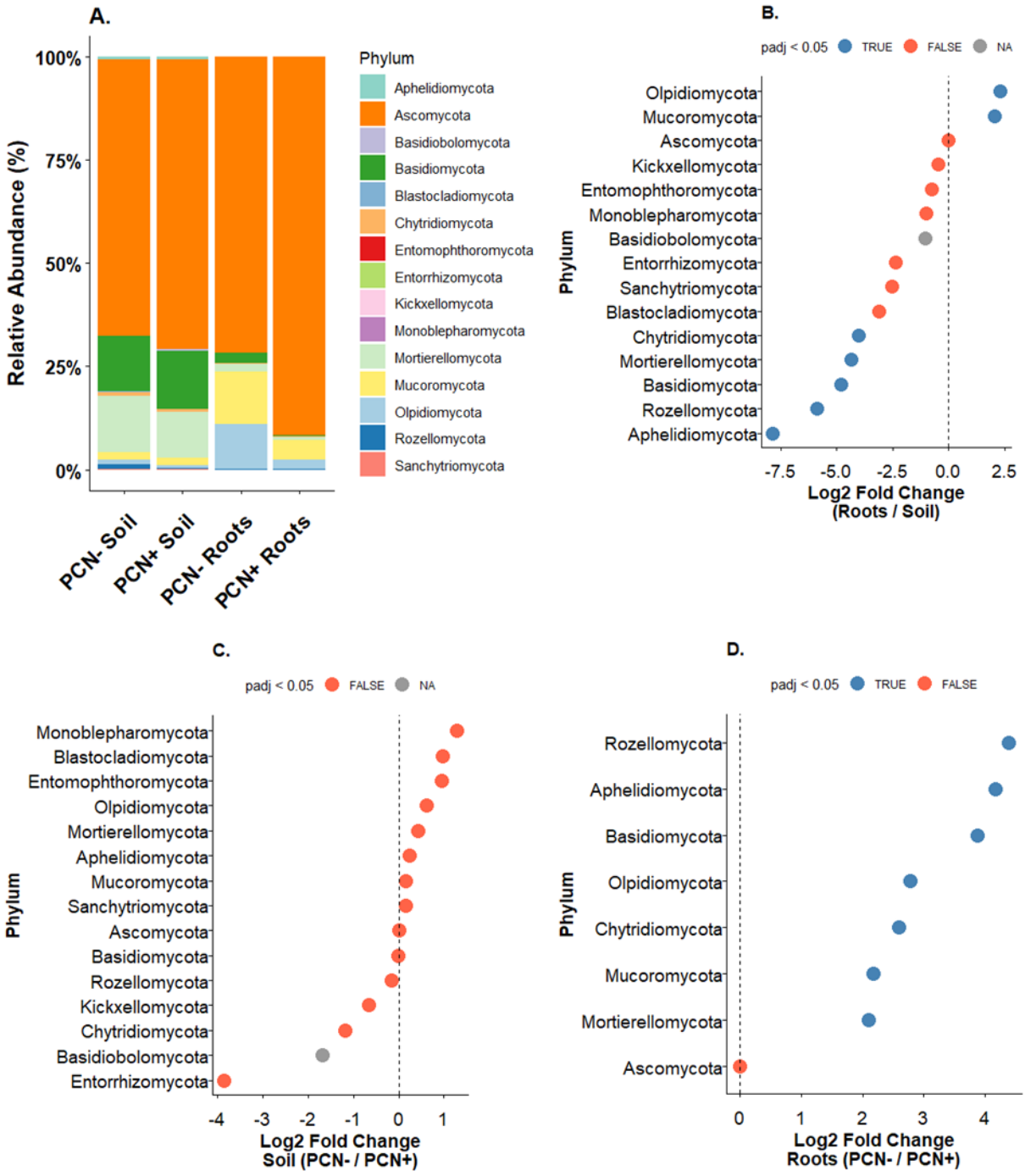

Figure 3.6 A. Relative abundance of **fungal Phyla (ITS dataset)** based on Sample type and PCN treatment. Differential abundance analysis using DESeq2 within **B**. Sample type, as well as within **C.** Soil and **D.** Roots based on PCN treatment. Absolute log_2 fold changes are shown as Roots/Soil (B) or PCN– / PCN+ (C, D); positive values indicate enrichment in Roots or PCN–, negative values in Soil or PCN+. Taxa present exclusively in one category are assigned a pseudo-log_2 fold change. Points are coloured by statistical significance: blue = padj < 0.05, red = padj ≥ 0.05, grey = padj unavailable (Table S3.11).

The vast majority of Mucoromycota, especially within roots, were assigned to the AM fungal class Glomeromycetes (Figure 3.7A). Although differential abundance analysis confirmed that Glomeromycetes were negatively affected by the presence of PCN treatment, this difference was not statistically significant when adjusting for multiple comparisons (Figure 3.7B; Table S3.12). The only Mucoromycotan Class confirmed to be significantly affected by PCN treatment was Paraglomeromycetes, a Class that was relatively rare across samples but exhibited a $\log_2$ fold change of ~5, indicating a strong decrease in the presence of PCN on the roots (Figure 3.7D; Table S3.12).

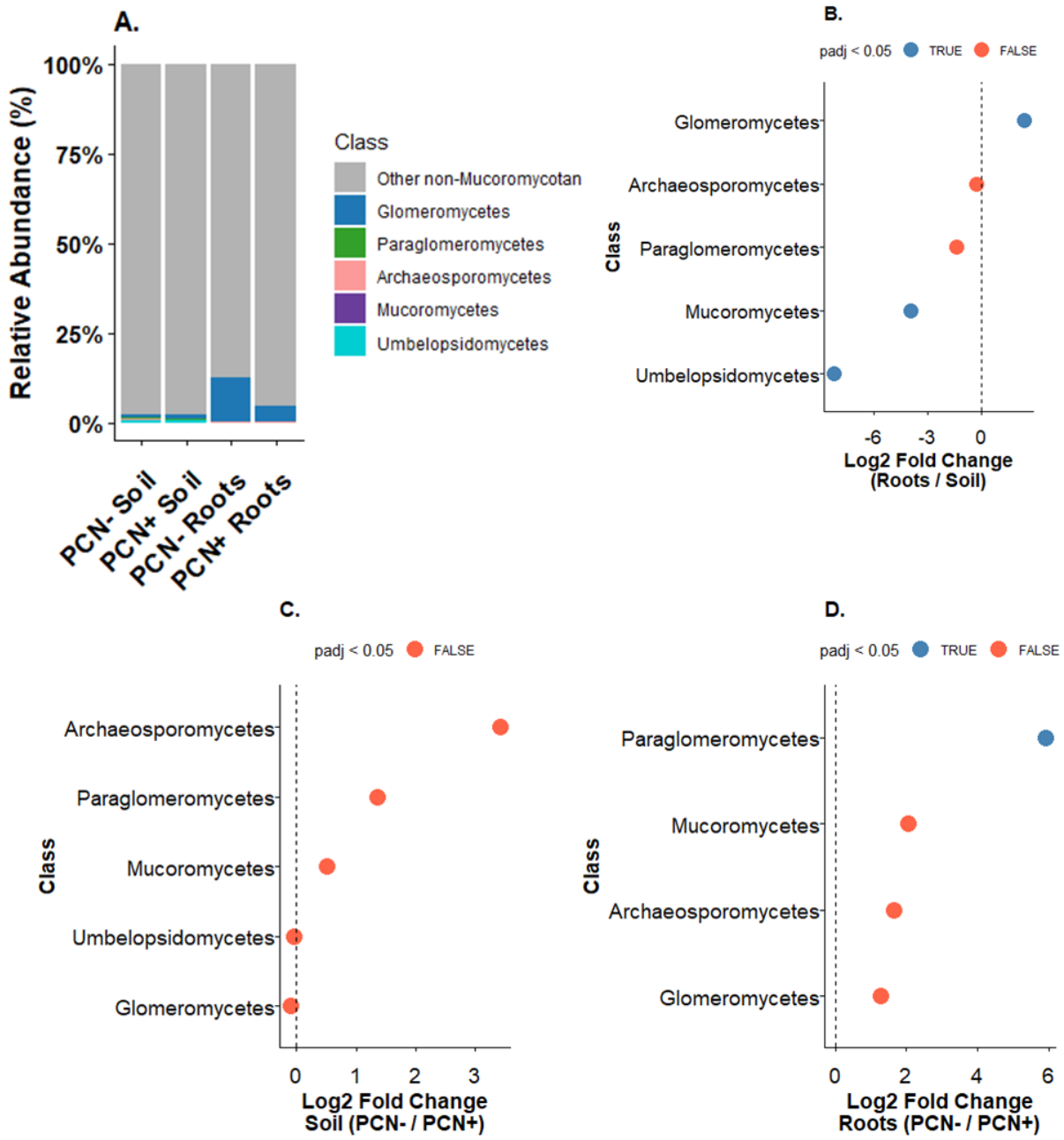

Figure 3.7 A. Relative abundance of fungal Classes **(ITS dataset)** based on Sample type and PCN treatment, highlighting only Mucoromycotan Classes. Differential abundance analysis using DESeq2 within **B**. Sample type, as well as within **C.** Soil and **D.** Roots based on PCN treatment. Absolute log_2 fold changes are shown as Roots/Soil (B) or PCN– / PCN+ (C, D); positive values indicate enrichment in Roots or PCN–, negative values in Soil or PCN+. Taxa present exclusively in one category are assigned a pseudo-log_2 fold change. Points are coloured by statistical significance: blue = padj < 0.05, red = padj ≥ 0.05, grey = padj unavailable (Table S3.12).

Focusing on Families within the Subphylum Glomeromycota, Gigasporaceae appeared more relatively abundant in soil, particularly PCN-free soil, based on both ITS (Figure 3.8A) and 18S primers (Figure 3.9A). Differential abundance analysis supported this trend, although it was not statistically significant (Figure 3.8B and 3.9B for ITS and 18S, respectively). Paraglomeraceae also appeared overall relatively more abundant in soil than in roots, especially with ITS primers (Figure 3.8A). This trend was supported by differential abundance analysis for both primer sets but reached statistical significance only with 18S, despite lower overall detection of Paraglomeraceae using this primer set (Figure 3.8B and 3.9B). Both primer datasets also indicated higher relative abundance of Polonosporaceae and Archaeosporaceae in soil, and more Glomeraceae in roots (Figure 3.8A and 3.9A for ITS and 18S, respectively), but differential abundance analysis confirmed this pattern only for Polonosporaceae and Archaeosporaceae using 18S (Figure 3.8B and Table S3.13 for ITS and Figure 3.9B and Table S3.14 for 18S). Diversisporaceae and Entrophosporaceae were also more abundant in soils than in roots (Figure 3.8B and Table S3.13 for ITS and Figure 3.9B and Table S3.14 for 18S).

Examining PCN effects, ITS primers suggested that PCN treatment reduced the relative abundance of Gigasporaceae but increased that of Archaeosporaceae in soils (Figure 3.8A), a pattern also suggested by 18S data (Figure 3.9A). While these trends were also reflected in differential abundance analysis, none were statistically significant after adjusting for multiple comparisons (Figure 3.8C and Table S3.13 for ITS and Figure 3.9D and Table S3.14 for 18S).

Within roots, ITS primers suggested that PCN treatment increased the relative abundance of Entrophosporaceae in roots at the expense of Glomeraceae (Figure 3.8A). However, differential abundance analysis showed that all Families tended to be negatively affected by

PCN, although none statistically so (Figure 3.8D; Table S3.13). In contrast, 18S primers showed that roots in general were dominated by Glomeraceae and revealed fewer PCN-related effects, with only Polonosporaceae appearing strongly reduced in PCN-infected roots (Figure 3.9D, Table S3.14).

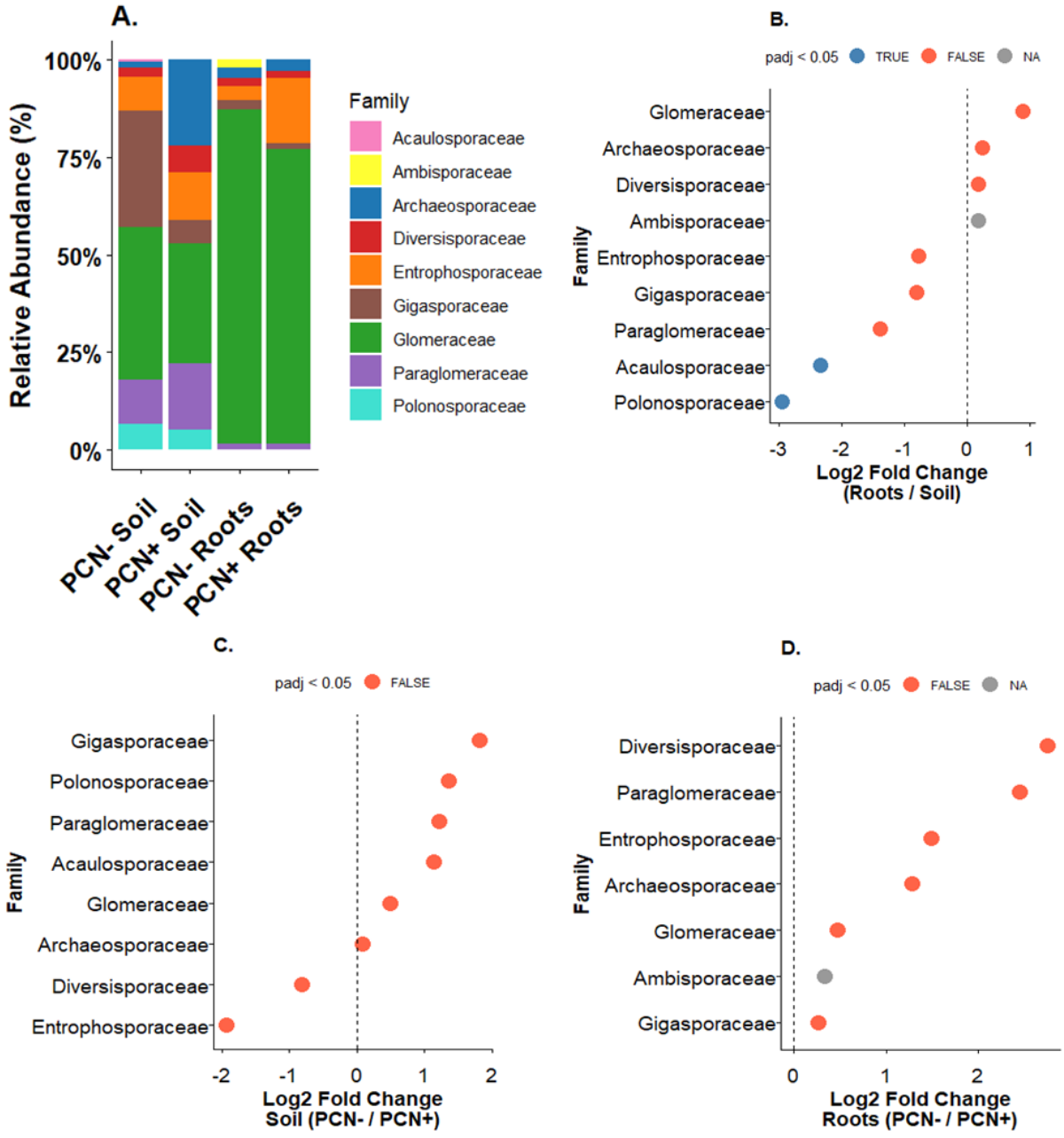

Figure 3.8 Relative abundance of **Glomeromycotan Families (ITS dataset)** based on Sample type and PCN treatment. Differential abundance analysis with DESeq2 within **B.** Sample type, as well as within **C.** Soil, **D.** Roots based on PCN treatment. Absolute log_2 fold changes are shown as Roots/Soil (B) or PCN– / PCN+ (C, D); positive values indicate enrichment in Roots or PCN–, negative values in Soil or PCN+. Taxa present exclusively in one category are assigned a pseudo-log_2 fold change. Points are coloured by statistical significance: blue = padj < 0.05, red = padj ≥ 0.05, grey = padj unavailable (Table S3.13).

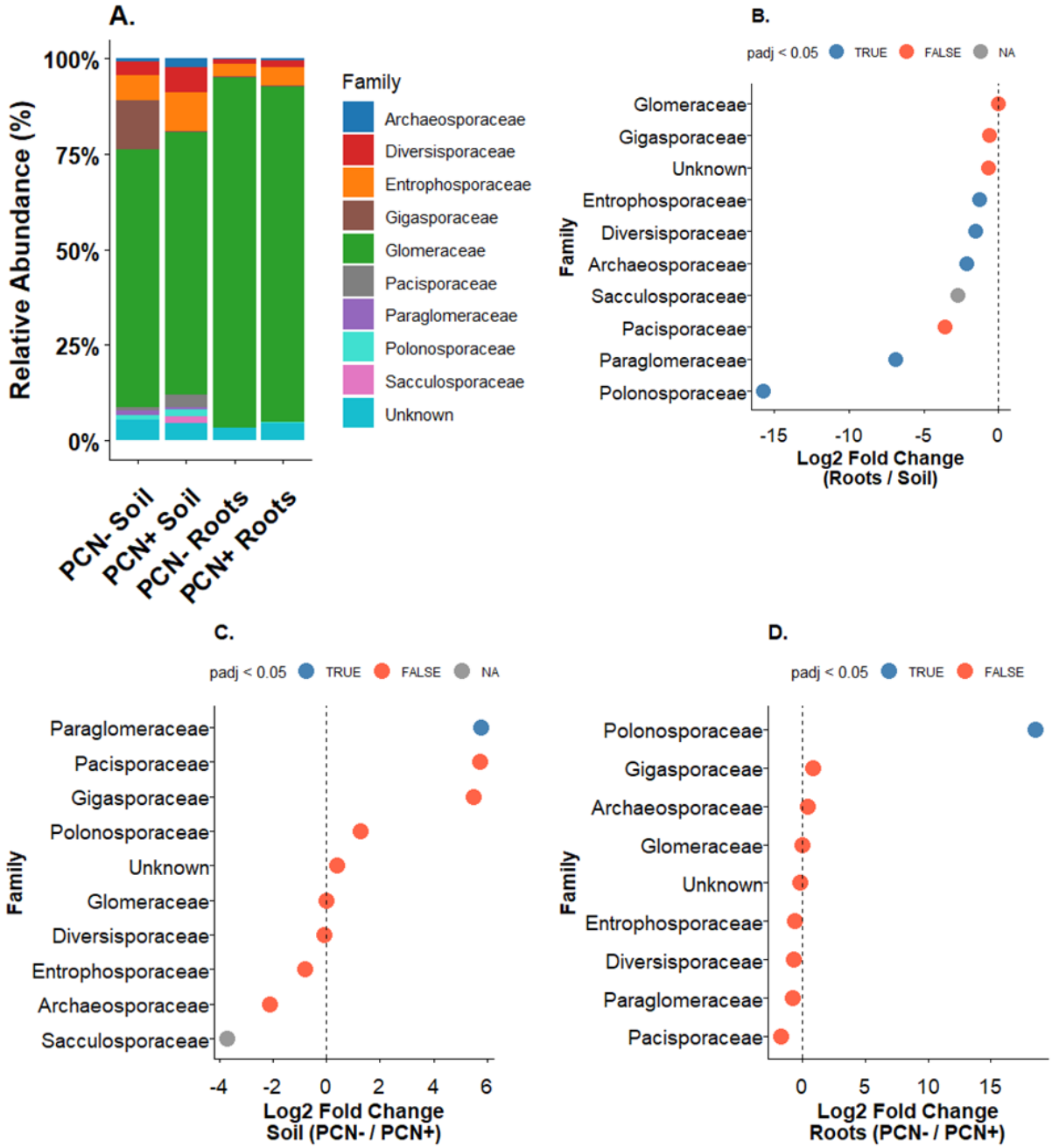

Figure 3.9 A. Relative abundance of **Glomeromycotan Families (18S dataset)** based on Sample type and PCN treatment. Differential abundance analysis using DESeq2 within **B.** Sample type, as well as within **C.** Soil, **D.** Roots based on PCN treatment. Absolute log_2 fold changes are shown as Roots/Soil (B) or PCN– / PCN+ (C, D); positive values indicate enrichment in Roots or PCN–, negative values in Soil or PCN+. Taxa present exclusively in one category are assigned a pseudo-log_2 fold change. Points are coloured by statistical significance: blue = padj < 0.05, red = padj ≥ 0.05, grey = padj unavailable (Table S3.14).

3.4.1.4 ITS and 18S primer comparison

In silico analysis of primer efficiency indicated that the ITS primers captured a higher percentage of sequences present in their respective reference database for each Glomeromycotan Family (Figure 3.10). However, despite this lower capture efficiency of the 18S primers, metabarcoding using 18S still allowed assignment to a greater absolute number of potential sequences for most families (except for Acaulosporaceae, Pervetustaceae, and Paraglomeraceae), because the 18S reference database used contained substantially more sequences overall (Figure 3.10).

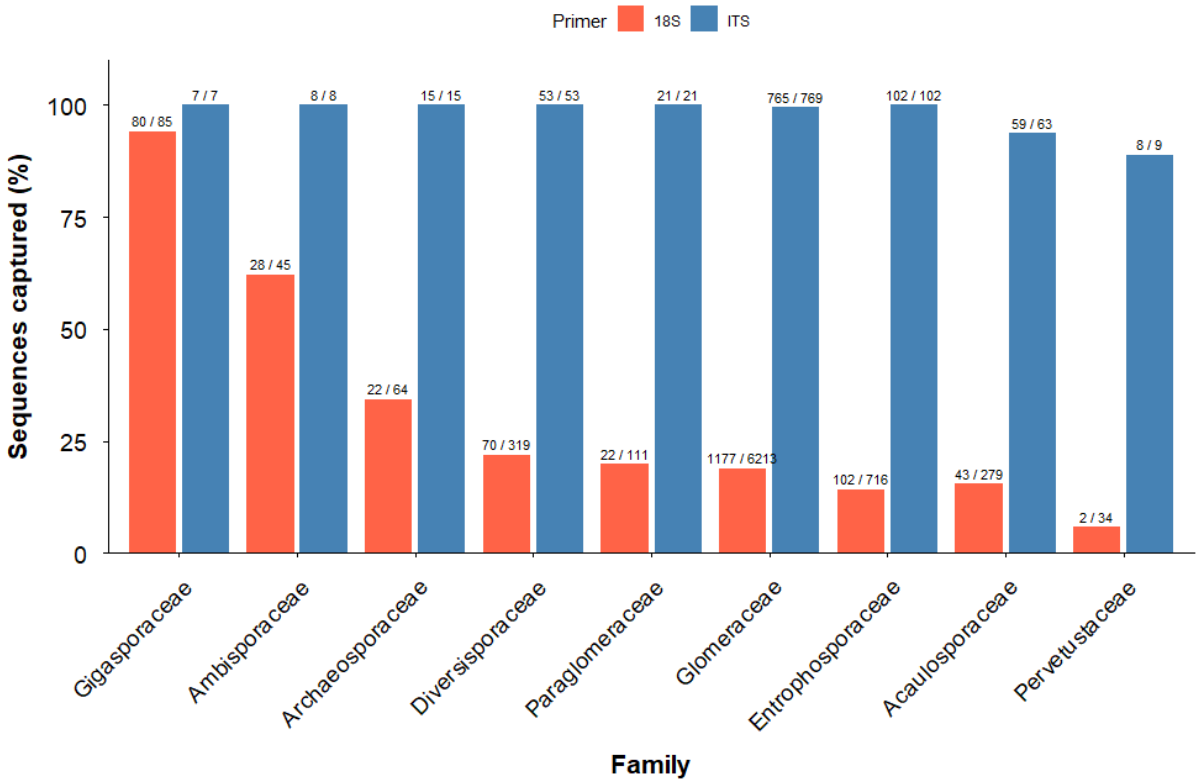

Figure 3.10 *In silico* analysis of primer efficiency showing the percentage (%) of sequences captured by each primer pair. The percentage was calculated as the number of sequences from each Glomeromycotan Family captured by each primer (using *cutadapt*) divided by the total number of sequences from that Family present in the relevant reference database. This calculation is shown above each relevant barplot.

Looking within my own data, most Glomeromycotan Families were successfully captured by both the ITS and the 18S primers, except for Acaulosporaceae and Ambisporaceae, which were uniquely identified by the ITS primers, and Pacisporaceae and Sacculosporaceae, which were uniquely identified by the 18S primers (Figure 3.11A). These families were detected at comparatively low abundances overall (Figure 3.11A), which may have contributed to their absence from either one of the primer datasets. As expected, the raw abundance for all Families was higher using the 18S primers, which largely only captured Glomeromycota (Figure 3.11B). When normalising abundances within each primer pair, considering only Families captured by both primers to some extent, Diversisporaceae and Entrophosporaceae appeared relatively more abundant with the 18S primers, whereas Paraglomeraceae and Polonosporaceae were relatively more abundant with the ITS primers (Figure 3.11C).

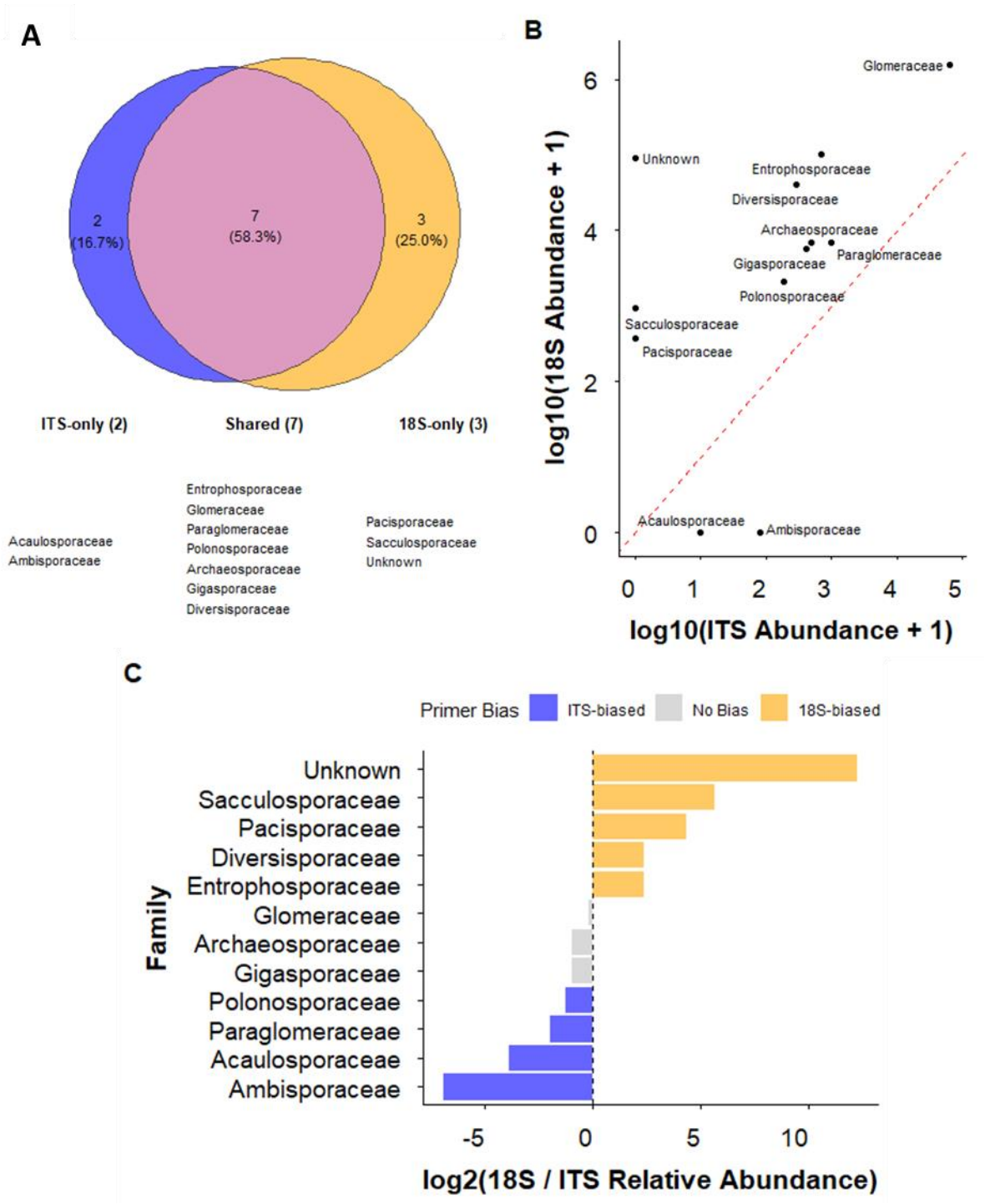

Figure 3.11 A. Venn diagram showing Glomeromycotan Families identified in root and soil samples using ITS and 18S primers, **B.** Relationship between the total abundance of each Glomeromycotan Family identified using ITS and 18S primers, and **C.** Log_2 fold change of the relative abundance of each Glomeromycotan Family identified using ITS and 18S primers. A family is highlighted as 'biased' if the log_2 fold change > than 2.

3.4.2 Bacteria

3.4.2.1 Alpha diversity

Using the 16S primers, 1055 ASVs were successfully assigned to at least the Phylum level and retained for all subsequent analyses. Of these, 1010 ASVs were also assigned to a Class level, 899 to an Order level, 791 to a Family level, 526 to a Genus level and 54 to a Species level.

Overall, similar to fungi, roots had a lower bacterial richness ($\chi^2 = 19.18$, $p < 0.01$) and diversity (Shannon: $\chi^2 = 64.37$, $p < 0.01$; Simpson: $\chi^2 = 93.82$, $p < 0.01$) than soil (Figure 3.12). That said, unlike fungi, there was no other statistically significant effect of PCN treatment within either sample type (Table S3.15).

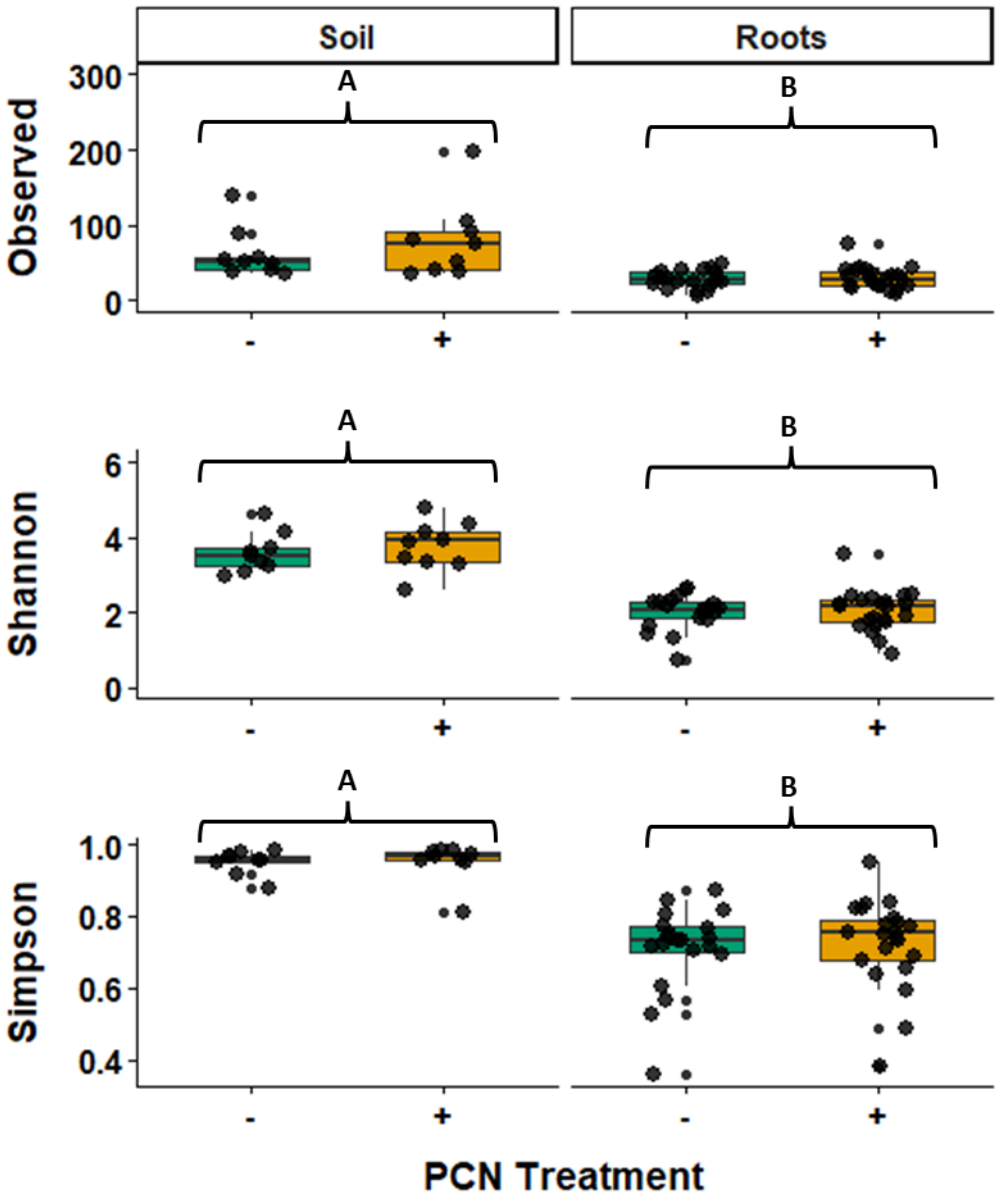

Figure 3.12 Observed richness and Alpha diversity **(16S dataset)** based on PCN treatment within soil and roots. Capital letters above grouped-boxplots indicate significant effects between soil and roots, whereas small letters above single boxplots indicate any PCN treatment differences within each sample type (Tables S3.15 and S3.16). Boxplots span the interquartile range (IQR), the line inside marks the median, and whiskers extend to 1.5 × IQR. Points outside are potential outliers. Plants without PCN are indicated by '–' and green bars, plants with PCN are indicated by '+' and orange bars.

3.4.2.2 Beta diversity

Bacterial community composition was largely driven by sample type (i.e., roots vs soil) alone ($R^2 = 0.44$, $F = 48.87$, $p < 0.01$), with no overall effect of PCN treatment (Figure 3.13; Table S3.17). However, when examining the effect of PCN treatment separately within roots and soil, root communities were significantly influenced by PCN, although the proportion of variation explained was small ($R^2 = 0.05$, $F = 2.07$, $p < 0.05$; Table S.18).

PCoA indicated that variation in community composition was associated with higher representation of the Classes Thermoleophilia, Bacilli (Families Bacillaceae and Planococcaceae), Nitrososphaerales and Alphaproteobacteria (Order Hyphomicrobiales) in soil, whereas Cyanobacteria and Alphaproteobacteria (Order Rickettsiales) were more associated with root samples (Figure 3.13).

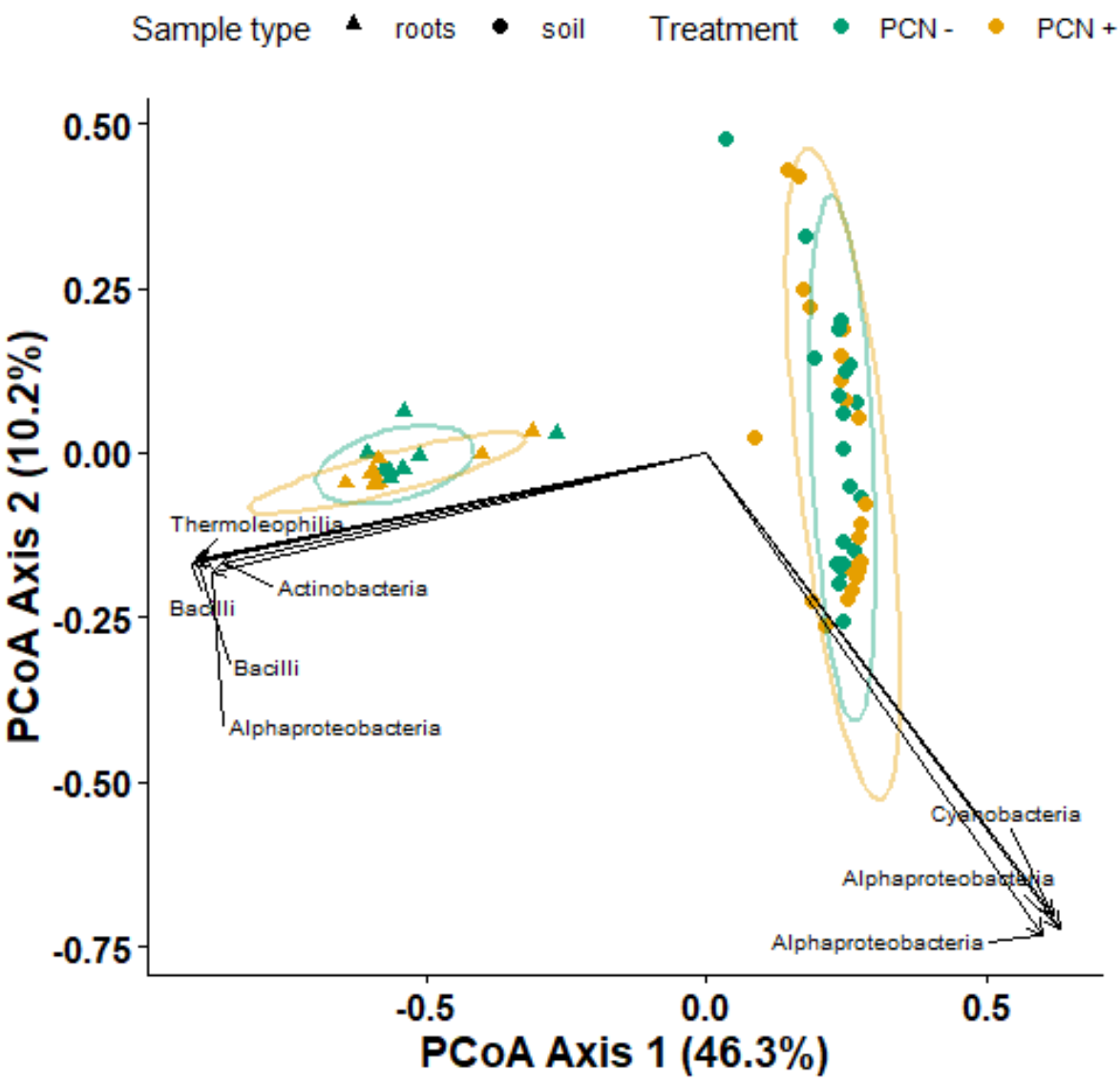

Figure 3.13 Principal Coordinates Analysis (PCoA) based on Bray-Curtis dissimilarity of bacterial communities (**16S dataset**) from soil and root samples. Points represent individual samples, coloured by treatment group ('PCN –' or 'PCN +') and shaped by sample type (roots or bulk soil). Ellipses show 95% confidence intervals for each treatment within each sample type. Arrows indicate the top 8 most influential ASVs, with labels based on Class assignment, highlighting the taxa most strongly associated with variation along the PCoA axes.

3.4.2.3 Relative and differential abundance

Relative abundances of bacterial Orders associated with plant cell-wall degrading enzymes or known to associate with AM fungi (Table S3.19) were generally higher in soil than in roots (Figure 3.14A). The notable exceptions were Pseudomonadales and, to a lesser, non-significant extent, Flavobacteriales, both of which showed higher relative abundance in root samples (Figure 3.14B; Table S3.20).

Regarding PCN treatment, most Orders exhibited shifts primarily in the soil. In particular, Sphingobacteriales were relatively more abundant in soil under PCN treatment (Figure 3.14A). Differential abundance analysis supported this pattern in both soil (Figure 3.14C) and roots (Figure 3.14D), although these trends were not statistically significant (Table S3.21). The only statistically significant change observed was the decrease of Pseudomonadales in soil containing PCN (Figure 3.14C).

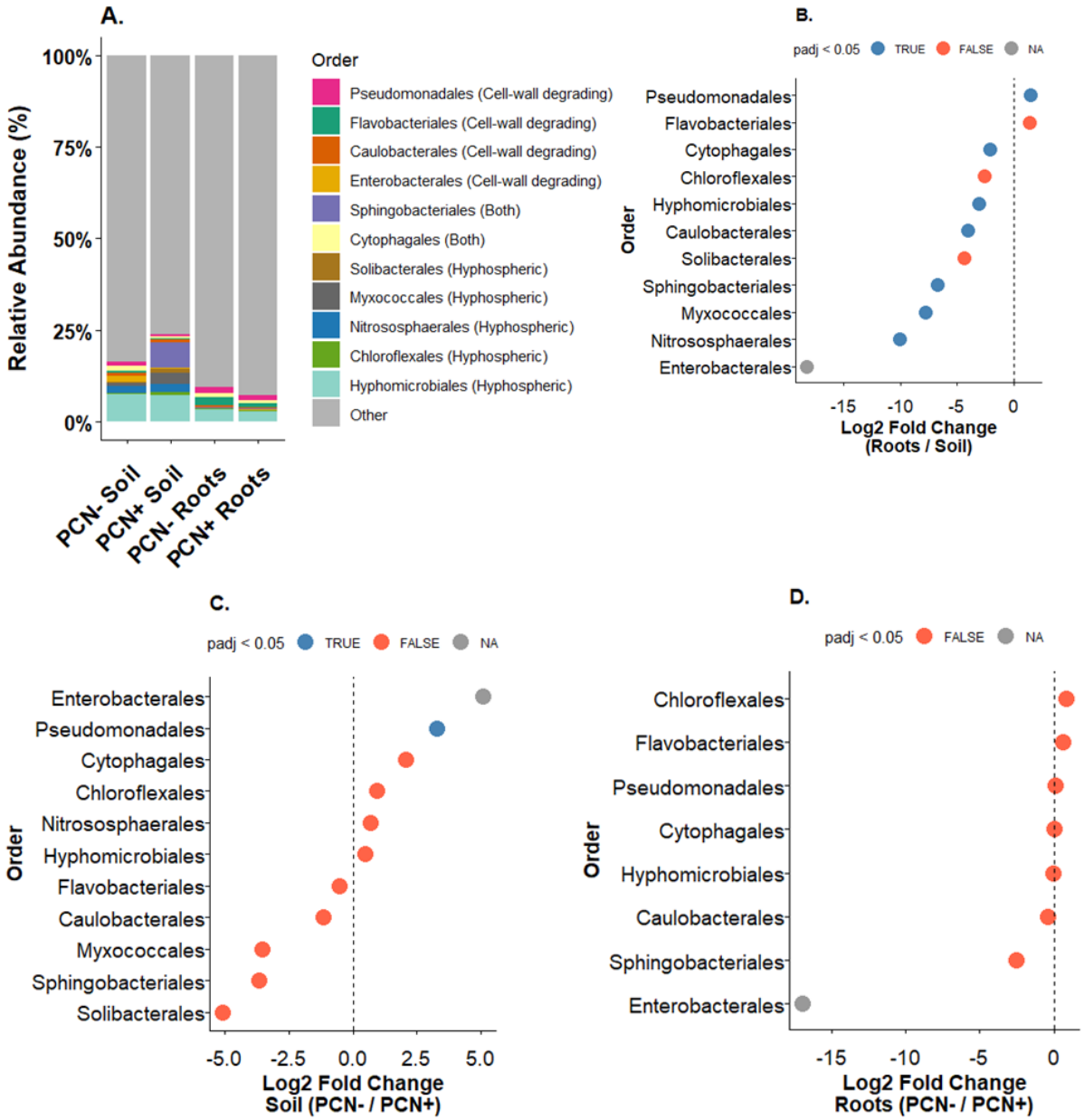

Figure 3.14 A. Relative abundance of **bacterial Orders (16S dataset)** from soil and root samples, highlighting only Orders enriched in plant cell-wall degrading enzymes or identified as hyphospheric (Table S3.15). Differential abundance was analysed using DESeq2 within **B.** Sample type, as well as within **C.** Soil, **D.** Roots, based on the PCN treatment. Absolute $\log_2$ fold changes are shown as Roots/Soil (B) or PCN– / PCN+ (C, D); positive values indicate enrichment in Roots or PCN–, negative values in Soil or PCN+. Taxa present exclusively in one category are assigned a pseudo-$\log_2$ fold change. Points are coloured by statistical significance: blue = padj < 0.05, red = padj ≥ 0.05, grey = padj unavailable (Table S3.21).

Relative abundance of bacterial Genera with potential phosphate-solubilising properties shifted particularly in the roots, with *Streptomyces* being relatively more abundant in roots without PCN, even though the opposite trend was seen in soil (Figure 3.15A). In any case, working with the raw count data and adjusting for differences in sequencing depth and variance between samples, it appears that *Streptomyces* and *Rhizobium* are indeed differentially more abundant in roots without PCN, albeit not statistically significantly so (Figure 3.15D).

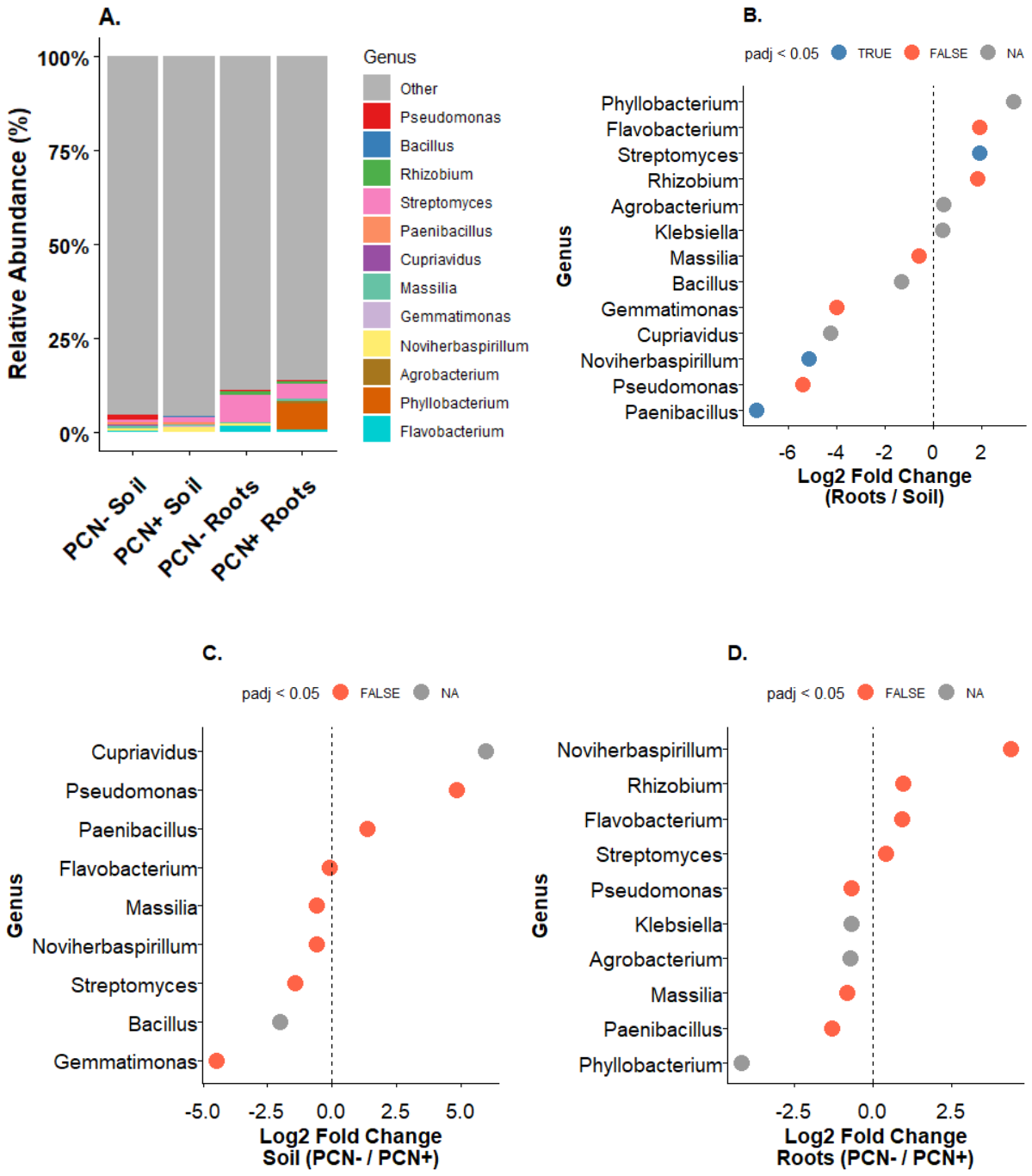

Figure 3.15 A. Relative abundance of **bacterial Genera (16S dataset)** in soil and root samples, highlighting Genera with phosphate-solubilising taxa (Table S3.20). Differential abundance was analysed using DESeq2 within **B.** Sample type, as well as within **C.** Soil, **D.** Roots, based on the PCN treatment. Log_2 fold changes are shown as Roots/Soil (B) or PCN– / PCN+ (C, D); positive values indicate enrichment in Roots or PCN–, negative values in Soil or PCN+. Taxa present in only one category are assigned a pseudo-log_2 fold change. Points are coloured by statistical significance: blue = padj < 0.05, red = padj ≥ 0.05, grey = padj unavailable (Table S3.22).

3.5 DISCUSSION

3.5.1 PCN treatment reduces root fungal diversity and alters community structure, while bacterial responses are limited to a few taxa

The overall aim of this chapter was to understand how the presence of the PCN, *Globodera pallida*, influences bacterial and fungal communities, with a particular focus on AM fungi. To achieve this, I used Illumina sequencing to characterise the richness, diversity and composition of microbial communities within both roots and surrounding soil. Roots generally harboured less diverse fungal and bacterial communities than soil, with lower observed richness and diversity indices (fungi: Figure 3.1; bacteria: Figure 3.12), suggesting that root-associated microbiomes are more selective or dominated by fewer taxa. This also agrees with previous studies (e.g., Lamelas et al., 2020; Yergaliyev et al. 2020; Toju and Tanaka, 2019) and further corroborates the ability of plant roots to regulate microbial entry, whether bacterial (Lundberg et al., 2012) or fungal (Edwards et al., 2015). Although not a universal trend as soil communities often drive root communities (e.g., Santos-Gonzalez et al., 2011; Inceoglu et al., 2013), selection at the root level is typically achieved by the plant host through biophysical and metabolic cues, as well as regulation of the plant immune system (Dodds and Rathjen, 2010).

Specifically, roots infected with PCN in my experiments exhibited lower total fungal richness and diversity than those without PCN, whereas no comparable effect was observed in soil samples (Figure 3.1) or for bacteria in either soil or root samples (Figure 3.12). The relationship between PCN and microbial communities has only recently been investigated in the context of ‘disease suppressive’ soils. One study reported a non-significant trend for higher bacterial richness in suppressive soils compared to conducive soils, with no clear

differences in fungal diversity or community composition (Kiige et al., 2025). Similar to my result, another study found no difference in fungal richness between PCN suppressive and conducive soils, although bacterial richness was higher in suppressive soils (van Himbeeck et al., 2025). Together, these findings suggest that PCN primarily influences fungal communities within the host root environment rather than in the surrounding soil, possibly through selective recruitment or suppression of root-associated fungi in response to infection. However, studies on PCN-microbe interactions remain limited, and the underlying mechanisms are likely complex, involving multiple biotic and abiotic factors.

Studies on root-knot nematode (RKN, *Meloidogyne* spp.)-infested soils have also reported mixed effects on microbial diversity. Some studies have observed reduced bacterial diversity in infested soils compared to non-infested soils (Zhou et al., 2019). In contrast, others have found no differences in rhizosphere soil but detected higher bacterial richness in RKN-infected roots compared to uninfected roots (Tian et al., 2015). Similarly, microbial richness has been reported to increase at early stages of RKN infection (3–30 days) but decrease by 60 days post-infection (Kudjordjie et al., 2024). Comparable variability has been observed with other nematode types; for instance, the addition of PPNs, as well as bacterial-, fungal-feeding, omnivorous, and carnivorous nematodes, can reduce fungal species richness in the rhizosphere (Wurst et al., 2009), while root herbivory by clover cyst nematodes (*Heterodera trifolii*) generally also has no effect or a negative effect on fungal and bacterial biomass, although low-level infestations can stimulate microbial growth, presumably via nematode-induced changes in root exudation (Yeates et al., 1998; Denton et al., 1998). These variable outcomes likely reflect context-dependent factors, including nematode species and feeding strategies, host plant traits, soil properties, levels of infection, as well as temporal dynamics, and whether roots or rhizosphere soil are sampled.

Similar to my results for diversity and richness, community composition of both fungi and bacteria was influenced by sample type (roots vs soil), whereas PCN treatment also exerted an influence on the community structure of root fungi (Figure 3.5; Tables S3.9 and S3.10). Recently, PCN ‘conducive’ soils have been found to contain a separate fungal and bacterial community composition from PCN ‘suppressive’ soil (van Himbeeck et al., 2025). RKN have also previously been found to influence bacterial and fungal communities of tomato plants, with some taxa being influenced more than others and distinct communities being formed

under nematode infection (Kudjordjie et al., 2024). Moreover, successional changes in RNK coincide with nematode development, indicating again that microbial community composition is highly dynamic (Kudjordjie et al., 2024). Early in their experiment (0–3 days post-infection), hub taxa were primarily fungal, whereas by 60 days post-infection, bacterial taxa dominated. Although not entirely analogous, most importantly due to the different types of PPN used, in my study, sampling at 7 weeks (~49 days) would fall closer to a phase when bacteria might dominate.

In any case, my results suggest that even low levels of PCN infection can reduce root fungal diversity and richness as well as impact community structure. However, metabarcoding does not provide information about microbial biomass, and techniques such as phospholipid fatty acid (PLFA) analysis or real-time qPCR would be more suitable for examining the effects on total microbial biomass. This is particularly interesting because PPN feeding can lead to C leakage from roots, which in turn may enhance microbial biomass (Yeates et al., 1998; Yeates et al., 1999) without necessarily impacting species richness or community structure.

3.5.2 What drives PCN-associated changes in fungal and bacterial communities?

Changes in the microbiome might be driven by the host plant, the PCN, and/or the microbes themselves. For example, PCN-associated microbiome changes may be plant-mediated (e.g., impacting plant defence mechanisms; Adam et al., 2014). Specifically, Jasmonic (JA) and Salicylic acid (SA), Strigolactones (SL) and Ethylene (ET) are thought to be important for PPN defence, but their effect might also be modulated indirectly by phytohormone-root microbiome effects (Doornbos et al., 2011; Carvalhais et al., 2015; Sikder et al., 2021; Liu et al., 2023). Indeed, growing evidence suggests that certain beneficial microorganisms can suppress PPN by triggering induced systemic resistance in plants (Topalović and Heuer, 2019), highlighting the importance of the plant host's ability to shape the microbiome to its advantage. Plant-defence mechanisms may therefore be complemented by shifts in soil microbiota, which plants can influence through metabolic and physiological adjustments (as will be explored further in Chapter 5). For example, root exudates play a central role in regulating soil fungal diversity and community composition (Broeckling et al., 2008; Badri and Vivanco, 2009), and changes in exudate profiles triggered by plant defence responses can further shape microbial communities (Carvalhais et al., 2015).

In one experiment, microbiomes from a flavonoid overexpressing line increased RKN invasion, whereas microbiomes harvested from the flavonoid-deficient lines significantly reduced invasion (Sikder et al., 2022). Microbiomes from the flavonoid-deficient lines also showed a higher abundance of several bacterial (e.g., *Chitinimonas*) and fungal (e.g., *Gibellulopsis nigrescens)* taxa, which are thought to be antagonistic with PPN (Sikder et al., 2022). PPN-antagonistic taxa typically act by reducing root invasion and triggering plant defence responses (Topalović et al., 2020). In my study, PPN-antagonistic fungal genera *Metapochonia*, *Clonostachys*, *Gibellulopsis, Pochonia* and *Acremonium* (Table S3.23) were found to be substantially reduced in roots with PCN (albeit only the first three were significantly so; Figure S3.2B), potentially pointing to the PCNs' ability to discourage their presence. *Metacordyceps*, another fungal genus which was recently found to be associated specifically with PCN 'suppressive' soil (van Himbeeck et al., 2025), was absent from my systems (Figure S3.2A and B).

PPN-antagonistic bacterial genera (Tables S3.23) showed a more mixed picture, with no statistically significant results (Figure S3.2C and D). However, it is worth noting that *Pseudomonas* was slightly increased in the roots in the presence of PCN (Figure S3.2C), despite being substantially less abundant in the soil under similar PCN conditions (Figure S3.2D). Such a pattern potentially points to the ability of the plant to preferentially recruit this genus with potential PCN-antagonistic properties (van Himbeeck et al., 2025). That said, the other study on PCN suppressive soils has identified *Pseudomonas* as having higher relative abundance in 'conducive' soils, suggesting a potential link between this genus and PCN infection (Kiige et al., 2025). These mixed results likely stem from the fact that *Pseudomonas* is known to contain pathogenic as well as plant-promoting strains (Raaijmakers and Mazzola, 2012; Mendes, Garbeva, and Raaijmakers, 2013), meaning that it likely also interacts with PCN in different ways.

As previously alluded to, the recruitment of PPN-antagonistic taxa by the plant hosts can create an evolutionary arms race, where it may also benefit PCNs to induce quantitative and qualitative changes in root exudates, phytohormones, and secondary metabolites, either to limit the plant's recruitment of PPN-antagonistic taxa or to recruit PPN-beneficial taxa directly. PPNs may also influence the microbiome more directly, as root damage can create opportunities for certain microbial species to colonise and potentially replace others, in some

cases increasing the abundance of PPN-beneficial taxa. Supporting this nematode-driven selection, fungal and bacterial taxa attached to RKN surfaces often have low relative abundance in the surrounding soil (Elhady et al., 2017), suggesting a selective recruitment process.

Moreover, it has been suggested that known cellulose-degrading bacterial Orders (e.g., Sphingobacteriales, Pseudomonadales, Flavobacteriales, Cytophagales, and Caulobacterales), which have an increased capacity to dissolve the plant cell wall, might be more enriched in RKN-infected roots because they potentially aid the formation of RKN-feeding sites (Tian and Zhang, 2015). In my study, although a substantially increased (albeit statistically insignificant) differential abundance of the Sphingobacteriales was observed in PCN-infected soil and roots, Pseudomonadales in the soil actually decreased in the presence of PCN (Figure 3.14C). This highlights once more the complexity and context-dependency of plant-nematode–microbe interactions, and suggests that even though PPN might favour infection sites where cellulose-degrading bacteria have already damaged the plant cell wall, these bacteria are not necessarily harboured on the PPN-surfaces as has been suggested for wood-feeding insects (Adams et al., 2011).

PCN-associated differences in fungal richness and community composition could also relate to the ability of PPN to encourage plant-detrimental consortia of bacteria, fungi, and viruses, collectively known as disease complexes (Back et al., 2002; Lamelas et al., 2020). These synergistic interactions are thought to arise through mechanisms such as the exploitation of PPN-induced wounds by soilborne pathogens (Karimi et al., 2000), as well as alterations in the rhizosphere environment and nematode-triggered physiological changes in the host, such as compromised host resistance (Back et al., 2002). In some cases, PPN-induced root damage can alter the composition of root exudates, making them more favourable to fungal pathogens (Bergeson, 1972). Indeed, more plant pathogens (e.g., *Plasmodiophorida*, *Oomycetes* and *Rhizoctonia* sp.) have been observed in plants that have PPN (Wilschut et al., 2019). Although the precise evolutionary drive for the emergence of such a PPN-fungal pathobiome remains unresolved, it has been proposed that plant pathogens entering the roots on the surface of PPN might protect them against PPP-antagonistic root endophytes (Topalović & Vestergård, 2021).

In any case, in my study, I did not observe an overall higher relative abundance of pathotrophic fungi in systems with PCN; on the contrary, roots without PCN showed the highest relative abundance of taxa singly defined as 'pathotrophs' by FUNGuild (Nguyen et al., 2016; Figure S3.1); although this analysis is limited by the multiple trophic mode assignments given to most taxa. Furthermore, looking more specifically at known potato-pathogenic fungal Genera in the roots, *Fusarium*, *Helminthosporium, Rhizoctonia*, and *Verticillium* were actually decreased in the presence of PCN (albeit the trend was statistically significant only for *Fusarium*; Figure S3.2B), whereas there was also no statistically significant difference in the recruitment of potential PPN-beneficial genera (Figure S3.2), suggesting that a different mechanism was in play in my experiments.

Finally, another, more general influence of PPN relates to the release of plant-derived C into the rhizosphere. It has been demonstrated that PPN feeding by *Rotylenchulus reniformis* can result in C 'leakage' and a subsequent increase in organic C in the soil, thereby enhancing microbial respiration and CO_2 release (Tu, Koenning, and Hu, 2003). PPN also contain cellulose-degrading genes, which means that they can increase the decomposability of roots (Smant et al., 1998) and thus further influence soil nutrient dynamics through feedbacks with saprotrophic microbes. Traditionally, bacteria (especially members of the order Burkholderiales; Vandenkoornhuyse et al., 2007) were thought to be better at consuming labile C and thus more dependent on plant exudates than fungi. If it is indeed true, PPN enhancement of labile C sources such as root exudates could benefit bacteria more than fungi (Newman, 1985). This could partly explain why bacterial richness and structure were overall unaffected by PCN in my study, as bacteria may benefit more than fungi from the increased labile C released into the soil under PPN infection. That said, more recently it has been proposed that fungi with saprotrophic capabilities (ectomycorrhizal fungi in particular) can also use substantial amounts of labile C (e.g., de Vries and Caruso, 2016), but more empirical research is needed to better understand soil food web dynamics.

In my case, again, there was no clear evidence that the relative abundance of taxa singly defined as 'saprotrophs' by FUNGuild (Nguyen et al., 2016) was increased under PCN-infected soil or roots in my experiment (Figure S3.1). However, as expected due to their role in organic matter decomposition, 'saprotrophs' were more abundant in soil rather than root samples (Rillig et al., 2025). Moreover, although the relative abundance of the phylum Ascomycota,

which includes many saprotrophs, was higher in roots under PCN infection, differential abundance analyses suggest that this pattern likely reflects declines in Basidiomycota, Olpidiomycota, and Mucoromycota. Overall, it appears that, contrary to all other Phyla, the abundance of Ascomycota remained unaffected by PCN infection, which suggests that Ascomycota neither benefited from a PCN-induced release of plant-derived C nor were they negatively affected by C resources being consumed by PCN, as has been suggested in other C-limiting conditions (Dumbrell et al., 2011).

Overall, the PPN-antagonistic fungal taxa *Metapochonia*, *Clonostachys*, and *Gibellulopsis* were the only taxa that exhibited significant trends consistent with expectations regarding the ability of PCN to manipulate the microbiome. Contrary to expectations, there was no clear indication that PCN increase the abundance of potato pathogenic fungal genera in PCN-free roots, or more generally, that of fungal 'pathotrophs' or 'saprotrophs'. Importantly, as discussed earlier, PCN infection directly disrupts root structure and function, while also indirectly affecting plant immune and chemical signalling. These combined effects likely drive the exclusion of certain fungal taxa and the overall shifts in community composition observed in roots. Consequently, the patterns seen for fungal genera probably reflect broader changes in fungal diversity, such as reduced richness and lower abundances of most Phyla in PCN-infected roots, rather than a direct ability of PCN to shape their microbial community. This interpretation also likely applies to 'pathotrophs' and 'saprotrophs', which, contrary to expectations, did not appear to be favoured by increased infection entry zones or by higher C exudation due to PCN. Instead, their patterns are more consistent with direct competition with PCN for root infection sites and, potentially, for C resources. More generally, the reduction in abundance of all Phyla except for Ascomycota under PCN infection ties in with evidence from trees where pathogen attacks can cause 'destabilisation in microbiome complexity', where an immune response is triggered by the plant in an effort to dampen the proliferation of the invading pathogen (Ginnan et al., 2020).

More detailed analyses could potentially identify individual ASVs that respond to PCN presence. Such taxa might include microbes that directly interact with PCN, opportunistic taxa that exploit PCN-induced changes in root exudation, or microbial groups involved in plant defence. Identifying these specific responses would be particularly informative if coupled with functional approaches (e.g., metagenomics, metatranscriptomics, or targeted assays such as

qPCR), as this would provide insight not only into which taxa are affected by PCN but also into their ecological roles. Indeed, not only is it difficult to translate presence into function, but moreover, microbes such as bacteria can transition from the dormant to the active state within minutes to hours (Blagodatskaya et al., 2013), reflecting the difficulty in effectively capturing their dynamics, especially in soil systems. Dissecting specific root regions, such as PCN-infected vs uninfected areas, would also likely be required to more accurately resolve these localised microbial responses.

Moreover, it is important to note that over time, any ability of PPNs to manipulate the microbiome could be further compromised as plants increasingly shape their microbial communities to defend against nematodes (Elhady et al., 2018). In fact, it could be argued that this process might be further accelerated in the presence of a common mycorrhizal network, which has been shown to mediate defence signals from infected plants to neighbouring uninfected plants (Babikova et al., 2013, 2013a; Song et al., 2010, 2014, 2015, 2019). All in all, it remains difficult to untangle plant-mediated, soil-mediated, and PCN-mediated effects, a challenge that is further compounded when considering potential AM fungal-mediated interactions in these systems.

3.5.3 PCN-associated changes in AM fungi

Similar to overall fungi, the richness of AM fungi in the roots was also negatively affected by PCN-treatment (Figure 3.3). Moreover, contrary to what was indicated by the root ink-vinegar staining results presented in Chapter 2, their abundance in the roots also seemed to decrease under PCN infection, particularly pronounced at the Phylum using the ITS primers (Figure 3.6D). Considering that AM fungi are obligate symbionts, and that C is likely the main limiting resource for AM fungal communities (Smith & Read, 2008; Helgason & Fitter, 2009), this would not be so surprising if a PCN-induced reduction in plant-C delivery to the MN had been observed in my experiment. In fact, ecological theory developed to explain plant succession predicts that an increase in a limiting resource such as C often decreases both diversity and community evenness, as dominant competitors monopolise resources and outcompete others (Tilman, 1987).

An alternative explanation for the observed PCN-associated effects on AM fungi is plant defence. Just as AM fungi can mediate plant defence responses against pests, including PPN (Schouteden et al., 2015; Jung et al., 2012), PCN infection could trigger plant defences that

inadvertently suppress beneficial fungi such as AM fungi. Mycorrhizal establishment is thought to depend on the partial suppression of SA-dependent responses, compensated by an enhancement of JA-regulated pathways (Pozo & Azcón-Aguilar, 2007). By contrast, PCN infection induces strong JA activation and, to a lesser degree, SA signalling (Nahar et al., 2011), and both pathways are required for effective defence against migratory nematodes such as *Hirschmanniella oryzae* (Nahar et al., 2012). In the context of my study, the activation of SA in PCN-infected roots could interfere with the SA suppression normally associated with AM colonisation, thereby preventing the successful establishment of more SA-sensitive AM taxa and reducing fungal richness overall. Of course, such a scenario necessitates the persistence of an active SA pathway, suggesting that PCN did not fully evade host defences via transcriptional reprogramming, a strategy that has been documented for other migratory PPN (Kyndt et al., 2012). However, cyst PPN are generally thought to exert a more localised defence-suppression effect than migratory species (Kyndt et al., 2013), creating a heterogeneous immune landscape within the plant. Namely, locally around syncytia, PCN can suppress plant defences to maintain the feeding structure, which may also favour AM colonisation; yet systemically, JA and SA responses are activated under PCN infection, generating a defence response that is less favourable for successful colonisation by a diverse fungal community.

Another possible explanation for the reduction in AM fungi under PCN infection in roots is that AM fungi are directly competing with PCN for space and for plant resources (Schouteden et al., 2015). It has been shown specifically that in the presence of PCN, AM fungi receive less plant-derived C (Bell et al., 2022). The quality of C received by the AM fungi is also influenced by the presence of PCN, with hexose supply being shut down but fatty acid supply being maintained (Bell et al., 2024). This could mean that AM taxa that rely heavily on sugars are at a disadvantage, while those better able to use fatty acids may be less affected. For instance, members of the Glomeraceae are considered ruderal and fast-growing (Chagnon et al., 2013), suggesting a greater reliance on sugar-based C flow and, as such, potentially an increased propensity to be negatively influenced by PCN. Indeed, a trend of reduced relative abundance of Glomeraceae under PCN was observed in this study, particularly in the soil (Figure 3.8A and 3.9A, for the ITS and 18S datasets, respectively), although it was not statistically supported by differential abundance analyses (Figure 3.8C and 3.9C, for the ITS and 18S datasets,

respectively). The lack of significance may reflect the relatively low levels of PCN infection used here, as well as the conservative nature of the statistical approach (e.g., DESeq2 is particularly stringent when model structures are complex and data variation is high).

Polonosporaceae, a recently described AM fungal family with limited ecological characterisation (Błaszkowski et al., 2021), were negatively influenced by PCN, particularly in the roots (Figure 3.9D), possibly also suggesting sensitivity to C-sugar limitation or competitive disadvantage under host stress. Paraglomeraceae exhibited a similar trend, both in root samples at the Class level (Paraglomeromycetes; Figure 3.7) and in soil samples at the family level (Figure 3.9C), indicating that they were the most sensitive taxon to PCN infection in this dataset. As one of the most ancient AM fungal lineages, Paraglomeraceae are characterised by small to mid-sized spores (Aguilar-Trigueros et al., 2019) and a preference for developing extensive extra-radical mycelium rather than investing in root colonisation (Hempel et al., 2007), a pattern that was also confirmed by this study (Figure 3.9B). These traits have been linked to their limited plant-growth promotion (Säle et al., 2015) and likely translate into greater reliance on readily available host C, which may explain their reduced abundance under PCN-infected conditions in my dataset.

In any case, establishing links between shifts in AM fungal taxa and functional changes remains challenging, as trait-based knowledge for AM fungi is still very limited, with most data coming from only a few strains, primarily within the Glomeraceae (Chagnon et al., 2013; Marro et al., 2022; Antunes et al., 2025). Moreover, the available information is often inconsistent, making it difficult to draw general conclusions (Chaudhary et al., 2022; Antunes et al., 2025; Camenzind et al., 2024). For example, a global meta-analysis on the effects of AM taxonomic groups on plants under various stresses revealed that different taxonomic groups influence plant performance differently with and without stress (Marro et al., 2022); however, this did not follow the expectations proposed by Chagnon et al. 2013. Namely, Diversisporales rather than Gigasporales were the most beneficial to plants without stress, and Gigasporales rather than Glomerales were the most beneficial to plants facing biotic stress (Marro et al., 2022). Although not directly comparable since prior meta-analyses did not assess relative abundance among AM fungal families and I did not measure family-level effects on plant performance, my findings diverge from those general trends. In my study, Gigasporaceae were not enriched in PCN-infected roots, as might be expected if they indeed

conferred resilience to PCN stress, although this might be related to the fact that they seemed to be severely negatively impacted by PCN conditions in the soil. Furthermore, although both my ITS and 18S data support the traditional view that Gigasporaceae invest in extensive hyphal networks while Glomeraceae dominate root colonisation (Maherali & Klironomos 2007; Sike et al., 2009), this was not confirmed by differential analysis of either dataset.

Of course, it is important to note that trait variations and predictions are further constrained by the fact that AM fungi are shaped by numerous factors, many of which are study-specific. For example, plant growth stage can influence microbial community dynamics (Hannula et al., 2012), particularly for root fungi (Hannula et al., 2010). Specifically, among AM fungi, fast-colonising species belonging to Glomeraceae like *Funneliformis mosseae* may dominate P-transfer early in plant growth, whereas slower colonisers, such as Gigasporaceae, become more prominent at later stages (Blažková et al., 2021). These patterns are also closely linked to the plant host's life cycle, as slower plant growth and reduced C allocation can favour slower-growing mycorrhizal species (Blažková et al., 2021).

Finally, beyond the influence of the plant and/or PCN in shaping the microbiome, microbes themselves exhibit preferences and limitations regarding where they can establish and grow. As discussed in earlier chapters, AM fungi in particular can, in some cases, discriminate between plant hosts according to which offer the highest returns in terms of plant host resources (Kiers et al., 2011). If the PCN-infected host resources are compromised (or are likely to be compromised in the future due to increased levels of PCN infection), then it would make sense for AM fungi to preferentially associate with uninfected hosts. Not all fungi are likely equally capable of switching their host association, and the timings and individual thresholds that might trigger such a change will vary among species, as AM taxa show high functional variation, including in growth patterns (Thonar et al., 2011; Pringle and Bever, 2002), the distance they acquire nutrients from (Thonar et al., 2011), and their mechanism of mediating plant growth (e.g., via nutrient provision or pathogen protection; Sikes et al., 2009; Sikes et al., 2010).

From a plant perspective, it has been proposed that co-colonisation by AM fungal species with different traits may limit the plant's ability to differentiate among fungal partners and preferentially allocate C to the most beneficial taxa (Verbruggen and Kiers, 2010; Hart et al., 2013). This could, in turn, constrain the fungi's ability to discriminate among plant hosts. In

my experiments, even if some AM taxa were able to switch host association, this would likely be reflected in the observed reduction in AM fungal richness under PCN treatment. Notably, the presence of a MN connecting plants appeared to exacerbate the differences between PCN-infected and PCN-free plants within the mixed treatment (−/+) compared to the contrasts between the entirely PCN-free (−/−) and PCN-infected (+/+) treatment combinations, as indicated by diversity measures (Figure 3.2) and the proportion of shared fungal ASVs (Figure 3.4A).

3.5.2 Considerations regarding the use of ITS and 18S primers for assessing AM fungi

Both ITS and 18S primers showed higher richness for Glomeromycotan fungi in roots than in soil, which has been shown using ITS primers previously (Berruti et al., 2017) and could suggest that both primers are amplifying root-dominant taxa more efficiently. It has also been hypothesised that low levels of AM fungal soil diversity described by ITS primers could be due to the lower ratio of AM fungal biomass relative to overall fungal biomass in soil compared to roots (Berruti et al., 2017). That said, both primer sets seemed to suggest that the abundance of most Glomeromycotan Families was overall higher in soil than in roots, which aligns with the expectation that the majority of their biomass is in the soil where their extensive extra-radical mycelium is formed (Helgason and Fitter, 2009).

Within roots, differences in Observed richness but not in Shannon or Simpson diversity (particularly in the 18S dataset) suggest that PCN presence influences mainly rare mycorrhizal taxa, while dominant taxa remain relatively unaffected. Moreover, the slight discrepancy between ITS and 18S results could be because each primer is picking out a different subset of Glomeromycotan fungi (Figure 3.11). For example, given that ITS primers can under-amplify certain taxa (especially those at low abundance, whose DNA may be masked by the high diversity of other fungi) PCN-associated differences may be overestimated when using ITS primers. On the other hand, if the 18S primers are overamplifying certain PCN-resilient taxa, this could obscure any PCN-associated differences.

It is well known that sequencing studies come with multiple inherent biases depending on the marker region, primer pair, PCR conditions and sequencing platform used (Paloi et al., 2021; 2023). Biases relating to the use of ITS and 18S-based primers have already been discussed extensively before (e.g., Hijri et al., 2006; Hempel et al., 2007; Stockinger et al., 2010; Van Geel et al., 2014; Kohout et al., 2014; Tedersoo and Lindahl, 2016; Lekberg et al., 2018; Suzuki

et al., 2020). Part of the issue lies in the difficulty of designing primers that can target all fungi equally, whilst excluding other organisms and plant DNA. There is also the difficulty of a single genetic locus giving a clear cutoff between intra- and interspecific genetic variation.

This is particularly difficult for fungi, as defining an individual fungal taxon is challenging. For example, AM fungi present coenocytic hyphae and spores, heterokaryotic nuclear organisation, and the ability to fuse to form vast networks (Kokkoris et al., 2020). Partly due to these reasons, they also present high intraspecific variability (Matthieu et al., 2018). In theory, the ITS primers should allow for more resolution in terms of species differentiation due to the more variable ITS1 region (Stockinger et al., 2010). Although this poses the danger of inflated diversity due to oversplitting (i.e., more unique ASVs identified whilst some are actually variants of the same individual), in this study, this has been controlled through LULU curation, which helps collapse intragenomic variants, and by working with ASVs that have been assigned to at least the Phylum level. For AM fungi, however, the ITS region is highly variable (i.e., exhibits high intraspecific variability; Thiery et al., 2016), which can hinder resolution of closely related species (Stockinger et al., 2009, 2010) and potentially lead to overestimation of Glomeromycotan richness.

However, this does not appear to have occurred in the present study, as overall Glomeromycotan richness was lower in the ITS dataset (Figure 3.3). This may reflect the limited characterisation of fungal diversity, including Glomeromycota (Öpik et al., 2013), which constrains accurate taxonomic assignment of ASVs from metabarcoding studies. Indeed, the comprehensiveness of reference databases is often the main factor driving bias when using different databases for taxonomy assignment (Berruti et al., 2017; Xue et al., 2019). This limitation is particularly pronounced for studies using the ITS region, which has been less widely applied in AM fungal metabarcoding, resulting in less complete reference databases. Additionally, the ITS primers used in this study span a slightly unconventional region, incorporating a portion of 18S to enhance capture of mycorrhizal fungi. Consequently, standard ITS reference databases are not fully suitable for taxonomic assignment, and, as indicated by my *in silico* analysis, the longer-read reference database used contained substantially fewer representative sequences for each Glomeromycotan family (Figure 3.10), potentially limiting the ability to assign taxonomy to some genuine Glomeromycotan ASVs.

To control for some of these biases, the use of primer combinations has also been suggested (Bellemain et al., 2010). Previously, general ITS (targeting ITS2) and AMF-specific 18S primers revealed similar trends in AM fungal community composition in three mountain vineyards (Berruti et al., 2017). Diversity measures across locations were also similar between the two primer sets, but the ITS primer underestimated AM fungal diversity in the soil (Berruti et al., 2017). More studies using ITS primers on soil samples have reported receiving low levels of Glomeromycota sequences (i.e., less than 5%; Leff et al., 2015; Tedersoo et al., 2015). That said, the difficulty in ensuring enough sequencing depth to capture Glomeromycota taxa has likely diminished with next-generation sequencing compared to older cloning and Sanger sequencing (Lekberg et al., 2018). Lekberg et al (2018) also compared a general fungal ITS primer (one that targeted the ITS2 region and is theoretically less representative of AM fungi) with 18S primers and detected some discrepancies in phylogenetic community composition, but no consistent difference in observed or extrapolated richness. In a different study looking at the traceability of AM inoculants in the field, 18S primers recovered a greater diversity than ITS primers targeting the ITS2 region (Berdeja et al., 2025), a trend which was also observed in this study. To further explain potential primer biases between the primers used in this study, a more in-depth *in silico* analysis paired with a metabarcoding study using artificial mock communities would be needed. Phylogenetic analysis would also help to assign phylogenetic placement and refine taxonomic assignments.

Chapter 4. Plant herbivory influences the movement of plant-fixed carbon through an arbuscular mycorrhizal network independently of microbial community changes

4.1 ABSTRACT

In Chapter 2, I presented evidence that plant-derived carbon (C) moves within a mycorrhizal network (MN) away from potato cyst nematode (PCN)-infected plants. In Chapter 3, I explored whether PCN-associated changes in the wider microbial environment could be influencing this C movement and found that a PCN-associated reduction in fungal richness—including arbuscular mycorrhizal (AM) fungi—may play a role. However, due to the lack of functional analysis and limited trait-based information on AM fungi, a conclusive assessment of the relative importance of microbial community changes versus the intrinsic capacity of AM fungi to preferentially move C within the MN could not be reached. In this chapter, I employ tripartite, compartmentalised *in vitro* microcosms, stripped of the microbial complexity found in soil, to further investigate MN-mediated C movement under simultaneous above- and below-ground herbivory (PCN and aphids) of host plants. I found that more plant-derived C was transported to a neighbouring compartment hosting a herbivore-free plant than to a compartment hosting a herbivore-infected plant. This trend was consistent regardless of the herbivore treatment of the ^{14}C-labelled plant. These findings underscore the capacity of AM fungal networks to regulate C movement according to the herbivore status of host plants. Importantly, this regulation appears independent of herbivore-induced changes in microbial communities and persists even when overall C delivery by host plants remains unchanged.

4.2 INTRODUCTION

The debate regarding the regulation of the carbon (C) for nutrient exchange in the arbuscular mycorrhizal (AM)-plant symbioses remains ongoing (e.g., Corrêa et al., 2023; Bunn et al., 2024). One of the key observations from reviewing the relevant literature (Chapter 1) was that aspects of the experimental design, such as the scale (e.g., Petri dish vs pot) and the medium (e.g., agar vs soil) of the study system, often correlated with the extent to which the findings supported a 'reciprocal rewards'-type regulation as described by Kiers et al. (2011), where plant and/or AM fungi can control aspects of the exchange of resources for their benefit. Specifically, it appears that, in comparison to larger-scale, soil-based experiments which employ whole plants under concurrent symbioses with other, non-AM organisms, the smaller-scale and more regulated or artificial an experiment is, the more likely it is to support a tightly regulated C-for-nutrient exchange (Chapter 1; Magkourilou et al., 2024).

Consistent with the above observation, the soil-based study described in Chapter 2 did not support a resource-based 'reciprocal rewards' model of regulation. Although plants without potato cyst nematode (PCN) infection received slightly more fungal-acquired ^{33}P, the AM fungi did not, in turn, receive more C from PCN-free plant hosts. However, it is important to note that these results stem from two separate experiments, which, although almost identical, limit our ability to link the C-for-nutrient exchange dynamics specifically within each system. Moreover, although soil-based experiments offer a more realistic setting for plant-AM symbioses to occur, soil complexity can create endless interactions which are difficult to track, and which could directly or indirectly influence the C-for-nutrient exchange between plant and AM fungi. This was partly explored in Chapter 3, where I found that PCN infection reduced root fungal species richness (including AM fungal richness) and also altered community structure and the relative abundance of various taxa. Although I could not specifically assess the direct implications of this on the C-for-nutrient exchange, in Chapter 3, I also discussed the many ways that such changes in microbial communities, whether predominantly plant, PCN or microbial-mediated, could influence the C-for-nutrient exchange via changes in C and nutrient cycling.

More specifically, instead of PCN-induced shifts in microbial communities influencing the distribution of fungal-acquired P and plant-derived C within the mycorrhizal network (MN), it is also possible that PCN-driven changes in C and P distribution within the MN are themselves

driving alterations in the microbial environment. Another unresolved question from the study presented in Chapter 2 was why the MN moved C away from the PCN-infected plant when, in reality, my results suggested that it was not receiving more C from the plant on that other side. In an attempt to gain more insights that could help explain the above, here, I set up a more controlled experiment, stripped of the complexity introduced by the soil microbiome.

As well as exposing plants to below-ground herbivory, I also introduced above-ground herbivory in the form of the aphid (*Myzus persicae*). Aphids are sap-sucking herbivores rather than root feeders, but similar to PCN (Bell et al., 2022), they have also been previously found to disrupt the C-for-nutrient exchange between plant hosts and their AM fungal symbionts (Charters et al., 2020). In a more complicated system involving two neighbouring plants presumably connected via an AM mycorrhizal network (MN), aphid-induced C losses to the MN were partly compensated by uninfected neighbours (Durant et al., 2023). Put another way, in that experiment, it seemed as if uninfested plants incurred an aphid-derived cost as they were the ones predominantly supporting the MN with C, without this being matched by an increased allocation of the fungal-acquired nutrient supply (Durant et al., 2023).

Aims

Here, I focus on plant-C and test whether simultaneous above- and below-ground herbivory on *in vitro* microcosms reduces plant C allocation to the MN, as observed in soil mesocosms. Using compartmentalised tripartite Petri dishes with three plants (each exposed or not to herbivory) and a shared AM fungal network, I also examine whether plant-derived C is preferentially directed to herbivore-free plants over those experiencing herbivory.

4.3 MATERIALS AND METHODS

4.3.1 Experimental design and establishment

Two different treatment combinations were established using tripartite plastic Petri dishes (90 mm diameter) where the dish's raised walls separated the three plant compartments, but AM fungi could grow on a thin layer of gel medium above the walls. Each experimental system consisted of an allocated 'labelled' plant and two 'receiver' plants. For each pair of receiver plants, one plant was exposed to above- and below-ground herbivory ('+'), whereas the other plant was not ('–'). Moreover, in some experimental systems, the 'labelled' plant was also exposed to herbivory, whereas in others, the 'labelled' plant was herbivore-free.

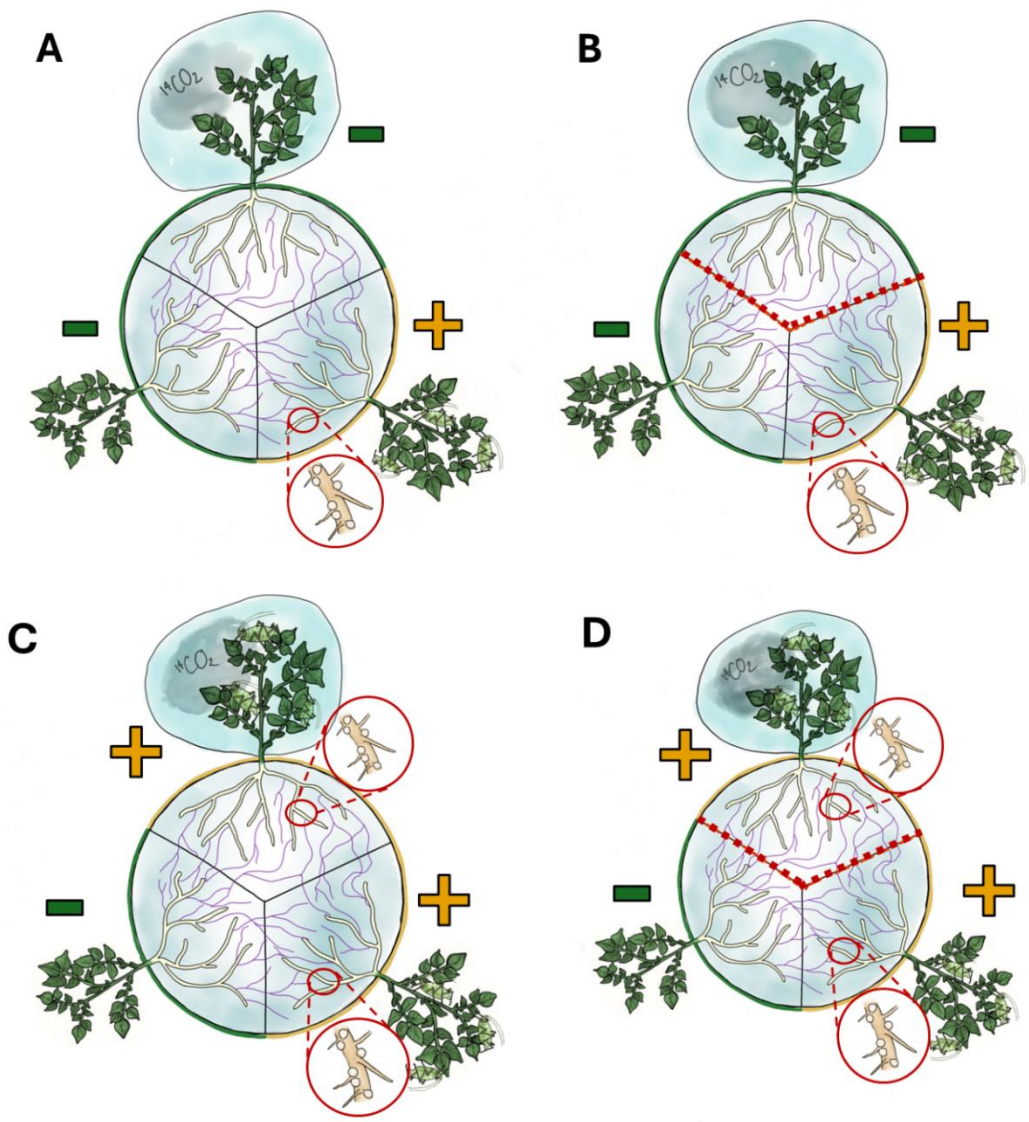

Figure 4.1 Treatment combinations used to test the effects of above-ground (aphids) and below-ground (PCN) herbivory on carbon exchange between plants and AM fungi in tripartite compartmentalised Petri dishes. Each system contained one 'donor' ^{14}C-labelled plant and two non-labelled 'receiver' plants, which could be connected via one or more *Rhizophagus irregularis* networks (purple lines). Plants without a biotic pressure are indicated by '–' with green borders, whereas plants experiencing a biotic pressure are indicated by '+' with orange borders. ^{14}C-labelled plants were either herbivore-free (**A**) or herbivore-infected '+' (**C**), while the receiver plants always had contrasting herbivory treatments. Panels **B** and **D** show the corresponding 'control' treatments, in which the MSR medium around the ^{14}C-labelled plant was trenched and backfilled to sever mycorrhizal connections with the rest of the dish.

To establish the systems, using heated forceps, small holes (~2 mm diameter) were made through the cover and base at each compartment edge of the tripartite Petri dish, which had already been filled with Modified Strullu-Romand (MSR) medium (see Table S4.1 for the recipe). Using these holes as a base for the stem, approximately two-week-old plantlets were then inserted into each of the three compartments of the Petri dishes. At the same time, a similar quantity of crushed AM fungal inoculum (*Rhizophagus irregularis* MUCL 41933; derived from an axenic Ri T-DNA transformed *Daucus carota* root organ culture) was added on top of the MSR medium, in the middle of each dish. The holes around the stems of the plantlets were blocked with autoclaved lanolin, and the Petri dishes were sealed with 3M™ Micropore Tape to prevent contamination. The Petri dishes were also wrapped in aluminium foil to keep the roots in darkness, while allowing the shoots to grow under light conditions. The systems were stored horizontally at room temperature under LED lights (XS1500, VIPASPECTRA; two panels of range 1000-800 µmol/m^2/s suspended at 24 cm) with a 14 h light / 10 h dark photoperiod.

Approximately four weeks later, the Petri dishes were opened under the flow hood so that the MSR media could be replenished, the roots trimmed to contain them within each compartment, more AM fungal inoculum added, and a total of approximately 30 PCN J2 juveniles pipetted on at three different positions on the roots of each '+' designated plant. The PCN juveniles had been hatched from cysts infused in filter-sterilised potato root exudate. The cysts had been treated in 0.1% malachite green for an hour and then left in sterile water overnight. The cysts were also then treated in an antimicrobial cocktail (see Table S4.2 for the recipe) at 4°C for approximately 9-24 h. After hatching, the J2s themselves were also treated in an antimicrobial cocktail (see Table S4.2 for the recipe) for 15 min, and washed in sterile water and 0.01% Tween before they were immediately added to the experimental systems as described above. Despite every effort to keep the system axenic, some amounts of fungal and bacterial contamination were observed, which resulted in almost half of the experimental systems that were originally set up being discarded. Finally, I only performed ^{14}C-labelling (see details below) on those systems that only showed minimal amounts of bacterial growth under microscopic evaluation. It is also worth noting that although I had confirmed successful PCN infection of roots using the same method in experimental trials (Figure 4.2B), in the actual experiment, it was not possible to visually confirm the levels of PCN infection on the roots

due to how densely the root systems developed. However, the growth of the AM mycelium was visually confirmed, and multiple hyphae were seen crossing the raised walls on the thin layer of MSR medium linking the compartments (Figures 4.2C and D).

Approximately three weeks after adding the PCN, two aphids (*Myzus persicae*) were placed on the leaves of the designated '+' plants and left to feed for two days, before the systems were ^{14}C-labelled, and then harvested. The aphids were retained within clip cages (see Durant et al., 2023 for more details). Empty clip cages were also added to the plants not exposed to aphids, to control for any potential impacts of the cages themselves.

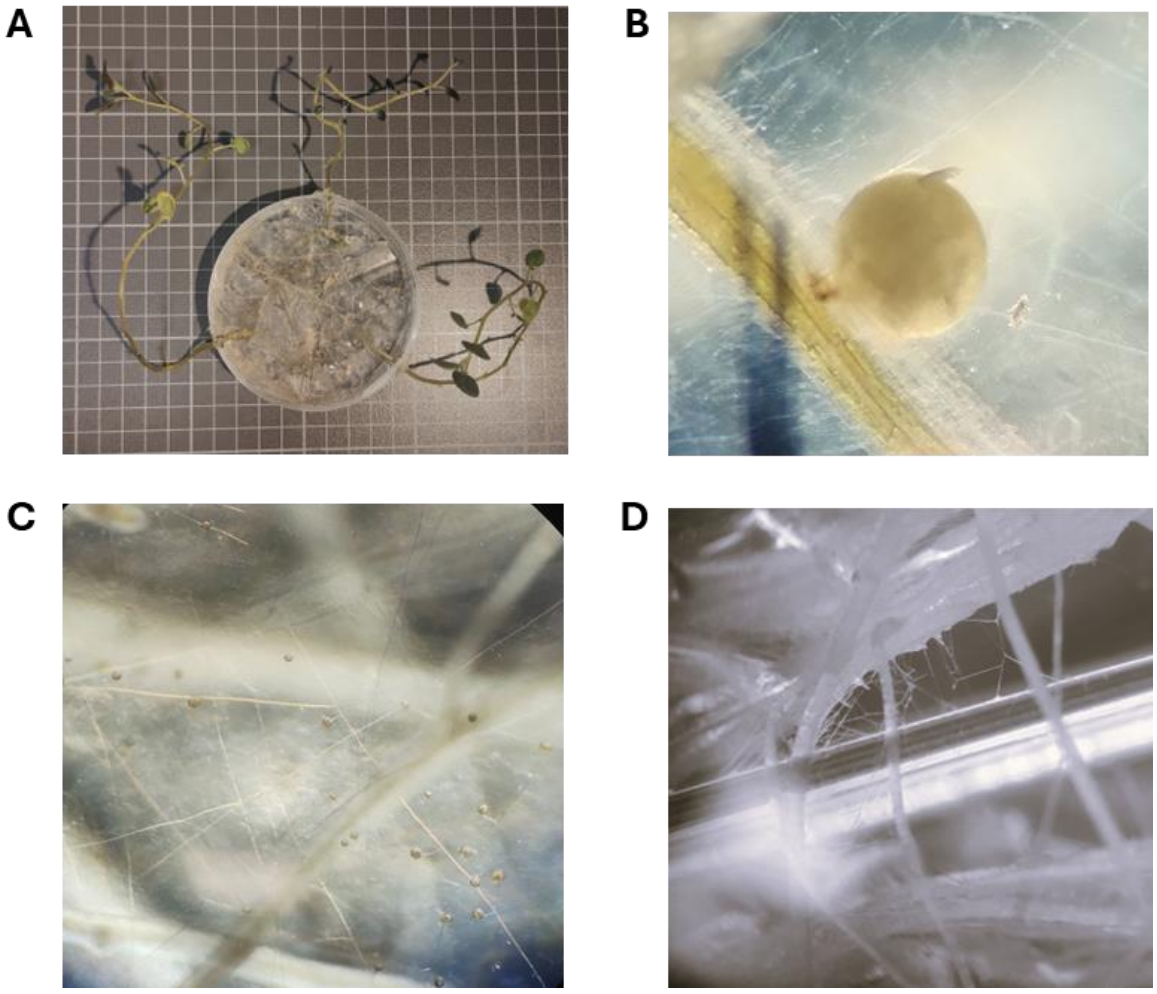

Figure 4.2 A. An example of the microcosms used to track the movement of plant-derived C within the AM fungal network using tripartite compartmentalised Petri dishes. Each system contained one ^{14}C-labelled 'donor' plant and two non-labelled 'receiver' plants; **B.** An example of a PCN cyst growing on roots in MSR medium, and **C.** and **D.** *Rhizophagus irregularis* networks growing in similar systems.

4.3.2 Tracing plant-to-fungus C transfer

Approximately eight weeks after establishment, the above-ground tissue of all plants was enclosed within polythene bags (Polybags Ltd., London, UK), sealed airtight using anhydrous lanolin and cable ties at the base of the plant stem. In the four 'Control Dishes' (two where the ^{14}C-labelled plant had a '+' treatment and two where the labelled plant had a '– ' treatment), the MSR medium around the plastic border surrounding the ^{14}C-labelled plant was trenched and removed (approximately 2mm) and then backfilled. These 'control' dishes were used to account for any movement of ^{14}C via diffusion and other non-fungal means, and to ensure that plant-fixed C transferred from the ^{14}C-labelled plants to the compartments around the non-labelled plants occurred via the MN.

$^{14}CO_2$ was liberated into the chamber of each of the allocated ^{14}C-labelled plants (n = 6 for '– ' and n = 7 for '+', including two trenched 'controls' for each) by adding 1.5 mL 10% lactic acid to a cuvette containing 100 µL ^{14}C-sodium bicarbonate (specific activity: 1.62 GBq $mmol^{-1}$; total activity released: 0.25 MBq; Perkin Elmer, USA). Plants were left in situ for 24 h post-labelling, at which point 1.5 mL of 2 M KOH was added to vials within each labelled chamber to capture any remaining gaseous $^{14}CO_2$. At the end of the experiment, root-free sub-samples of the MSR medium containing AM fungal mycelium were collected from each of the three compartments per Petri dish to estimate the amount of recently fixed plant-derived C allocated to the fungus (i.e., fungal C; see below for details).

4.3.3 Quantification of host-fixed C in fungi

An average of 27 mg of the freeze-dried MSR medium containing the AM mycelium from each of the three compartments per Petri dish was weighed in triplicate into Combusto-cones (PerkinElmer, Beaconsfield, UK). ^{14}C was measured following sample oxidation (Model 307 Packard Sample Oxidiser; Isotech, Chesterfield, UK) with released $^{14}CO_2$ from burnt agar medium samples trapped in 10 mL of the liquid scintillant CarbonTrap and mixed with 10 mL CarbonCount (Meridian Biotechnologies Ltd., Tadworth, UK). Radioactivity was quantified by liquid scintillation counting (Packard Tri-Carb 4910TR; PerkinElmer). The total C (i.e., $^{12}CO_2$ and $^{14}CO_2$) contained in each MSR sub-sample was calculated by quantifying the total CO_2 volume and content mass in the labelling chamber and the proportion of the supplied $^{14}CO_2$ that was photosynthetically fixed by the plant during the 24 h labelling period (see Durant et al., 2023 for detailed equations as adapted from Cameron et al., 2008).

The distribution of ^{14}C was also visually assessed in one randomly selected microcosm. After labelling, the sample was exposed to a phosphor storage screen for 24 h in a dark cassette. The phosphor screen was then scanned using a Typhoon FLA 7000 imaging system using the 'phosphorimaging' mode at 100 µm resolution with a photomultiplier tube setting of 500V.

4.3.4 Statistical analysis

All statistical analyses and figure construction were performed in RStudio (RStudio Team, 2025) using the R programming language (R Core Team, 2023). The total C per dish (as a concentration ng per gram) was log-transformed to meet general linear models assumptions and analysed with one-way ANOVA to test whether the biotic treatment of the ^{14}C-labelled plant influenced the overall amount of C transferred. Assumptions for the use of general linear models were validated by plotting residuals versus fitted values, square root residuals versus fitted values, normal qq plot, and constant leverage using the *autoplot* function of the `ggplot2` R package (Wickham, 2014). The effect of trenching the MSR medium around the designated 'control' Petri dish was tested using the proportion of C in each compartment relative to the total for each dish. This was analysed using beta regression mixed-effects models (*glmmTMB*) to account for the bounded nature of the response variable (0–1) and potential heteroscedasticity, with 'Petri dish' also included as a random effect to account for paired measurements. A similar model was used to test the effect of the biotic treatment of the ^{14}C-labelled plant as well as the effect of the plant on the 'receiving' compartments, as well as their interaction. Model assumptions were evaluated using residual diagnostics from the `DHARMa` R package (Hartig, 2025), including checks for linearity, dispersion, zero-inflation, and uniformity of residuals.

4.4 RESULTS

The total C recovered per Petri dish did not statistically differ based on the treatment of the ^{14}C-labelled plants ($F = 0.16$; $p = 0.70$; Figure 4.3). This suggests that labelled plants delivered the same amount of total C below-ground regardless of whether they were under biotic pressure ('+') or not ('–').

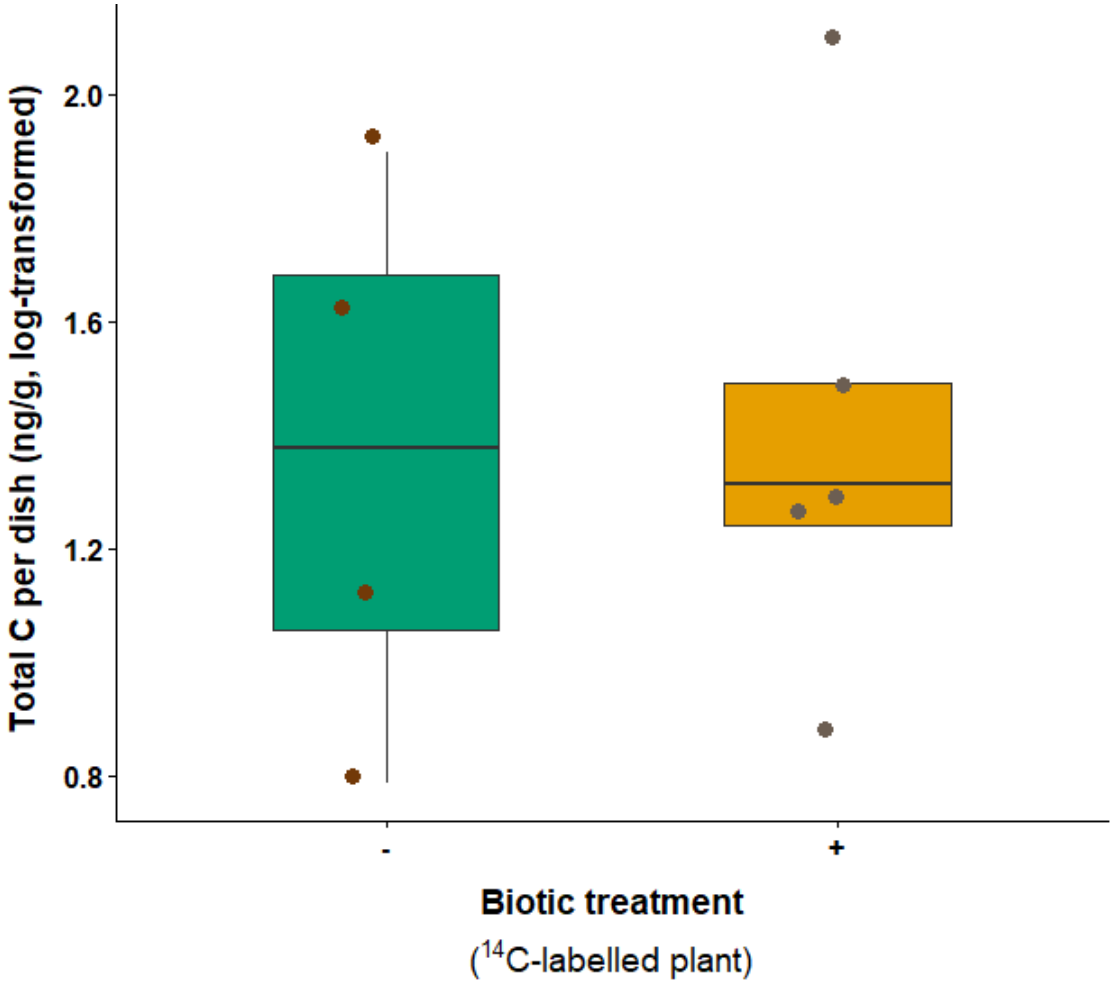

Figure 4.3 Total plant-derived C recovered in each Petri dish based on the herbivory treatment of the ^{14}C-labelled plant. Boxplots span the interquartile range (IQR), the line inside marks the median, and whiskers extend to 1.5 × IQR. Points outside are potential outliers. Labelled plants without herbivory are indicated by '–' and green colour, whereas those with herbivory are indicated by '+' and orange colour.

As expected, the largest proportion of C recovered from the experimental systems was retained around the compartments of the ^{14}C-labelled plants ($\chi^2 = 22.99$, $p < 0.01$; Figure 4.4). This pattern was observed both when the ^{14}C-labelled plants received a biotic treatment and when they did not ($\chi^2 = 1.95$, $p = 0.16$). However, an interaction effect indicated that retention around the compartments of the ^{14}C-labelled plants was slightly more pronounced when the labelled plants were herbivore-free ($\chi^2 = 3.92$, $p = 0.0477$; Figure 4.4). In any case, a substantial amount of C was indeed transferred *away* from the ^{14}C-labelled plant towards the non-labelled compartments.

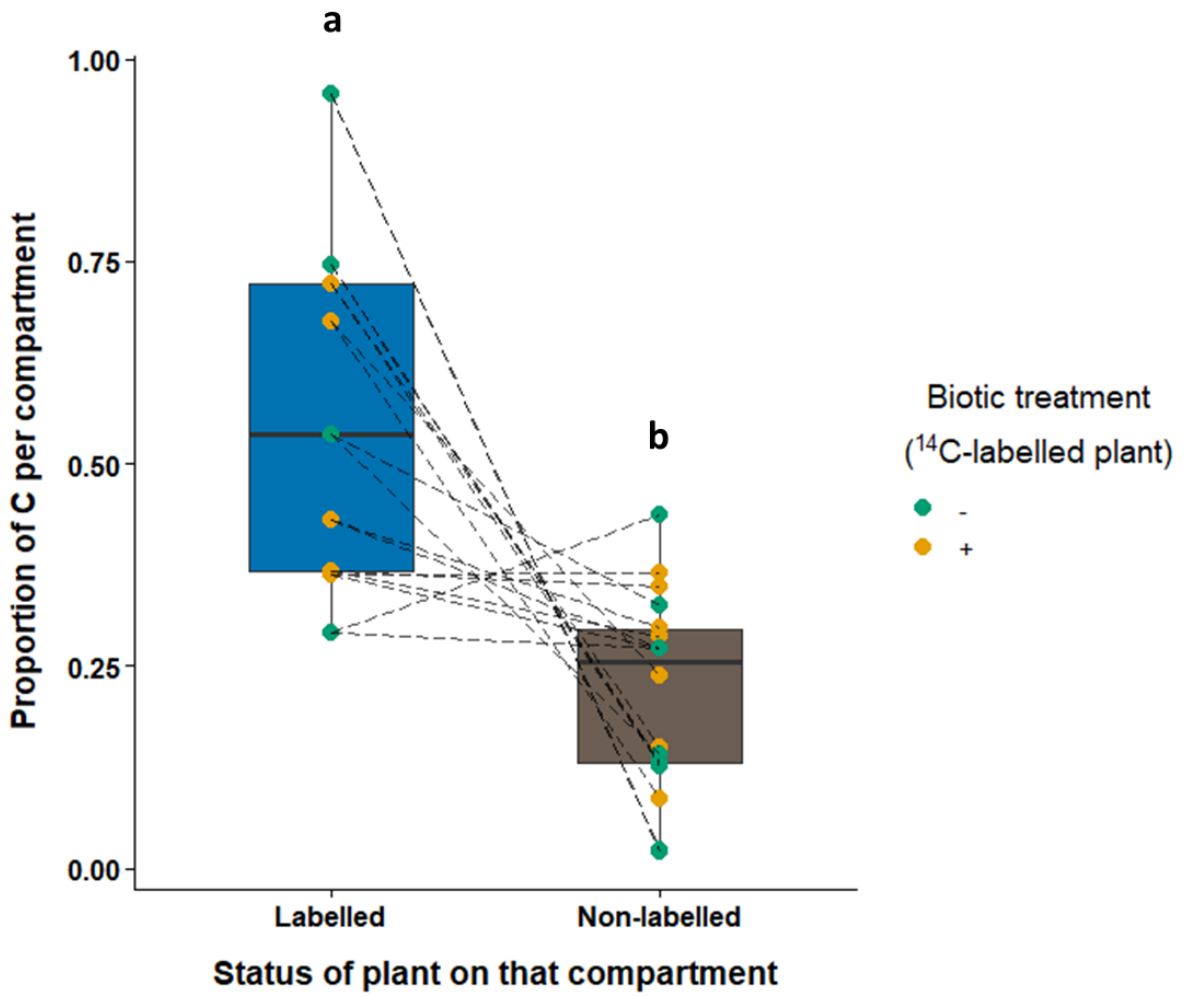

Figure 4.4 Proportion of C contained in each compartment based on whether that compartment was around the ^{14}C-labelled plant or not. Proportion calculations are based on concentration values (i.e., ng of C g^{-1} tissue). Letters above boxplots indicate significant differences based on the 'labelled' or 'non-labelled' status of the compartment ($p < 0.05$; Generalised Linear Mixed Model). Dashed lines connect compartments belonging to the same microcosm. Boxplots span the interquartile range (IQR), the line inside marks the median, and whiskers extend to 1.5 × IQR. Points outside are potential outliers. The individual points are also coloured based on whether the ^{14}C-labelled plant in that microcosm was exposed to herbivory (indicated by '+' and orange colour) or not (indicated by '–' and the green colour).

Importantly, the proportion of C that moved to compartments around the non-labelled plants in the 'control dishes' (where the hyphal connections were severed just before ^{14}C-labelling) was significantly lower than the proportion of C that moved to the compartments around the

non-labelled plants in the 'connected dishes' (where hyphal connections were left intact; Figure 4.5). This indicates that transfer in the 'connected dishes' was not merely due to diffusion or other, non-fungal means.

Within the 'connected dishes', the proportion of C that moved to the compartments around the non-labelled plants was significantly higher if these plants were herbivore-free ('–') than if they were exposed to herbivores ('+'). This did not appear to be further influenced by the herbivore treatment of the ^{14}C-labelled plant (Figure 4.5).

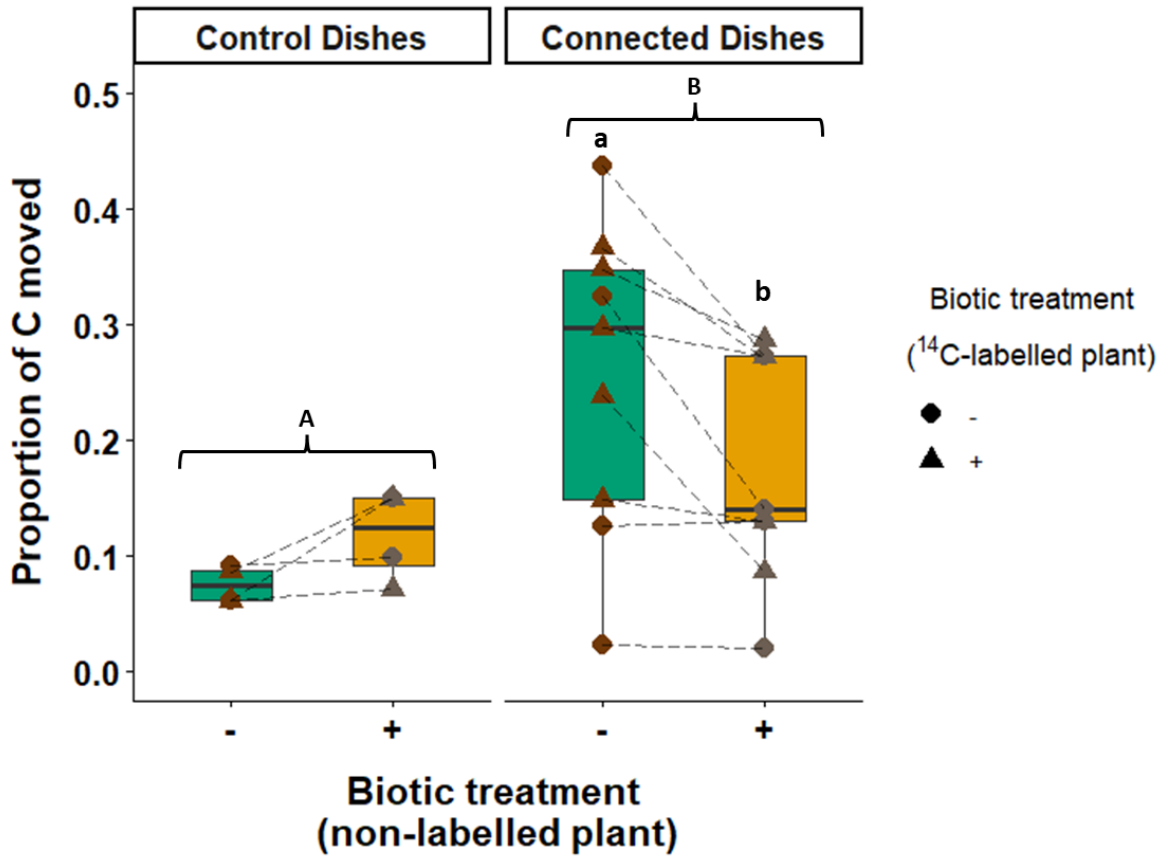

Figure 4.5 Proportion of C derived from the ^{14}C-labelled plant that is contained in the compartments of non-labelled plants, shown according to their herbivory treatment. Proportion calculations are based on concentration values (i.e., ng of C g^{-1} tissue). The 'Control Dishes' panel refers to the microcosms where the hyphal connections were severed just before labelling, whereas the 'Connected Dishes' panel refers to the microcosms where the hyphal connections were left intact. Dashed lines connect compartments belonging to the same microcosm. Capital letters above grouped boxplots indicate significant differences based on the 'severing control treatment', whereas small letters indicate differences based on the 'biotic treatment' of the non-labelled plant ($p < 0.05$; Generalised Linear Mixed Model). Boxplots span the interquartile range (IQR), the line inside marks the median, and whiskers extend to 1.5 × IQR. Points outside are potential outliers. Compartments of herbivore-free non-labelled plants are indicated by '−' and green colour, whereas compartments of non-labelled plants with herbivory are indicated by '+' and orange colour. Shapes denote the herbivory treatment of ^{14}C-labelled plant as per legend.

The qualitative data visually confirmed that the compartment around the herbivore-free plant (−) had a slightly higher concentration of ^{14}C than that around the herbivore-infested plant (+). That said, as per the quantitative data, it appears that most of the ^{14}C was retained around the labelled plant (Figure 4.6B). Moreover, it is worth noting that based on the quantitative data, the system that was randomly picked for visual inspection was not the most extreme example in terms of C movement to the non-labelled compartments. Specifically, the non-labelled compartments contained approximately 25% of the detected C, whereas the average for all the other systems was 44%. The overall concentration of C detected across the system was also relatively low at 84.9 (ng/g) vs the average of 526.0 (ng/g), which might explain why the signal that was picked up is not more pronounced.

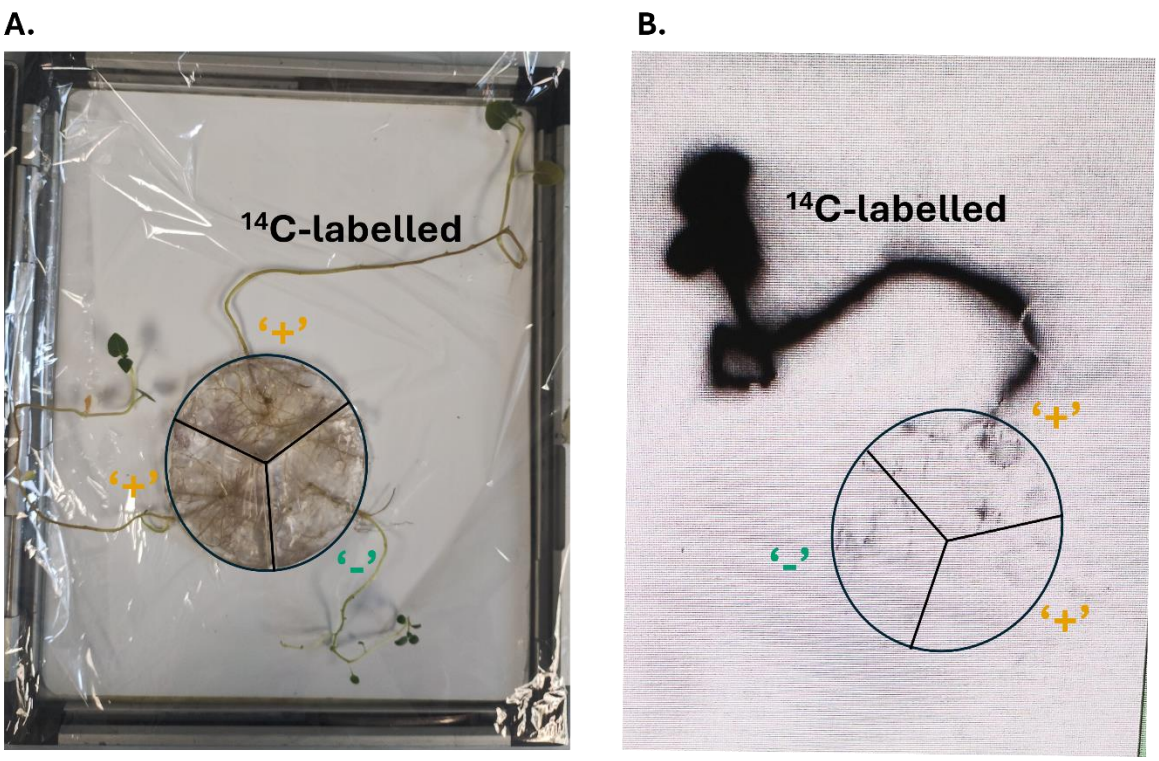

Figure 4.6 A ^{14}C-labelled experimental microcosm consisting of one ^{14}C-labelled 'donor' plant and two non-labelled 'receiver' plants, connected by an AM fungal network. The system is placed on a phosphor storage screen just before scanning, and **B.** Detection of ^{14}C in the same experimental system after scanning using a Typhoon FLA 7000 imaging system. The sample was exposed to the phosphor storage screen for 24 h in a dark cassette, after which the screen was scanned in Storage Phosphor mode at 100 µm resolution with a PMT setting of 500. Signal intensity is shown in grayscale, with darker areas corresponding to stronger ^{14}C emission. Compartments without herbivory treatment are indicated by '–', whereas compartments with herbivory are indicated by '+'.

4.5 DISCUSSION

Previously, plant herbivory by aphids (Charters et al., 2020) or PCN (Bell et al., 2022) has been found to lead to a reduction in the amount of plant-C allocated to AM fungi, although the fungal-acquired provision of nutrients to the plants was largely maintained. Similar to Chapter 2, this herbivore-induced C reduction was not confirmed here using simultaneous aphid and PCN infection, as the total plant-derived C retrieved across the Petri dishes did not differ based on the herbivore treatment of the ^{14}C-labelled plants (Figure 4.3). However, in contrast

to the work done by Charters et al. (2020) and PCN (Bell et al. 2022), where single plants were used, here I used compartmentalised microcosms with three neighbouring plants, possibly connected by the same MN. As it was also discussed in Chapter 2, plant–plant interactions can strongly influence the amount of resources invested below-ground (Weiner & Thomas, 1992), and this also appears to be the case here. Common mycorrhizal networks (CMNs) may intensify competition between neighbouring hosts (Merrild et al., 2013; Weremijewicz et al., 2016), and potentially force plants to adjust their below-ground C allocation in relation to the C supplied by their neighbours (Wyatt et al., 2014).

Based on their finding that plant-C allocation to the AM network increased only when one plant was infested by aphids compared to when both plants were infested, Durant et al. (2023) hypothesised that the uninfested plant was the primary C contributor to the MN in the (−/+) scenario. However, the individual contributions of each plant were not directly measured, leaving open the possibility that aphid-infested plants also increased their C allocation when neighbouring an uninfested plant—perhaps to compete with the uninfested plant and maintain their association with the MN. If so, the uninfested plants would not have been the sole C providers to the MN.

As discussed in Chapter 2, once assimilated by the MN, plant-derived C moved away from the PCN-infested plants in a soil-based system of two neighbouring plants. Interestingly, the movement of C was not influenced by the PCN infection status of the plant on the other side (i.e., C moved similarly towards PCN-infected and PCN-free plants), although this comparison was somewhat limited by a lack of replication. Here, by using compartmentalised microcosms with three plants, I was able to more fully explore the spatial distribution of plant-fixed C. Similar to Chapter 2, it appears that the MN was distributing plant-derived C away from the herbivore-infected plants (Figure 4.5), even in the absence of a plant-herbivore-induced reduction in the total amount of plant-C delivered to the MN (Figure 4.1). However, in contrast to Chapter 2, rather than just comparing how much C stayed versus how much C moved away from the ^{14}C-labelled plant based on the PCN treatment combination, here, I could compare how much C moved away from the labelled plant towards a herbivore-infected or a herbivore-free neighbouring plant situated at an equal distance. This is important because it enhances the evidence for the preferential nature of the C transfer. Moreover, importantly, I could confirm the movement of C within MN in the absence of any herbivore-

associated changes in the soil or root microbiome, which, as discussed extensively in Chapter 3, could have directly or indirectly influenced the C-for-P exchange.

Interactions between aphids and plant-parasitic nematodes (PPN), such as PCN, are not well understood. In general, it is thought that the presence of herbivorous insects may influence PPN activity, and conversely, PPN can positively or negatively affect shoot-feeding herbivorous insects (Wondafrash, Dam, and Tytgat, 2013). For example, root-feeding by the cyst nematode *Heterodera schachtii* can lead to reduced aphid body size (Hol et al., 2010) and infection by root-knot nematodes has been shown to trigger defence responses against aphids, partly mediated by changes in plant volatile organic compounds (Shi et al., 2022), with similar effects reported for other insect herbivores (Guo and Ge, 2017; Hong et al., 2010). If this applies in the current experiment, aphid-induced damage may have been limited, as plants had already experienced two weeks of root herbivory before aphid addition. Ultimately, this would suggest that the effect of herbivory on C movement within the MN could be even more pronounced under a more coordinated herbivore attack. In any case, as with soil-based mesocosms, evidence from these *in vitro* microcosms supports the idea that even low levels of herbivory can alter the distribution of plant-derived C within the MN, and that this occurs without a corresponding reduction in the overall C supplied by plants to the MN. More importantly, this experiment suggests that such changes can take place independently of herbivore-associated shifts in the microbial environment. Future work could further confirm the mechanisms through microbial inoculation experiments, in which communities from PCN-infected or uninfected plants are transferred to PCN-free plants, and the resulting distribution of fungal-acquired P and plant-derived C is monitored as before.

Chapter 5. Neighbouring plant infection by parasitic nematodes does not alter non-volatile metabolites via below-ground signalling, but induces subtle shifts in headspace VOCs

5.1 ABSTRACT

Plants use metabolites, such as volatile organic compounds (VOCs), for internal coordination and external communication with other plants and organisms. Mycorrhizal networks (MNs) can act as conduits for below-ground defence signalling, including the transfer of defence-related VOCs. Building on the previous chapter, where I showed that PCN-induced changes in C distribution within MNs can occur independently of microbial shifts or overall C allocation, here, as another alternative mechanism, I test whether PCN infection alters leaf non-volatile metabolites and VOCs in focal and neighbouring plants. To do so, I analysed metabolites using MALDI-TOF MS and VOCs GC-MS. Leaf non-volatile metabolite composition and intensity were overall unaffected by PCN infection. However, in mixed treatments, infected plants consistently exhibited higher defence-related metabolite intensities than their uninfected neighbours, suggesting no defence-related signalling between plants. This further suggests that the increased contribution of fungal-acquired P to PCN-free hosts in the mixed treatment (as observed in Chapter 2) did not translate into AM-mediated priming of plant defences. In contrast, VOC profiles were significantly shaped by neighbour PCN status: PCN-free plants adjacent to infected neighbours displayed distinct blends, likely driven by Tricyclene—the most abundant compound—even though no single VOC showed significant log-fold changes with PCN treatment. These findings suggest that PCN influence VOC profiles through subtle, coordinated, system-wide shifts rather than changes in individual metabolites. The mechanism is likely below-ground, and future work should determine whether this occurs via root exudation, below-ground VOC diffusion, or MN connectivity. In any case, plant–plant communication via VOCs does not appear to play a role in shaping AM resource allocation in my systems.

5.2 INTRODUCTION

Plants do not live in isolation; rather, they form interactions with con-specific and heterospecific plant neighbours as well as with other above- and below-ground organisms. As one strategy to mediate these interactions, plants release a diverse array of volatile organic compounds (VOCs) that serve as chemical signals (Badlwin, 2010). For example, when under herbivore attack, stressed plants often modulate their VOC emissions, releasing blends of herbivore-induced plant volatiles (HIPVs) that act as airborne cues, including terpenes, green leaf volatiles (GLVs), benzenoids, or jasmonate-related volatiles (Turlings and Erb, 2018). These volatiles can act as an internal signal in response to herbivore attack (Frost et al., 2007) or as an inter-plant signal to potentially prime neighbouring 'naïve' plants to activate defence pathways in anticipation of stress (Farmer and Ryan, 1990). In some cases, the emitted VOCs also recruit natural enemies of herbivores (Thaler, 1999), thereby potentially contributing to indirect defence strategies (Dicke and Baldwin, 2010). It has also been suggested that plant microbial pathogens can also manipulate plant VOCS to attract insect vectors (Hammerbacher et al., 2019). As well as activating plant defences, VOCs are also thought to suppress plant defences, although the mechanisms for this are less clear (Erb, 2018). Importantly, the specificity and intensity of VOC signalling can vary with the nature of the stress, the identity of the emitting plant, and the ecological context, suggesting a highly dynamic communication system (McCormick, et al., 2012).

Beyond airborne volatiles, non-volatile metabolites also play critical roles in signalling within an individual plant, as, among other things, they contribute to the regulation of plant defences and stress responses, albeit in a more localised manner than VOCs (Li et al., 2023). For example, below-ground, AM fungi colonisation has been found to promote root-feeding nematodes by suppressing benzoxazinoid defence compounds in the roots (Frew et al., 2018). Above-ground, leaf metabolites such as phenolics, flavonoids, alkaloids, and amino acid derivatives not only act as signalling molecules modulating resource allocation and tolerance to stress but can also act as direct deterrents against herbivores and pathogens (Naoumkina et al., 2010; Cheynier et al., 2013; Li et al., 2023). Alongside these metabolites, phytohormones such as Jasmonic acid (JA), Salicylic acid (SA) and Ethylene (ET) function as central signalling molecules, often mediating the activation of systemic acquired resistance (SAR) and induced systemic resistance (ISR) and priming tissues against subsequent attack

(Pieterse et al., 2012). This often also means that root-induced responses can alter leaf responses (Dam and Oomen, 2008).

Together, VOCs, metabolites, and defence-related compounds such as phytohormones integrate local stress perception into systemic signalling networks, enabling coordinated physiological adjustments within individual plants. Through the release of VOCs in both the above-ground phyllosphere and the below-ground rhizosphere, similar signalling processes can also mediate interactions at a distance, for example, between plants or between plants and insects, or even microbes (Junker and Tholl, 2013; Brosset and Blande, 2022). That said, there is very little information about how plant-parasitic nematodes (PPN), and PCN in particular, might influence above-ground plant VOC release, as, somewhat understandably, given the below-ground feeding strategy, the majority of the research has focused on changes in below-ground VOCs (e.g., Kihika et al., 2017). However, syncytia of feeding female PCN are thought to be connected with the phloem via plasmodesmata (Hofmann et al., 2006). Thus, PCN infection could also manifest in changes above-ground. For example, above-ground tissues of root-knot nematode (RKN)-infected plants have been found to show a reduced expression of SA-related genes (Kyndt et al. 2012; Hamamouch et al. 2011). In fact, similar ISRs in plants (Wondafrash, Dam, and Tytgat, 2013; van Dam et al., 2008) as well as other changes in leaf and phloem plant metabolomes (Pajar et al., 2024) are thought to mediate interactions between PPN and above-ground herbivores. Specifically for headspace VOCs, although no study has directly measured changes after PCN infection, the cyst nematode *Heterodera glycines* has been shown to alter foliar VOC emissions of soybean (*Glycine max*; Constantino et al., 2021) and the PPN *Xiphinema index* to alter the VOC emissions of grapevines (*Vitis vinifera* L.; Castorina et al., 2020).

Here, I employ a similar experimental design as in the previous chapters to monitor any potato cyst nematode (PCN)-induced changes in the profile and intensity of in-leaf metabolites as well as VOCs released from the plants. Measuring both volatile and non-volatile metabolites is important because they have been shown to respond differently to different above-ground herbivore stresses (Mezzomo et al., 2023), and the same could also be true for below-ground stresses such as PCN infection. I also assess the influence of having neighbouring plants connected via common mycorrhizal networks (CMNs), as CMNs can transfer defence signals and other stress-induced responses (Babikova et al., 2013; Song et

al., 2010, 2014, 2015, 2019). In fact, plant VOC collection has been used to verify this, as experiments have demonstrated that plants under aphid attack and neighbouring, uninfested plants produced a similar VOC profile (defined in particular by methyl salicylate; Babikova et al., 2013). Importantly, this occurred only when potential hyphal links below-ground were retained; when links were severed, neighbours' VOC profiles remained unresponsive (Babikova et al., 2013). Moreover, it was shown that aphids were repelled by the headspace samples collected from the infested plants and their hyphal-linked uninfested neighbours, whereas parasitoid wasps, a key aphid predator, were attracted to the VOCs (Babikova et al., 2013). A similar study confirmed this and showed that such aphid-induced changes in the VOC profile via CMNs can occur as early as 24 hours after aphid attack (Babikova et al., 2013). Subsequent research reinforced this CMN-mediated priming whereby caterpillar herbivory on one tomato plant elevated defence-related VOC pathways in CMN-connected neighbours and reduced caterpillar performance on those neighbouring plants (Song et al., 2014).

However, experimental design caveats remain, particularly regarding the need to distinguish CMN-mediated signalling from diffusion through soil or shared airspace (Figueirido et al, 2021). Against this backdrop, investigating how PCN infection alters the profile of above-ground volatile and non-volatile secondary metabolites in neighbouring potato plants grown in mesocosms inoculated with AM fungi has the potential to demonstrate the extent of plant signalling and community defence dynamics. This is also linked to evidence from Chapter 3, suggesting that PCN infection can reduce fungal diversity and alter community structure, as soil microbial communities can influence the release of defence-related metabolites from the below-ground as well as the above-ground parts of the plants (Joosten et al., 2009). In fact, even rare soil microorganisms, such as some of the rarer AM fungal taxa that seemed to be lost under PCN infection, seem to be important in eliciting above-ground and below-ground plant defences (Hol et al., 2010).

Aims

Here, I examine in-leaf metabolites collected from the plants used in the ^{33}P tracing experiment described in Chapter 2, as well as VOCs collected from the headspace of plants set up in similar mesocosms with contrasting PCN treatments. The initial longer-term objective of the experiment from which VOCs were collected was to test whether a priming effect could be observed in the experimental mesocosms—that is, whether a plant 'naïve' to

PCN infection but connected via a CMN to a PCN-infected plant would respond more effectively to a subsequent PCN infection. If such an effect were detected, the intention was to follow up with a second experiment designed to more clearly disentangle the below-ground mechanisms involved (i.e., distinguishing between root exudation/VOC diffusion and CMN connectivity). However, an aphid infestation in the plant growth chambers compromised the validity of continuing with the experiment. As a result, only the first stage of the anticipated dataset is presented in this chapter. Specifically, the aims of this study are to:

1. Characterise changes in leaf non-volatile metabolites and VOCs induced by PCN infection in potato plants;
2. Assess whether PCN infection induces changes in leaf metabolites and VOCs in neighbouring, uninfected plants connected via a CMN. Specifically, could the preferential allocation of fungal-acquired P to PCN-free plants in the mixed treatments, as observed in Chapter 2, be driving changes in defence-related metabolites (or vice versa)?
3. If such changes are detected in neighbouring plants, evaluate whether they could arise from above-ground (i.e., shared headspace) and/or below-ground mechanisms (i.e., root exudation and VOC diffusion, or CMN connectivity, though without the ability to further resolve between potential mechanisms).

5.3 MATERIALS AND METHODS

5.3.1 Leaf metabolites

5.3.1.1 Collection

The metabolic profile of plant leaves from Block 3 of the ^{33}P-tracing experiment, described in Chapter 2, was analysed. Leaves were collected from weeks 5 and 7 of plant growth, with week 5 corresponding to the addition of the ^{33}P tracer to the containers and week 7 being the week the experiment was harvested.

500 µL of methanol/chloroform/water (2.5:1:1 v/v/v –20 °C) was first added to 50 mg of leaf sample from each plant, whilst keeping the samples on ice. Samples were then homogenised using metallic beads (two 3 mm stainless steel beads per sample) and a FastPrep-24™ (MP Biomedicals, USA) at 5.5 m s^{-1} for 2 x 30 sec periods and an incubation step for 5 minutes between homogenisations. Samples were then vortexed and left on ice for 5 minutes, before

vortexing again and centrifuging (14,000 rpm, 2 min, 4 °C). For each sample, the supernatant was then collected, and the pellet re-extracted with 250 µL of methanol/chloroform (1:1 v/v stored at -20 °C), followed by another centrifugation (14,000 rpm, 2 min, 4 °C). The supernatant was again collected, and the two supernatants were combined. 175 µL of chilled, distilled water and 100 µL of chloroform were then added to the merged supernatants, followed by centrifugation (14,000 rpm, 15 min, 4 °C). The chloroform and aqueous phases were then separated and each centrifuged (14,000 rpm, 2 min, 4 °C) before the supernatants were collected again and stored at -20 °C until further use.

Preliminary trials were carried out with different dilutions and buffer–matrix ratios to minimise matrix suppression effects and to avoid overloading the MALDI spot. Based on these optimisations, 10 µL of the aqueous phase was diluted 1:100 with a buffer (methanol/water 1:1 v/v + 0.1% trifluoroacetic acid). From this dilution, 10 µL was then mixed 1:1 with a matrix solution (α-Cyano-4-hydroxycinnamic acid in methanol at 5 mg mL^{-1} + 0.1% trifluoroacetic acid) prior to spotting for analysis. Finally, a 1 µL aliquot was spotted onto a stainless-steel MALDI target plate (preheated at 40 °C using a heat block) in technical triplicate, and the plate was left to dry at room temperature before being loaded into the mass spectrometry instrument.

5.3.1.2 MALDI-TOF Mass Spectrometry

Matrix-assisted laser desorption/ionisation time-of-flight mass spectrometry (MALDI-TOF MS) was performed to analyse the molecular composition of the samples. Measurements were carried out using a SYNAPT G2 MS System (Waters, USA) operated in positive ion mode only. The mass spectra were acquired over an m/z range of 50–1200 Da. A spiral laser raster pattern was used for sample ablation, ensuring uniform desorption across the target spot. The laser energy was set to 340 arbitrary units, optimised to achieve sufficient ionisation without inducing sample degradation. Each sample was analysed for a total acquisition time of 2 minutes to ensure adequate signal accumulation and reproducibility.

5.3.1.3 Processing and analysis

Raw MALDI-TOF spectra were acquired in profile mode and converted into the open mzML format using Mass-Up (López-Fernández et al., 2015). All subsequent processing and analysis were performed in R (R Core Team, 2025) using RStudio (RStudio Team, 2025) and packages `MALDIquant` and `MALDIquantForeign` packages (Gibb & Strimmer, 2012).

To reduce technical variability, replicate scans were first grouped by sample and averaged to generate one spectrum per sample. Intensities were then square-root transformed to stabilise variance, and spectra were smoothed using a Savitzky–Golay filter (Savitzky & Golay, 1964) to suppress high-frequency noise, followed by baseline correction with the SNIP algorithm (Ryan et al., 1988) to improve peak detection. Intensities were normalised by total ion current (TIC), a standard approach to correct for variation in ionisation efficiency across spectra (Rubakhin et al., 2005). The majority of one sample had been lost during homogenization, and as expected, no obvious spectra were recovered so this was removed from all subsequent analysis.

For all other samples, technical replicates (three for each biological sample) were averaged to yield representative consensus spectra for each sample. In three cases where there were also biological duplicates (i.e., samples from the sample individual that were run separately on the MALDI-TOF), these were also merged into a single consensus spectrum for each sample.

Peak detection was performed using a median absolute deviation (MAD)–based approach (Gibb & Strimmer, 2012). Different peak detection parameters were assessed visually, but ultimately, peak detection was performed using a half-window size of 180, a signal-to-noise (SNR) ratio threshold of 5, and a minimum relative intensity threshold of 0.005. To ensure comparability across samples, peak alignment was carried out using a warping-based approach with a mass tolerance of 0.001 Da, and diagnostic plots were inspected to confirm alignment quality, at which point one spectrum was removed.

The resulting aligned peak lists were combined into a comprehensive peak table containing the m/z values and corresponding intensities for each sample. The dataset was reshaped into a wide-format matrix with samples as rows and m/z bins as columns, with missing peaks treated as zero intensity. This final binned intensity matrix was used for all subsequent statistical and multivariate analyses.

A principal component analysis (PCA) was performed on the centred and scaled intensity matrix using the *prcomp* function. To identify the m/z features most strongly driving separation along the first two principal components, feature loadings were extracted, ranked by their combined contribution to PC1 and PC2, and the top 10 were plotted as biplot arrows on the PCA plot. Sample scores were visualised, with points grouped by PCN treatment and

growth stage. To formally test treatment effects while accounting for week-to-week variation, PERMANOVA was applied using the *adonis2* function from the `vegan` R package (Oksanen et al., 2022). Bray–Curtis dissimilarities were computed from the intensity matrix, and models included PCN treatment, PCN treatment of neighbour, growth week, and any relevant interactions, with permutations also stratified by growth week where appropriate.

To focus on defence-related metabolites (e.g., jasmonates, abscisic acid, salicylic acid, glycoalkaloids, and phenolic acids), a reference table of expected m/z values and adducts was constructed from published molecular weights (Table S5.1). Observed peaks were matched to targets using a tolerance of ±900 ppm. Matched peaks were then collapsed at the metabolite level, summing intensities across adducts within each sample, while retaining the associated m/z values for reporting.

To test for treatment-specific differences in defence metabolites, peak intensities were summarised per sample and compared between groups using two-sample t-tests, with false discovery rate (FDR) correction applied to control for multiple testing (Benjamini & Hochberg, 1995). Results are presented as $\log_2$ fold changes (PCN+/PCN−), with significance assigned at adjusted $p < 0.05$. In addition, the total defence metabolite intensity per sample was analysed using a mixed-effects model, with PCN treatment of the focal plant and its interaction with growth week included as fixed effects. A random intercept for mesocosm was added to account for non-independence among plants within the same mesocosm and repeated measures across weeks. Following visual inspection of the data, a further mixed-effects model was applied to the mixed treatment combination (PCN−/PCN+), with PCN treatment included as a main effect and a random intercept for mesocosm and for growth week to account for non-independence among plants within the same mesocosm and repeated measures across weeks. Significance of all model parameters was assessed using the *Anova* (Type III) function in R with the `lmerTest` package (Kuznetsova et al., 2017).

For comparison, the total intensity of non-defence metabolites was also computed by removing all peaks that matched defence-related m/z values and summing the remaining intensities per sample. This allowed defence-related metabolites to be evaluated relative to the broader metabolic background. The model parameterisation and testing were as for the defence metabolites described above.

5.3.2 Leaf Volatile Organic Compounds (VOCs)

5.3.2.1 Collection

Four containers were established for each of the two treatment combinations: (a) PCN–/PCN– and (b) PCN–/PCN+, following the setup described in Chapter 2. VOCs were collected from the headspace of individual plants. Air samples were drawn using a pump (11.6 L min^{-1}; WELCH MP 065 E, 18V, Germany) connected via plastic tubing to cups enclosing the plant leaves. Each cup contained an adsorption tube packed with activated charcoal (Supelco ORBO™ 32). Sampling was conducted at week 5 of plant growth (corresponding to the addition of ^{33}P in the tracing experiment described in Chapter 2) and lasted for approximately six hours, from 11:00 to 17:00 h. After sampling, adsorption tubes were sealed with manufacturer-supplied caps and stored at –20 °C until analysis.

5.3.2.2 Adsorption tube elution

Caps were removed from the adsorption tubes, and 5 µL of an internal standard solution (tetralin in ethanol, 80 µg mL^{-1}) was injected through the glass wool plug into the charcoal adsorbent. The tubes were then placed into gas chromatography (GC) vials and positioned in a vacuum manifold. Subsequently, 250 µL of dichloromethane was eluted through each tube. The eluates were sealed in GC vials and stored at –80 °C for no more than 48 h before being analysed.

5.3.2.3 Gas Chromatography-Mass Spectrometry (GC-MS)

Volatile and semi-volatile compounds were analysed using a gas chromatograph (PerkinElmer Clarus 680) coupled with a thermal desorber (PerkinElmer TurboMatrix 650) and a mass spectrometer (PerkinElmer Clarus SQ 8T). Sample introduction was performed at 1 µL aliquots for each sample via thermal desorption under standard conditions according to the manufacturer's guidelines.

The GC injector was maintained at 225 °C and operated in split mode with a split ratio of 100:1, held for 0.7 minutes before switching to full flow. Chromatographic separation was achieved on an Elite-5ms capillary column (30 m × 0.25 mm i.d., 0.25 µm film thickness; PerkinElmer), with helium as the carrier gas at a constant flow rate of 1.0 mL/min. The oven temperature program was as follows: an initial hold at 40 °C for 5 minutes, followed by a ramp of 8 °C/min to 180 °C, then a second ramp of 20 °C/min to 220 °C, which was held for 10 minutes. The total runtime was 30 minutes.

Mass spectrometric detection was performed in electron ionisation (EI) mode at 70 eV (EI auto). Full-scan data were acquired across a mass range of m/z 33–350 over a retention time window of 6 to 30 minutes.

5.3.2.4 Processing and analysis

Initial data acquisition and analysis were carried out using TurboMass software (version 6.1.0.1963; PerkinElmer). First, chromatograms of all samples were visually inspected to confirm the presence of VOC peaks. Compound identification was based on comparison of retention times and mass spectra with the NIST Mass Spectral Library (version 2.2). For each detected peak, retention time and m/z values were recorded, and peak integration was subsequently performed in TurboMass, with spectra of each pre-selected compound purified. The internal standard was applied to correct for sample-to-sample variation in the desorption procedure. Chromatograms were smoothed using the Savitzky–Golay method (Savitzky & Golay, 1964), with join valley, peak tailing, and baseline parameters set to default values of 30%, 50%, and 10%, respectively. These parameters were incorporated into the quantification method, which was then applied across all samples (see Table S5.11 for peaks included in the integration method). Peak areas for each sample were then manually inspected and adjusted in the TurboMass software.

The raw data were then imported into R (R Core Team, 2025) using RStudio (RStudio Team, 2025) and organised in long format with sample names, compound identities, and peak areas. The intensity for each compound detected in the background control sample was subtracted from each of the sample intensities, removing quite a few compounds in the process. Furthermore, to limit the impact of extreme outliers, only compounds detected in at least 2 of the 15 samples were retained for downstream analyses. Finally, total emission per compound was calculated as the sum across samples, and a log-transformation (log1p) was applied to normalise the data and reduce skewness.

PCA was performed on log-transformed VOC data (centred and scaled) to visualise patterns in VOC profiles. Top contributing VOCs were identified based on the sum of absolute loadings on the first two principal components. Arrows representing these VOCs were scaled proportionally and plotted on the PCA biplot with labels for the top compounds. Bray–Curtis dissimilarity was computed from the log-transformed VOC data to quantify compositional differences. Permutational multivariate analysis of variance (PERMANOVA, adonis2) with

Bray–Curtis dissimilarity was used to test the effects of PCN treatment of the focal plant, the PCN treatment of the neighbouring plant, and their interaction on VOC composition.

For each VOC, mean abundance per PCN treatment and neighbour treatment was calculated, and $\log_2$ fold changes were computed using an adaptive pseudocount (half the minimum non-zero value across all VOCs). Wilcoxon rank-sum tests were applied to assess statistical differences between treatment groups. Top compounds with the largest absolute fold changes were visualised using dot plots. Linear mixed-effects models (*lmer*) and linear models (*lm*) were used to test for the effects of PCN treatment and PCN neighbour treatment on total VOC emissions and VOC classes (e.g., Aldehydes, Benzenoids, Monoterpenoids, Sesquiterpenoids), with log-transformation applied to correct for skewness and reduce the influence of outliers where necessary. Significance of all model parameters was assessed using the *Anova* (Type III) function in R.

5.4 RESULTS

5.4.1 Leaf metabolomics

To assess the overall effect of PCN treatment on the leaf metabolite profile, Principal Component Analysis (PCA) was performed on the scaled intensity data. The first two principal components explained a combined 61.38% of the total variance (PC1: 49.7%, PC2: 11.68%; Figure 5.1). The PCA scores plot revealed a clear separation along PC1 according to the growth week that the samples were taken from(Figure 5.1; Table S5.2). This separation was statistically confirmed ($R^2 = 0.85$, $F = 238.67$, $p < 0.01$) and was also found to be primarily driven by elevated intensities of m/z features 771.25 (likely ID: Tamarixetin) and 455.03 (likely ID: Gangleodin) being more pronounced at week 7 of growth whereas, m/z peak 933.31 (likely ID: Torososide B) was more pronounced in week 5 of growth. PCN treatment did not prove to be a statistically significant factor overall or when comparing individually within each growth week (Figure 5.1; Tables S5.2 and S5.3).

The relative total intensity of metabolites was also influenced by growth week, but again it was not influenced by PCN treatment, overall or within each growth week (Tables S5.4 and S5.5)

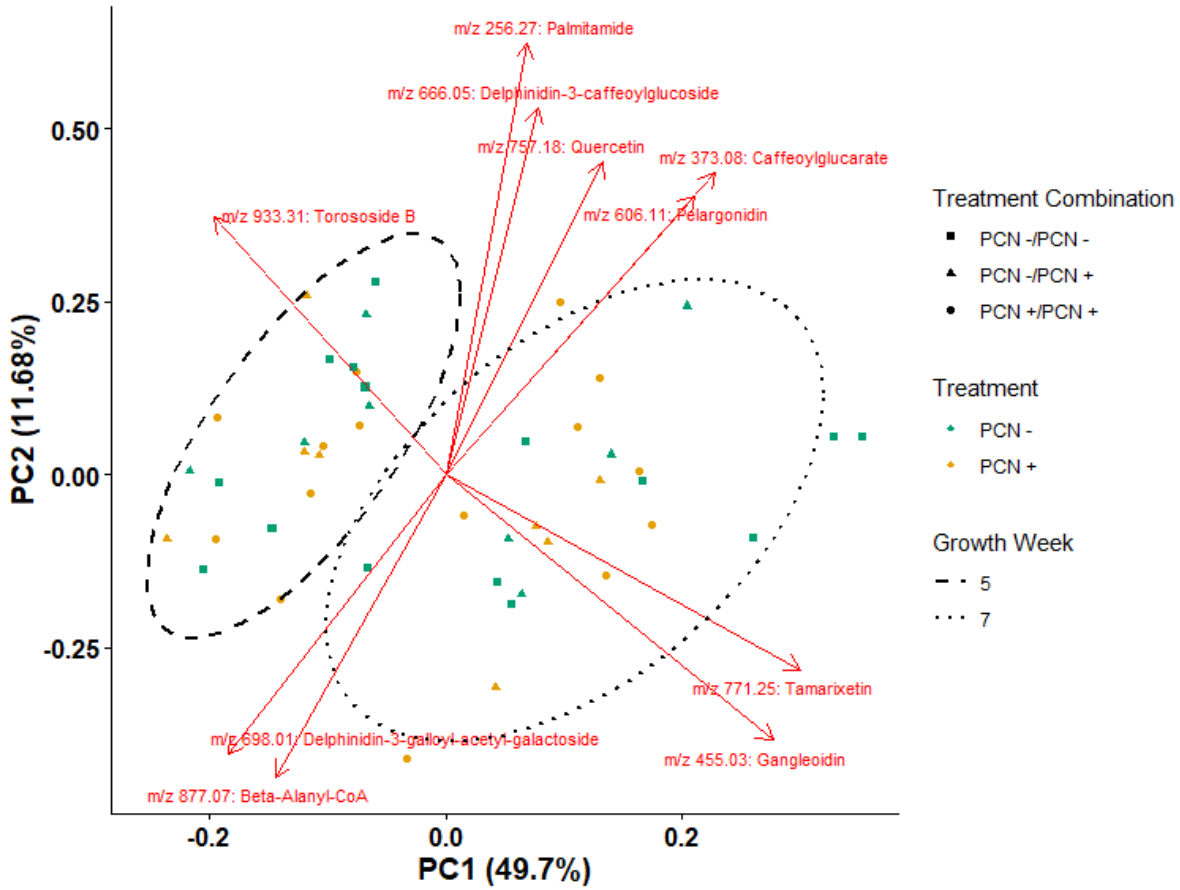

Figure 5.1 Principal Component Analysis (PCA) of MALDI-TOF metabolomics data from potato leaf samples. Points represent individual samples coloured by treatment group ('PCN −' or 'PCN +') and shaped by PCN treatment combination (PCN−/PCN−; PCN−/PCN+; PCN+/PCN+). Ellipses indicate 95% confidence intervals for leaf samples taken at growth weeks 5 and 7. Red arrows show the top 10 metabolites driving the separation, labelled with m/z and short metabolite name. Full metabolite identities, adducts, and additional notes are provided in Table S.5.1. Metabolite IDs are tentative, and were annotated via the CEU MassBatch database using a tolerance of 100 mDa in positive ion mode, considering possible adducts [M+H]+, [M+Na]+, [M+K]+ across the LipidMaps, Metlin, and KEGG databases.

A more targeted approach was also employed to specifically search for potential defence-related metabolites listed in Table S5.6. Of the 26 metabolites screened, 10 were successfully detected in my dataset. Among these, α-Chaconine exhibited by far the highest intensity, with a mean relative abundance approximately an order of magnitude higher than other

metabolites detected (e.g., ~14 times higher than Solanidine and ~25–50 times higher than jasmonates, phenolics, and amino acids).

Generally, defence-related metabolites showed higher intensities in the leaves of PCN-free plants except for the most abundant metabolites overall, such as α-Chaconine, Solanidine, and α-Solanine (Figure 5.2). In any case, the observed log_2 fold changes were relatively small and not statistically significant, suggesting that when looked at individually, the defence-related metabolites measured in this study were not substantially influenced by PCN treatment under these experimental conditions.

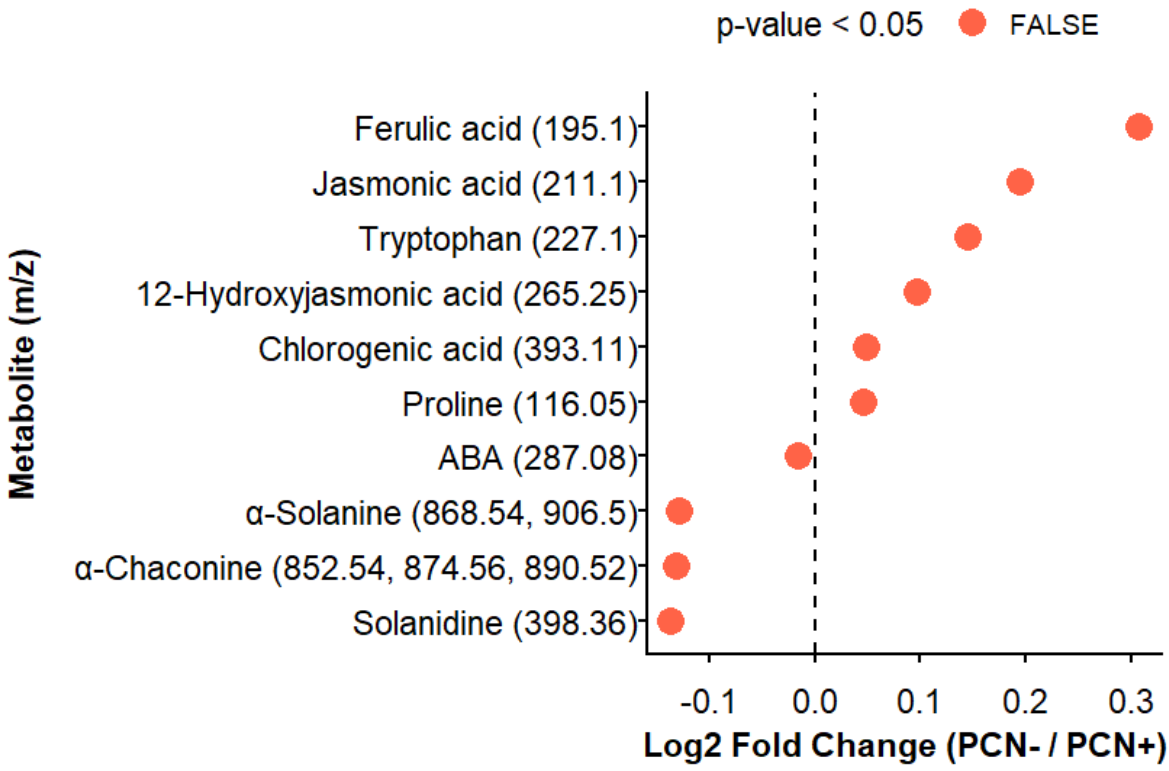

Figure 5.2 Log_2 fold change of candidate defence-related metabolites in potato leaves based on PCN treatment. Each point represents a measured metabolite matched to its expected m/z value and potential adducts ([M+H]+, [M+Na]+, [M+K]+). The x-axis shows the log_2 fold change in intensity between PCN-free and PCN-infected plants (PCN−/ PCN+); negative values indicate a decrease in PCN+. The y-axis lists metabolite names (tentative IDs) and corresponding m/z values. Point colour reflects statistical significance (t-test p-value < 0.05, FDR-adjusted; Table S5.5), and the dashed vertical line at zero indicates no change in abundance between treatments.

The total intensity of defence-related m/z values (which, as already mentioned, was largely dominated by α-Chaconine) was generally higher in week 5 compared with week 7 (χ^2 = 28.18, p < 0.01), whereas it was not overall influenced by PCN treatment (Figure 5.3; Table S5.8). Pairwise comparisons further confirmed the overall lack of PCN treatment, even within growth weeks (Table S5.9). Interestingly, however, within the mixed treatment combination (−/+), PCN-infected plants consistently showed higher metabolite intensities relative to their uninfected neighbours (χ^2 = 28.18, p = 0.01; Figure 5.3).

In contrast, when considering all other (i.e., non-defence) metabolites, the opposite temporal trend was observed, with total intensity being higher in growth week 7 (χ^2 = 18.19, p < 0.01; Figure S4.S). Similar to the defence-related subset, there was no detectable effect of PCN treatment overall (χ^2 = 0.56, p = 0.45), within each growth week (Growth week 5: t-ratio = -0.71, p = 0.49; Growth week 7: t-ratio = -0.0, p = 0.49) or within the mixed combination (χ^2 = 2.00, p = 0.16; Figure S5.1).

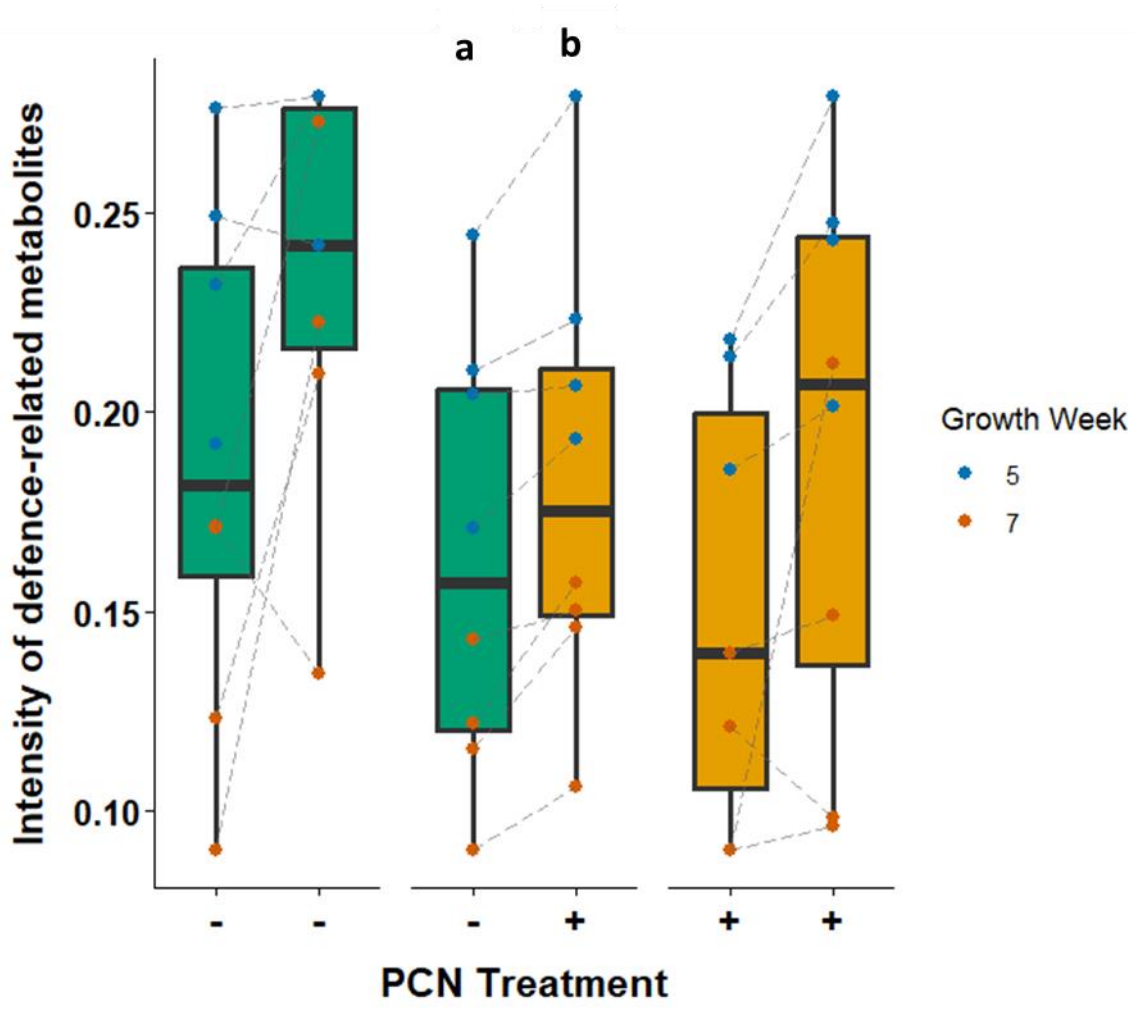

Figure 5.3 Total intensity values of defence-related m/z peaks detected in potato leaves across both sampling timepoints (weeks 5 and 7), split per mesocosm. Boxplots span the interquartile range (IQR), the line inside marks the median, and whiskers extend to 1.5 × IQR; points outside are potential outliers. Letters above boxplots indicate significant PCN treatment effects within the '−/+' mesocosms across both growth weeks ($p < 0.05$). Plants without PCN are indicated by '−' and green boxplots, while plants with PCN are indicated by '+' and orange boxplots. Individual points represent biological replicates, with colours denoting the sampling timepoint (Growth Week 5 in blue, Week 7 in reddish-brown). Dashed lines connect paired m/z peaks across each side of the same mesocosm for a given timepoint. Intensities were calculated as the summed abundance of tentative defence-related metabolites (Table S5.6), measured by MALDI-TOF MS in positive ion mode.

5.4.1 Leaf Volatile Organic Compounds

To assess the overall effect of PCN treatment on the leaf VOCs profile, a PCA was performed on the scaled, relative intensity data. The first two principal components explained a combined 61.38% of the total variance (PC1: 30.73%, PC2: 17.72%; Figure 5.4). The PCA scores plot hinted at some separation based on the PCN treatment as well as the PCN treatment of the neighbour (Figure 5.4); with only the influence of the PCN treatment of the neighbour being statistically confirmed ($R^2 = 0.83$, $F = 3.00$, $p = 0.04$; Table S5.10). Overall, the separation was primarily driven by Monoterpenes (e.g., β-Sesquiphellandrene) and Sesquiterpenes (e.g., β-Caryophyllene).

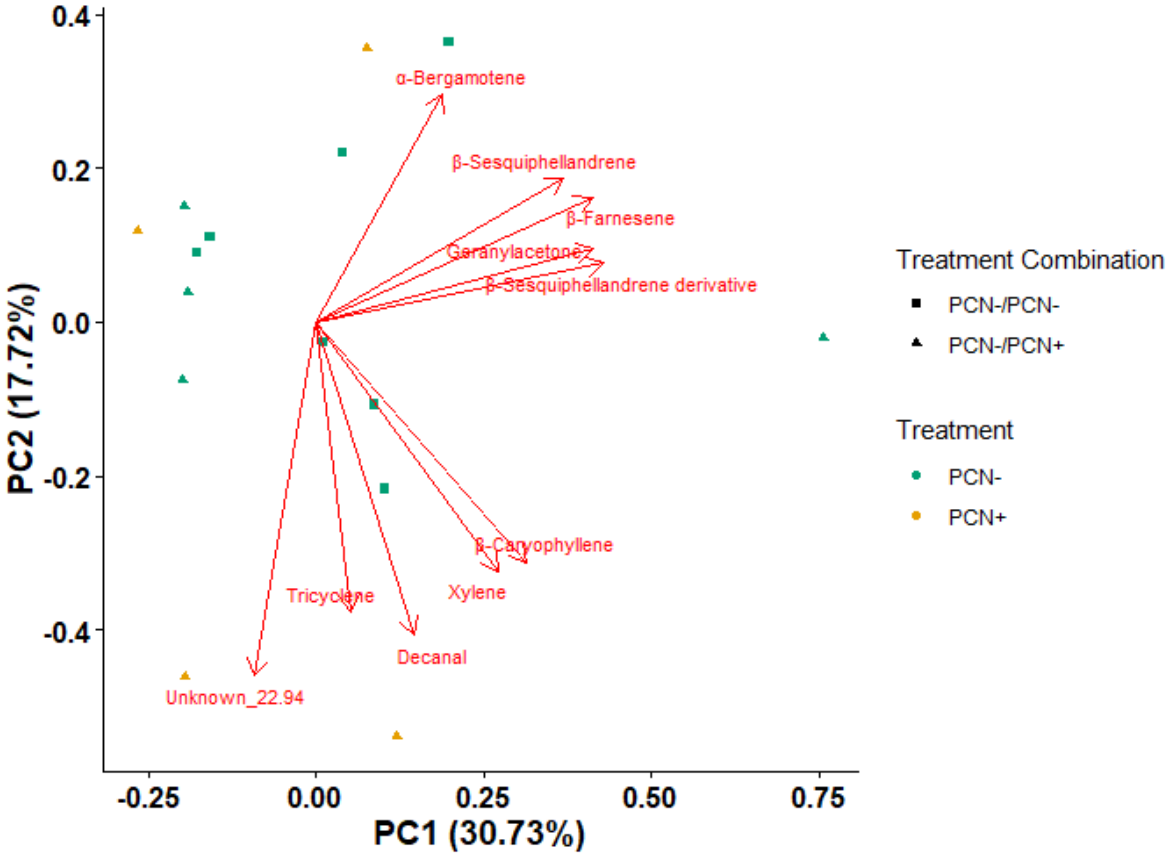

Figure 5.4 Principal Component Analysis (PCA) of log-transformed GC-MS metabolomics data from potato leaves. Points represent individual samples coloured by treatment group ('PCN −' or 'PCN +') and shaped by PCN treatment combination (PCN−/PCN−; PCN−/PCN+). Red arrows show the top 10 VOCs driving the separation, with tentative VOCs ID assignment performed using the NIST library (version 2.2). Further details about the VOCs included in the analysis are provided in Table S.5.11.

Among the 14 VOCs retained after excluding those also detected in the 'background' control, Tricyclene showed by far the highest intensity, with mean levels roughly an order of magnitude greater than the other detected metabolites (~25× higher than β-Sesquiphellandrene, the second most abundant VOC).

Overall, the $\log_2$ fold changes in the emission of individual VOCs varied, and none reached statistical significance, likely due to variability in the dataset (Table S5.12). Nonetheless, a trend was observed in which VOC emissions tended to decrease under PCN infection of the plant (Figure 5.5A) and also when the neighbouring plant was infected (Figure 5.5B).

Interestingly, the most abundant VOCs, Tricyclene and β-Sesquiphellandrene, showed the opposite pattern, with increased emissions under these PCN conditions.

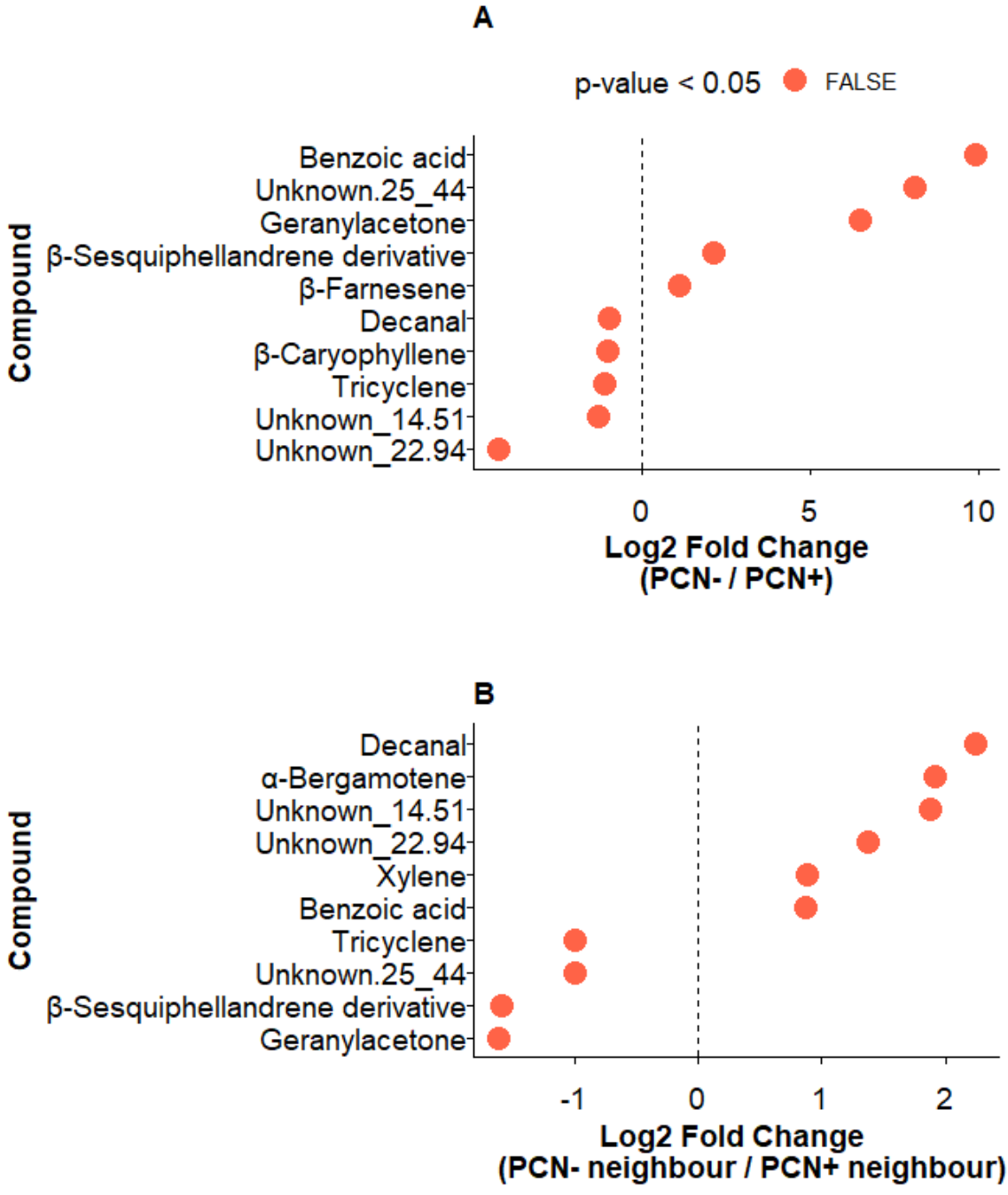

Figure 5.5 Log_2 fold change of normalised emission intensities of VOCs emitted from potato leaves, shown for **A.** the PCN treatment of the plant and **B.** the PCN treatment of the neighbouring plant. Fold changes were calculated with a small pseudocount added to all intensities to avoid division by zero. The colour of each point indicates whether the difference between treatments is statistically significant (p-value < 0.05; Table S5.12). The dashed vertical line at zero represents no change in intensities between treatments. VOC ID assignment is tentative and was performed using the NIST library (version 2.2).

VOC emissions varied substantially across PCN treatments and VOC classes, with few clear patterns emerging (Figure 5.6). Crucially, PCN-free plants neighbouring PCN-infected plants did not show a different emission for any of the VOC classes, compared to PCN-free plants neighbouring PCN-free plants (Table S5.12). The only noticeable trend was for the 'Unknown' VOCs where there was a reduction in emission from PCN-free plants with PCN-infected neighbours (Figure 5.6).

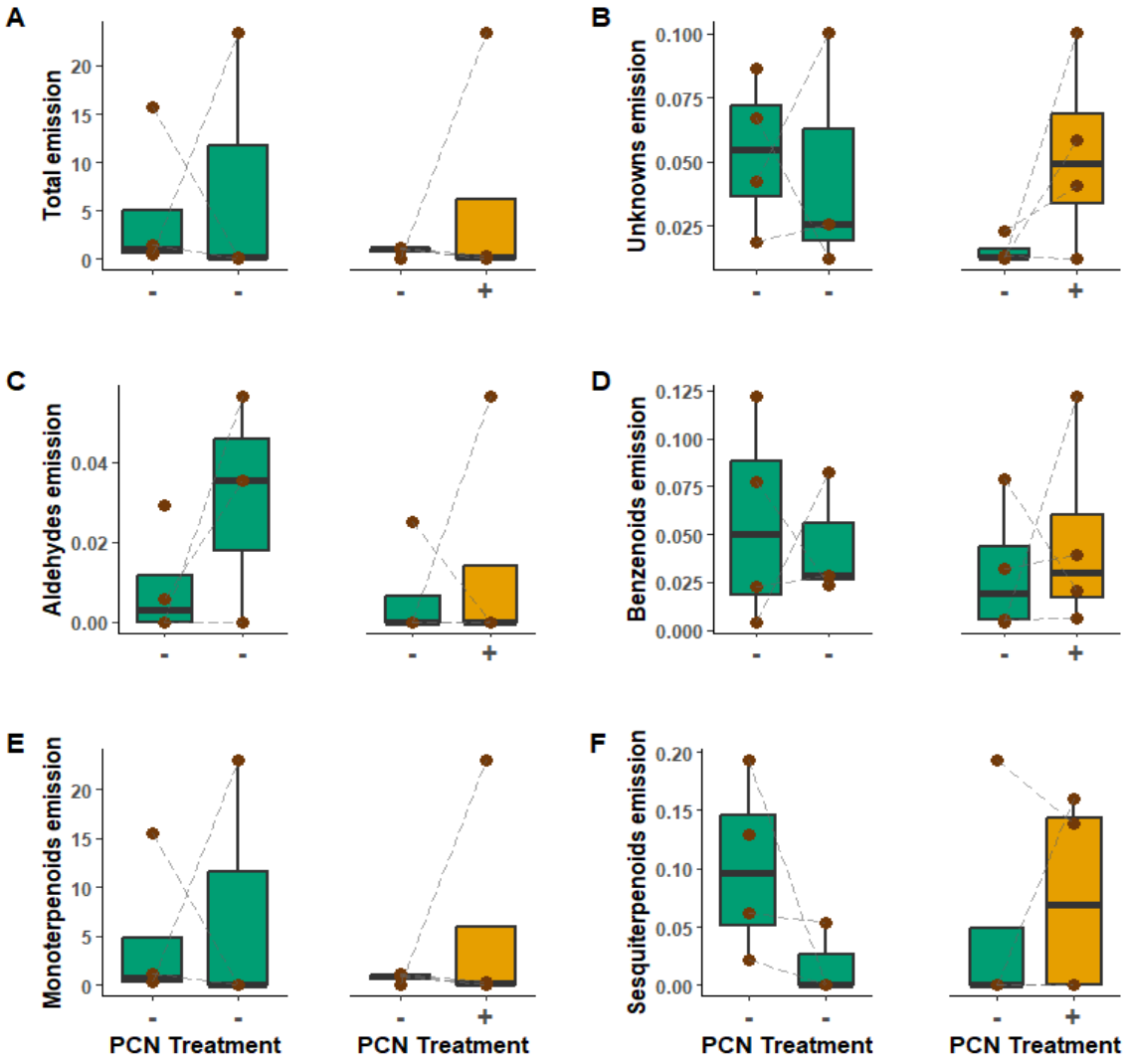

Figure 5.6 VOCs relative emission intensity from potato leaves, split per mesocosm. **A.** Total emission across all VOCs detected above the background threshold, **B.** VOCs of unknown ID, **C.** Aldehydes (i.e., Decanal), **D.** Benzenoids (i.e., Toluene, Xylene, Benzoic acid), E. Monoterpenoids (i.e., β-Sesquiphellandrene, Tricyclene), and **F.** Sesquiterpenoids (i.e., β-Caryophyllene, α-Bergamotene, Geranylacetone, β-Farnesene). ID assignment is tentative and was performed using the NIST library (version 2.2). Boxplots span the interquartile range (IQR), the line inside marks the median, and whiskers extend to 1.5 × IQR; points outside are potential outliers. Plants without PCN are indicated by '–' and green boxplots, while plants with PCN are indicated by '+' and orange boxplots. Individual points represent biological replicates, with dashed lines connecting paired VOCs across each side of the same mesocosm.

5.5 DISCUSSION

The main aims of these experiments were to characterise changes in leaf non-volatile metabolites and VOCs induced by PCN infection in potato plants, and assess whether PCN infection also induces changes in leaf metabolites and VOCs in neighbouring, uninfected plants connected via a CMN. Overall, leaf non-volatile metabolites were influenced more strongly by time (i.e., growth week) than by PCN treatment. Although some defence-related metabolites appeared to vary with PCN infection, the underlying variability meant that these trends were not statistically significant. α-Chaconine was the most abundant defence-related metabolite, which is consistent with the fact that α-Chaconine and α-Solanine account for approximately 95 % of potato glycoalkaloids (Lachman et al., 2001). Glycoalkaloids such as α-Chaconine and α-Solanine are well-known defence-related metabolites (Friedman, 2006; Pariera Dinkins et al., 2008), and in this study, both showed a slightly higher relative abundance in the leaves of PCN-infected plants. In a previous study, α-Chaconine and α-Solanine, together with chlorogenic acid, were found to be more abundant in the leaves of potato plants whose tubers had been damaged by the moth *Tecia solanivora*, whilst the same plants also exhibited reduced growth of the above-ground herbivore *Spodoptera exigua* (Kumar et al., 2016). Caterpillar larvae reared on a mixture of the same metabolites showed reduced growth, confirming the defensive role of these compounds against above-ground herbivores (Kumar et al., 2016). In my study, however, chlorogenic acid actually showed the opposite trend, where its abundance was slightly higher in PCN-free plants.

Ferulic acid, a phenylpropanoid alongside compounds such as flavonoids, lignin, and other phenolic acids (Dixon et al., 2022), showed the largest reduction in the leaves of PCN-infected plants. Since phenylpropanoid pathways are closely linked to pathogen resistance (Yadav et al., 2020; 2022) and PPN tolerance in plants (Singh et al., 2021), this reduction, although statistically insignificant—likely due to underlying variation in the data and the relatively low PCN infection levels used—could still be biologically meaningful. It may reflect a PCN-induced metabolic shift in which the plant reallocates phenylpropanoids such as ferulic acid from leaves to roots to reinforce local defences against PCN. If true, this would contrast with earlier findings suggesting that even under below-ground herbivore attack, roots generally accumulate fewer secondary metabolites than leaves, and that metabolite translocation is more effective from roots to shoots than in the opposite direction (Erb et al., 2009).

Alternatively, transcriptome studies have shown that PPN can modulate the phenylpropanoid biosynthetic pathway (Shukla et al., 2017; Iberkleid et al., 2015). In this context, PCN may actively downregulate ferulic acid production in the roots as a strategy to suppress host defences, with possible downstream consequences for ferulic acid concentrations in leaves.

The defence-related metabolite JA, which is known to mediate systemic responses alongside SA and ET (Pieterse et al., 2012), was also found to be in lower relative abundance in leaves of PCN-infected plants. This is contrary to predictions that would expect root PPN infection to induce JA accumulation in above-ground tissues (e.g., van Dam et al., 2008). Although many studies investigate JA induction up to 7–10 days after nematode infection (e.g., Shi et al., 2022), the absence of detectable signalling in this study is unlikely to be due to the timing of sampling (5 and 8 weeks after PCN inoculation), as elevated JA levels have been observed in roots even 30 days post-inoculation with RKNs, the latest time point assessed in that study (Mbaluto et al., 2020). More likely, the lack of a clear signal could be due to the relatively low level of PCN infection employed in this study which reflected the conditions of most infected fields in England at 10 eggs per gram of soil (Minnis et al., 2002), the variability of the response depending on PPN species (van Dam et al., 2008) and PPN lifestage (Mbaluto et al., 2020), and the ability of PPN to secrete protein effectors that suppress JA production (Haegeman et al., 2012; Mantelin et al., 2015), which is partly responsible for the transient nature of the JA-response (Kyndt et al., 2012).

Interestingly, defence-related metabolites were more abundant at week 5 of growth, whereas the other metabolites peaked at week 7 (Figure 5.3). This suggests that between weeks 5 and 7, plants shifted resources away from defence and toward other functions, such as growth and reproductive investment, such as tuber bulking (Thornton, 2020). In addition, within the mixed treatment (−/+), defence-related metabolites consistently accumulated to higher levels in PCN-infected plants compared with their PCN-free neighbours across both sampling weeks, whereas such a pattern was not observed for the non-defence-related metabolites. This would be expected given that infected plants are dealing with an active infection. Surprisingly, however, PCN-free plants in the mixed treatment (−/+) did not show higher levels of defence-related metabolites compared to PCN-free plants in the (−/−) treatment. This suggests that the slightly increased contribution of fungal-acquired P to PCN-free hosts in the mixed treatment (as observed in Chapter 2) did not translate into AM-

mediated priming of plant defences (Jung et al., 2012; Pozo et al., 2015). More detailed analyses (e.g., qPCR of defence-related genes) would be needed to confirm this.

Overall, although there were some indications that PCN treatment caused some differences, especially in defence-related metabolites, there was no indication that these differences translated to neighbours (i.e., PCN-free plants neighbouring PCN-free plants did not show different patterns to PCN-free plants neighbouring PCN-infected plants). As such, it appears from this experiment that no inter-plant mechanism, whether above-ground (i.e., shared headspace) or below-ground (i.e., root exudation and VOC diffusion, or CMN connectivity), seemed to come into play to influence leaf metabolites under PCN infection. It might well be that, based on the below-ground lifestyle of PCN, these changes occur first around the roots and that a higher infection or a longer timescale is needed to pick up the signal above-ground.

For VOCs, although overall composition did not change significantly in response to PCN infection itself, the presence of a PCN-infected neighbour had a detectable effect on the VOC profiles of nearby plants (Table S5.10). Specifically, PCN-free plants growing next to PCN-infected plants (−/+) produced VOC profiles that were more similar to those of the infected plants than to PCN-free plants growing next to other PCN-free plants (−/−). In contrast, PCN-free plants neighbouring other PCN-free plants (−/−) showed no such shift. Because all plants shared the same headspace, airborne transmission alone cannot explain this pattern. Instead, this suggests the involvement of a below-ground signalling mechanism, likely mediated through root exudation or mycorrhizal connections.

That said, interestingly, examination of individual VOCs revealed that the intensity of VOCs was not consistently altered by the PCN treatment of the focal plant (Figure 5.5A) or of the neighbouring plant (Figure 5.5B). Still, the effect was likely driven by Tricyclene, the most abundant VOC overall, which showed a trend to be more pronounced in PCN-free plants when neighbouring a PCN-infected plant. Although Tricyclene has been recorded as a plant VOC before (e.g., Courtois et al., 2009; Zhao et al., 2011), not much is known about its function; however, the monoterpene biosynthetic pathway is known to be responsive to stress or signalling cues internally within a plant (Frank et al., 2021) as well as to support SAR within and between plants (Riedmeier et al., 2017; Wenig et al., 2019). A field study using sagebrush plants (*Artemisia tridentata*) found that plants that emitted more Tricyclene (alongside Camphor and Camphene) received less chewing damage from above-ground herbivores

(Karban et al., 2016). Other monoterpenes (i.e, β-Linalool and γ-Terpinene) have also been found to be emitted from tomato (*Solanum lycopersicon)*, another Solanaceae plant, following caterpillar-induced damage (Zebelo et al., 2014). Overall, the observed Tricyclene response highlights that, while the broader VOC profile showed limited PCN treatment effects, specific compounds can potentially act as sensitive indicators of plant physiological responses.

The paired VOC emission profiles of the plants in the same mesocosm showed a lot of variation between and within PCN treatment, as well as based on the VOC class (Figure 5.6). Within the mixed treatment combination (−/+), only the emission of 'Unknown' VOCs appeared to show a consistent trend. This pattern reflected an increase in VOC emission under PCN treatment, which was actually driven by a reduction in emission from PCN-free plants with PCN-infected neighbours. The three 'Unknown' VOCs were detected at retention times 15.51, 22.94, and 25.44. As with all other peaks, tentative identification was made based on mass spectral matches to the NIST library; however, these matches were of low probability and often suggested a mix of compounds, all unlikely to be plant VOCs. Without external standards, the identities of these compounds cannot be fully confirmed. This is a common limitation of GC–MS when relying solely on library matches, as co-elution, matrix effects, or minor differences in derivatisation or ionisation can lead to misidentification or ambiguous assignment. In general, the reported VOCs identities in this study should be considered tentative, and future studies using authentic external standards will be necessary to validate them.

Similarly, limitations also come with the MALDI-TOF MS, which was used to identify leaf non-volatile metabolites. While MALDI-TOF MS provides a rapid and high-throughput method for profiling leaf metabolites, it offers limited structural information, making it difficult to distinguish isomers or confidently identify compounds without further MS/MS analysis. The choice of matrix can introduce interference in the low-mass range and bias, which metabolite classes are ionised, while the lack of chromatographic separation increases the chance of overlapping peaks in complex plant extracts. In addition, sensitivity is lower for compounds present at low abundance, and ion suppression effects may mask biologically relevant metabolites. Although preliminary trials were conducted to assess the optimal level of sample dilution and buffer–matrix ratios for my samples, some of the caveats remain, and the ID of

metabolites is tentative. This analysis should thus be considered as a screening tool, with complementary techniques required for detailed metabolite quantification, such as High-Performance Liquid Chromatography (HPLC) and identification, such as Liquid Chromatography–Mass Spectrometry (LC-MS).

Chapter 6. General Discussion

6.1 Summary of main results

Plants typically form multiple, concurrent biotic associations with other organisms. However, research often focuses on interactions between individual symbionts and plant hosts. As discussed in **Chapter 1**, specifically for the symbioses of plants with arbuscular mycorrhizal (AM) fungi, our current understanding of resource allocation and regulation relies substantially on evidence gained from experimental systems consisting of single plants. While such approaches have significantly advanced our understanding, to increase the ecological relevance of the results, it is necessary to go beyond this approach and investigate the role of competing root symbionts, especially on neighbouring plants connected via mycorrhizal networks (MN).

Building on previous work that has shown that plant infection with potato cyst nematodes (PCN) disrupt the carbon (C)-for-nutrient exchange in AM fungal symbioses (Bell et al., 2022), in **Chapter 2**, I found that in the presence of two neighbouring plants potentially linked by a CMN, plant-C supply to the fungus was not negatively affected by the PCN infection (Figure 2.6). However, PCN infection influenced the movement of plant-derived C once below-ground as the MN distributed C away from PCN-infected hosts (Figure 2.7). In the same Chapter, I also presented evidence for the ability of the MN to provide their PCN-free hosts with more fungal-acquired phosphorus (P) relative to their PCN-infected neighbours (Figure 2.5). Overall, the presence of a MN interconnecting neighbouring host plants appears to mitigate the difference in the amount of plant-derived C delivered to AM fungi by infected versus uninfected hosts. This is consistent with predictions from biological market theory (BMT), which suggest that host-imposed 'punishment' may be less effective in the presence of a CMN, as if one plant withholds resources, the CMN can still receive C from other connected plants (Kiers and Denison, 2008).

However, in **Chapter 3**, I explored how PCN infection might influence the microbial diversity of the roots and the soil as an alternative explanation for what might be affecting the distribution of P and C within the system. The results suggest that fungal species diversity and richness were reduced in PCN-infected roots (Figure 3.1) and that fungal root community structure also differed based on PCN infection (Figure 3.5). This was also true for AM fungi, where it appears that their overall richness (Figure 3.3) as well as their abundance in the roots

decreased under PCN infection, especially evident at the Phylum level when using the ITS primers (Figure 3.6D). Overall, Chapter 3 suggests that PCN may indirectly, through changes in the microbiome, influence the C-for-P exchange in AM-plant symbioses. This could serve as an alternative or complementary explanation to the notion that AM fungi actively adjust P and C allocation depending on their needs and the PCN infection status of their host plants. That said, it remains possible that the opposite is also true, where differences in the P and C allocation are driving microbial community shifts.

To clarify this further, in **Chapter 4,** I revisited resource allocation in the AM-plant symbioses, focusing entirely on C. The results confirmed that herbivory, above- and below-ground, did not reduce overall C allocation (Figure 4.3). Instead, the MN directed C towards the compartments that contained plants that were not experiencing herbivory (Figure 4.5). These results are important as they confirmed that even without the PCN-associated effect on the microbiome, the MN alone can influence the distribution of plant-derived C within the system. Using a single '^{14}C-labelled' plant and two 'receiver' plants within each system also strengthens the results, as any variation in the physiology of the '^{14}C-labelled' plant (e.g., size, photosynthetic rates, etc.) that might influence the results is inherently accounted for.

Finally, **Chapter 5** examined how PCN-induced changes in P and C distribution within the plant–MN system could both influence and be influenced by plant metabolites, and whether such changes affected neighbouring PCN-free plants connected to the same MNs. I found that PCN infection might slightly increase or decrease individual defence-related non-volatile metabolites in plant leaves, although plant growth stage remained the primary driver (Figure 5.1). The most abundant leaf metabolite detected, α-Chaconine, showed a trend, albeit statistically insignificant, to be increased in the leaves of PCN-infected plants (Figure 5.2). Overall, the total abundance of defence-related metabolites peaked at week 5 of growth and showed a consistent trend to be higher in leaves of PCN-infected plants relative to their PCN-free neighbours (Figure 5.3). This indicates that while PCN treatment influenced the infected plant, the effect was not transmitted to neighbouring uninfected plants, and there was no evidence of a link between mycorrhizal P distribution and AM-mediated priming of plant defences. On the other hand, volatile organic compounds (VOCs) emitted by plants appeared less influenced by the PCN treatment of the emitting plant itself. Instead, PCN-free plants displayed distinct VOC profiles depending on whether their neighbour was PCN-infected or

not (Figure 5.4), pointing to a possible below-ground signalling pathway. This effect was largely driven by Tricyclene, the most abundant VOC, which showed elevated emissions in PCN-free plants neighbouring PCN-infected plants (Figure 5.5), although variability in the data limited statistical significance. Overall, findings from this chapter suggest that PCN infection can induce below-ground signalling that modulates above-ground VOC emissions to some extent, but does not alter in-leaf metabolite profiles.

6.2 C-for-nutrient exchange and fungal diversity

Metabarcoding analysis revealed that PCN infection led to reduced AM-fungal richness in my soil-based experiments. However, total AM root colonisation assessed through ink-vinegar staining was not found to be impacted. This suggests that PCN infection likely influenced low-abundance or rare AM fungal taxa, and although fewer taxa colonised PCN-infected roots, those that did likely compensated for losses in colonisation by other taxa. Previous research has also found no effect of PPN on AM colonisation (e.g., Vos et al., 2012), which highlights that, as well as the quantity, the quality of AM colonisation is also important. For example, it has been suggested that plants may benefit from being colonised by more AM fungal species (Crossay et al., 2019) or more diverse AM communities (van der Heijden et al., 1998; Wagg et al., 2011), although the pattern is not universal (e.g., Sendek et al., 2019). Importantly, it has also been shown that increasing the number of AM fungal species in a system does not necessarily translate to changes in the overall level of AM colonisation, even though other benefits can occur, such as increased shoot biomass and increased plant P acquisition via AM fungi (Weber et al., 2025). Moreover, in the same study, under increased AM fungal richness, plants acquired this extra P without substantially increasing total C allocation (Weber et al., 2025). My observations align with both of these recent findings, suggesting that greater AM fungal diversity can enhance P supply through complementary nutrient acquisition strategies and competition among fungi for host C, ultimately meaning that plants effectively gain more P at a lower C cost. However, in my systems, plants were able to reduce the C:P ratio only when they were PCN-free, and their plant neighbours were PCN-infected, highlighting the level of influence other symbionts can have on the C-for-nutrient dynamics.

Another possible explanation for the patterns of P and C distribution observed in my systems, as explored in Chapter 3, is that PCN alter the microbiome. Specifically for P, a PCN-associated

reduction in AM fungal species richness might decrease the functional complementarity between the remaining AM taxa and their host (Powell & Rillig, 2018). Functional complementarity is particularly important because higher AM fungal richness increases the likelihood that roots are colonised by species with a high capacity for P provision, whereas a reduction in richness could limit access to these 'high-performing' partners. Following a similar logic, it has been proposed that low P availability may select for functionally similar AM fungal species exhibiting highly efficient P uptake (Buil et al., 2025). Moreover, colonisation by a greater number of, and likely more functionally varied, species could allow access to a wider range of P pools through their different growth strategies (spatial partitioning; Thonar et al., 2011) or enable complementary roles at different stages of plant growth or environmental conditions according to seasonal patterns (complementary phenology; Pringle and Bever, 2022).

However, it is important to note that these patterns are only expectations, and that complementarity between plant and mycorrhizal fungal communities is not always enhanced by greater diversity in the other (Wagg et al., 2015). Moreover, as with other traits, the P-provisioning capacity of AM fungal species is highly context-dependent (Johnson et al., 1997). Increased AM fungal richness likely entails the coexistence of both 'expensive' and 'cheaper' species, which can influence plant C allocation in different ways. For example, the presence of 'cheaper' partners may reduce the C cost of 'expensive' species, potentially because greater species richness promotes more 'cooperative' behaviour and enhances P provision (Argüello et al., 2016). Conversely, 'expensive' species may stimulate higher C consumption by 'cheaper' partners (Blažková et al., 2021), particularly if high sink strength is an inherent trait of certain fungi (Ji and Bever, 2016), thereby increasing the overall C flow into the AM fungal community to maintain allocation across partners of differing quality (Wyatt et al., 2014). Pertinent to my experiments, increased AM fungal richness has been shown to make otherwise 'uncooperative/expensive' taxa behave more 'cooperatively/cheaply' (Argüello et al., 2016). This suggests that the higher P provision observed in PCN-free plants in the mixed treatment may not necessarily be driven by the presence of particular taxa unique to their roots, but rather by the same taxa performing differently when embedded in the larger and more functionally diverse communities found around PCN-free roots.

Finally, even if AM fungal diversity remains unchanged, the amount of P acquired by AM fungi can still be indirectly affected by observed changes in overall fungal diversity. One of the reasons for this is that fungi can mediate the P and N cycles by releasing extracellular enzymes that convert organic P or N compounds to smaller products or mineral forms (Sinsabaugh, 1994; Richardson and Simpson, 2011). Such interactions have been demonstrated in experimental systems, where non-mycorrhizal fungi enhance organic P mobilisation and thereby increase the inorganic P available to AM fungi and their hosts (Jiang et al., 2021; Wang et al., 2023). Conversely, the PCN-associated reduction in fungal richness and diversity observed here could limit organic P mineralisation by free-living fungi, decreasing the pool of inorganic P available to AM fungi. This, in turn, may reduce the amount of P that AM fungi can supply to their hosts, which could lower the C they receive in return and potentially decrease AM fungal abundance. Of course, the outcome would still depend on the specific plant–AM fungal interactions, as under low P, plant dependence on mycorrhizal associations is likely to increase, potentially leading to greater plant-C allocation to the MN (Ji and Bever, 2016), which could then fuel MN growth and enhance its capacity to scavenge for P. Further research is needed to decipher the strength of each of these mechanisms and to better understand the extent to which free-living fungi may also mediate the functional complementarity between plant hosts and AM fungi as discussed above.

In any case, and despite the complexity in interpreting the results, monitoring AM fungal diversity in experiments is a step in the right direction, as biotic factors (i.e., plant and AM taxa identity) appear to be more important than abiotic factors (i.e., soil pH, soil texture, and experimental duration) in explaining mycorrhizal growth responses (Wang et al., 2023). While characterising the mycorrhizal community is a useful first step, future research should go further by linking community composition to the functional traits of individual AM fungal taxa, thereby enabling hypotheses about how shifts in AM fungal communities affect plant nutrient acquisition to be tested. This remains a challenging task, not only because of the high diversity of AM fungi, but also because their traits can vary at the physiological level (Janoušková and Jansa, 2025) and can change during the course of their interaction with plant hosts—partly because, as already discussed, the composition of the fungal community itself can change over time (Jansa et al., 2008; Blažková et al., 2021).

Trait-based and functional analyses are important not only for identifying which fungal taxa are most capable of supplying P (or other benefits) to the plant, but also for understanding their associated C demands. Under a 'reciprocal rewards' framework (e.g., Kiers et al., 2011), if AM fungi provided more P to PCN-free plants than to their infected neighbours, it would be expected that they would, in return, receive increased C from those PCN-free plants. However, this pattern was not observed in my experiments. What could not be determined here, however, is which individual AM fungal isolates were responsible for providing P, and how much C those same isolates were receiving. It remains possible that the isolates providing most of the P to PCN-free plants were also those receiving most of the C from the same plants, even if the overall amount of C transferred below ground did not differ between treatments. That said, theory predicts that such precise C allocation would reduce the diversity of fungal partners (Lekberg and Koide, 2014), which was not observed in this study. It would therefore be valuable to test this more explicitly in longer-term experiments. Stable isotope probing (SIP) using $^{13}CO_2$ pulse-labelling of plants, combined with lipid biomarker analysis (i.e., using phospholipid fatty acids for total fungi and neutral lipid fatty acids for AM fungi) and/or nucleic acid–based approaches (DNA-SIP), as applied in previous studies (Clochiatti et al., 2021; Maillard et al., 2023; Nuccio et al., 2022), could help disentangle the interactions between PCN, AM fungi, free-living fungal communities, and bacteria.

6.3 C-for-nutrient exchange and bacterial diversity

In addition to free-living soil fungi, bacteria also play a crucial role in mobilising both organic and mineral-bound P, and shifts in bacterial community composition could therefore influence the availability of P to AM fungi. In my study, I explored bacterial diversity and community structure in an attempt to relate these patterns to the AM-mediated distribution of C and P. However, interpretation of these findings is constrained by our incomplete understanding of how AM fungi interact with bacteria. In particular, it remains unclear how much C flows from AM fungi to bacteria, what the chemical identity of AM hyphal exudates is, and which bacterial processes these exudates may induce (Duan et al., 2024). Similar to what was discussed for AM fungi, targeted functional assays assessing the saprophytic capacity of the soil microbiome would be needed to determine whether the specific bacterial taxa detected in my system can solubilise P and thereby influence AM fungi.

Previous studies have shown that AM fungi can actively influence the composition and function of their surrounding bacterial communities. For example, AM fungi have been found to recruit bacteria harbouring phosphatase genes and thereby increase alkaline phosphatase activity in the hyphosphere (Zhang et al., 2018). Building on this, metagenomic approaches have been used to reveal shifts in the relative abundance of a wider set of microbial P-transformation genes in response to AM fungal activity (Dai et al., 2020). More recently, studies have gone further to link these functional changes to actual P fluxes, showing that specific microbial genes (i.e., CAZy genes) involved in phytate mobilisation can directly contribute to mycorrhizal P uptake pathways (Wang et al., 2023). Together, these studies highlight a progression from documenting microbial recruitment to identifying functional potential, to quantifying functional consequences, offering a framework that could be applied to better understand how hyphospheric bacteria influence AM-mediated nutrient transfer.

A more in-depth exploration linking bacterial taxa to functional genes—and ideally to gene expression—associated with organic P mineralisation is needed to better connect the observed patterns of C and P distribution in my systems with potential PCN-induced shifts in bacterial community composition. Moreover, the composition of bacteria in and around the hyphae is different from that in the soil and the roots (Zhang et al., 2022), so it would be useful for a more detailed analysis of the hyphosphere to be included. For example, in one study, richness and diversity of the bacteria were significantly higher in the hyphosphere than in the rhizosphere, leading the authors to suggest that in the rhizosphere, bacteria and AM fungi are competing for resources, whereas in the hyphosphere, bacteria are feeding on AM fungal exudates (Huang et al., 2023). Future studies should also assess more distinct soil and plant compartments—such as P-rich versus P-poor soil patches or specific dynamics around PCN infection zones —to better resolve spatial dynamics. Inoculation experiments under controlled and possibly P-limited conditions could then confirm whether specific bacterial taxa appearing more sensitive to PCN (e.g., Pseudomonadales) in my system are responsible for enhancing AM-mediated P delivery to PCN-free plants.

6.4 Beyond a resource-based biological markets framework

The evolution and dynamics of bidirectional nutrient exchange between AM fungi and host plants are often explained using Biological Market Theory (BMT; Noë & Kiers, 2018), which suggests that nutrients are traded commodities and partners can assess costs and benefits to

preferentially interact with those offering the best exchange rates (Werner et al., 2014). Access to alternative partners is necessary for such discrimination, and CMNs allow AM fungi to reach multiple hosts. Most studies have focused on the nutritional benefits of AM fungi and CMNs to plants (e.g., Fellbaum et al., 2014; van't Padje et al., 2020, 2021; Whiteside et al., 2019) and used BMT to explain symbiosis stability (Noë & Kiers, 2018). However, AM fungi can also provide non-nutritional benefits, including mycorrhizal-induced pathogen resistance (Cameron et al., 2013) and defence priming, reducing the impacts of parasites (Jung et al., 2012).

Specifically for PPN, the potential for CMNs to confer additional benefits, as shown in other systems (e.g., Alaux et al., 2020), warrants further investigation, as CMNs may enable systemic priming of defence responses in plants that are not directly attacked by PCN but are connected to infected plants. PPN secrete effector molecules to promote root colonisation (Rai et al., 2015), suppress plant defence responses (Chen et al., 2018), and reprogram host cells to form metabolically active feeding sites that accumulate plant resources (Rodiuc et al., 2014). In PCN-resistant potato varieties, recognition of these effectors is thought to trigger localised cell death, collapse of the feeding site, and ultimately nematode mortality (Postma et al., 2012). Co-colonisation by other root symbionts, such as AM fungi, could potentially interfere with these processes.

AM fungi have in some cases been shown to reduce PPN infection, although evidence remains equivocal (e.g., De La Peña et al., 2006; Garita et al., 2019; Vos et al., 2012), and it is unclear to what extent such protective effects depend on improved nutrient acquisition (Schouteden et al., 2015). More recently, it was shown that while AM colonisation can enhance PCN reproductive capacity, it also increases plant tolerance to PCN infestation, allowing plants to better withstand the negative impacts of the pest (Bell et al., 2022). These findings, together with suggestions that shifts in AM fungal communities may be driven by the level of pest or pathogen protection they offer rather than by changes in C-for-nutrient exchange ratios (Frew et al., 2024), point to a broader interpretation of BMT in the context of AM–plant symbioses. Rather than being solely defined by a tightly coupled reciprocal rewards system based on resource allocation, these symbioses could still be conceptualised as 'markets' but with 'services' (e.g., pathogen defence) as well as 'goods' (e.g., nutrients or C) being exchanged, and their evolutionary stability likely shaped by multiple selective pressures.

It has long been recognised that microbial symbioses with plants are multifunctional, so considering as many of these functions as possible is crucial for interpreting experimental outcomes (Sikes et al., 2010). For example, increased AM fungal richness has been associated not only with greater P provision to plants, as discussed earlier, but also with enhanced protection against fungal pathogens when plants are colonised by more diverse AM fungal communities (Sikes et al., 2009). In contrast, in my system, the PCN-associated reduction in overall AM fungal richness could reflect plants under stress becoming more selective in identifying and excluding 'uncooperative' AM fungi. This aligns with the idea that such 'uncooperative' taxa tend to perform better in more diverse communities (Hart et al., 2013). It is therefore not surprising that the effects of AM fungal richness may vary depending on the type of plant antagonist involved, with higher richness potentially enhancing defences against some root pathogens but not conferring the same benefits against pests such as PCN, where C allocation might be retained even if the AM species are 'uncooperative'. It, of course, remains possible that AM fungal richness is also determined by the fungi themselves, as well as indirectly shaped by the plant host and/or PCN.

Both my ITS and 18S datasets hint towards the traditional view that Gigasporaceae invest more in developing extensive extraradical hyphal networks, whereas Glomeraceae are more concentrated within roots (Maherali and Klironomos, 2007; Sikes et al., 2009; Sikes, 2010). More specifically, my data indicate a trend for Gigasporaceae abundance to be higher in PCN-free compartments—particularly in soil—which corresponds with the increased AM-derived ^{33}P received by plants in those compartments. This aligns with previous findings that greater soil colonisation by AM fungal hyphae is correlated with increased shoot P concentration (Powell et al., 2009). In contrast, although Glomeraceae were slightly more abundant in roots, they did not appear to contribute to fungal pathogen protection in my study as previously suggested (Sikes et al., 2009; Sikes, 2010). If anything, their modestly higher abundance in PCN-free roots coincided with an elevated relative abundance of 'pathotrophs' as defined by FUNGuild (Nguyen et al., 2016). Notably, the known potato-pathogenic fungal genus *Fusarium* was also more abundant in PCN-free roots, which, as mentioned, showed slightly higher Glomeraceae abundance. This lack of apparent protective effect could reflect context dependency in Glomeraceae-mediated pathogen suppression, which has been shown to vary

with host species, nutrient availability, and the composition of co-occurring AM fungal taxa (Sikes, 2010).

The rationale behind Chapter 5 was that CMNs can function as a highway for plant-plant communication via phytohormones, disease resistance and induced defence signals (e.g., Barto et al., 2012; Song et al., 2010). This has previously been demonstrated when plant VOCs caused by aphid herbivory were expressed in aphid-free plants, only when these aphid-free plants were connected to aphid-infested plants via a CMN (Babikova et al., 2013). Crucially, the VOCs produced in aphid-free plants were found to elicit the same insect responses (i.e., repelling aphids and attracting parasitoid wasps to act as natural enemies) as those produced after aphid infestation (Babikova et al., 2013).

In my experiment, I found evidence that VOC profiles of PCN-free plants were influenced by the PCN treatment of their neighbouring plants, with the monoterpene Tricyclene likely contributing strongly to these differences. This suggests the involvement of a below-ground signalling mechanism that affects the emission of headspace VOCs. An alternative explanation could be a resource-reallocation mechanism, whereby the increased ^{33}P received by PCN-free plants relative to their infected neighbours drives changes in VOC production. However, if this were the case, PCN-free plants in the mixed treatment (i.e., −/+) would be expected to form a distinct cluster, separate from both the PCN-free plants in the '−/−' treatment and the PCN-infected plants in the mixed treatment—yet this pattern was not observed. On the other hand, it appears that below-ground signalling may have, to some extent, mediated plant–plant communication and influenced plant–C delivery dynamics. Specifically, if the altered metabolic profiles of PCN-infected plants were transmitted to neighbouring plants—as suggested by the observed shifts in the VOC emissions of PCN-free plants—those neighbours may, in turn, have adjusted their own C allocation to the fungi. This supports the hypothesis proposed in Chapter 3 that, in the '−/+' treatment, uninfected plants could have reduced their C allocation to the MN to match that of their infected neighbours. Such a mechanism would explain why a PCN-induced reduction in C allocation is not evident in systems of neighbouring plants, despite being observed in systems of single plants (Bell et al., 2022). More research is needed to verify this, as the observed differences in VOCs in my experiment appeared to be driven primarily by Tricyclene, and similar patterns were not detected in the in-leaf metabolites.

In any case, monitoring the effects of PCN infection on the VOC profile of infected plants, as well as on neighbouring plants, as done in my experiments, is crucial for assessing the role of MNs in plant–plant communication. However, the extent to which the signalling resulting in different VOCs occurred via MNs or via other below-ground mechanisms, such as root exudation, remains unclear and requires further investigation. In fact, even if the above-ground pathways are controlled or accounted for, below-ground VOCs also need to be considered, as these can be emitted from roots and even from fungi and bacteria (Martínez-Medina et al., 2017). It would be useful for future experiments to disentangle the evolutionary drivers behind developing below-ground signalling mechanisms, considering that above-ground air signalling is likely more direct and faster, and to further determine the specific influence of below-ground pathways such as root exudation and mycorrhizal connections (e.g., is the speed of defence-related signals similar via both mechanisms and under what circumstances is one mechanism more useful than the other?).

Furthermore, while my study examined potential PCN-induced changes in both volatile and non-volatile plant metabolites, future work should test the actual impact of any below-ground signalling by infecting with PCN 'naïve' plants that have been connected via a MN to PCN-infected neighbours and comparing their responses to infecting 'naïve' plants connected to other PCN-free neighbours, as was originally planned for the next stage of my experiment before the aphid infestation in the greenhouse chamber. Gaining deeper insights would further require incorporating transcriptomic approaches (e.g., RNA-seq), followed by targeted gene expression analyses (e.g., qPCR). For potato in particular, it would be valuable to conduct such experiments using both susceptible and PCN-resistant varieties to determine whether maintaining a connection to a CMN involves a trade-off with the plant host's own defence system. Understanding whether and how the AM fungal community is shaped directly by the distribution of plant-derived C or indirectly through its contribution to plant defences is also an important open question.

More broadly, research using a wider range of plant species and diverse organisms that might influence AM fungal function is needed to clarify the role of MNs in modulating the C-for-nutrient exchange of the symbiosis and/or improving plant host defences. Increasing the temporal and spatial resolution of experimental studies will also be paramount to fully appreciate the contribution of AM fungi and MNs to ecosystem functioning (reviewed by

Alaux et al., 2021), especially their role in C cycling and storage (e.g., Averill et al., 2014; Hawkins et al., 2023; van der Heijden et al., 2015; Wurzburger et al., 2017) and their potential applications in agricultural systems (Rillig et al., 2019; Thirkell et al., 2017). If BMT were expanded to incorporate these additional ecological and functional scenarios, it might converge with other frameworks explaining C-for-nutrient exchange (e.g., source–sink dynamics) in predicting similar outcomes. Ultimately, more research is needed to understand the multiple ways that other symbionts influence the C-for-nutrient exchange—directly or indirectly—so that these interactions can be incorporated into predictive models.

6.5 What could a PPN-induced movement of C through mycorrhizal networks mean for global C-cycling?

PPNs are among the most abundant and diverse life forms on Earth, and most plants encounter them at some point during their life cycle (Sohlenius, 1980). Likewise, approximately 82% of plant species form associations with mycorrhizal fungi, including 72% with AM fungi and around 2% with ectomycorrhizal (EcM) fungi (Brundrett and Tedersoo, 2018). Both PPN (De Deyn et al., 2003) and mycorrhizal fungi (Tedersoo et al., 2020; van der Heijden et al., 1998) are known to drive plant succession in natural ecosystems, and—as explored throughout this thesis in the context of PCN and AM fungi in particular—they can also influence each other. From a biotic perspective, soil organic carbon (SOC) dynamics depend largely on plant productivity and the subsequent allocation of plant-derived C between above- and below-ground tissues (Creighton et al., 2007). Both of these processes can be affected by PPN and mycorrhizal fungi. Once translocated below-ground, plant-derived C can be utilised by the plant, consumed directly by phytophagous organisms such as PPN, acquired by plant mutualists such as mycorrhizal fungi, or released into the soil where it becomes available to the broader microbial community.

Despite C metabolism and transport in AM fungi being a subject of study for a long time (e.g., Bago, Pfeffer, and Shachar-Hill., 2000), our understanding of how mycorrhizal fungi influence soil C dynamics remains limited. Still, we do know that mycorrhizal fungi typically receive up to around 20% of plant photosynthates (Jakobsen and Rosendahl, 1990; Hobbie, 2006; Drigo et al., 2010). There are also thought to be three main and complementary pathways by which mycorrhizal fungi in general contribute to C cycling: providing substrates for decomposition

(Soudzilovskaia et al., 2015), affecting plant litter quality and quantity (Averill et al., 2019), and shaping the microbial and environmental context of litter breakdown (Frey, 2019). In terms of decomposition, it is thought that mycorrhizal fungi can reduce decomposition through a phenomenon known as the 'Gadgil effect', where mycorrhizal fungi compete with free-living fungi for nutrient resources and thus limit their activity (Gadgil, 1971). On the other hand, mycorrhizal fungi can also increase (aka prime) decomposition through the activation of plant exudation, which can release saprotrophic fungi from C limitation (Paterson et al., 2016). Finally, mycorrhizal fungi also contribute to increased decomposition through their own exudation (Shahzad et al., 2015) as well as their necromass acting as a food source for saprotrophic organisms (Wilkinson, Alexander, and Johnson, 2011). Traditionally, EcM fungi were thought to be more likely to reduce decomposition through the 'Gadgil effect', whereas AM fungi were more likely to prime decomposition (Frey, 2019). However, a recent meta-analysis has suggested that, irrespective of their type, mycorrhizal fungi are more likely to promote decomposition and thus negatively influence soil C storage (Choreño-Parra and Treseder, 2024).

Despite increasing evidence of the importance of mycorrhizal fungi as a global C pool (Hawkins et al., 2023), we still know relatively little about how plant-derived C is distributed once it enters the fungal mycelium and how this influences wider soil C cycling. Understanding the drivers of C movement within the MN is particularly important given that extraradical hyphae of AM fungi may constitute around 15% of SOC (Leake et al., 2004). In this study, I focused exclusively on AM fungi, the most widespread type of mycorrhizal association, which colonise approximately 55% of global vegetation and are common in herbaceous plants such as potato, my model organism (Soudzilovskaia et al., 2019). Using both soil- and medium-based experimental designs, I observed that plant-derived C moves within an AM fungal MN and that this movement is influenced by biotic factors, namely whether the plant producing the C—or neighbouring plants connected to the same MN—are subjected to phytophagy.

AM networks exhibit rapid turnover, with individual hyphae disintegrating within 5–7 days of formation (Friese & Allen, 1991; Staddon et al., 2003), suggesting that much of the plant-derived C they transport may be quickly respired or made available to free-living saprotrophs. While earlier I discussed how PCN-associated changes in free-living fungal communities could influence AM fungal diversity and the C-for-P exchange, my findings could also be interpreted

in the opposite direction: that PCN-induced movement of C within the AM network shapes the diversity of surrounding soil fungi, particularly saprotrophs. For example, C translocated toward PCN-free compartments could stimulate saprotrophic activity, potentially explaining the observed increase in overall fungal richness and the slightly higher relative abundance of 'saprotrophs' (as classified by FUNGuild; Nguyen et al., 2016) in both PCN-free soil and roots. In fact, this interpretation is further supported by evidence from the *in vitro* experiment, where plant-derived C preferentially moved via the MN toward microcosm compartments containing PCN-free plants, even in the absence of a complex soil microbial community.

Besides AM fungi, EcM fungi represent another important type of mycorrhizal association. Although they form symbioses with only ~2% of land plants, their host species account for over 25% of global vegetation (Brundrett and Tedersoo, 2018). AM and EcM fungi are hypothesised to differ in their influence on C cycling (Soudzilovskaia et al., 2015), with EcM fungi showing a stronger positive correlation with below-ground C stocks (Soudzilovskaia et al., 2019). Consequently, it is interesting to consider how herbivory might shape the movement of C within EcM MNs. EcM plants are estimated to allocate more C to their fungal partners than AM plants (Leake et al., 2004), and their extraradical mycelium is likely more extensive and exhibits slower turnover than that of AM fungi (Leake et al., 2004). Soils in ecosystems dominated by EcM fungi also contain more C per unit N than AM-dominated soils (Averill et al., 2014), potentially because EcM fungi compete with free-living decomposers for N, thereby slowing decomposition (Orwin et al., 2011). Taken together, these factors suggest that herbivore-induced effects on C distribution within EcM MNs could be particularly pronounced. On the other hand, if PPN reduce EcM species richness—as I observed PCN do for AM fungal richness—the overall CO_2 efflux from soil might also be reduced (Wilkinson, Alexander, and Johnson, 2010).

There is limited information on how PPN might influence EcM hosts, as these are largely trees and woody shrubs (Smith & Read, 2010), and most research on PPN focuses on crops (Kantor et al., 2022). Consequently, the global impact of PPN on forests may be underestimated (Khan, 2012). PPN can be classified according to their feeding strategy into ectoparasites, migratory endoparasites, and sedentary endoparasites such as PCN (Sijmons et al., 1994). Early research indicates that migratory root-feeding nematodes, such as *Pratylenchus* spp., can negatively interact with EcM of forest trees (Marks et al., 1987; Hanel, 1998). These

interactions extend further, as for example, inoculation of EcM oak (*Quercus robur*) with *Pratylenchus penetrans* reduced bacterial biomass in the rhizosphere, although plant-derived C detected in bacteria was enhanced (Maboreke et al., 2017).

PPN feeding style likely influences how plant-derived C moves within MNs. Unlike sedentary endoparasites such as PCN, which establish long-lived feeding sites composed of metabolically active host cells that act as strong carbon sinks, migratory endoparasites like *Pratylenchus* kill the cells they feed on, leaving necrotic tissue behind (Sijmons et al., 1994). This suggests that while PCN infection may reduce C supply to mycorrhizal fungi, some supply of C to the AM fungi will likely be maintained and then distributed within MNs. In contrast, *Pratylenchus* infection likely disrupts root integrity and, depending on the level of damage, halts C flow through affected regions, reducing the amount of plant-derived C entering MNs altogether.

PPN feeding styles are highly diverse, and EcM hosts can also be impacted by some above-ground PPN as well. For instance, *Bursaphelenchus xylophilus* inhabits the trunk and branches of trees, causing pine wilt disease (Mamiya, 1983), and is under regulatory control in the US due to its potential for extensive forestry damage (APHIS, 2025; Dwinell, 1997). Another example is *Litylenchus crenatae mccannii*, a nematode recognised in 2020 for causing beech leaf disease in the US state of Ohio, which, within a year, had spread to nine further states (Carta et al., 2020; Kantor et al., 2022). Because these above-ground PPN attack photosynthetic tissues rather than roots, they are likely to reduce the plant's overall photosynthetic capacity and carbohydrate production. A reduction in photosynthate supply would be expected to limit the amount of recent C available for below-ground allocation, including to EcM fungi. Whether above- or below-ground, a PPN-induced reduction in C allocation to EcM fungi could diminish SOM accumulation, especially in forests where EcM fungi play a key role in soil C storage. Understanding how the C that is delivered below-ground gets distributed within MNs would allow for better predictions of soil C losses and could inform management strategies to prevent them. This is particularly important as such effects may be exacerbated under warming climates, which could facilitate the poleward expansion of PPN or other herbivores into boreal and taiga regions dominated by EcM trees (Brundrett and Tedersoo, 2018).

In general, it is important to consider how PPN-induced shifts in the movement of C within MNs might interact with future climate conditions, which are projected to involve a rise in atmospheric CO_2 from current levels of ~420 ppm to 800–1000 ppm by 2100, representing an increase of approximately 90–140% (IPCC, 2021). For example, Charters et al. (2020) found that allocation of plant C to AM fungi decreased following aphid herbivory and that this reduction persisted under elevated CO_2 conditions (800 ppm). This suggests that the PCN-induced effects detected in my experiments could similarly persist under future CO_2 levels. In fact, they could even be amplified, as several studies have shown that plant C allocation to AM fungi can increase by up to 25% under elevated CO_2 (Drigo et al., 2010), which could increase the flow of C through MNs. Greater C flux could in turn stimulate microbial activity and enhance below-ground C turnover, thereby increasing the amount of C respired back into the atmosphere (Cheng et al., 2012). That said, under a more gradual rise in CO_2, this positive priming effect on decomposers may be less pronounced as soil microbial communities have more time to adjust their functioning to changing conditions (Klironomos et al., 2005). Still, although it is very difficult to predict how exactly soil and rhizosphere communities will respond to a changing climate, plant root exudation and thus microbial C flow are likely to be influenced (Drigo et al., 2013), which will undoubtedly shift the composition of the soil food web. Future research incorporating a broader range of host plants, mycorrhizal types, and combinations of biotic stresses such as herbivory, under varying abiotic conditions like elevated CO_2, will be crucial not only for improving our understanding of current MN-mediated C dynamics but also for enhancing our ability to predict their responses under future climate scenarios.

6.6 Wider considerations

Several aspects of the experimental design were chosen to reconcile practical constraints with biological relevance. For example, experiments involving ^{14}C-isotopic labelling require a careful balance between allowing sufficient time for the isotope to be taken up by the plant and distributed within the system and avoiding excessive labelling periods that would allow the isotope to be recycled and respired to the point where it can no longer be traced. Longer labelling times also increase the likelihood that labelled C exuded from AM fungi will be taken up by other saprotrophic fungi, as AM fungi are known to mediate the transfer of plant-

derived C to the wider microbial community (Nottingham et al., 2013). Indeed, experiments using ^{13}C have shown that labelling periods longer than 24 h result in greater ^{13}C enrichment of non-AM taxa, although even within 24 h, not only AM fungi but also other fungal taxa—most notably members of the Ascomycota—can become enriched (Hannula et al., 2012; 2020). Although somewhat debated, this likely reflects plant-derived C being passed to other fungi via exudation from AM fungi themselves, rather than being directly consumed from root exudates (Drigo et al., 2010; Kaiser et al., 2015; Hünninghaus et al., 2019).

In any case, labelling for 24 h enabled me to trace plant-derived C through the system, though this represents only a brief snapshot in time and does not necessarily capture the longer-term C dynamics, which may differ substantially over the full course of my experiment—or more importantly, over the longer timescales at which such interactions occur in nature. Moreover, this short labelling period preferentially captures recently-fixed C sources such as hexose sugars, whereas other C forms, such as fatty acids—which take longer to be constructed by the plant and are typically used for storage—are less likely to be traced. This is an important consideration because recent work has shown that plant herbivory can limit the delivery of hexose sugars to AM fungi, while C delivery in the form of fatty acids is largely maintained (Bell et al., 2024). If such dynamics occur in my systems, then the apparent redistribution of C away from infected hosts could actually be an underestimate. It could be useful for future experiments to validate these results using ^{13}C rather than ^{14}C labelling, since ^{13}C-labelling is less sensitive and typically requires longer pulse periods to achieve detectable incorporation.

In my P-tracing experiment, I applied ^{33}P in the form of soluble inorganic orthophosphate because it is widely regarded as the principal form that AM fungi supply to their hosts (Smith & Read, 2010). However, organic P is the predominant form in some soils (Walker and Syers, 1976; Harrison, 1987) and occurs alongside insoluble inorganic forms such as crystalline apatite (Raven et al., 2018). From a plant's perspective, the C cost of acquiring these different P pools depends largely on whether the plant (or its symbionts) can access the P form directly and on its concentration levels in the soil (Raven et al., 2018). Although, somewhat spatially separated, the inorganic P acquired by AM fungi is generally considered to originate from the same pool that is in principle also accessible to plants; yet, there is growing evidence that mycorrhizal roots can also exploit otherwise inaccessible insoluble inorganic P sources in the

soil (e.g., rock phosphate; Cabello et al., 2005; Duponnois et al., 2005). That said, the actual phosphate-solubilising capabilities of AM fungi remain somewhat contested.

Although early reports suggested that AM fungi might produce extracellular phosphatases (Gianinazzi et al., 1979), genomic analyses indicate that AM taxa have a reduced repertoire of genes for plant-cell-wall and polysaccharide degradation and apparently lack phytase genes (Tisserant et al., 2013; Miyauchi et al., 2020). The current understanding is that without these genes, it is unlikely that AM fungi can effectively hydrolyse complex organic P such as phytate — a major component of soil organic P (Liu et al., 2022). Nonetheless, some *in vitro* studies have indicated that AM hyphae can contribute to organic-P hydrolysis and transport of this P within the MN (Joner, Ravnskov, and Jakobsen, 2000), with the released inorganic P then transported to the root organ culture (Koide and Kabir, 2000). Acid phosphatase activity has also been detected on extraradical hyphae of *Rhizophagus clarus* (Sato et al., 2015). More recently, *Rhizophagus irregularis* was shown to mobilise P from phytic acid (both in free form and bound to goethite; Andrino et al., 2019) and to access apatite-bound P (Andrino et al., 2021).

Most likely, mechanisms underlying the enhanced P uptake observed in past studies of AM symbioses primarily reflect hyphal exploration of a larger soil volume and/or synergistic interactions with P-solubilising microorganisms (Antunes et al., 2007). Specifically, as already discussed, AM fungi cooperate with soil microorganisms that possess the enzymatic machinery to mineralise organic P, with hyphal exudates potentially stimulating microbial phosphatase activity and thereby releasing inorganic P that becomes accessible to both the fungus and its host plant (Zhang et al., 2018). This also ties in with the evidence suggesting that AM fungi can influence the degradation of organic matter and subsequently acquire and transfer a portion of released nutrients to their associated host plants, not directly through mobilising organically bound nutrients but through associations with other microbes (Bunn et al., 2019).

Regardless of whether AM fungi can access organic P directly or indirectly, this process appears to require substantially greater mycelial growth and host C investment than the uptake of soluble mineral P (Andrino et al., 2019; 2021). This implies that the dynamics of the C-for-P exchange in plant–AM symbioses are influenced by the form of P available. It would therefore be valuable to confirm the results presented here using a range of P forms, and

ideally to link this back to specific AM fungal isolates and bacterial strains. Different AM taxa may specialise in scavenging orthophosphate, whereas others may rely more on bacterial partners to solubilise mineral P sources such as apatite or to hydrolyse organic P forms such as phytic acid. Such functional differences could also relate to the longevity of hyphae or their patterns of mycelial development—for example, whether an AM taxon invests more in soil exploration to reach new hosts or in root colonisation of existing host (Hart et al., 2001; Hart and Reader, 2002).

Although trait-based approaches are urgently needed, it remains challenging to test how AM fungal families (and even more so individual species) truly differ in these traits under controlled yet realistic conditions (Lekberg and Koide, 2014). Pot experiments, as presented in this thesis, for example, come with inherent limitations, particularly when studying MNs, as fungal traits may not be expressed in pots as they are in natural settings. For example, soil temperature in pots likely fluctuates more than that in the ground, with unknown consequences for AM fungal growth and the capacity of MNs to transfer nutrients. Pot experiments are also usually time-bound, running up to a few weeks, and although the AM fungi are very active during the first 3 to 8-9 weeks of the symbiosis (Jansa et al., 2008; Blažková et al., 2021), our understanding of how communities shift past these few initial weeks and how this might influence their overall functioning is very limited.

Furthermore, comparisons of the relative abundance of AM families are not only limited by the lack of trait-based information on AM fungal families, but should also be caveated by the fact that AM fungi orders have varying genome sizes, ranging from approximately 150 Mb in *Rhizophagus* species to 784 Mb in *Gigaspora margarita* (Venice et al., 2020), whereas the ancestral sister lineage *Paraglomus occultum* contains an exceptionally small genome of 39.6 Mb (Malar et al., 2022). Such a large variation means that the rRNA copy numbers are likely to also vary, and indeed, rRNA copy numbers of fungi vary substantially across phylogenetic scales and ecological roles (Lofgren et al., 2019), which could lead to an overestimation of the relative abundance of taxa with higher copy numbers in metabarcoding datasets.

Another consideration for future studies is the levels of P in the soil. Although this was not specifically determined in this study, previous experiments using soil and sand from the same suppliers had an estimated 20.5 mg/L of P, which is considered a medium soil P concentration

(Bell et al., 2022). It would be interesting to corroborate the findings under different levels of soil P, as it is well known that levels of soil P influence mycorrhizal functioning (Hoeksema et al., 2010), and in particular, under high P, plants may rely less on the mycorrhizal pathway for their P uptake (Johnson et al., 1997; Johnson, 2010). It would also be interesting to test how PCN infection might influence the movement of other nutrients, such as N, given that N and P dynamics are interdependent (Vance, 2001). Although ^{15}N was applied together with ^{33}P in my experiments, it was not detected above background levels in plant shoots, likely because the amount added was small relative to the size of the experimental mesocosms.

Another important detail is that a microbial filtrate of the PCN inoculum (e.g., obtained by removing the nematodes while retaining the associated microbial community) was not applied to the PCN-free compartments in my experiments. However, the metabarcoding analysis showed that soil community profiles were similar across PCN treatments (i.e., PCN− and PNC+) and therefore root-level differences were not driven by the characteristics of the microbial communities present in the soil used to add the PCN. Furthermore, the results regarding the PCN-mediated C movement within the MN were further corroborated using the compartmentalised microcosm, which was stripped of the microbial diversity seen in soil.

Relevant to this point, here I examined how microbial communities might be shaped by PCN treatment; however, the primary determinant of microbial community structure is often soil type, which can be considered as a microbial seed bank. The plant species and genotype then select which microbial taxa can grow in the roots (Philippot et al., 2013). It is thus important for the results to be corroborated using different soil types, different starting soil communities, as well as different plant species at different plant growth stages, which might be better or worse than at shaping their rhizosphere microbiome. The effect of plant community diversity should also be considered, as this can influence the rhizosphere microbiota, including AM fungi (Hausmann et al. 2009), as well as above-ground processes such as VOC release (Kigathi et al., 2019).

My experimental design used for the experiments conducted in soil mesocosms did not include an air gap compartment between the two mesocosm compartments as used in some other studies (e.g., Shen et al., 2020), as the focus was on monitoring the functioning of MNs in soil. This does, however, come with the limitation that limited root contact through the mesh barrier cannot be fully excluded. AM-free controls were not included because the

primary aim was to examine interactions among plants, AM fungi, and PCN within a naturally mycorrhizal context. While AM-free controls can help separate mycorrhizal from non-mycorrhizal nutrient transfer, they can also hinder interpretations, as non-mycorrhizal plants show different exudation patterns and also change their direct (aka non-mycorrhizal) nutrient pathways (Smith and Read, 2010). Moreover, although my results suggest that on average 30% of AM fungal ASVs were shared across both sides of the soil-based mesocosms, the continuity of the MN(s) between the two plants has not been formally established, and throughout the thesis, I have refrained from using the term 'CMN' to refer to my systems.

As recently discussed, however, the definition of CMNs as 'physical, continuous linkages among the roots of at least two different individual plants, by the same genetic individual of mycorrhizal fungus' (Karst et al., 2023) may represent a rather special case. This strict definition ensures that any resource transfer is interpreted as occurring exclusively via direct hyphal connections—a condition that is rarely demonstrated in experimental studies (Lehman & Rillig, 2025). Rillig et al. (2025) argue instead that the term CMN should encompass MNs more broadly, regardless of whether hyphal continuity is proven, since many of their ecological functions (e.g., mediation of defence signalling, as discussed in Chapter 5) do not necessarily require direct hyphal links. They further propose the term Common Fungal Network (CFN), which includes networks formed by non-mycorrhizal fungi. Such networks are likely widespread in natural systems, potentially more biologically significant than mycorrhizal networks in some contexts, yet often remain underexplored (Lehman & Rillig, 2025).

Finally, although initial tuber size was not formally quantified in any of the experiments, tubers were visually assessed to ensure comparable size and distributed evenly among treatments, reducing the likelihood of systematic size-related bias. Moreover, previous preliminary experiments in which tuber size was measured did not reveal any relationship between tuber size and subsequent plant growth (unpublished data), supporting the validity of this approach. Nevertheless, explicitly recording initial tuber mass could provide additional precision in future studies.

6.7 Conclusion

The work presented in this thesis demonstrates the inherent complexity of studying ecologically relevant experimental systems. It is well recognised that mycorrhizal functioning

is highly context-dependent, and the diversity of mycorrhizal fungi described to date likely represents only a fraction of what exists. Even so, trait-based information for the AM fungi already discovered is limited and often contradictory, which constrains our ability to interpret findings and make broader generalisations. This complexity is further compounded by the presence of other symbionts, such as PCN or bacteria, as demonstrated throughout this thesis. Gathering robust trait-based information will require accurate characterisation of mycorrhizal diversity, yet current molecular tools—including the primers used here—capture only a subset of this diversity and introduce their own biases.

Finally, while the C-for-nutrient exchange is a fundamental feature of AM fungal–plant symbioses, experimental studies must be expanded to monitor this process under a wider range of biotic and abiotic conditions. As well as the quantity and the quality of the C delivered to the MN (see Bell et al., 2024), the distribution of this C within MNs needs to be further explored (see Chapter 2; Magkourilou et al., 2024), as it likely has important ramifications not only for the basic functioning of mycorrhizal fungi but also for their role in ecosystem processes such as C cycling. Furthermore, conceptual frameworks should not be confined to a rigid, resource-based biological markets perspective; rather, alternative hypotheses, including those incorporating other mycorrhizal benefits conferred to plants, such as increased defence, should be explored. If broadened in this way, my findings suggest the BMT could remain a relevant and valuable model for understanding AM fungal symbioses.

References

Adam, M., Westphal, A., Hallmann, J., & Heuer, H. (2014). Specific microbial attachment to root knot nematodes in suppressive soil. *Applied and Environmental Microbiology*, *80*(9), 2679–2686. https://doi.org/10.1128/AEM.03905-13/

Adams, A. S., Jordan, M. S., Adams, S. M., Suen, G., Goodwin, L. A., Davenport, K. W., Currie, C. R., & Raffa, K. F. (2011). Cellulose-degrading bacteria associated with the invasive woodwasp Sirex noctilio. *The ISME Journal*, *5*(8), 1323–1331. https://doi.org/10.1038/ISMEJ.2011.14

Aguilar-Trigueros, C. A., Hempel, S., Powell, J. R., Cornwell, W. K., & Rillig, M. C. (2019). Bridging reproductive and microbial ecology: a case study in arbuscular mycorrhizal fungi. *The ISME Journal*, *13*(4), 873–884. https://doi.org/10.1038/S41396-018-0314-7

Alaux, P.-L., Naveau, F., Declerck, S., & Cranenbrouck, S. (2020). Common Mycorrhizal Network Induced JA/ET Genes Expression in Healthy Potato Plants Connected to Potato Plants Infected by Phytophthora infestans. *Frontiers in Plant Science*, *11*, 503121. https://doi.org/10.3389/fpls.2020.00602

Alaux, P.-L., Zhang, Y., Gilbert, L., & Johnson, D. (2021). Can common mycorrhizal fungal networks be managed to enhance ecosystem functionality? *Plants, People, Planet*, *3*(5), 433–444. https://doi.org/10.1002/PPP3.10178

Andrino, A., Boy, J., Mikutta, R., Sauheitl, L., & Guggenberger, G. (2019). Carbon investment required for the mobilization of inorganic and organic phosphorus bound to goethite by an arbuscular mycorrhiza (Solanum lycopersicum x Rhizophagus irregularis). *Frontiers in Environmental Science*, *7*(MAR), 422350. https://doi.org/10.3389/FENVS.2019.00026/

Andrino, A., Guggenberger, G., Sauheitl, L., Burkart, S., & Boy, J. (2021). Carbon investment into mobilization of mineral and organic phosphorus by arbuscular mycorrhiza. *Biology and Fertility of Soils*, *57*(1), 47–64. https://doi.org/10.1007/S00374-020-01505-5/F

Antunes, P. M., Schneider, K., Hillis, D., & Klironomos, J. N. (2007). Can the arbuscular mycorrhizal fungus Glomus intraradices actively mobilize P from rock phosphates? *Pedobiologia*, *51*(4), 281–286. https://doi.org/10.1016/J.PEDOBI.2007.04.007

Antunes, P. M., Stürmer, S. L., Bever, J. D., Chagnon, P. L., Chaudhary, V. B., Deveautour, C., Fahey, C., Kokkoris, V., Lekberg, Y., Powell, J. R., Aguilar-Trigueros, C. A., & Zhang, H. (2025). Enhancing consistency in arbuscular mycorrhizal trait-based research to improve predictions of function. *Mycorrhiza 2025 35:2*, *35*(2), 1–25. https://doi.org/10.1007/S00572-025-01187-7

Argüello, A., O'Brien, M. J., van der Heijden, M. G. A., Wiemken, A., Schmid, B., & Niklaus, P. A. (2016). Options of partners improve carbon for phosphorus trade in the arbuscular mycorrhizal mutualism. *Ecology Letters*, *19*(6), 648–656. https://doi.org/10.1111/ELE.12601

Averill, C., Bhatnagar, J. M., Dietze, M. C., Pearse, W. D., & Kivlin, S. N. (2019). Global imprint of mycorrhizal fungi on whole-plant nutrient economics. *Proceedings of the National Academy of Sciences of the United States of America*, *116*(46), 23163–23168. https://doi.org/10.1073/PNAS.1906655116/SUPPL_FILE/PNAS.1906655116.SD01.CSV

Averill, C., Turner, B. L., & Finzi, A. C. (2014a). Mycorrhiza-mediated competition between plants and decomposers drives soil carbon storage. *Nature*, *505*(7484), 543–545. https://doi.org/10.1038/NATURE12901

Averill, C., Turner, B. L., & Finzi, A. C. (2014b). Mycorrhiza-mediated competition between plants and decomposers drives soil carbon storage. *Nature 2014 505:7484*, *505*(7484), 543–545. https://doi.org/10.1038/nature12901

Avital, S., Rog, I., Livne-Luzon, S., Cahanovitc, R., & Klein, T. (2022). Asymmetric belowground carbon transfer in a diverse tree community. *Molecular Ecology*, *31*(12), 3481–3495. https://doi.org/10.1111/MEC.16477

Awaydul, A., Zhu, W., Yuan, Y., Xiao, J., Hu, H., Chen, X., Koide, R. T., & Cheng, L. (2019). Common mycorrhizal networks influence the distribution of mineral nutrients between an invasive plant, Solidago canadensis, and a native plant, Kummerowa striata. *Mycorrhiza*, *29*(1), 29–38. https://doi.org/https://doi.org/10.1007/s00572-018-0873-5

Babikova, Z., Gilbert, L., Bruce, T. J. A., Birkett, M., Caulfield, J. C., Woodcock, C., Pickett, J. A., & Johnson, D. (2013). Underground signals carried through common mycelial networks warn neighbouring plants of aphid attack. *Ecology Letters*, *16*(7), 835–843. https://doi.org/10.1111/ELE.12115

Babikova, Z., Johnson, D., Bruce, T., Pickett, J. A., & Gilbert, L. (2013). How rapid is aphid-induced signal transfer between plants via common mycelial networks? *Communicative & Integrative Biology*, *6*(6), e25904. https://doi.org/10.4161/CIB.25904

Back, M. A., Haydock, P. P. J., & Jenkinson, P. (2002). Disease complexes involving plant parasitic nematodes and soilborne pathogens. *Plant Pathology*, *51*(6), 683–697. https://doi.org/10.1046/J.1365-3059.2002.00785.X

Badri, D. v., & Vivanco, J. M. (2009). Regulation and function of root exudates. *Plant, Cell and Environment*, *32*(6), 666–681. https://doi.org/10.1111/J.1365-3040.2009.01926.X

Bago, B., & Bécard, G. (2002). Bases of the obligate biotrophy of arbuscular mycorrhizal fungi. *Mycorrhizal Technology in Agriculture*, 33–48. https://doi.org/10.1007/978-3-0348-8117-3_3

Bago, B., Pfeffer, P. E., & Shachar-Hill, Y. (2000). Carbon Metabolism and Transport in Arbuscular Mycorrhizas. *Plant Physiology*, *124*(3), 949–958. https://doi.org/10.1104/PP.124.3.949

Baldwin, I. T. (2010). Plant volatiles. *Current Biology*, *20*(9), R392–R397. https://doi.org/10.1016/j.cub.2010.02.052

Barto, E. K., Weidenhamer, J. D., Cipollini, D., & Rillig, M. C. (2012). Fungal superhighways: do common mycorrhizal networks enhance below ground communication? *Trends in Plant Science*, *17*(11), 633–637. https://doi.org/10.1016/J.TPLANTS.2012.06.007

Been, T. H., & Schomaker, C. H. (2000). Development and evaluation of sampling methods for fields with infestation foci of potato cyst nematodes (Globodera rostochiensis and G. pallida). *Phytopathology*, *90*(6), 647–656. https://doi.org/10.1094/PHYTO.2000.90.6.647

Bell, C. A., Magkourilou, E., Ault, J. R., Urwin, P. E., & Field, K. J. (2024). Phytophagy impacts the quality and quantity of plant carbon resources acquired by mutualistic arbuscular mycorrhizal fungi. *Nature Communications 2024 15:1*, *15*(1), 1–14. https://doi.org/10.1038/s41467-024-45026-3

Bell, C. A., Magkourilou, E., Barker, H., Barker, A., Urwin, P. E., & Field, K. J. (2023). Arbuscular mycorrhizal fungal-induced tolerance is determined by fungal identity and pathogen density. *Plants, People, Planet*, *5*(2), 241–253. https://doi.org/10.1002/PPP3.10338

Bell, C. A., Magkourilou, E., Urwin, P. E., & Field, K. J. (2021). The influence of competing root symbionts on below-ground plant resource allocation. *Ecology and Evolution*, *11*(7), 2997–3003. https://doi.org/10.1002/ECE3.7292

Bell, C. A., Magkourilou, E., Urwin, P. E., & Field, K. J. (2022). Disruption of carbon for nutrient exchange between potato and arbuscular mycorrhizal fungi enhanced cyst nematode fitness and host pest tolerance. *New Phytologist*, *234*(1), 269–279. https://doi.org/10.1111/NPH.17958

Bellemain, E., Carlsen, T., Brochmann, C., Coissac, E., Taberlet, P., & Kauserud, H. (2010). ITS as an environmental DNA barcode for fungi: An in silico approach reveals potential PCR biases. *BMC Microbiology*, *10*(1), 1–9. https://doi.org/10.1186/1471-2180-10-189

Benjamini, Y., & Hochberg, Y. (1995). Controlling the False Discovery Rate: A Practical and Powerful Approach to Multiple Testing. *Journal of the Royal Statistical Society: Series B (Methodological)*, *57*(1), 289–300. https://doi.org/10.1111/J.2517-6161.1995.TB02031.X

Bennett, A. E., & Groten, K. (2022). The Costs and Benefits of Plant-Arbuscular Mycorrhizal Fungal Interactions. *Annual Review of Plant Biology*, *73*, 649–672. https://doi.org/10.1146/ANNUREV-ARPLANT-102820-124504

Berdeja, M. P., Reynolds, N. K., Pawlowska, T., & Heuvel, J. E. V. (2025). Commercial bioinoculants improve colonization but do not alter the arbuscular mycorrhizal fungal community of greenhouse-grown grapevine roots. *Environmental Microbiome*, *20*(1), 1–15. https://doi.org/10.1186/S40793-025-00676-8/

Berdeni, D., Cotton, T. E. A., Daniell, T. J., Bidartondo, M. I., Cameron, D. D., & Evans, K. L. (2018). The effects of arbuscular mycorrhizal fungal colonisation on nutrient status, growth, productivity, and canker resistance of apple (Malus pumila). *Frontiers in Microbiology*, *9*(JUL). https://doi.org/https://doi.org/10.3389/fmicb.2018.01461

Berendsen, R. L., Pieterse, C. M. J., & Bakker, P. A. H. M. (2012). The rhizosphere microbiome and plant health. *Trends in Plant Science*, *17*(8), 478–486. https://doi.org/10.1016/J.TPLANTS.2012.04.001/ASSET/8021BF9C-1688-47F2-B480-97C85DFC5CEC/MAIN.ASSETS/GR3.JPG

Bergeson, G. B. (1972). Concepts of nematode—Fungus associations in plant disease complexes: A review. *Experimental Parasitology*, *32*(2), 301–314. https://doi.org/10.1016/0014-4894(72)90037-9

Bergmann, J., Weigelt, A., van der Plas, F., Laughlin, D. C., Kuyper, T. W., Guerrero-Ramirez, N., Valverde-Barrantes, O. J., Bruelheide, H., Fresche, G. T., Iversen, C. M., Kattge, J., McCormack, M. L., Meier, I. C., Rillig, M. C., Roumet, C., Semchenko, M., Sweeney, C. J., van Ruijven, J., York, L. M., & Mommer, L. (2020). The fungal collaboration gradient dominates the root economics space in plants. *Science Advances*, *6*(27). https://doi.org/https://doi.org/10.1126/sciadv.aba3756

Berruti, A., Desirò, A., Visentin, S., Zecca, O., & Bonfante, P. (2017). ITS fungal barcoding primers versus 18S AMF-specific primers reveal similar AMF-based diversity patterns in roots and soils of three mountain vineyards. *Environmental Microbiology Reports*, *9*(5), 658–667. https://doi.org/10.1111/1758-2229.12574

Bever, J. D., Richardson, S. C., Lawrence, B. M., Holmes, J., & Watson, M. (2009). Preferential allocation to beneficial symbiont with spatial structure maintains mycorrhizal mutualism. *Ecology Letters*, *12*(1), 13–21. https://doi.org/10.1111/J.1461-0248.2008.01254.X

Bianciotto, V., Bandi, C., Minerdi, D., Sironi, M., Tighy, H. V., & Bonfante, P. (1996). An obligately endosymbiotic mycorrhizal fungus itself harbors obligately intracellular bacteria. *Applied and Environmental Microbiology*, *62*(8), 3005–3010. https://doi.org/10.1128/AEM.62.8.3005-3010.1996

Blagodatskaya, E., & Kuzyakov, Y. (2013). Active microorganisms in soil: Critical review of estimation criteria and approaches. *Soil Biology and Biochemistry*, *67*, 192–211. https://doi.org/10.1016/J.SOILBIO.2013.08.024

Błaszkowski, J., Niezgoda, P., Meller, E., Milczarski, P., Zubek, S., Malicka, M., Uszok, S., Casieri, L., Goto, B. T., & Magurno, F. (2021). New taxa in Glomeromycota: Polonosporaceae fam. nov., Polonospora gen. nov., and P. polonica comb. nov. *Mycological Progress*, *20*(8), 941–951. https://doi.org/10.1007/S11557-021-01726-4

Blažková, A., Jansa, J., Püschel, D., Vosátka, M., & Janoušková, M. (2021). Is mycorrhiza functioning influenced by the quantitative composition of the mycorrhizal fungal community? *Soil Biology and Biochemistry*, *157*, 108249. https://doi.org/10.1016/J.SOILBIO.2021.108249

Bleve-Zacheo, T., & Melillo, M. T. (1997). The Biology of Giant Cells. In *Cellular and Molecular Aspects of Plant-Nematode Interactions* (pp. 65–79). Springer, Dordrecht. https://doi.org/10.1007/978-94-011-5596-0_6

Broeckling, C. D., Broz, A. K., Bergelson, J., Manter, D. K., & Vivanco, J. M. (2008). Root exudates regulate soil fungal community composition and diversity. *Applied and Environmental Microbiology*, *74*(3), 738–744. https://doi.org/10.1128/AEM.02188-07

Brosset, A., & Blande, J. D. (2022). Volatile-mediated plant–plant interactions: volatile organic compounds as modulators of receiver plant defence, growth, and reproduction. *Journal of Experimental Botany*, *73*(2), 511–528. https://doi.org/10.1093/JXB/ERAB487

Brundrett, M. C., & Tedersoo, L. (2018). Evolutionary history of mycorrhizal symbioses and global host plant diversity. *New Phytologist*, *220*(4), 1108–1115. https://doi.org/10.1111/NPH.14976

Bücking, H., Mensah, J. A., & Fellbaum, C. R. (2016). Common mycorrhizal networks and their effect on the bargaining power of the fungal partner in the arbuscular mycorrhizal symbiosis. *Communicative & Integrative Biology*, *9*(1). https://doi.org/10.1080/19420889.2015.1107684

Bücking, H., & Shachar-Hill, Y. (2005). Phosphate uptake, transport and transfer by the arbuscular mycorrhizal fungus Glomus intraradices is stimulated by increased carbohydrate availability. *New Phytologist*, *165*(3), 899–912. https://doi.org/10.1111/J.1469-8137.2004.01274.X

Buil, P. A., Jansa, J., Rozmoš, M., Kotianová, M., Bukovská, P., Grilli, G., Marro, N., & Janoušková, M. (2025). Soil cropping selects for nutrient efficient but more costly indigenous mycorrhizal fungal communities. *Biology and Fertility of Soils*, *61*(5), 841–859. https://doi.org/10.1007/S00374-025-01900-W/

Bunn, R. A., Corrêa, A., Joshi, J., Kaiser, C., Lekberg, Y., Prescott, C. E., Sala, A., & Karst, J. (2024). What determines transfer of carbon from plants to mycorrhizal fungi? *New Phytologist*, *244*(4), 1199–1215. https://doi.org/10.1111/NPH.20145

Bunn, R. A., Simpson, D. T., Bullington, L. S., Lekberg, Y., & Janos, D. P. (2019). Revisiting the 'direct mineral cycling' hypothesis: arbuscular mycorrhizal fungi colonize leaf litter, but why? *The ISME Journal*, *13*(8), 1891–1898. https://doi.org/10.1038/S41396-019-0403-2

Cabello, M., Irrazabal, G., Bucsinszky, A. M., Saparrat, M., & Schalamuk, S. (2005). Effect of an arbuscular mycorrhizal fungus, Glomus mosseae, and a rock-phosphate-solubilizing fungus, Penicillium thomii, on Mentha piperita growth in a soilless medium. *Journal of Basic Microbiology*, *45*(3), 182–189. https://doi.org/10.1002/JOBM.200410409

Cahanovitc, R., Livne-Luzon, S., Angel, R., & Klein, T. (2022). Ectomycorrhizal fungi mediate belowground carbon transfer between pines and oaks. *The ISME Journal 2022 16:5*, *16*(5), 1420–1429. https://doi.org/10.1038/s41396-022-01193-z

Callahan, B. J., McMurdie, P. J., Rosen, M. J., Han, A. W., Johnson, A. J. A., & Holmes, S. P. (2016). DADA2: High-resolution sample inference from Illumina amplicon data. *Nature Methods 2016 13:7*, *13*(7), 581–583. https://doi.org/10.1038/nmeth.3869

Camacho, C., Coulouris, G., Avagyan, V., Ma, N., Papadopoulos, J., Bealer, K., & Madden, T. L. (2009). BLAST+: Architecture and applications. *BMC Bioinformatics*, *10*(1), 1–9. https://doi.org/10.1186/1471-2105-10-421/

Camenzind, T., Aguilar-Trigueros, C. A., Heuck, M. K., Maerowitz-McMahan, S., Rillig, M. C., Cornwell, W. K., & Powell, J. R. (2024). Progressing beyond colonization strategies to understand arbuscular mycorrhizal fungal life history. *New Phytologist*, *244*(3), 752–759. https://doi.org/10.1111/NPH.20090

Cameron, D. D., Johnson, I., Leake, J. R., & Read, D. J. (2007). Mycorrhizal Acquisition of Inorganic Phosphorus by the Green-leaved Terrestrial Orchid Goodyera repens. *Annals of Botany*, *99*(5), 831–834. https://doi.org/10.1093/AOB/MCM018

Cameron, D. D., Johnson, I., Read, D. J., & Leake, J. R. (2008). Giving and receiving: measuring the carbon cost of mycorrhizas in the green orchid, Goodyera repens. *New Phytologist*, *180*(1), 176–184. https://doi.org/10.1111/J.1469-8137.2008.02533.X

Cameron, D. D., Neal, A. L., van Wees, S. C. M., & Ton, J. (2013). Mycorrhiza-induced resistance: more than the sum of its parts? *Trends in Plant Science*, *18*(10), 539–545. https://doi.org/10.1016/J.TPLANTS.2013.06.004

Caris, C., Hördt, W., Hawkins, H. J., Römheld, V., & George, E. (1998). Studies of iron transport by arbuscular mycorrhizal hyphae from soil to peanut and sorghum plants. *Mycorrhiza*, *8*(1), 35–39. https://doi.org/10.1007/S005720050208

Carta, L. K., Handoo, Z. A., Li, S., Kantor, M., Bauchan, G., McCann, D., Gabriel, C. K., Yu, Q., Reed, S., Koch, J., Martin, D., & Burke, D. J. (2020). Beech leaf disease symptoms caused by newly recognized nematode

subspecies Litylenchus crenatae mccannii (Anguinata) described from Fagus grandifolia in North America. *Forest Pathology*, *50*(2), e12580. https://doi.org/10.1111/EFP.12580

Carvalhais, L. C., Dennis, P. G., Badri, D. v., Kidd, B. N., Vivanco, J. M., & Schenk, P. M. (2015). Linking Jasmonic acid signaling, root exudates, and rhizosphere microbiomes. *Molecular Plant-Microbe Interactions*, *28*(9), 1049–1058. https://doi.org/10.1094/MPMI-01-15-0016-R/

Castelli, J. P., & Casper, B. B. (2003). INTRASPECIFIC AM FUNGAL VARIATION CONTRIBUTES TO PLANT–FUNGAL FEEDBACK IN A SERPENTINE GRASSLAND. *Ecology*, *84*(2), 323–336. https://doi.org/https://doi.org/10.1890/0012-9658

Castorina, G., Grassi, F., Consonni, G., Vitalini, S., Oberti, R., Calcante, A., Ferrari, E., Bononi, M., & Iriti, M. (2020). Characterization of the Biogenic Volatile Organic Compounds (BVOCs) and Analysis of the PR1 Molecular Marker in Vitis vinifera L. Inoculated with the Nematode Xiphinema index. *International Journal of Molecular Sciences 2020, Vol. 21, Page 4485*, *21*(12), 4485. https://doi.org/10.3390/IJMS21124485

Cessna, S., Demmig-Adams, B., Adams, W. W., & Cessna, I. S. (2010). Exploring Photosynthesis and Plant Stress Using Inexpensive Chlorophyll Fluorometers. *Journal of Natural Resources and Life Sciences Education*, *39*(1), 22–30. https://doi.org/10.4195/JNRLSE.2009.0024U

Chagnon, P. L., Bradley, R. L., Maherali, H., & Klironomos, J. N. (2013). A trait-based framework to understand life history of mycorrhizal fungi. *Trends in Plant Science*, *18*(9), 484–491. https://doi.org/10.1016/J.TPLANTS.2013.05.001/

Charters, M. D., Sait, S. M., Correspondence, K. J. F., & Field, K. J. (2020). Aphid Herbivory Drives Asymmetry in Carbon for Nutrient Exchange between Plants and an Arbuscular Mycorrhizal Fungus. *Current Biology*, *30*. https://doi.org/10.1016/j.cub.2020.02.087

Chaudhary, V. B., Holland, E. P., Charman-Anderson, S., Guzman, A., Bell-Dereske, L., Cheeke, T. E., Corrales, A., Duchicela, J., Egan, C., Gupta, M. M., Hannula, S. E., Hestrin, R., Hoosein, S., Kumar, A., Mhretu, G., Neuenkamp, L., Soti, P., Xie, Y., & Helgason, T. (2022). What are mycorrhizal traits? *Trends in Ecology & Evolution*, *37*(7), 573–581. https://doi.org/10.1016/J.TREE.2022.04.003

Chen, J., Hu, L., Sun, L., Lin, B., Huang, K., Zhuo, K., & Liao, J. (2018). A novel Meloidogyne graminicola effector, MgMO237, interacts with multiple host defence-related proteins to manipulate plant basal immunity and promote parasitism. *Molecular Plant Pathology*, *19*(8), 1942–1955. https://doi.org/10.1111/MPP.12671

Cheng, L., Booker, F. L., Tu, C., Burkey, K. O., Zhou, L., Shew, H. D., Rufty, T. W., & Hu, S. (2012). Arbuscular mycorrhizal fungi increase organic carbon decomposition under elevated CO2. *Science*, *337*(6098), 1084–1087. https://doi.org/10.1126/SCIENCE.1224304/

Choreño-Parra, E. M., & Treseder, K. K. (2024). Mycorrhizal fungi modify decomposition: a meta-analysis. *New Phytologist*, *242*(6), 2763–2774. https://doi.org/10.1111/NPH.19748

Chowdhury, S., Lange, M., Malik, A. A., Goodall, T., Huang, J., Griffiths, R. I., & Gleixner, G. (2022). Plants with arbuscular mycorrhizal fungi efficiently acquire Nitrogen from substrate additions by shaping the decomposer community composition and their net plant carbon demand. *Plant and Soil*, *475*(1–2), 473–490. https://doi.org/10.1007/S11104-022-05380-X

Clavijo McCormick, A., Unsicker, S. B., & Gershenzon, J. (2012). The specificity of herbivore-induced plant volatiles in attracting herbivore enemies. *Trends in Plant Science*, *17*(5), 303–310. https://doi.org/10.1016/J.TPLANTS.2012.03.012/ASSET/416B2A67-BCC4-400E-B914-F8FB0D42806B/

Clocchiatti, A., Hannula, S. E., Hundscheid, M. P. J., klein Gunnewiek, P. J. A., & de Boer, W. (2021). Stimulated saprotrophic fungi in arable soil extend their activity to the rhizosphere and root microbiomes of crop seedlings. *Environmental Microbiology*, *23*(10), 6056. https://doi.org/10.1111/1462-2920.15563

Constantino, N., Oh, Y., Şennik, E., Andersen, B., Warden, M., Oralkan, Ö., & Dean, R. A. (2021). Soybean Cyst Nematodes Influence Aboveground Plant Volatile Signals Prior to Symptom Development. *Frontiers in Plant Science*, *12*, 749014. https://doi.org/10.3389/FPLS.2021.749014/

Corrêa, A., Ferrol, N., & Cruz, C. (2023). Testing the trade-balance model: resource stoichiometry does not sufficiently explain AM effects. *New Phytologist*. https://doi.org/10.1111/NPH.19432

Courtois, E. A., Paine, C. E. T., Blandinieres, P. A., Stien, D., Bessiere, J. M., Houel, E., Baraloto, C., & Chave, J. (2009). Diversity of the volatile organic compounds emitted by 55 species of tropical trees: A survey in French Guiana. *Journal of Chemical Ecology*, *35*(11), 1349–1362. https://doi.org/10.1007/S10886-009-9718-1/

Crossay, T., Majorel, C., Redecker, D., Gensous, S., Medevielle, V., Durrieu, G., Cavaloc, Y., & Amir, H. (2019). Is a mixture of arbuscular mycorrhizal fungi better for plant growth than single-species inoculants? *Mycorrhiza*, *29*(4), 325–339. https://doi.org/10.1007/S00572-019-00898-Y/

Cruz-Paredes, C., Svenningsen, N. B., Nybroe, O., Kjøller, R., Frøslev, T. G., & Jakobsen, I. (2019). Suppression of arbuscular mycorrhizal fungal activity in a diverse collection of non-cultivated soils. *FEMS Microbiology Ecology*, *95*(3), 20. https://doi.org/10.1093/FEMSEC/FIZ020

de Deyn, G. B., Raaijmakers, C. E., Zoomer, H. R., Berg, M. P., de Ruiter, P. C., Verhoef, H. A., Bezemer, T. M., & van der Putten, W. H. (2003). Soil invertebrate fauna enhances grassland succession and diversity. *Nature*, *422*(6933), 711–713. https://doi.org/10.1038/NATURE01548;KWRD

de Kesel, J., Conrath, U., Flors, V., Luna, E., Mageroy, M. H., Mauch-Mani, B., Pastor, V., Pozo, M. J., Pieterse, C. M. J., Ton, J., & Kyndt, T. (2021). The Induced Resistance Lexicon: Do's and Don'ts. *Trends in Plant Science*, *26*(7), 685–691. https://doi.org/10.1016/j.tplants.2021.01.001

de La Peña, E., Echeverría, S. R., van der Putten, W. H., Freitas, H., & Moens, M. (2006). Mechanism of control of root-feeding nematodes by mycorrhizal fungi in the dune grass Ammophila arenaria. *New Phytologist*, *169*(4), 829–840. https://doi.org/10.1111/J.1469-8137.2005.01602.X

de Novais, C. B., Pepe, A., Siqueira, J. O., Giovannetti, M., & Sbrana, C. (2017). Compatibility and incompatibility in hyphal anastomosis of arbuscular mycorrhizal fungi. *Scientia Agricola*, *74*(5), 411–416. https://doi.org/10.1590/1678-992X-2016-0243

de Vries, F. T., & Caruso, T. (2016). Eating from the same plate? Revisiting the role of labile carbon inputs in the soil food web. *Soil Biology and Biochemistry*, *102*, 4–9. https://doi.org/10.1016/J.SOILBIO.2016.06.023

Delavaux, C. S., Smith-Ramesh, L. M., & Kuebbing, S. E. (2017). Beyond nutrients: a meta-analysis of the diverse effects of arbuscular mycorrhizal fungi on plants and soils. *Ecology*, *98*(8), 2111–2119. https://doi.org/10.1002/ECY.1892

Denton, C. S., Bardgett, R. D., Cook, R., & Hobbs, P. J. (1998). Low amounts of root herbivory positively influence the rhizosphere microbial community in a temperate grassland soil. *Soil Biology and Biochemistry*, *31*(1), 155–165. https://doi.org/10.1016/S0038-0717(98)00118-7

Dicke, M., & Baldwin, I. T. (2010). The evolutionary context for herbivore-induced plant volatiles: beyond the "cry for help." *Trends in Plant Science*, *15*(3), 167–175. https://doi.org/10.1016/J.TPLANTS.2009.12.002

Dodds, P. N., & Rathjen, J. P. (2010). Plant immunity: towards an integrated view of plant–pathogen interactions. *Nature Reviews Genetics 2010 11:8*, *11*(8), 539–548. https://doi.org/10.1038/nrg2812

Doidy, J., van Tuinen, D., Lamotte, O., Corneillat, M., Alcaraz, G., & Wipf, D. (2012). The Medicago truncatula Sucrose Transporter Family: Characterization and Implication of Key Members in Carbon Partitioning towards Arbuscular Mycorrhizal Fungi. *Molecular Plant*, *5*(6), 1346–1358. https://doi.org/10.1093/MP/SSS079

Doornbos, R. F., Geraats, B. P. J., Kuramae, E. E., van Loon, L. C., & Bakker, P. A. H. M. (2011). Effects of jasmonic acid, ethylene, and salicylic acid signaling on the rhizosphere bacterial community of Arabidopsis thaliana. *Molecular Plant-Microbe Interactions*, *24*(4), 395–407. https://doi.org/10.1094/MPMI-05-10-0115

Drigo, B., Kowalchuk, G. A., Knapp, B. A., Pijl, A. S., Boschker, H. T. S., & van Veen, J. A. (2013). Impacts of 3 years of elevated atmospheric CO2 on rhizosphere carbon flow and microbial community dynamics. *Global Change Biology*, *19*(2), 621–636. https://doi.org/10.1111/GCB.12045

Drigo, B., Pijl, A. S., Duyts, H., Kielak, A. M., Gamper, H. A., Houtekamer, M. J., Boschker, H. T. S., Bodelier, P. L. E., Whiteley, A. S., Veen, J. A. van, & Kowalchuk, G. A. (2010). Shifting carbon flow from roots into associated microbial communities in response to elevated atmospheric CO2. *Proceedings of the National Academy of Sciences*, *107*(24), 10938–10942. https://doi.org/10.1073/PNAS.0912421107

Duan, S., Feng, G., Limpens, E., Bonfante, P., Xie, X., & Zhang, L. (2024). Cross-kingdom nutrient exchange in the plant–arbuscular mycorrhizal fungus–bacterium continuum. *Nature Reviews Microbiology 2024 22:12*, *22*(12), 773–790. https://doi.org/10.1038/s41579-024-01073-7

Duan, S., Jin, Z., Zhang, L., & Declerck, S. (2025). Mechanisms of cooperation in the plants-arbuscular mycorrhizal fungi-bacteria continuum. *The ISME Journal*, *19*(1), 23. https://doi.org/10.1093/ISMEJO/WRAF023

Dumbrell, A. J., Ashton, P. D., Aziz, N., Feng, G., Nelson, M., Dytham, C., Fitter, A. H., & Helgason, T. (2011). Distinct seasonal assemblages of arbuscular mycorrhizal fungi revealed by massively parallel pyrosequencing. *New Phytologist*, *190*(3), 794–804. https://doi.org/10.1111/J.1469-8137.2010.03636.X

Duponnois, R., Colombet, A., Hien, V., & Thioulouse, J. (2005). The mycorrhizal fungus Glomus intraradices and rock phosphate amendment influence plant growth and microbial activity in the rhizosphere of Acacia holosericea. *Soil Biology and Biochemistry*, *37*(8), 1460–1468. https://doi.org/10.1016/J.SOILBIO.2004.09.016

Durant, E., Hoysted, G. A., Howard, N., Sait, S. M., Childs, D. Z., Johnson, D., & Field, K. J. (2023). Herbivore-driven disruption of arbuscular mycorrhizal carbon-for-nutrient exchange is ameliorated by neighboring plants. *Current Biology*, *33*(12), 2566-2573.e4. https://doi.org/10.1016/J.CUB.2023.05.033

Dwinell, L. D. (1997). The pinewood nematode: Regulation and mitigation. *Annual Review of Phytopathology*, *35*(Volume 35, 1997), 153–166. https://doi.org/10.1146/ANNUREV.PHYTO.35.1.153

Edwards, J., Johnson, C., Santos-Medellín, C., Lurie, E., Podishetty, N. K., Bhatnagar, S., Eisen, J. A., Sundaresan, V., & Jeffery, L. D. (2015). Structure, variation, and assembly of the root-associated microbiomes of rice. *Proceedings of the National Academy of Sciences of the United States of America*, *112*(8), E911–E920. https://doi.org/10.1073/PNAS.1414592112/SUPPL_FILE/PNAS.1414592112.SD01.XLSX

Elhady, A., Adss, S., Hallmann, J., & Heuer, H. (2018). Rhizosphere microbiomes modulated by pre-crops assisted plants in defense against plant-parasitic nematodes. *Frontiers in Microbiology*, *9*(JUN), 376555. https://doi.org/10.3389/FMICB.2018.01133/

Elhady, A., Giné, A., Topalovic, O., Jacquiod, S., Sørensen, S. J., Sorribas, F. J., & Heue, H. (2017). Microbiomes associated with infective stages of root-knot and lesion nematodes in soil. *PLOS ONE*, *12*(5), e0177145. https://doi.org/10.1371/JOURNAL.PONE.0177145

Elliott, A. J., Daniell, T. J., Cameron, D. D., & Field, K. J. (2021). A commercial arbuscular mycorrhizal inoculum increases root colonization across wheat cultivars but does not increase assimilation of mycorrhiza-acquired nutrients. *Plants, People, Planet*, *3*(5), 588–599. https://doi.org/10.1002/PPP3.10094

Ellouze, W., Hamel, C., DePauw, R. M., Knox, R. E., Cuthbert, R. D., & Singh, A. K. (2015). Potential to breed for mycorrhizal association in durum wheat. *Https://Doi.Org/10.1139/Cjm-2014-0598*, *62*(3), 263–271. https://doi.org/10.1139/CJM-2014-0598

Emmett, B. D., Lévesque-Tremblay, V., & Harrison, M. J. (2021). Conserved and reproducible bacterial communities associate with extraradical hyphae of arbuscular mycorrhizal fungi. *The ISME Journal*, *15*(8), 2276–2288. https://doi.org/10.1038/S41396-021-00920-2

Erb, M. (2018). Volatiles as inducers and suppressors of plant defense and immunity — origins, specificity, perception and signaling. *Current Opinion in Plant Biology*, *44*, 117–121. https://doi.org/10.1016/J.PBI.2018.03.008

Erb, M., Flors, V., Karlen, D., de Lange, E., Planchamp, C., D'Alessandro, M., Turlings, T. C. J., & Ton, J. (2009). Signal signature of aboveground-induced resistance upon belowground herbivory in maize. *The Plant Journal*, *59*(2), 292–302. https://doi.org/10.1111/J.1365-313X.2009.03868.X

Faghihinia, M., & Jansa, J. (2022). Mycorrhiza governs plant-plant interactions through preferential allocation of shared nutritional resources: A triple (13C, 15N and 33P) labeling study. *Frontiers in Plant Science*, *13*, 4987. https://doi.org/10.3389/FPLS.2022.1047270

Farmer, E. E., & Ryan, C. A. (1990). Interplant communication: airborne methyl jasmonate induces synthesis of proteinase inhibitors in plant leaves. *Proceedings of the National Academy of Sciences*, *87*(19), 7713–7716. https://doi.org/10.1073/PNAS.87.19.7713

Fellbaum, C. R., Gachomo, E. W., Beesetty, Y., Choudhari, S., Strahan, G. D., Pfeffer, P. E., Kiers, E. T., & Bücking, H. (2012). Carbon availability triggers fungal nitrogen uptake and transport in arbuscular mycorrhizal symbiosis. *Proceedings of the National Academy of Sciences*, *109*(7), 2666–2671. https://doi.org/10.1073/PNAS.1118650109

Fellbaum, C. R., Mensah, J. A., Cloos, A. J., Strahan, G. E., Pfeffer, P. E., Kiers, E. T., & Bücking, H. (2014). Fungal nutrient allocation in common mycorrhizal networks is regulated by the carbon source strength of individual host plants. *New Phytologist*, *203*(2), 646–656. https://doi.org/10.1111/NPH.12827

Fenwick, D. W. (1940). Methods for the Recovery and Counting of Cysts of Heterodera schachtii from Soil. *Journal of Helminthology*, *18*(4), 155–172. https://doi.org/10.1017/S0022149X00031485

Field, K. J., Cameron, D. D., Leake, J. R., Tille, S., Bidartondo, M. I., & Beerling, D. J. (2012). Contrasting arbuscular mycorrhizal responses of vascular and non-vascular plants to a simulated Palaeozoic CO2 decline. *Nature Communications 2012 3:1*, *3*(1), 1–8. https://doi.org/10.1038/ncomms1831

Figueiredo, A. F., Boy, J., & Guggenberger, G. (2021). Common Mycorrhizae Network: A Review of the Theories and Mechanisms Behind Underground Interactions. *Frontiers in Fungal Biology*, *2*, 735299. https://doi.org/10.3389/FFUNB.2021.735299/XML

Finlay, R., & Söderström, B. (1992). Mycorrhiza and Carbon Flow to the Soil. In *Mycorrhizal functioning: an integrative plant-fungal process* (pp. 134–160). Springer Science & Business Media.

Fitter, A. H. (2006). What is the link between carbon and phosphorus fluxes in arbuscular mycorrhizas? A null hypothesis for symbiotic function. *New Phytologist*, *172*(1), 3–6. https://doi.org/10.1111/J.1469-8137.2006.01861.X

Fitter, A. H., Graves, J. D., Watkins, N. K., Robinson, D. G., & Scrimgeour, C. (1998). Carbon transfer between plants and its control in networks of arbuscular mycorrhizas. *Functional Ecology*, *12*(3), 406–412. https://doi.org/10.1046/J.1365-2435.1998.00206.X

Forczek, S. T., Bukovská, P., Püschel, D., Janoušková, M., Blažková, A., & Jansa, J. (2022). Drought rearranges preferential carbon allocation to arbuscular mycorrhizal community members co-inhabiting roots of Medicago truncatula. *Environmental and Experimental Botany*, *199*, 104897. https://doi.org/10.1016/J.ENVEXPBOT.2022.104897

Francis, R., & Read, D. J. (1984). Direct transfer of carbon between plants connected by vesicular–arbuscular mycorrhizal mycelium. *Nature 1984 307:5946*, *307*(5946), 53–56. https://doi.org/10.1038/307053a0

Frank, L., Wenig, M., Ghirardo, A., van der Krol, A., Vlot, A. C., Schnitzler, J. P., & Rosenkranz, M. (2021). Isoprene and β-caryophyllene confer plant resistance via different plant internal signalling pathways. *Plant, Cell & Environment*, *44*(4), 1151–1164. https://doi.org/10.1111/PCE.14010

Frew, A. (2022). Root herbivory reduces species richness and alters community structure of root-colonising arbuscular mycorrhizal fungi. *Soil Biology and Biochemistry*, *171*, 108723. https://doi.org/10.1016/J.SOILBIO.2022.108723

Frew, A., Antunes, P. M., Cameron, D. D., Hartley, S. E., Johnson, S. N., Rillig, M. C., & Bennett, A. E. (2022). Plant herbivore protection by arbuscular mycorrhizas: a role for fungal diversity? *New Phytologist*, *233*(3), 1022–1031. https://doi.org/10.1111/NPH.17781

Frew, A., Öpik, M., Oja, J., Vahter, T., Hiiesalu, I., & Aguilar-Trigueros, C. A. (2023). Herbivory-driven shifts in arbuscular mycorrhizal fungal community assembly: increased fungal competition and plant phosphorus benefits. *New Phytologist*. https://doi.org/10.1111/NPH.19474

Frew, A., Powell, J. R., Glauser, G., Bennett, A. E., & Johnson, S. N. (2018). Mycorrhizal fungi enhance nutrient uptake but disarm defences in plant roots, promoting plant-parasitic nematode populations. *Soil Biology and Biochemistry*, *126*, 123–132. https://doi.org/10.1016/J.SOILBIO.2018.08.019

Frew, A., Weinberger, N., Powell, J., Watts-Williams, S. J., & Aguilar-Trigueros, C. A. (2024). Community assembly of root-colonising arbuscular mycorrhizal fungi: Beyond carbon and into defence? *The ISME Journal*. https://doi.org/10.1093/ismejo/wrae007/7584592

Frey, S. D. (2019). Mycorrhizal Fungi as Mediators of Soil Organic Matter Dynamics. *Annual Review of Ecology, Evolution, and Systematics*, *50*(Volume 50, 2019), 237–259. https://doi.org/10.1146/ANNUREV-ECOLSYS-110617-062331/CITE/REFWORKS

Friedman, M. (2006). Potato Glycoalkaloids and Metabolites: Roles in the Plant and in the Diet. *Journal of Agricultural and Food Chemistry*, *54*(23), 8655–8681. https://doi.org/10.1021/JF061471T

Friese, C. F., & Allen, M. F. (1991). The Spread of Va Mycorrhizal Fungal Hyphae in the Soil: Inoculum Types and External Hyphal Architecture. *Mycologia*, *83*(4), 409–418. https://doi.org/10.1080/00275514.1991.12026030

Fritz, M., Jakobsen, I., Lyngkjær, M. F., Thordal-Christensen, H., & Pons-Kühnemann, J. (2006). Arbuscular mycorrhiza reduces susceptibility of tomato to Alternaria solani. *Mycorrhiza*, *16*(6), 413–419. https://doi.org/10.1007/S00572-006-0051-Z

Frost, C. J., Appel, H. M., Carlson, J. E., de Moraes, C. M., Mescher, M. C., & Schultz, J. C. (2007). Within-plant signalling via volatiles overcomes vascular constraints on systemic signalling and primes responses against herbivores. *Ecology Letters*, *10*(6), 490–498. https://doi.org/10.1111/J.1461-0248.2007.01043.X

Gadgil, R., & Gadgil, P. (1971). Mycorrhiza and litter decomposition. *Nature*, *233*, 133–133. https://www.nature.com/articles/233133a0

Garita, S. A., Bernardo, V. F., Guimarães, M. D. A., Arango, M. C., & Ruscitti, M. F. (2019). Mycorrhization and grafting improve growth in the tomato and reduce the population of Nacobbus aberrans. *Revista Ciência Agronômica*, *50*(4), 609–615. https://doi.org/10.5935/1806-6690.20190072

Gehring, C. A., & Whitham, T. G. (2002). *Mycorrhizae-Herbivore Interactions: Population and Community Consequences*. 295–320. https://doi.org/10.1007/978-3-540-38364-2_12

Ghignone, S., Salvioli, A., Anca, I., Lumini, E., Ortu, G., Petiti, L., Cruveiller, S., Bianciotto, V., Piffanelli, P., Lanfranco, L., & Bonfante, P. (2012). The genome of the obligate endobacterium of an AM fungus reveals an interphylum network of nutritional interactions. *The ISME Journal*, *6*(1), 136–145. https://doi.org/10.1038/ISMEJ.2011.110

GIANINAZZI, S., GIANINAZZI-PEARSON, V., & DEXHEIMER, J. (1979). ENZYMATIC STUDIES ON THE METABOLISM OF VESICULAR-ARBUSCULAR MYCORRHIZA. III. ULTRASTRUCTURAL LOCALIZATION OF ACID AND ALKALINE PHOSPHATASE IN ONION ROOTS INFECTED BY GLOMUS MOSSEAE (NICOL. & GERD.). *New Phytologist*, *82*(1), 127–132. https://doi.org/10.1111/J.1469-8137.1979.TB07566.X

Gibb, S., & Strimmer, K. (2012). MALDIquant: a versatile R package for the analysis of mass spectrometry data. *Bioinformatics*, *28*(17), 2270–2271. https://doi.org/10.1093/BIOINFORMATICS/BTS447

Ginnan, N. A., Dang, T., Bodaghi, S., Ruegger, P. M., McCollum, G., England, G., Vidalakis, G., Borneman, J., Rolshausen, P. E., & Caroline Roper, M. (2020). Disease-Induced Microbial Shifts in Citrus Indicate Microbiome-

Derived Responses to Huanglongbing Across the Disease Severity Spectrum. https://doi.org/10.1094/PBIOMES-04-20-0027-R

Giovannetti, M., Sbrana, C., Avio, L., & Strani, P. (2004). Patterns of below-ground plant interconnections established by means of arbuscular mycorrhizal networks. *New Phytologist*, *164*(1), 175–181. https://doi.org/10.1111/J.1469-8137.2004.01145.X

Govindarajulu, M., Pfeffer, P. E., Jin, H., Abubaker, J., Douds, D. D., Allen, J. W., Bücking, H., Lammers, P. J., & Shachar-Hill, Y. (2005). Nitrogen transfer in the arbuscular mycorrhizal symbiosis. *Nature*, *435*(7043), 819–823. https://doi.org/10.1038/nature03610

Graves, J. D., Watkins, N. K., Fitter, A. H., Robinson, D. G., & Scrimgeour, C. (1997). Intraspecific transfer of carbon between plants linked by a common mycorrhizal network. *Plant and Soil*, *192*(2), 153–159. https://doi.org/10.1023/A:1004257812555

Grime, J. P., Mackey, J. M., Hillier, S. H., & Read, D. J. (1988). Mycorrhizal infection and plant species diversity. *Nature 1988 334:6179*, *334*(6179), 202–202. https://doi.org/10.1038/334202b0

Grime, J. P., Mackey, J. M. L., Hillier, S. H., & Read, D. J. (1987). Floristic diversity in a model system using experimental microcosms. *Nature*, *328*(6129), 420–422. https://doi.org/10.1038/328420a0

Guo, H., & Ge, F. (2017). Root nematode infection enhances leaf defense against whitefly in tomato. *Arthropod-Plant Interactions*, *11*(1), 23–33. https://doi.org/10.1007/S11829-016-9462-8/TABLES/2

Haegeman, A., Mantelin, S., Jones, J. T., & Gheysen, G. (2012). Functional roles of effectors of plant-parasitic nematodes. *Gene*, *492*(1), 19–31. https://doi.org/10.1016/j.gene.2011.10.040

Hamamouch, N., Li, C., Seo, P. J., Park, C. M., & Davis, E. L. (2011). Expression of Arabidopsis pathogenesis-related genes during nematode infection. *Molecular Plant Pathology*, *12*(4), 355–364. https://doi.org/10.1111/J.1364-3703.2010.00675

Hamilton, A. C. L. H. R. I., & Smith, B. L. D. L. M. (2000). Acquisition of Cu, Zn, Mn and Fe by mycorrhizal maize (Zea mays L.) grown in soil at different P and micronutrient levels. *Mycorrhiza*, *9*.

Hammer, E. C., Pallon, J., Wallander, H., & Olsson, P. A. (2011). Tit for tat? A mycorrhizal fungus accumulates phosphorus under low plant carbon availability. *FEMS Microbiology Ecology*, *76*(2), 236–244. https://doi.org/10.1111/J.1574-6941.2011.01043.X

Hammerbacher, A., Coutinho, T. A., & Gershenzon, J. (2019). Roles of plant volatiles in defence against microbial pathogens and microbial exploitation of volatiles. *Plant Cell and Environment*, *42*(10), 2827–2843. https://doi.org/10.1111/PCE.13602

Hanel, L. (1998). Distribution of nematodes in soil, mycorrhizal soil, mycorrhizae and roots of spruce forests at the Boubin Mount., Czech Republic. *Biologia (Slovak Republic)*, *53*(5), 593–603.

Hannula, S. E., Boschker, H. T. S., de Boer, W., & van Veen, J. A. (2012). 13C pulse-labeling assessment of the community structure of active fungi in the rhizosphere of a genetically starch-modified potato (Solanum tuberosum) cultivar and its parental isoline. *New Phytologist*, *194*(3), 784–799. https://doi.org/10.1111/J.1469-8137.2012.04089.X

Hannula, S. E., de Boer, W., & van Veen, J. A. (2010). In situ dynamics of soil fungal communities under different genotypes of potato, including a genetically modified cultivar. *Soil Biology and Biochemistry*, *42*(12), 2211–2223. https://doi.org/10.1016/J.SOILBIO.2010.08.020

Hannula, S. E., Morriën, E., de Hollander, M., van der Putten, W. H., van Veen, J. A., & de Boer, W. (2017). Shifts in rhizosphere fungal community during secondary succession following abandonment from agriculture. *ISME Journal*, *11*(10), 2294–2304. https://doi.org/10.1038/ISMEJ.2017.90

Hannula, S. E., Morriën, E., van der Putten, W. H., & de Boer, W. (2020). Rhizosphere fungi actively assimilating plant-derived carbon in a grassland soil. *Fungal Ecology*, *48*, 100988. https://doi.org/10.1016/J.FUNECO.2020.100988

Hart, M. M., Forsythe, J., Oshowski, B., Bücking, H., Jansa, J., & Kiers, E. T. (2013). Hiding in a crowd - Does diversity facilitate persistence of a low-quality fungal partner in the mycorrhizal symbiosis? *Symbiosis*, *59*(1), 47–56. https://doi.org/10.1007/S13199-012-0197-8/

Hart, M. M., & Reader, R. J. (2002). Taxonomic basis for variation in the colonization strategy of arbuscular mycorrhizal fungi. *New Phytologist*, *153*(2), 335–344. https://doi.org/10.1046/J.0028-646X.2001.00312.X

Hart, M. M., Reader, R. J., & Klironomos, J. N. (2001). Life-history strategies of arbuscular mycorrhizal fungi in relation to their successional dynamics. *Mycologia*, *93*(6), 1186–1194. https://doi.org/10.1080/00275514.2001.12063251

Hartig, F. (2025). DHARMa: Residual Diagnostics for Hierarchical (Multi-Level / Mixed) Regression Models. In *CRAN: Contributed Packages* (R package version 0.4.7). Comprehensive R Archive Network (CRAN). https://doi.org/10.32614/CRAN.PACKAGE.DHARMA

Hausmann, N. T., & Hawkes, C. v. (2009). Plant neighborhood control of arbuscular mycorrhizal community composition. *New Phytologist*, *183*(4), 1188–1200. https://doi.org/10.1111/J.1469-8137.2009.02882.X

Hawkins, H.-J., Cargill, R. I. M., van Nuland, M. E., Hagen, S. C., Field, K. J., Sheldrake, M., Soudzilovskaia, N. A., & Kiers, E. T. (2023). Mycorrhizal mycelium as a global carbon pool. *Current Biology*, *33*(11), 560–573. https://doi.org/10.1016/J.CUB.2023.02.027

Helgason, T., & Fitter, A. H. (2009). Natural selection and the evolutionary ecology of the arbuscular mycorrhizal fungi (Phylum Glomeromycota). *Journal of Experimental Botany*, *60*(9), 2465–2480. https://doi.org/10.1093/JXB/ERP144

Hempel, S., Renker, C., & Buscot, F. (2007). Differences in the species composition of arbuscular mycorrhizal fungi in spore, root and soil communities in a grassland ecosystem. *Environmental Microbiology*, *9*(8), 1930–1938. https://doi.org/10.1111/J.1462-2920.2007.01309.X;WGROUP:STRING:PUBLICATION

Henriksson, N., Marshall, J., Högberg, M. N., Högberg, P., Polle, A., Franklin, O., & Näsholm, T. (2023). Re-examining the evidence for the mother tree hypothesis – resource sharing among trees via ectomycorrhizal networks. *New Phytologist*. https://doi.org/10.1111/NPH.18935

Herman, D. J., Firestone, M. K., Nuccio, E., & Hodge, A. (2012). Interactions between an arbuscular mycorrhizal fungus and a soil microbial community mediating litter decomposition. *FEMS Microbiology Ecology*, *80*(1), 236–247. https://doi.org/10.1111/J.1574-6941.2011.01292.X

Hestrin, R., Hammer, E. C., Mueller, C. W., & Lehmann, J. (2019). Synergies between mycorrhizal fungi and soil microbial communities increase plant nitrogen acquisition. *Communications Biology*, *2*(1), 1–9. https://doi.org/10.1038/S42003-019-0481-8

Hijri, I., Sýkorová, Z., Oehl, F., Ineichen, K., Mäder, P., Wiemken, A., & Redecker, D. (2006). Communities of arbuscular mycorrhizal fungi in arable soils are not necessarily low in diversity. *Molecular Ecology*, *15*(8), 2277–2289. https://doi.org/10.1111/J.1365-294X.2006.02921.X

Hobbie, E. A. (2006). CARBON ALLOCATION TO ECTOMYCORRHIZAL FUNGI CORRELATES WITH BELOWGROUND ALLOCATION IN CULTURE STUDIES. *Ecology*, *87*(3), 563–569. https://doi.org/10.1890/05-0755

Hodge, A., & Fitter, A. H. (2010). Substantial nitrogen acquisition by arbuscular mycorrhizal fungi from organic material has implications for N cycling. *Proceedings of the National Academy of Sciences of the United States of America*, *107*(31), 13754–13759. https://doi.org/10.1073/PNAS.1005874107/

Hoeksema, J. D., Chaudhary, V. B., Gehring, C. A., Johnson, N. C., Karst, J., Koide, R. T., Pringle, A., Zabinski, C., Bever, J. D., Moore, J. C., Wilson, G. W. T., Klironomos, J. N., & Umbanhowar, J. (2010). A meta-analysis of

context-dependency in plant response to inoculation with mycorrhizal fungi. *Ecology Letters*, *13*(3), 394–407. https://doi.org/10.1111/J.1461-0248.2009.01430.X

Hofmann, J., & Grundler, F. M. W. (2006). Females and males of root-parasitic cyst nematodes induce different symplasmic connections between their syncytial feeding cells and the phloem in Arabidopsis thaliana. *Plant Physiology and Biochemistry*, *44*(5–6), 430–433. https://doi.org/10.1016/J.PLAPHY.2006.06.006

Hol, W. H. G., de Boer, W., Termorshuizen, A. J., Meyer, K. M., Schneider, J. H. M., van Dam, N. M., van Veen, J. A., & van der Putten, W. H. (2010). Reduction of rare soil microbes modifies plant–herbivore interactions. *Ecology Letters*, *13*(3), 292–301. https://doi.org/10.1111/J.1461-0248.2009.01424.X

Hong, S. C., Donaldson, J., & Gratton, C. (2010). Soybean Cyst Nematode Effects on Soybean Aphid Preference and Performance in the Laboratory. *Environmental Entomology*, *39*(5), 1561–1569. https://doi.org/10.1603/EN10091

Huang, H., Liu, S., Du, Y., Tang, J., Hu, L., & Chen, X. (2023). Carbon allocation mediated by arbuscular mycorrhizal fungi alters the soil microbial community under various phosphorus levels. *Fungal Ecology*, *62*, 101227. https://doi.org/10.1016/J.FUNECO.2023.101227

Hünninghaus, M., Dibbern, D., Kramer, S., Koller, R., Pausch, J., Schloter-Hai, B., Urich, T., Kandeler, E., Bonkowski, M., & Lueders, T. (2019). Disentangling carbon flow across microbial kingdoms in the rhizosphere of maize. *Soil Biology and Biochemistry*, *134*, 122–130. https://doi.org/10.1016/J.SOILBIO.2019.03.007

Iberkleid, I., Sela, N., & Brown Miyara, S. (2015). Meloidogyne javanica fatty acid- and retinol-binding protein (Mj-FAR-1) regulates expression of lipid-, cell wall-, stress- and phenylpropanoid-related genes during nematode infection of tomato. *BMC Genomics*, *16*(1), 1–26. https://doi.org/10.1186/S12864-015-1426-3/

Inceoğlu, O., van Overbeek, L. S., Salles, J. F., & van Elsas, J. D. (2013). Normal Operating Range of Bacterial Communities in Soil Used for Potato Cropping. *Applied and Environmental Microbiology*, *79*(4), 1160–1170. https://doi.org/10.1128/AEM.02811-12

Ingraffia, R., Giambalvo, D., Frenda, A. S., Roma, E., Ruisi, P., & Amato, G. (2021). Mycorrhizae differentially influence the transfer of nitrogen among associated plants and their competitive relationships. *Applied Soil Ecology*, *168*, 104127. https://doi.org/10.1016/J.APSOIL.2021.104127

Jakobsen, I., & Rosendahl, L. (1990). Carbon flow into soil and external hyphae from roots of mycorrhizal cucumber plants. *New Phytologist*, *115*(1), 77–83. https://doi.org/10.1111/J.1469-8137.1990.TB00924.X

Janoušková, M., & Jansa, J. (2025). More for less: how mycorrhizal fungal diversity benefits plant communities. *New Phytologist*, *248*(2), 438–440. https://doi.org/10.1111/NPH.70377

Jansa, J., Smith, F. A., & Smith, S. E. (2008). Are there benefits of simultaneous root colonization by different arbuscular mycorrhizal fungi? *New Phytologist*, *177*(3), 779–789. https://doi.org/10.1111/J.1469-8137.2007.02294.X

Ji, B., & Bever, J. D. (2016). Plant preferential allocation and fungal reward decline with soil phosphorus: implications for mycorrhizal mutualism. *Ecosphere*, *7*(5), e01256. https://doi.org/10.1002/ECS2.1256

Jiang, F., Zhang, L., Zhou, J., George, T. S., & Feng, G. (2021). Arbuscular mycorrhizal fungi enhance mineralisation of organic phosphorus by carrying bacteria along their extraradical hyphae. *New Phytologist*, *230*(1), 304–315. https://doi.org/10.1111/NPH.17081

Jiang, Y., Wang, W., Xie, Q., Liu, N., Liu, L., Wang, D., Zhang, X., Yang, C., Chen, X., Tang, D., & Wang, E. (2017). Plants transfer lipids to sustain colonization by mutualistic mycorrhizal and parasitic fungi. *Science*, *356*(6343), 1172–1173. https://doi.org/10.1126/SCIENCE.AAM9970

Johnson, D., Leake, J. R., & Read, D. J. (2001). Novel in-growth core system enables functional studies of grassland mycorrhizal mycelial networks. *New Phytologist*, *152*(3), 555–562. https://doi.org/10.1046/J.0028-646X.2001.00273.X

Johnson, N. C., Graham, J. H., & Smith, F. A. (1997). Functioning of mycorrhizal associations along the mutualism-parasitism continuum. *New Phytologist*, *135*(4), 575–585. https://doi.org/10.1046/J.1469-8137.1997.00729.X

Joner, E. J., Ravnskov, S., & Jakobsen, I. (2000). Arbuscular mycorrhizal phosphate transport under monoxenic conditions using radio-labelled inorganic and organic phosphate. *Biotechnology Letters*, *22*(21), 1705–1708. https://doi.org/10.1023/A:1005684031296/

Joosten, L., Mulder, P. P. J., Klinkhamer, P. G. L., & van Veen, J. A. (2009). Soil-borne microorganisms and soil-type affect pyrrolizidine alkaloids in Jacobaea vulgaris. *Plant and Soil*, *325*(1), 133–143. https://doi.org/10.1007/S11104-009-9963-7/

Jung, S. C., Martinez-Medina, A., Lopez-Raez, J. A., & Pozo, M. J. (2012). Mycorrhiza-Induced Resistance and Priming of Plant Defenses. *Journal of Chemical Ecology*, *38*(6), 651–664. https://doi.org/10.1007/s10886-012-0134-6

Junker, R. R., & Tholl, D. (2013). Volatile organic compound mediated interactions at the plant-microbe interface. *Journal of Chemical Ecology*, *39*(7), 810–825. https://doi.org/10.1007/S10886-013-0325-9

Kaiser, C., Kilburn, M. R., Clode, P. L., Fuchslueger, L., Koranda, M., Cliff, J. B., Solaiman, Z. M., & Murphy, D. v. (2015). Exploring the transfer of recent plant photosynthates to soil microbes: mycorrhizal pathway vs direct root exudation. *New Phytologist*, *205*(4), 1537–1551. https://doi.org/10.1111/NPH.13138

Kakouridis, A., Yuan, M., Nuccio, E. E., Hagen, J. A., Fossum, C. A., Moore, M. L., Estera-Molina, K. Y., Nico, P. S., Weber, P. K., Pett-Ridge, J., & Firestone, M. K. (2024). Arbuscular mycorrhiza convey significant plant carbon to a diverse hyphosphere microbial food web and mineral-associated organic matter. *New Phytologist*, *242*(4), 1661–1675. https://doi.org/10.1111/NPH.19560

Kantor, M., Handoo, Z., Carta, L., & Li, S. (2022). First Report of Beech Leaf Disease, Caused by Litylenchus crenatae mccannii, on American Beech (Fagus grandifolia) in Virginia. *Plant Disease*, *106*(6), 1764. https://doi.org/10.1094/PDIS-08-21-1713-PDN

Kantor, M., Handoo, Z., Kantor, C., & Carta, L. (2022). Top Ten Most Important U.S.-Regulated and Emerging Plant-Parasitic Nematodes. *Horticulturae 2022, Vol. 8, Page 208*, *8*(3), 208. https://doi.org/10.3390/HORTICULTURAE8030208

Karban, R., Grof-Tisza, P., & Blande, J. D. (2016). CHEMOTYPIC Variation in Volatiles and Herbivory for Sagebrush. *Journal of Chemical Ecology*, *42*(8), 829–840. https://doi.org/10.1007/S10886-016-0741-8

Karimi, M., van Montagu, M., & Gheysen, G. (2000). Nematodes as vectors to introduce Agrobacterium into plant roots. *Molecular Plant Pathology*, *1*(6), 383–387. https://doi.org/10.1046/J.1364-3703.2000.00043.X

Karst, J., Jones, M. D., & Hoeksema, J. D. (2023). Positive citation bias and overinterpreted results lead to misinformation on common mycorrhizal networks in forests. *Nature Ecology & Evolution 2023 7:4*, *7*(4), 501–511. https://doi.org/10.1038/s41559-023-01986-1

Keymer, A., Pimprikar, P., Wewer, V., Huber, C., Brands, M., Bucerius, S. L., Delaux, P. M., Klingl, V., von Röpenack-Lahaye, E., Wang, T. L., Eisenreich, W., Dörmann, P., Parniske, M., & Gutjahr, C. (2017). Lipid transfer from plants to arbuscular mycorrhiza fungi. *ELife*, *6*. https://doi.org/10.7554/ELIFE.29107

Khan, M. R. (2012). Nematodes, an Emerging Threat to Global Forests: Assessment and Management. *Plant Pathology Journal*, *11*(4), 99–113. https://doi.org/10.3923/PPJ.2012.99.113

Kiers, E. T., & Denison, R. F. (2008). Sanctions, cooperation, and the stability of plant-rhizosphere mutualisms. *Annual Review of Ecology, Evolution, and Systematics*, *39*, 215–236. https://doi.org/10.1146/ANNUREV.ECOLSYS.39.110707.173423

Kiers, E. T., Duhamel, M., Beesetty, Y., Mensah, J. A., Franken, O., Verbruggen, E., Fellbaum, C. R., Kowalchuk, G. A., Hart, M. M., Bago, A., Palmer, T. M., West, S. A., Vandenkoornhuyse, P., Jansa, J., & Bücking, H. (2011).

Reciprocal Rewards Stabilize Cooperation in the Mycorrhizal Symbiosis. *Science*, *333*(6044), 880–882. https://doi.org/10.1126/SCIENCE.1208473

Kiers, E. T., & van der Heijden, M. G. A. (2006). Mutualistic stability in the arbuscular mycorrhizal symbiosis: exploring hypotheses of evolutionary cooperation. *CONCEPTS & SYNTHESIS EMPHASIZING NEW IDEAS TO STIMULATE RESEARCH IN ECOLOGY Ecology*, *87*(7), 1627–1636. https://doi.org/10.1890/0012-9658

Kiers, E. T., West, S. A., Wyatt, G. A. K., Gardner, A., Bücking, H., & Werner, G. D. A. (2016). Misconceptions on the application of biological market theory to the mycorrhizal symbiosis. *Nature Plants 2016 2:5*, *2*(5), 1–2. https://doi.org/10.1038/nplants.2016.63

Kigathi, R. N., Weisser, W. W., Reichelt, M., Gershenzon, J., & Unsicker, S. B. (2019). Plant volatile emission depends on the species composition of the neighboring plant community. *BMC Plant Biology*, *19*(1), 1–17. https://doi.org/10.1186/S12870-018-1541-9/

Kihika, R., Murungi, L. K., Coyne, D., Ng'ang'a, M., Hassanali, A., Teal, P. E. A., & Torto, B. (2017). Parasitic nematode Meloidogyne incognita interactions with different Capsicum annum cultivars reveal the chemical constituents modulating root herbivory. *Scientific Reports 2017 7:1*, *7*(1), 1–10. https://doi.org/10.1038/s41598-017-02379-8

Kiige, J. K., Kavoo, A. M., Mwajita, M. R., Mogire, D., Ogada, S., Wekesa, T. B., & Kiirika, L. M. (2025). Metagenomic characterization of bacterial abundance and diversity in potato cyst nematode suppressive and conducive potato rhizosphere. *PLOS ONE*, *20*(5), e0323382. https://doi.org/10.1371/JOURNAL.PONE.0323382

Klironomos, J. H., Allen, M. F., Rillig, M. C., Piotrowski, J., Makvandi-Hejad, S., Wolfe, B. E., & Powell, J. R. (2005). Abrupt rise in atmospheric CO2 overestimates community response in a model plant-soil system. *Nature*, *433*(7026), 621–624. https://doi.org/10.1038/NATURE03268;KWRD

Klironomos, J. N. (2003). Variation in plant response to native and exotic arbuscular mycorrhizal fungi. *Ecology*, *84*(9), 2292–2301. https://doi.org/10.1890/02-0413

Koegel, S., Ait Lahmidi, N., Arnould, C., Chatagnier, O., Walder, F., Ineichen, K., Boller, T., Wipf, D., Wiemken, A., & Courty, P. E. (2013). The family of ammonium transporters (AMT) in Sorghum bicolor: two AMT members are induced locally, but not systemically in roots colonized by arbuscular mycorrhizal fungi. *New Phytologist*, *198*(3), 853–865. https://doi.org/10.1111/NPH.12199

Koegel, S., Mieulet, D., Baday, S., Chatagnier, O., Lehmann, M. F., Wiemken, A., Boller, T., Wipf, D., Bernèche, S., Guiderdoni, E., & Courty, P. E. (2017). Phylogenetic, structural, and functional characterization of AMT3;1, an ammonium transporter induced by mycorrhization among model grasses. *Mycorrhiza*, *27*(7), 695–708. https://doi.org/10.1007/S00572-017-0786-8/

Kohout, P., Sudová, R., Janoušková, M., Čtvrtlíková, M., Hejda, M., Pánková, H., Slavíková, R., Štajerová, K., Vosátka, M., & Sýkorová, Z. (2014). Comparison of commonly used primer sets for evaluating arbuscular mycorrhizal fungal communities: Is there a universal solution? *Soil Biology and Biochemistry*, *68*, 482–493. https://doi.org/10.1016/J.SOILBIO.2013.08.027

Koide, R. T., & Kabir, Z. (2000). Extraradical hyphae of the mycorrhizal fungus Glomus intraradices can hydrolyse organic phosphate. *New Phytologist*, *148*(3), 511–517. https://doi.org/10.1046/J.1469-8137.2000.00776.X

Kokkoris, V., & Hart, M. (2019). In vitro propagation of arbuscular mycorrhizal fungi may drive fungal evolution. *Frontiers in Microbiology*, *10*(OCT), 2420. https://doi.org/10.3389/FMICB.2019.02420/B

Kokkoris, V., Stefani, F., Dalpé, Y., Dettman, J., & Corradi, N. (2020). Nuclear Dynamics in the Arbuscular Mycorrhizal Fungi. *Trends in Plant Science*, *25*(8), 765–778. https://doi.org/10.1016/j.tplants.2020.05.002

Koricheva, J., Gange, A. C., & Jones, T. (2009). Effects of mycorrhizal fungi on insect herbivores: a meta-analysis. *Ecology*, *90*(8), 2088–2097. https://doi.org/10.1890/08-1555.1

Kudjordjie, E. N., Santos, S. S., Topalović, O., & Vestergård, M. (2024). Distinct changes in tomato-associated multi-kingdom microbiomes during Meloidogyne incognita parasitism. *Environmental Microbiome*, *19*(1), 1–18. https://doi.org/10.1186/S40793-024-00597-Y/

Kuhlgert, S., Austic, G., Zegarac, R., Osei-Bonsu, I., Hoh, D., Chilvers, M. I., Roth, M. G., Bi, K., TerAvest, D., Weebadde, P., & Kramer, D. M. (2016). MultispeQ Beta: a tool for large-scale plant phenotyping connected to the open PhotosynQ network. *Royal Society Open Science*, *3*(10). https://doi.org/10.1098/RSOS.160592

Kumar, A., Sharma, S., & Mishra, S. (2016). Evaluating effect of arbuscular mycorrhizal fungal consortia and Azotobacter chroococcum in improving biomass yield of Jatropha curcas. *Plant Biosystems - An International Journal Dealing with All Aspects of Plant Biology*, *150*(5), 1056–1064. https://doi.org/10.1080/11263504.2014.1001001

Kuznetsova, A., Brockhoff, P. B., & Christensen, R. H. B. (2017). lmerTest Package: Tests in Linear Mixed Effects Models. *Journal of Statistical Software*, *82*(13), 1–26. https://doi.org/10.18637/JSS.V082.I13

Kyndt, T., Nahar, K., Haegeman, A., de Vleesschauwer, D., Höfte, M., & Gheysen, G. (2012). Comparing systemic defence-related gene expression changes upon migratory and sedentary nematode attack in rice. *Plant Biology*, *14*(SUPPL. 1), 73–82. https://doi.org/10.1111/J.1438-8677.2011.00524.X

Kyndt, T., Vieira, P., Gheysen, G., & de Almeida-Engler, J. (2013). Nematode feeding sites: Unique organs in plant roots. *Planta*, *238*(5), 807–818. https://doi.org/10.1007/S00425-013-1923-Z

Lachman, J., Hamouz, K., Orsák, M., & Pivec, V. (2001). Potato glycoalkaloids and their significance in plant protection and human nutrition-review. *Rostlinna Vyroba*, *47*, 181–191. https://doi.org/10.5555/20013068044

Lamelas, A., Desgarennes, D., López-Lima, D., Villain, L., Alonso-Sánchez, A., Artacho, A., Latorre, A., Moya, A., & Carrión, G. (2020). The Bacterial Microbiome of Meloidogyne-Based Disease Complex in Coffee and Tomato. *Frontiers in Plant Science*, *11*, 510816. https://doi.org/10.3389/FPLS.2020.00136

Larimer, A. L., Clay, K., & Bever, J. D. (2014). Synergism and context dependency of interactions between arbuscular mycorrhizal fungi and rhizobia with a prairie legume. *Ecology*, *95*(4), 1045–1054. https://doi.org/10.1890/13-0025.1

Leake, J., Johnson, D., Donnelly, D., Muckle, G., Boddy, L., Read, D., Leake, J. R., Johnson, D., Muckle, G. E., Read, D. J., Donnelly, D. P., & Boddy, L. (2004). Networks of power and influence: the role of mycorrhizal mycelium in controlling plant communities and agroecosystem functioning. *Canadian Journal of Botany*, *82*(8), 1016–1045. https://doi.org/10.1139/B04-060

Leff, J. W., Jones, S. E., Prober, S. M., Barberán, A., Borer, E. T., Firn, J. L., Harpole, W. S., Hobbie, S. E., Hofmockel, K. S., Knops, J. M. H., McCulley, R. L., la Pierre, K., Risch, A. C., Seabloom, E. W., Schütz, M., Steenbock, C., Stevens, C. J., & Fierer, N. (2015). Consistent responses of soil microbial communities to elevated nutrient inputs in grasslands across the globe. *Proceedings of the National Academy of Sciences of the United States of America*, *112*(35), 10967–10972. https://doi.org/10.1073/PNAS.1508382112

Lehmann, A., & Rillig, M. C. (2025). Systematic mapping of experimental approaches to studying common mycorrhizal networks in arbuscular mycorrhiza. *Plants, People, Planet*, *7*(4), 920–933. https://doi.org/10.1002/PPP3.10618

Lehmann, A., Veresoglou, S. D., Leifheit, E. F., & Rillig, M. C. (2014). Arbuscular mycorrhizal influence on zinc nutrition in crop plants – A meta-analysis. *Soil Biology and Biochemistry*, *69*, 123–131. https://doi.org/10.1016/J.SOILBIO.2013.11.001

Leifheit, E. F., Verbruggen, E., & Rillig, M. C. (2015). Arbuscular mycorrhizal fungi reduce decomposition of woody plant litter while increasing soil aggregation. *Soil Biology and Biochemistry*, *81*, 323–328. https://doi.org/10.1016/J.SOILBIO.2014.12.003

Leigh, J., Fitter, A. H., & Hodge, A. (2011). Growth and symbiotic effectiveness of an arbuscular mycorrhizal fungus in organic matter in competition with soil bacteria. *FEMS Microbiology Ecology*, *76*(3), 428–438. https://doi.org/10.1111/J.1574-6941.2011.01066.X

Lekberg, Y., Hammer, E. C., & Olsson, P. A. (2010). Plants as resource islands and storage units – adopting the mycocentric view of arbuscular mycorrhizal networks. *FEMS Microbiology Ecology*, *74*(2), 336–345. https://doi.org/10.1111/J.1574-6941.2010.00956.X

Lekberg, Y., & Koide, R. T. (2014). Integrating physiological, community, and evolutionary perspectives on the arbuscular mycorrhizal symbiosis. *Botany*, *92*(4), 241–251. https://doi.org/10.1139/CJB-2013-0182

Lekberg, Y., Vasar, M., Bullington, L. S., Sepp, S.-K., Antunes, P. M., Bunn, R., Larkin, B. G., & Öpik, M. (2018). More bang for the buck? Can arbuscular mycorrhizal fungal communities be characterized adequately alongside other fungi using general fungal primers? *New Phytologist*, *220*(4), 971–976. https://doi.org/10.1111/nph.15035

Lerat, S., Gauci, R., Catford, J., Vierheilig, H., Piché, Y., & Lapoint, L. (2002). 14C transfer between the spring ephemeral Erythronium americanum and sugar maple saplings via arbuscular mycorrhizal fungi in natural stands. *Oecologia*, *132*(2), 181–187. https://doi.org/10.1007/s00442-002-0958-9

Li, Y., Nan, Z., Matthew, C., Wang, Y., & Duan, T. (2023). Arbuscular mycorrhizal fungus changes alfalfa (Medicago sativa) metabolites in response to leaf spot (Phoma medicaginis) infection, with subsequent effects on pea aphid (Acyrthosiphon pisum) behavior. *New Phytologist*. https://doi.org/10.1111/NPH.18924

Litton, C. M., Raich, J. W., & Ryan, M. G. (2007). Carbon allocation in forest ecosystems. *Global Change Biology*, *13*(10), 2089–2109. https://doi.org/10.1111/J.1365-2486.2007.01420.X

Liu, J., Maldonado-Mendoza, I., Lopez-Meyer, M., Cheung, F., Town, C. D., & Harrison, M. J. (2007). Arbuscular mycorrhizal symbiosis is accompanied by local and systemic alterations in gene expression and an increase in disease resistance in the shoots. *The Plant Journal*, *50*(3), 529–544. https://doi.org/10.1111/J.1365-313X.2007.03069.X

Liu, R., Chen, M., Liu, B., Huang, K., Mao, Z., Li, H., & Zhao, J. (2023). A root-knot nematode effector manipulates the rhizosphere microbiome for establishing parasitism relationship with hosts. *Frontiers in Microbiology*, *14*, 1217863. https://doi.org/10.3389/FMICB.2023.1217863

Liu, X., Han, R., Cao, Y., Turner, B. L., & Ma, L. Q. (2022). Enhancing Phytate Availability in Soils and Phytate-P Acquisition by Plants: A Review. *Environmental Science & Technology*, *56*(13), 9196–9219. https://doi.org/10.1021/ACS.EST.2C00099

Lofgren, L. A., Uehling, J. K., Branco, S., Bruns, T. D., Martin, F., & Kennedy, P. G. (2019). Genome-based estimates of fungal rDNA copy number variation across phylogenetic scales and ecological lifestyles. *Molecular Ecology*, *28*(4), 721–730. https://doi.org/10.1111/MEC.14995

López-Fernández, H., Santos, H. M., Capelo, J. L., Fdez-Riverola, F., Glez-Peña, D., & Reboiro-Jato, M. (2015). Mass-Up: An all-in-one open software application for MALDI-TOF mass spectrometry knowledge discovery. *BMC Bioinformatics*, *16*(1), 1–12. https://doi.org/10.1186/S12859-015-0752-4

Love, M. I., Huber, W., & Anders, S. (2014). Moderated estimation of fold change and dispersion for RNA-seq data with DESeq2. *Genome Biology*, *15*(12), 1–21. https://doi.org/10.1186/S13059-014-0550-8

Lumini, E., Bianciotto, V., Jargeat, P., Novero, M., Salvioli, A., Faccio, A., Bécard, G., & Bonfante, P. (2007). Presymbiotic growth and sporal morphology are affected in the arbuscular mycorrhizal fungus Gigaspora margarita cured of its endobacteria. *Cellular Microbiology*, *9*(7), 1716–1729. https://doi.org/10.1111/J.1462-5822.2007.00907.X

Lundberg, D. S., Lebeis, S. L., Paredes, S. H., Yourstone, S., Gehring, J., Malfatti, S., Tremblay, J., Engelbrektson, A., Kunin, V., Rio, T. G. del, Edgar, R. C., Eickhorst, T., Ley, R. E., Hugenholtz, P., Tringe, S. G., & Dangl, J. L.

(2012). Defining the core Arabidopsis thaliana root microbiome. *Nature 2012 488:7409*, *488*(7409), 86–90. https://doi.org/10.1038/nature11237

M, L., C, T., RL, B., Y, S., RA, W., E, F., & J, J. (2011). Symbiont identity matters: carbon and phosphorus fluxes between Medicago truncatula and different arbuscular mycorrhizal fungi. *Mycorrhiza*, *21*(8), 689–702. https://doi.org/10.1007/S00572-011-0371-5

Ma, J., Wang, W., Yang, J., Qin, S., Yang, Y., Sun, C., Pei, G., Zeeshan, M., Liao, H., Liu, L., & Huang, J. (2022). Mycorrhizal symbiosis promotes the nutrient content accumulation and affects the root exudates in maize. *BMC Plant Biology*, *22*(1), 1–13. https://doi.org/10.1186/S12870-021-03370-2/

Maboreke, H. R., Graf, M., Grams, T. E. E., Herrmann, S., Scheu, S., & Ruess, L. (2017). Multitrophic interactions in the rhizosphere of a temperate forest tree affect plant carbon flow into the belowground food web. *Soil Biology and Biochemistry*, *115*, 526–536. https://doi.org/10.1016/J.SOILBIO.2017.09.002

Magkourilou, E., Bell, C. A., Daniell, T. J., & Field, K. J. (2024). The functionality of arbuscular mycorrhizal networks across scales of experimental complexity and ecological relevance. *Functional Ecology*, *00*, 1–16. https://doi.org/10.1111/1365-2435.14618

Maherali, H., & Klironomos, J. N. (2007). Influence of Phylogeny on Fungal Community Assembly and Ecosystem Functioning. *Science*, *316*(5832), 1746–1748. https://doi.org/10.1126/SCIENCE.1143082

Maillard, F., Michaud, T. J., See, C. R., DeLancey, L. C., Blazewicz, S. J., Kimbrel, J. A., Pett-Ridge, J., & Kennedy, P. G. (2023). Melanization slows the rapid movement of fungal necromass carbon and nitrogen into both bacterial and fungal decomposer communities and soils. *MSystems*. https://doi.org/10.1128/MSYSTEMS.00390-23

Mantelin, S., Thorpe, P., & Jones, J. T. (2015). Suppression of Plant Defences by Plant-Parasitic Nematodes. *Advances in Botanical Research*, *73*, 325–337. https://doi.org/10.1016/BS.ABR.2014.12.011

Marks, G. C., Winoto-Suatmadji, R., & Smith, I. W. (1987). Effects of nematode control on shoot, root and mycorrhizal development of Pinus radiata seedlings growing in a nursery soil infested with Pratylenchus penetrans. *Australian Forestry Research*, *17*, 1–10. https://www.cabidigitallibrary.org/doi/full/10.5555/19880619917

Marro, N., Grilli, G., Soteras, F., Caccia, M., Longo, S., Cofré, N., Borda, V., Burni, M., Janoušková, M., & Urcelay, C. (2022). The effects of arbuscular mycorrhizal fungal species and taxonomic groups on stressed and unstressed plants: a global meta-analysis. *New Phytologist*, *235*(1), 320–332. https://doi.org/10.1111/NPH.18102

Martin, M. (2011). Cutadapt removes adapter sequences from high-throughput sequencing reads. *EMBnet.Journal*, *17*(1), 10–12.

Martina, J., Karol, K., Cameron, W., Helena, Š., Petra, C., & Miroslav, V. (2013). Effects of Inoculum Additions in the Presence of a Preestablished Arbuscular Mycorrhizal Fungal Community. *Applied and Environmental Microbiology*, *79*(20), 6507–6515. https://doi.org/10.1128/AEM.02135-13

Martinez Arbizu, P. (2020). *pairwiseAdonis: Pairwise multilevel comparison using adonis* (R package version 0.4).

Martínez-Medina, A., van Wees, S. C. M., & Pieterse, C. M. J. (2017). Airborne signals from Trichoderma fungi stimulate iron uptake responses in roots resulting in priming of jasmonic acid-dependent defences in shoots of Arabidopsis thaliana and Solanum lycopersicum. *Plant, Cell & Environment*, *40*(11), 2691–2705. https://doi.org/10.1111/PCE.13016

Masson-Delmotte, V., Zhai, P., Pirani A., Connors, S. L., Pean, C., Berger., S., Caud, N., Chen, Y., Goldfarb, L., Gomis, M. I., Huang, M., Leitzell, K., Lonnoy, E., Matthews, J. B. R., Maycock, T. K., Waterfield, T., Yelekci, O., Yu, R., & Zhou, B. (2021). *Climate Change 2021 - the Physical Science Basis Contribution of Working Group I to*

the Sixth Assessment Report of the Intergovernmental Panel on Climate Change. https://search.informit.org/doi/abs/10.3316/informit.315096509383738

Mathieu, S., Cusant, L., Roux, C., & Corradi, N. (2018). Arbuscular mycorrhizal fungi: intraspecific diversity and pangenomes. *New Phytologist*, *220*(4), 1129–1134. https://doi.org/10.1111/NPH.15275

Mathu Malar, C., Wang, Y., Stajich, J. E., Kokkoris, V., Villeneuve-Laroche, M., Yildirir, G., & Corradi, N. (2022). Early branching arbuscular mycorrhizal fungus Paraglomus occultum carries a small and repeat-poor genome compared to relatives in the Glomeromycotina. *Microbial Genomics*, *8*(4), 000810. https://doi.org/10.1099/MGEN.0.000810

Mbaluto, C. M., Ahmad, E. M., Fu, M., Martínez-Medina, A., & van Dam, N. M. (2020). The impact of Spodoptera exigua herbivory on Meloidogyne incognita-induced root responses depends on the nematodes' life cycle stages. *AoB PLANTS*, *12*(4). https://doi.org/10.1093/AOBPLA/PLAA029

McGonigle, T. P., Miller, M. H., Evans, D. G., Fairchild, G. L., & Swan, J. A. (1990). A new method which gives an objective measure of colonization of roots by vesicular—arbuscular mycorrhizal fungi. *New Phytologist*, *115*(3), 495–501. https://doi.org/10.1111/J.1469-8137.1990.TB00476.X

McLaren, M. R., & Callahan, B. J. (n.d.). *Silva 138.1 prokaryotic SSU taxonomic training data formatted for DADA2*. Zenodo. https://doi.org/10.5281/ZENODO.4587955

McMurdie, P. J., & Holmes, S. (2013). phyloseq: An R Package for Reproducible Interactive Analysis and Graphics of Microbiome Census Data. *PLOS ONE*, *8*(4), e61217. https://doi.org/10.1371/JOURNAL.PONE.0061217

Mendes, R., Garbeva, P., & Raaijmakers, J. M. (2013). The rhizosphere microbiome: significance of plant beneficial, plant pathogenic, and human pathogenic microorganisms. *FEMS Microbiology Reviews*, *37*(5), 634–663. https://doi.org/10.1111/1574-6976.12028

Meng, L., Zhang, A., Wang, F., Han, X., Wang, D., & Li, S. (2015). Arbuscular mycorrhizal fungi and rhizobium facilitate nitrogen uptake and transfer in soybean/maize intercropping system. *Frontiers in Plant Science*, *6*(MAY), 1–10. https://doi.org/10.3389/FPLS.2015.00339

Merrild, M. P., Ambus, P., Rosendahl, S., & Jakobsen, I. (2013). Common arbuscular mycorrhizal networks amplify competition for phosphorus between seedlings and established plants. *New Phytologist*, *200*(1), 229–240. https://doi.org/10.1111/NPH.12351

Mezzomo, P., Weinhold, A., Aurová, K., Jorge, L. R., Kozel, P., Michálek, J., Nováková, N., Seifert, C. L., Volfová, T., Engström, M., Salminen, J. P., Sedio, B. E., & Volf, M. (2023). Leaf volatile and nonvolatile metabolites show different levels of specificity in response to herbivory. *Ecology and Evolution*, *13*(5), e10123. https://doi.org/10.1002/ECE3.10123

Mikkelsen, B. L., Rosendahl, S., & Jakobsen, I. (2008). Underground resource allocation between individual networks of mycorrhizal fungi. *New Phytologist*, *180*(4), 890–898. https://doi.org/10.1111/J.1469-8137.2008.02623.X

Minnis, S. T., Haydock, P. P. J., Ibrahim, S. K., Grove, I. G., Evans, K., & Russell, M. D. (2002). Potato cyst nematodes in England and Wales - occurrence and distribution. *Annals of Applied Biology*, *140*(2), 187–195. https://doi.org/10.1111/J.1744-7348.2002.TB00172.X

Miyauchi, S., Kiss, E., Kuo, A., Drula, E., Kohler, A., Sánchez-García, M., Morin, E., Andreopoulos, B., Barry, K. W., Bonito, G., Buée, M., Carver, A., Chen, C., Cichocki, N., Clum, A., Culley, D., Crous, P. W., Fauchery, L., Girlanda, M., … Martin, F. M. (2020). Large-scale genome sequencing of mycorrhizal fungi provides insights into the early evolution of symbiotic traits. *Nature Communications 2020 11:1*, *11*(1), 1–17. https://doi.org/10.1038/s41467-020-18795-w

Moens, M., & Perry, R. N. (2009). Migratory plant endoparasitic nematodes: A group rich in contrasts and divergence. *Annual Review of Phytopathology*, *47*, 313–332. https://doi.org/10.1146/ANNUREV-PHYTO-080508-081846

Moore, J. C., de Ruiter, P. C., Hunt, H. W., Coleman, D. C., & Freckman, D. W. (1996). Microcosms and soil ecology: Critical linkages between field studies and modelling food webs. *Ecology*, *77*(3), 694–705. https://doi.org/10.2307/2265494

Morriën, E. (2016). Understanding soil food web dynamics, how close do we get? *Soil Biology and Biochemistry*, *102*, 10–13. https://doi.org/10.1016/J.SOILBIO.2016.06.022

Mosse, B., & Phillips, J. M. (1971). The Influence of Phosphate and Other Nutrients on the Development of Vesicular-arbuscular Mycorrhiza in Culture. *Microbiology*, *69*(2), 157–166. https://doi.org/10.1099/00221287-69-2-157

Muneer, M. A., Chen, X., Munir, M. Z., Nisa, Z. U., Saddique, M. A. B., Mehmood, S., Su, D., Zheng, C., & Ji, B. (2023). Interplant transfer of nitrogen between C3 and C4 plants through common mycorrhizal networks under different nitrogen availability. *Journal of Plant Ecology*, *16*(2). https://doi.org/10.1093/JPE/RTAC058

Murphy, J., & Riley, J. P. (1962). A modified single solution method for the determination of phosphate in natural waters. *Analytica Chimica Acta*, *27*(C), 31–36. https://doi.org/10.1016/S0003-2670(00)88444-5

Nahar, K., Kyndt, T., de Vleesschauwer, D., Höfte, M., & Gheysen, G. (2011). The Jasmonate Pathway Is a Key Player in Systemically Induced Defense against Root Knot Nematodes in Rice. *Plant Physiology*, *157*(1), 305–316. https://doi.org/10.1104/PP.111.177576

Nahar, K., Kyndt, T., Nzogela, Y. B., & Gheysen, G. (2012). Abscisic acid interacts antagonistically with classical defense pathways in rice–migratory nematode interaction. *New Phytologist*, *196*(3), 901–913. https://doi.org/10.1111/J.1469-8137.2012.04310.X

Naoumkina, M. A., Zhao, Q., Gallego-Giraldo, L., Dai, X., Zhao, P. X., & Dixon, R. A. (2010). Genome-wide analysis of phenylpropanoid defence pathways. *Molecular Plant Pathology*, *11*(6), 829–846. https://doi.org/10.1111/J.1364-3703.2010.00648.X

Naumann, M., Schüßler, A., & Bonfante, P. (2010). The obligate endobacteria of arbuscular mycorrhizal fungi are ancient heritable components related to the Mollicutes. *The ISME Journal*, *4*(7), 862–871. https://doi.org/10.1038/ISMEJ.2010.21

Newman, E. (1985). The rhizosphere: carbon sources and microbial populations. In A. Fitter, D. Atkinson, D. Read, & M. Usher (Eds.), *Ecological Interactions in Soil: Plants, Microbes and Animals* (pp. 107–119). Blackwell Scientific Publications Oxford. https://doi.org/10.5555/19851999297

Nguyen, N. H., Song, Z., Bates, S. T., Branco, S., Tedersoo, L., Menke, J., Schilling, J. S., & Kennedy, P. G. (2016). FUNGuild: An open annotation tool for parsing fungal community datasets by ecological guild. *Fungal Ecology*, *20*, 241–248. https://doi.org/10.1016/J.FUNECO.2015.06.006

Nicol, J. M., Turner, S. J., Coyne, D. L., Nijs, L. den, Hockland, S., & Maafi, Z. T. (2011). Current Nematode Threats to World Agriculture. *Genomics and Molecular Genetics of Plant-Nematode Interactions*, 21–43. https://doi.org/10.1007/978-94-007-0434-3_2

Noë, R. (2021). Waste Can Be Traded with Mutualistic Partners. *Trends in Ecology & Evolution*, *36*(3), 175–176. https://doi.org/10.1016/J.TREE.2020.11.005

Noë, R., & Kiers, E. T. (2018). Mycorrhizal Markets, Firms, and Co-ops. *Trends in Ecology & Evolution*, *33*(10), 777–789. https://doi.org/10.1016/J.TREE.2018.07.007

Nottingham, A. T., Turner, B. L., Winter, K., Chamberlain, P. M., Stott, A., & Tanner, E. V. J. (2013). Root and arbuscular mycorrhizal mycelial interactions with soil microorganisms in lowland tropical forest. *FEMS Microbiology Ecology*, *85*(1), 37–50. https://doi.org/10.1111/1574-6941.12096

Nuccio, E. E., Blazewicz, S. J., Lafler, M., Campbell, A. N., Kakouridis, A., Kimbrel, J. A., Wollard, J., Vyshenska, D., Riley, R., Tomatsu, A., Hestrin, R., Malmstrom, R. R., Firestone, M., & Pett-Ridge, J. (2022). HT-SIP: a semi-automated stable isotope probing pipeline identifies cross-kingdom interactions in the hyphosphere of arbuscular mycorrhizal fungi. *Microbiome*, *10*(1), 1–20. https://doi.org/10.1186/S40168-022-01391-Z

Ochola, J., Cortada, L., Ng'ang'a, M., Hassanali, A., Coyne, D., & Torto, B. (2020). Mediation of Potato–Potato Cyst Nematode, G. rostochiensis Interaction by Specific Root Exudate Compounds. *Frontiers in Plant Science*, *11*, 523480. https://doi.org/10.3389/FPLS.2020.00649

Offre, P., Pivato, B., Siblot, S., Gamalero, E., Corberand, T., Lemanceau, P., & Mougel, C. (2007). Identification of Bacterial Groups Preferentially Associated with Mycorrhizal Roots of Medicago truncatula. *Applied and Environmental Microbiology*, *73*(3), 913–921. https://doi.org/10.1128/AEM.02042-06

Oksanen, Blanchet, Friendly, Kindt, Legendre, McGlinn, & Minchin. (2020). *VEGAN Community Ecology R Package* (2.5-6).

Olsson, O., Olsson, P. A., & Hammer, E. C. (2014). Phosphorus and carbon availability regulate structural composition and complexity of AM fungal mycelium. *Mycorrhiza*, *24*(6), 443–451. https://doi.org/10.1007/S00572-014-0557-8

Olsson, P. A., Rahm, J., & Aliasgharzad, N. (2010). Carbon dynamics in mycorrhizal symbioses is linked to carbon costs and phosphorus benefits. *FEMS Microbiology Ecology*, *72*(1), 125–131. https://doi.org/10.1111/J.1574-6941.2009.00833.X

Öpik, M., Zobel, M., Cantero, J. J., Davison, J., Facelli, J. M., Hiiesalu, I., Jairus, T., Kalwij, J. M., Koorem, K., Leal, M. E., Liira, J., Metsis, M., Neshataeva, V., Paal, J., Phosri, C., Põlme, S., Reier, Ü., Saks, Ü., Schimann, H., … Moora, M. (2013). Global sampling of plant roots expands the described molecular diversity of arbuscular mycorrhizal fungi. *Mycorrhiza*, *23*(5), 411–430. https://doi.org/10.1007/S00572-013-0482-2

Orwin, K. H., Kirschbaum, M. U. F., St John, M. G., & Dickie, I. A. (2011). Organic nutrient uptake by mycorrhizal fungi enhances ecosystem carbon storage: a model-based assessment. *Ecology Letters*, *14*(5), 493–502. https://doi.org/10.1111/J.1461-0248.2011.01611.X

Pajar, J. A., Otto, P., Leonar, A. L., Döll, S., & van Dam, N. M. (2024). Dual nematode infection in Brassica nigra affects shoot metabolome and aphid survival in distinct contrast to single-species infection. *Journal of Experimental Botany*, *75*(22), 7317–7336. https://doi.org/10.1093/JXB/ERAE364

Paloi, S., Kumla, J., Karunarathna, S. C., Lumyong, S., & Suwannarach, N. (2023). Taxonomic and phylogenetic evidence reveal two new Russula species (Russulaceae, Russulales) from northern Thailand. *Mycological Progress*, *22*(10), 1–13. https://doi.org/10.1007/S11557-023-01921-5

Paloi, S., Mhuantong, W., Luangsa-Ard, J. J., & Kobmoo, N. (2021). Using high-throughput amplicon sequencing to evaluate intragenomic variation and accuracy in species identification of cordyceps species. *Journal of Fungi*, *7*(9), 767. https://doi.org/10.3390/JOF7090767/S1

Pariera Dinkins, C. L., Peterson, R. K. D., Gibson, J. E., Hu, Q., & Weaver, D. K. (2008). Glycoalkaloid responses of potato to Colorado potato beetle defoliation. *Food and Chemical Toxicology*, *46*(8), 2832–2836. https://doi.org/10.1016/J.FCT.2008.05.023

Paterson, E., Sim, A., Davidson, J., & Daniell, T. J. (2016). Arbuscular mycorrhizal hyphae promote priming of native soil organic matter mineralisation. *Plant and Soil*, *408*(1–2), 243–254. https://doi.org/10.1007/S11104-016-2928-8

Pérez-De-Luque, A., Tille, S., Johnson, I., Pascual-Pardo, D., Ton, J., & Cameron, D. D. (2017). The interactive effects of arbuscular mycorrhiza and plant growth-promoting rhizobacteria synergistically enhance host plant defences against pathogens. *Scientific Reports 2017 7:1*, *7*(1), 1–10. https://doi.org/10.1038/s41598-017-16697-4

Pfeffer, P. E., Douds, D. D., Bücking, H., Schwartz, D. P., & Shachar-Hill, Y. (2004). The fungus does not transfer carbon to or between roots in an arbuscular mycorrhizal symbiosis. *New Phytologist*, *163*(3), 617–627. https://doi.org/10.1111/J.1469-8137.2004.01152.X

Philippot, L., Raaijmakers, J. M., Lemanceau, P., & van der Putten, W. H. (2013). Going back to the roots: The microbial ecology of the rhizosphere. *Nature Reviews Microbiology*, *11*(11), 789–799. https://doi.org/10.1038/NRMICRO3109

Pieterse, C. M. J., van der Does, D., Zamioudis, C., Leon-Reyes, A., & van Wees, S. C. M. (2012). Hormonal modulation of plant immunity. *Annual Review of Cell and Developmental Biology*, *28*, 489–521. https://doi.org/10.1146/ANNUREV-CELLBIO-092910-154055

Posada, R. H., Madriñan, S., & Rivera, E. L. (2012). Relationships between the litter colonization by saprotrophic and arbuscular mycorrhizal fungi with depth in a tropical forest. *Fungal Biology*, *116*(7), 747–755. https://doi.org/10.1016/J.FUNBIO.2012.04.003

Postma, W. J., Slootweg, E. J., Rehman, S., Finkers-Tomczak, A., Tytgat, T. O. G., van Gelderen, K., Lozano-Torres, J. L., Roosien, J., Pomp, R., van Schaik, C., Bakker, J., Goverse, A., & Smant, G. (2012). The Effector SPRYSEC-19 of Globodera rostochiensis Suppresses ---Mediated Disease Resistance in Plants. *Plant Physiology*, *160*(2), 944–954. https://doi.org/10.1104/PP.112.200188

Powell, J. R., Parrent, J. L., Hart, M. M., Klironomos, J. N., Rillig, M. C., & Maherali, H. (2009). Phylogenetic trait conservatism and the evolution of functional trade-offs in arbuscular mycorrhizal fungi. *Proceedings of the Royal Society B: Biological Sciences*, *276*(1676), 4237–4245. https://doi.org/10.1098/RSPB.2009.1015

Powell, J. R., & Rillig, M. C. (2018). Biodiversity of arbuscular mycorrhizal fungi and ecosystem function. *New Phytologist*, *220*(4), 1059–1075. https://doi.org/10.1111/NPH.15119

Pozo, M. J., & Azcón-Aguilar, C. (2007). Unraveling mycorrhiza-induced resistance. *Current Opinion in Plant Biology*, *10*(4), 393–398. https://doi.org/10.1016/J.PBI.2007.05.004

Prescott, C. E., Grayston, S. J., Helmisaari, H. S., Kaštovská, E., Körner, C., Lambers, H., Meier, I. C., Millard, P., & Ostonen, I. (2020). Surplus Carbon Drives Allocation and Plant–Soil Interactions. *Trends in Ecology & Evolution*, *35*(12), 1110–1118. https://doi.org/10.1016/J.TREE.2020.08.007

Prescott, C. E., Grayston, S. J., Helmisaari, H. S., Kaštovská, E., Körner, C., Lambers, H., Meier, I. C., Millard, P., & Ostonen, I. (2021). Rhizosphere 'Trade' Is an Unnecessary Analogy: Response to Noë. *Trends in Ecology & Evolution*, *36*(3), 176–177. https://doi.org/10.1016/J.TREE.2020.12.005

Price, J. A., Coyne, D., Blok, V. C., & Jones, J. T. (2021). Potato cyst nematodes Globodera rostochiensis and G. pallida. *Molecular Plant Pathology*, *22*(5), 495–507. https://doi.org/10.1111/MPP.13047

Pringle, A., & Bever, J. D. (2002). Divergent phenologies may facilitate the coexistence of arbuscular mycorrhizal fungi in a North Carolina grassland. *American Journal of Botany*, *89*(9), 1439–1446. https://doi.org/10.3732/AJB.89.9.1439

R Core Team. (2023). *R: A Language and Environment for Statistical Computing*. R Foundation for Statistical Computing. https://www.R-project.org

Raaijmakers, J. M., & Mazzola, M. (2012). Diversity and natural functions of antibiotics produced by beneficial and plant pathogenic bacteria. *Annual Review of Phytopathology*, *50*(Volume 50, 2012), 403–424. https://doi.org/10.1146/ANNUREV-PHYTO-081211-172908

Rasmann, S., de Vos, M., Casteel, C. L., Tian, D., Halitschke, R., Sun, J. Y., Agrawal, A. A., Felton, G. W., & Jander, G. (2012). Herbivory in the previous generation primes plants for enhanced insect resistance. *Plant Physiology*, *158*(2), 854–863. https://doi.org/10.1104/PP.111.187831

Raven, J. A., Lambers, H., Smith, S. E., & Westoby, M. (2018). Costs of acquiring phosphorus by vascular land plants: patterns and implications for plant coexistence. *New Phytologist*, *217*(4), 1420–1427. https://doi.org/10.1111/NPH.14967

Redecker, D., Kodner, R., & Graham, L. E. (2000). Glomalean fungi from the Ordovician. *Science*, *289*(5486), 1920–1921. https://doi.org/10.1126/science.289.5486.1920

Řezáčová, V., Zemková, L., Beskid, O., Püschel, D., Konvalinková, T., Hujslová, M., Slavíková, R., & Jansa, J. (2018). Little cross-feeding of the mycorrhizal networks shared between C3-panicum bisulcatum and C4-panicum maximum under different temperature regimes. *Frontiers in Plant Science*, *9*, 449. https://doi.org/10.3389/FPLS.2018.00449/

Richardson, A. E., & Simpson, R. J. (2011). Soil Microorganisms Mediating Phosphorus Availability Update on Microbial Phosphorus. *Plant Physiology*, *156*(3), 989–996. https://doi.org/10.1104/PP.111.175448

Riedlmeier, M., Ghirardo, A., Wenig, M., Knappe, C., Koch, K., Georgii, E., Dey, S., Parker, J. E., Schnitzler, J. P., & Vlot, A. C. (2017). Monoterpenes Support Systemic Acquired Resistance within and between Plants. *The Plant Cell*, *29*(6), 1440–1459. https://doi.org/10.1105/TPC.16.00898

Rillig, M. C., Aguilar-Trigueros, C. A., Camenzind, T., Cavagnaro, T. R., Degrune, F., Hohmann, P., Lammel, D. R., Mansour, I., Roy, J., van der Heijden, M. G. A., & Yang, G. (2019). Why farmers should manage the arbuscular mycorrhizal symbiosis. *New Phytologist*, *222*(3), 1171–1175. https://doi.org/10.1111/NPH.15602

Rillig, M. C., Lehmann, A., Mounts, I. R., & Bock, B. M. (2025). Concurrent common fungal networks formed by different guilds of fungi. *New Phytologist*, *246*(1), 33–38. https://doi.org/10.1111/NPH.20418

Robinson, D. G., Ammer, C., Polle, A., Bauhus, J., Aloni, R., Annighöfer, P., Baskin, T. I., Blatt, M. R., Bolte, A., Bugmann, H., Cohen, J. D., Davies, P. J., Draguhn, A., Hartmann, H., Hasenauer, H., Hepler, P. K., Kohnle, U., Lang, F., Löf, M., … Näsholm, T. (2023). Mother trees, altruistic fungi, and the perils of plant personification. *Trends in Plant Science*. https://doi.org/10.1016/J.TPLANTS.2023.08.010

Robinson, D. G., & Fitter, A. (1999). The magnitude and control of carbon transfer between plants linked by a common mycorrhizal network. *Journal of Experimental Botany*, *50*(330), 9–13. https://doi.org/10.1093/JXB/50.330.9

Rodiuc, N., Vieira, P., Banora, M. Y., & de Almeida Engler, J. (2014). On the track of transfer cell formation by specialized plant-parasitic nematodes. *Frontiers in Plant Science*, *5*(MAY), 160. https://doi.org/10.3389/FPLS.2014.00160

Rozmoš, M., Bukovská, P., Hršelová, H., Kotianová, M., Dudáš, M., Gančarčíková, K., & Jansa, J. (2021). Organic nitrogen utilisation by an arbuscular mycorrhizal fungus is mediated by specific soil bacteria and a protist. *The ISME Journal 2021 16:3*, *16*(3), 676–685. https://doi.org/10.1038/s41396-021-01112-8

RStudio Team. (2022). *RStudio: Integrated Development for R*. RStudio. http://www.rstudio.com/.

Rubakhin, S. S., Jurchen, J. C., Monroe, E. B., & Sweedler, J. v. (2005). Imaging mass spectrometry: fundamentals and applications to drug discovery. *Drug Discovery Today*, *10*(12), 823–837. https://doi.org/10.1016/S1359-6446(05)03458-6

Ruiz-Lozano, J. M., Aroca, R., Zamarreño, Á. M., Molina, S., Andreo-Jiménez, B., Porcel, R., García-Mina, J. M., Ruyter-Spira, C., & López-Ráez, J. A. (2016). Arbuscular mycorrhizal symbiosis induces strigolactone biosynthesis under drought and improves drought tolerance in lettuce and tomato. *Plant, Cell & Environment*, *39*(2), 441–452. https://doi.org/10.1111/PCE.12631

Ryan, C. G., Clayton, E., Griffin, W. L., Sie, S. H., & Cousens, D. R. (1988). SNIP, a statistics-sensitive background treatment for the quantitative analysis of PIXE spectra in geoscience applications. *Nuclear Instruments and Methods in Physics Research Section B: Beam Interactions with Materials and Atoms*, *34*(3), 396–402. https://doi.org/10.1016/0168-583X(88)90063-8

Säle, V., Aguilera, P., Laczko, E., Mäder, P., Berner, A., Zihlmann, U., van der Heijden, M. G. A., & Oehl, F. (2015). Impact of conservation tillage and organic farming on the diversity of arbuscular mycorrhizal fungi. *Soil Biology and Biochemistry*, *84*, 38–52. https://doi.org/10.1016/J.SOILBIO.2015.02.005

Salmeron-santiago, I. A., Martínez-trujillo, M., Valdez-alarcón, J. J., Pedraza-santos, M. E., Santoyo, G., Pozo, M. J., & Chávez-bárcenas, A. T. (2022). An Updated Review on the Modulation of Carbon Partitioning and Allocation in Arbuscular Mycorrhizal Plants. *Microorganisms*, *10*(1), 75. https://doi.org/10.3390/MICROORGANISMS10010075

Santos-González, J. C., Nallanchakravarthula, S., Alström, S., & Finlay, R. D. (2011). Soil, But Not Cultivar, Shapes the Structure of Arbuscular Mycorrhizal Fungal Assemblages Associated with Strawberry. *Microbial Ecology*, *62*(1), 25–35. https://doi.org/10.1007/S00248-011-9834-7/METRICS

Sato, T., Ezawa, T., Cheng, W., & Tawaraya, K. (2015). Release of acid phosphatase from extraradical hyphae of arbuscular mycorrhizal fungus Rhizophagus clarus. *Soil Science and Plant Nutrition*, *61*(2), 269–274. https://doi.org/10.1080/00380768.2014.993298

Savitzky, A., & Golay, M. J. E. (1964). Smoothing and Differentiation of Data by Simplified Least Squares Procedures. *Analytical Chemistry*, *36*(8), 1627–1639. https://doi.org/10.1021/AC60214A047/ASSET/AC60214A047.FP.PNG_V03

Sawers, R. J. H., Svane, S. F., Quan, C., Grønlund, M., Wozniak, B., Gebreselassie, M.-N., González-Muñoz, E., Montes, R. A. C., Baxter, I., Goudet, J., Jakobsen, I., & Paszkowski, U. (2017). Phosphorus acquisition efficiency in arbuscular mycorrhizal maize is correlated with the abundance of root-external hyphae and the accumulation of transcripts encoding PHT1 phosphate transporters. *New Phytologist*, *214*(2), 632–643. https://doi.org/10.1111/NPH.14403

Scheublin, T. R., Sanders, I. R., Keel, C., & van der Meer, J. R. (2010). Characterisation of microbial communities colonising the hyphal surfaces of arbuscular mycorrhizal fungi. *The ISME Journal*, *4*(6), 752–763. https://doi.org/10.1038/ISMEJ.2010.5

Schouteden, N., Waele, D. de, Panis, B., & Vos, C. M. (2015). Arbuscular mycorrhizal fungi for the biocontrol of plant-parasitic nematodes: A review of the mechanisms involved. *Frontiers in Microbiology*, *6*(NOV), 1280. https://doi.org/10.3389/FMICB.2015.01280/

Schütz, L., Saharan, K., Mäder, P., Boller, T., & Mathimaran, N. (2022). Rate of hyphal spread of arbuscular mycorrhizal fungi from pigeon pea to finger millet and their contribution to plant growth and nutrient uptake in experimental microcosms. *Applied Soil Ecology*, *169*, 104156. https://doi.org/10.1016/J.APSOIL.2021.104156

Selosse, M. A., Richard, F., He, X., & Simard, S. W. (2006). Mycorrhizal networks: des liaisons dangereuses? *Trends in Ecology & Evolution*, *21*(11), 621–628. https://doi.org/10.1016/J.TREE.2006.07.003

Semchenko, M., Zobel, K., & Hutchings, M. J. (2010). To compete or not to compete: An experimental study of interactions between plant species with contrasting root behaviour. *Evolutionary Ecology*, *24*(6), 1433–1445. https://doi.org/10.1007/S10682-010-9401-6/

Sendek, A., Karakoç, C., Wagg, C., Domínguez-Begines, J., do Couto, G. M., van der Heijden, M. G. A., Naz, A. A., Lochner, A., Chatzinotas, A., Klotz, S., Gómez-Aparicio, L., & Eisenhauer, N. (2019). Drought modulates interactions between arbuscular mycorrhizal fungal diversity and barley genotype diversity. *Scientific Reports*, *9*(1), 1–15. https://doi.org/10.1038/S41598-019-45702-1

Shahzad, T., Chenu, C., Genet, P., Barot, S., Perveen, N., Mougin, C., & Fontaine, S. (2015). Contribution of exudates, arbuscular mycorrhizal fungi and litter depositions to the rhizosphere priming effect induced by grassland species. *Soil Biology and Biochemistry*, *80*, 146–155. https://doi.org/10.1016/J.SOILBIO.2014.09.023

Shen, K., Cornelissen, J. H. C., Wang, Y., Wu, C., He, Y., Ou, J., Tan, Q., Xia, T., Kang, L., Guo, Y., & Wu, B. (2020). AM Fungi Alleviate Phosphorus Limitation and Enhance Nutrient Competitiveness of Invasive Plants via Mycorrhizal Networks in Karst Areas. *Frontiers in Ecology and Evolution*, *8*, 125. https://doi.org/10.3389/FEVO.2020.00125

Sherrill-Mix, S. (2025). taxonomizr: Functions to Work with NCBI Accessions and Taxonomy [R package taxonomizr version 0.10.7]. In *CRAN: Contributed Packages* (R package version 0.10.7). Comprehensive R Archive Network (CRAN). https://doi.org/10.32614/CRAN.PACKAGE.TAXONOMIZR

Shi, J. H., Liu, H., Pham, T. C., Hu, X. J., Liu, L., Wang, C., Foba, C. N., Wang, S. B., & Wang, M. Q. (2022). Volatiles and hormones mediated root-knot nematode induced wheat defense response to foliar herbivore aphid. *Science of The Total Environment*, *815*, 152840. https://doi.org/10.1016/J.SCITOTENV.2021.152840

Shukla, N., Yadav, R., Kaur, P., Rasmussen, S., Goel, S., Agarwal, M., Jagannath, A., Gupta, R., & Kumar, A. (2017). Transcriptome analysis of root-knot nematode (Meloidogyne incognita)-infected tomato (Solanum lycopersicum) roots reveals complex gene expression profiles and metabolic networks of both host and nematode during susceptible and resistance responses. *Molecular Plant Pathology*, *19*(3), 615. https://doi.org/10.1111/MPP.12547

Sijmons, P. C., Atkinson, H. J., & Wyss, U. (1994). Parasitic strategies of root nematodes and associated host cell responses. *Annual Review of Phytopathology*, *32*(Volume 32,), 235–259. https://doi.org/10.1146/ANNUREV.PY.32.090194.001315/CITE/REFWORKS

Sikder, M. M., Vestergård, M., Kyndt, T., Kudjordjie, E. N., & Nicolaisen, M. (2021). Phytohormones selectively affect plant parasitic nematodes associated with Arabidopsis roots. *New Phytologist*, *232*(3), 1272–1285. https://doi.org/10.1111/NPH.17549

Sikder, M. M., Vestergård, M., Kyndt, T., Topalović, O., Kudjordjie, E. N., & Nicolaisen, M. (2022). Genetic disruption of Arabidopsis secondary metabolite synthesis leads to microbiome-mediated modulation of nematode invasion. *The ISME Journal*, *16*(9), 2230–2241. https://doi.org/10.1038/S41396-022-01276-X

Sikes, B. A., Cottenie, K., & Klironomos, J. N. (2009). Plant and fungal identity determines pathogen protection of plant roots by arbuscular mycorrhizas. *Journal of Ecology*, *97*(6), 1274–1280. https://doi.org/10.1111/J.1365-2745.2009.01557.X

Sikes, B. A., Powell, J. R., & Rillig, M. C. (2010). Deciphering the relative contributions of multiple functions within plant-microbe symbioses. *Ecology*, *91*(6), 1591–1597. https://doi.org/10.1890/09-1858.1

Simard, S. W., Perry, D. A., Jones, M. D., Myrold, D. D., Durall, D. M., & Molina, R. (1997). Net transfer of carbon between ectomycorrhizal tree species in the field. *Nature 1997 388:6642*, *388*(6642), 579–582. https://doi.org/10.1038/41557

Singh, R. R., Pajar, J. A., Audenaert, K., & Kyndt, T. (2021). Induced Resistance by Ascorbate Oxidation Involves Potentiating of the Phenylpropanoid Pathway and Improved Rice Tolerance to Parasitic Nematodes. *Frontiers in Plant Science*, *12*, 713870. https://doi.org/10.3389/FPLS.2021.713870

Sinsabaugh, R. S. (1994). Enzymic analysis of microbial pattern and process. *Biology and Fertility of Soils*, *17*(1), 69–74. https://doi.org/10.1007/BF00418675

Smant, G., Stokkermans, J. P. W. G., Yan, Y., de Boer, J. M., Baum, T. J., Wang, X., Hussey, R. S., Gommers, F. J., Henrissat, B., Davis, E. L., Helder, J., Schots, A., & Bakker, J. (1998). Endogenous cellulases in animals: Isolation of β-1,4-endoglucanase genes from two species of plant-parasitic cyst nematodes. *Proceedings of the National Academy of Sciences of the United States of America*, *95*(9), 4906–4911. https://doi.org/10.1073/PNAS.95.9.4906

Smith, S. E., & Read, D. J. (2010). *Mycorrhizal symbiosis*. Academic press.

Smith, S. E., & Smith, F. A. (2011). Roles of Arbuscular Mycorrhizas in Plant Nutrition and Growth: New Paradigms from Cellular to Ecosystem Scales., 227–250. https://doi.org/10.1146/ANNUREV-ARPLANT-042110-103846

Sohlenius, B. (1980). Abundance, Biomass and Contribution to Energy Flow by Soil Nematodes in Terrestrial Ecosystems. *Oikos*, *34*(2), 186. https://doi.org/10.2307/3544181

Song, Y., Chen, D., Lu, K., Sun, Z., & Zeng, R. (2015). Enhanced tomato disease resistance primed by arbuscular mycorrhizal fungus. *Frontiers in Plant Science*, *6*(September), 163569. https://doi.org/10.3389/FPLS.2015.00786

Song, Y., Wang, M., Zeng, R., Groten, K., & Baldwin, I. T. (2019). Priming and filtering of antiherbivore defences among Nicotiana attenuata plants connected by mycorrhizal networks. *Plant, Cell & Environment*, *42*(11), 2945–2961. https://doi.org/10.1111/PCE.13626

Song, Y. Y., Ye, M., Li, C., He, X., Zhu-Salzman, K., Wang, R. L., Su, Y. J., Luo, S. M., & Zeng, R. sen. (2014). Hijacking common mycorrhizal networks for herbivore-induced defence signal transfer between tomato plants. *Scientific Reports 2014 4:1*, *4*(1), 1–8. https://doi.org/10.1038/srep03915

Song, Y. Y., Zeng, R. sen, Xu, J. F., Li, J., Shen, X., & Yihdego, W. G. (2010). Interplant Communication of Tomato Plants through Underground Common Mycorrhizal Networks. *PLOS ONE*, *5*(10), e13324. https://doi.org/10.1371/JOURNAL.PONE.0013324

Soudzilovskaia, N. A., van Bodegom, P. M., Terrer, C., Zelfde, M. van't, McCallum, I., Luke McCormack, M., Fisher, J. B., Brundrett, M. C., de Sá, N. C., & Tedersoo, L. (2019). Global mycorrhizal plant distribution linked to terrestrial carbon stocks. *Nature Communications*, *10*(1), 1–10. https://doi.org/10.1038/S41467-019-13019-2

Soudzilovskaia, N. A., van der Heijden, M. G. A., Cornelissen, J. H. C., Makarov, M. I., Onipchenko, V. G., Maslov, M. N., Akhmetzhanova, A. A., & van Bodegom, P. M. (2015). Quantitative assessment of the differential impacts of arbuscular and ectomycorrhiza on soil carbon cycling. *New Phytologist*, *208*(1), 280–293. https://doi.org/10.1111/NPH.13447

Spatafora, J. W., Chang, Y., Benny, G. L., Lazarus, K., Smith, M. E., Berbee, M. L., Bonito, G., Corradi, N., Grigoriev, I., Gryganskyi, A., James, T. Y., O'Donnell, K., Roberson, R. W., Taylor, T. N., Uehling, J., Vilgalys, R., White, M. M., & Stajich, J. E. (2016). A phylum-level phylogenetic classification of zygomycete fungi based on genome-scale data. *Mycologia*, *108*(5), 1028–1046. https://doi.org/10.3852/16-042

Spohn, M., Ermak, A., & Kuzyakov, Y. (2013). Microbial gross organic phosphorus mineralization can be stimulated by root exudates – A 33P isotopic dilution study. *Soil Biology and Biochemistry*, *65*, 254–263. https://doi.org/10.1016/J.SOILBIO.2013.05.028

Staddon, P. L., Ramsey, C. B., Ostle, N., Ineson, P., & Fitter, A. H. (2003). Rapid Turnover of Hyphae of Mycorrhizal Fungi Determined by AMS Microanalysis of 14C. *Science*, *300*(5622), 1138–1140. https://doi.org/10.1126/SCIENCE.1084269

Stockinger, H., Krüger, M., & Schüßler, A. (2010). DNA barcoding of arbuscular mycorrhizal fungi. *New Phytologist*, *187*(2), 461–474. https://doi.org/10.1111/J.1469-8137.2010.03262.X

Stockinger, H., Walker, C., & Schüßler, A. (2009). 'Glomus intraradices DAOM197198', a model fungus in arbuscular mycorrhiza research, is not Glomus intraradices. *New Phytologist*, *183*(4), 1176–1187. https://doi.org/10.1111/J.1469-8137.2009.02874.X

Suzuki, K., Takahashi, K., & Harada, N. (2020). Evaluation of primer pairs for studying arbuscular mycorrhizal fungal community compositions using a MiSeq platform. *Biology and Fertility of Soils*, *56*(6), 853–858. https://doi.org/10.1007/S00374-020-01431-6

Svenningsen, N. B., Watts-Williams, S. J., Joner, E. J., Battini, F., Efthymiou, A., Cruz-Paredes, C., Nybroe, O., & Jakobsen, I. (2018). Suppression of the activity of arbuscular mycorrhizal fungi by the soil microbiota. *The ISME Journal 2018 12:5*, *12*(5), 1296–1307. https://doi.org/10.1038/s41396-018-0059-3

Symanczik, S., Lehmann, M. F., Wiemken, A., Boller, T., & Courty, P. E. (2018). Effects of two contrasted arbuscular mycorrhizal fungal isolates on nutrient uptake by Sorghum bicolor under drought. *Mycorrhiza*, *28*(8), 779–785. https://doi.org/10.1007/S00572-018-0853-9

Tedersoo, L., Anslan, S., Bahram, M., Põlme, S., Riit, T., Liiv, I., Kõljalg, U., Kisand, V., Nilsson, R. H., Hildebrand, F., Bork, P., & Abarenkov, K. (2015). Shotgun metagenomes and multiple primer pair-barcode combinations of amplicons reveal biases in metabarcoding analyses of fungi. *MycoKeys 10: 1-43*, *10*, 1–43. https://doi.org/10.3897/MYCOKEYS.10.4852

Tedersoo, L., Bahram, M., & Zobel, M. (2020). How mycorrhizal associations drive plant population and community biology. *Science*, *367*(6480). https://doi.org/10.1126/science.aba1223

Tedersoo, L., & Brundrett, M. C. (2017). *Evolution of Ectomycorrhizal Symbiosis in Plants*. 407–467. https://doi.org/10.1007/978-3-319-56363-3_19

Tedersoo, L., & Lindahl, B. (2016). Fungal identification biases in microbiome projects. *Environmental Microbiology Reports*, *8*(5), 774–779. https://doi.org/10.1111/1758-2229.12438

Tennant, D. (1975). A Test of a Modified Line Intersect Method of Estimating Root Length. *The Journal of Ecology*, *63*(3), 995. https://doi.org/10.2307/2258617

Thaler, J. S. (1999). Jasmonate-inducible plant defences cause increased parasitism of herbivores. *Nature*, *399*(6737), 686–688. https://doi.org/10.1038/21420

Thirkell, T. J., Cameron, D. D., & Hodge, A. (2016). Resolving the 'nitrogen paradox' of arbuscular mycorrhizas: fertilization with organic matter brings considerable benefits for plant nutrition and growth. *Plant, Cell & Environment*, *39*(8), 1683–1690. https://doi.org/10.1111/PCE.12667

Thirkell, T. J., Campbell, M., Driver, J., Pastok, D., Merry, B., & Field, K. J. (2021). Cultivar-dependent increases in mycorrhizal nutrient acquisition by barley in response to elevated CO2. *Plants, People, Planet*, *3*(5), 553–566. https://doi.org/10.1002/PPP3.10174

Thirkell, T. J., Charters, M. D., Elliott, A. J., Sait, S. M., & Field, K. J. (2017). Are mycorrhizal fungi our sustainable saviours? Considerations for achieving food security. *Journal of Ecology*, *105*(4), 921–929. https://doi.org/10.1111/1365-2745.12788

Thirkell, T. J., Pastok, D., & Field, K. J. (2020). Carbon for nutrient exchange between arbuscular mycorrhizal fungi and wheat varies according to cultivar and changes in atmospheric carbon dioxide concentration. *Global Change Biology*, *26*(3), 1725–1738. https://doi.org/10.1111/GCB.14851

Thonar, C., Schnepf, A., Frossard, E., Roose, T., & Jansa, J. (2011). Traits related to differences in function among three arbuscular mycorrhizal fungi. *Plant and Soil*, *339*(1), 231–245. https://doi.org/10.1007/S11104-010-0571-3/

Thornton, M. (2020). Potato Growth and Development. *Potato Production Systems*, 19–33. https://doi.org/10.1007/978-3-030-39157-7_2

Tian, B. Y., Cao, Y., & Zhang, K. Q. (2015). Metagenomic insights into communities, functions of endophytes and their associates with infection by root-knot nematode, Meloidogyne incognita, in tomato roots. *Scientific Reports 2015 5:1*, *5*(1), 1–15. https://doi.org/10.1038/srep17087

Tisserant, E., Kohler, A., Dozolme-Seddas, P., Balestrini, R., Benabdellah, K., Colard, A., Croll, D., da Silva, C., Gomez, S. K., Koul, R., Ferrol, N., Fiorilli, V., Formey, D., Franken, P. H., Helber, N., Hijri, M., Lanfranco, L., Lindquist, E., Liu, Y., … Martin, F. (2012). The transcriptome of the arbuscular mycorrhizal fungus Glomus intraradices (DAOM 197198) reveals functional tradeoffs in an obligate symbiont. *New Phytologist*, *193*(3), 755–769. https://doi.org/10.1111/J.1469-8137.2011.03948.X

Tisserant, E., Malbreil, M., Kuo, A., Kohler, A., Symeonidi, A., Balestrini, R., Charron, P., Duensing, N., Frei Dit Frey, N., Gianinazzi-Pearson, V., Gilbert, L. B., Handa, Y., Herr, J. R., Hijri, M., Koul, R., Kawaguchi, M., Krajinski, F., Lammers, P. J., Masclaux, F. G., … Martin, F. (2013). Genome of an arbuscular mycorrhizal fungus provides insight into the oldest plant symbiosis. *Proceedings of the National Academy of Sciences of the United States of America*, *110*(50), 20117–20122. https://doi.org/10.1073/pnas.1313452110

Toju, H., & Tanaka, Y. (2019). Consortia of anti-nematode fungi and bacteria in the rhizosphere of soybean plants attacked by root-knot nematodes. *Royal Society Open Science*, *6*(3). https://doi.org/10.1098/RSOS.181693;JOURNAL:JOURNAL:RSOS;WGROUP:STRING:PUBLICATION

Topalović, O., Bredenbruch, S., Schleker, A. S. S., & Heuer, H. (2020). Microbes Attaching to Endoparasitic Phytonematodes in Soil Trigger Plant Defense Upon Root Penetration by the Nematode. *Frontiers in Plant Science*, *11*, 512362. https://doi.org/10.3389/FPLS.2020.00138

Topalović, O., & Heuer, H. (2019). Plant-Nematode Interactions Assisted by Microbes in the Rhizosphere. *Current Issues in Molecular Biology*, *30*, 75–88. https://doi.org/10.21775/CIMB.030.075

Topalović, O., & Vestergård, M. (2021). Can microorganisms assist the survival and parasitism of plant-parasitic nematodes? *Trends in Parasitology*, *37*(11), 947–958. https://doi.org/10.1016/J.PT.2021.05.007

Treseder, K. K. (2004). A meta-analysis of mycorrhizal responses to nitrogen, phosphorus, and atmospheric CO2 in field studies. *New Phytologist*, *164*(2), 347–355. https://doi.org/10.1111/J.1469-8137.2004.01159.X

Tu, C., Koenning, S. R., & Hu, S. (2003). Root-parasitic nematodes enhance soil microbial activities and nitrogen mineralization. *Microbial Ecology*, *46*(1), 134–144. https://doi.org/10.1007/S00248-002-1068-2

Turlings, T. C. J., & Erb, M. (2018). Tritrophic Interactions Mediated by Herbivore-Induced Plant Volatiles: Mechanisms, Ecological Relevance, and Application Potential. *Annual Review of Entomology*, *63*(Volume 63, 2018), 433–452. https://doi.org/10.1146/ANNUREV-ENTO-020117-043507

Turner, S. J., & Rowe, J. A. (2006). Cyst nematodes. *Plant Nematology. Wallingford, Oxfordshire: CAB International*, 90–122.

Turner, S., & Subbotin, S. (2013). Cyst nematodes. In R. Perry & M. Moens (Eds.), *Plant Nematology* (2nd ed., pp. 110–143). CAB International. http://www.russjnematology.com/subbotin/Reprint/Chap4_Cyst_Nematodes.pdf

U.S. Regulated Plant Pest Table | Animal and Plant Health Inspection Service. (2025). https://www.aphis.usda.gov/plant-imports/regulated-pest-list

van Dam, N. M., & Oomen, M. W. A. T. (2008a). Root and shoot jasmonic acid applications differentially affect leaf chemistry and herbivore growth. *Plant Signaling & Behavior*, *3*(2), 91–98. https://doi.org/10.4161/PSB.3.2.5220

van Dam, N. M., & Oomen, M. W. A. T. (2008b). Root and shoot jasmonic acid applications differentially affect leaf chemistry and herbivore growth. *Plant Signaling & Behavior*, *3*(2), 91–98. https://doi.org/10.4161/PSB.3.2.5220

van der Heijden, M. G. A., Klironomos, J. N., Ursic, M., Moutoglis, P., Streitwolf-Engel, R., Boller, T., Wiemken, A., & Sanders, I. R. (1998). Mycorrhizal fungal diversity determines plant biodiversity, ecosystem variability and productivity. *Nature 1998 396:6706*, *396*(6706), 69–72. https://doi.org/10.1038/23932

van der Heijden, M. G. A., Martin, F. M., Selosse, M. A., & Sanders, I. R. (2015). Mycorrhizal ecology and evolution: the past, the present, and the future. *New Phytologist*, *205*(4), 1406–1423. https://doi.org/10.1111/NPH.13288

van der Heijden, M. G. A., & Walder, F. (2016). Reply to 'Misconceptions on the application of biological market theory to the mycorrhizal symbiosis.' *Nature Plants 2016 2:5*, *2*(5), 1–1. https://doi.org/10.1038/nplants.2016.62

van Geel, M., Busschaert, P., Honnay, O., & Lievens, B. (2014). Evaluation of six primer pairs targeting the nuclear rRNA operon for characterization of arbuscular mycorrhizal fungal (AMF) communities using 454 pyrosequencing. *Journal of Microbiological Methods*, *106*, 93–100. https://doi.org/10.1016/J.MIMET.2014.08.006

van Himbeeck, R., Geisen, S., van Schaik, C., van den Elsen, S., Berendsen, R., Bertran, A., Schepel, E., & Helder, J. (2025). Patchy Distribution of Potato Cyst Nematodes Within Single Arable Fields Reveals Local Disease Suppressiveness Mediated by Disparate Microbial Communities. *Environmental Microbiology*, *27*(5), e70113. https://doi.org/10.1111/1462-2920.70113

van ’t Padje, A., Bonfante, P., Ciampi, L. T., & Kiers, E. T. (2021). Quantifying Nutrient Trade in the Arbuscular Mycorrhizal Symbiosis Under Extreme Weather Events Using Quantum-Dot Tagged Phosphorus. *Frontiers in Ecology and Evolution*, *0*, 153. https://doi.org/10.3389/FEVO.2021.613119

Vance, C. P. (2001). Symbiotic Nitrogen Fixation and Phosphorus Acquisition. Plant Nutrition in a World of Declining Renewable Resources. *Plant Physiology*, *127*(2), 390–397. https://doi.org/10.1104/PP.010331

Vandenkoornhuyse, P., Mahé, S., Ineson, P., Staddon, P., Ostle, N., Cliquet, J. B., Francez, A. J., Fitter, A. H., & Young, J. P. W. (2007). Active root-inhabiting microbes identified by rapid incorporation of plant-derived carbon into RNA. *Proceedings of the National Academy of Sciences of the United States of America*, *104*(43), 16970–16975. https://doi.org/10.1073/PNAS.0705902104

van’t Padje, A., Oyarte Galvez, L., Klein, M., Hink, M. A., Postma, M., Shimizu, T., & Kiers, E. T. (2020). Temporal tracking of quantum-dot apatite across in vitro mycorrhizal networks shows how host demand can influence fungal nutrient transfer strategies. *The ISME Journal 2020 15:2*, *15*(2), 435–449. https://doi.org/10.1038/s41396-020-00786-w

van’t Padje, A., Werner, G. D. A., & Kiers, E. T. (2021). Mycorrhizal fungi control phosphorus value in trade symbiosis with host roots when exposed to abrupt ‘crashes’ and ‘booms’ of resource availability. *New Phytologist*, *229*(5), 2933–2944. https://doi.org/10.1111/NPH.17055

Venice, F., Chialva, M., Domingo, G., Novero, M., Carpentieri, A., Salvioli di Fossalunga, A., Ghignone, S., Amoresano, A., Vannini, C., Lanfranco, L., & Bonfante, P. (2021). Symbiotic responses of Lotus japonicus to two isogenic lines of a mycorrhizal fungus differing in the presence/absence of an endobacterium. *The Plant Journal*, *108*(6), 1547–1564. https://doi.org/10.1111/TPJ.15578

Verbruggen, E., el Mouden, C., Jansa, J., Akkermans, G., Bücking, H., West, S. A., & Kiers, T. E. (2012). Spatial structure and interspecific cooperation: Theory and an empirical test using the mycorrhizal mutualism. *American Naturalist*, *179*(5). https://doi.org/10.1086/665032

Verbruggen, E., & Toby Kiers, E. (2010). Evolutionary ecology of mycorrhizal functional diversity in agricultural systems. *Evolutionary Applications*, *3*(5–6), 547–560. https://doi.org/10.1111/J.1752-4571.2010.00145.X

Verbruggen, E., van der Heijden, M. G. A., Weedon, J. T., Kowalchuk, G. A., & Rö-Ling, W. F. M. (2012). Community assembly, species richness and nestedness of arbuscular mycorrhizal fungi in agricultural soils. *Molecular Ecology*, *21*(10), 2341–2353. https://doi.org/10.1111/J.1365-294X.2012.05534.X

Veresoglou, S. D., Johnson, D., Mola, M., Yang, G., & Rillig, M. C. (2022). Evolutionary bet-hedging in arbuscular mycorrhiza-associating angiosperms. *New Phytologist*, *233*(5), 1984–1987. https://doi.org/10.1111/NPH.17852

Vierheilig, H., Coughlan, A. P., Wyss, U., & Piché, Y. (1998). Ink and vinegar, a simple staining technique for arbuscular-mycorrhizal fungi. *Applied and Environmental Microbiology*, *64*(12), 5004–5007. https://doi.org/10.1128/aem.64.12.5004-5007.1998

Voets, L., Goubau, I., Olsson, P. A., Merckx, R., & Declerck, S. (2008). Absence of carbon transfer between Medicago truncatula plants linked by a mycorrhizal network, demonstrated in an experimental microcosm. *FEMS Microbiology Ecology*, *65*(2), 350–360. https://doi.org/10.1111/J.1574-6941.2008.00503.X

Vos, C., Claerhout, S., Mkandawire, R., Panis, B., de Waele, D., & Elsen, A. (2012). Arbuscular mycorrhizal fungi reduce root-knot nematode penetration through altered root exudation of their host. *Plant and Soil*, *354*(1–2), 335–345. https://doi.org/10.1007/S11104-011-1070-X

Vos, C., Geerinckx, K., Mkandawire, R., Panis, B., de Waele, D., & Elsen, A. (2012). Arbuscular mycorrhizal fungi affect both penetration and further life stage development of root-knot nematodes in tomato. *Mycorrhiza*, *22*(2), 157–163. https://doi.org/10.1007/S00572-011-0422-Y

Vos, C. M., Tesfahun, A. N., Panis, B., de Waele, D., & Elsen, A. (2012). Arbuscular mycorrhizal fungi induce systemic resistance in tomato against the sedentary nematode Meloidogyne incognita and the migratory

nematode Pratylenchus penetrans. *Applied Soil Ecology*, *61*, 1–6. https://doi.org/10.1016/J.APSOIL.2012.04.007

Vos, C., van den Broucke, D., Lombi, F. M., de Waele, D., & Elsen, A. (2012). Mycorrhiza-induced resistance in banana acts on nematode host location and penetration. *Soil Biology and Biochemistry*, *47*, 60–66. https://doi.org/10.1016/J.SOILBIO.2011.12.027

Wagg, C., Barendregt, C., Jansa, J., & van der Heijden, M. G. A. (2015). Complementarity in both plant and mycorrhizal fungal communities are not necessarily increased by diversity in the other. *Journal of Ecology*, *103*(5), 1233–1244. https://doi.org/10.1111/1365-2745.12452

Wagg, C., Jansa, J., Schmid, B., & van der Heijden, M. G. A. (2011). Belowground biodiversity effects of plant symbionts support aboveground productivity. *Ecology Letters*, *14*(10), 1001–1009. https://doi.org/10.1111/J.1461-0248.2011.01666.X

Wahab, A., Muhammad, M., Munir, A., Abdi, G., Zaman, W., Ayaz, A., Khizar, C., & Reddy, S. P. P. (2023). Role of Arbuscular Mycorrhizal Fungi in Regulating Growth, Enhancing Productivity, and Potentially Influencing Ecosystems under Abiotic and Biotic Stresses. *Plants 2023, Vol. 12, Page 3102*, *12*(17), 3102. https://doi.org/10.3390/PLANTS12173102

Walder, F., Brulé, D., Koegel, S., Wiemken, A., Boller, T., & Courty, P. E. (2015). Plant phosphorus acquisition in a common mycorrhizal network: regulation of phosphate transporter genes of the Pht1 family in sorghum and flax. *New Phytologist*, *205*(4), 1632–1645. https://doi.org/10.1111/NPH.13292

Walder, F., Niemann, H., Natarajan, M., Lehmann, M. F., Boller, T., & Wiemken, A. (2012). Mycorrhizal Networks: Common Goods of Plants Shared under Unequal Terms of Trade. *Plant Physiology*, *159*(2), 789–797. https://doi.org/10.1104/PP.112.195727

Walder, F., & van der Heijden, M. G. A. (2015). Regulation of resource exchange in the arbuscular mycorrhizal symbiosis. *Nature Plants*, *1*(11), 1–7. https://doi.org/10.1038/nplants.2015.159

Walker, T. W., & Syers, J. K. (1976). The fate of phosphorus during pedogenesis. *Geoderma*, *15*(1), 1–19. https://doi.org/10.1016/0016-7061(76)90066-5

Wang, B., & Qiu, Y.-L. (2006). Phylogenetic distribution and evolution of mycorrhizas in land plants. *Mycorrhiza 2006 16:5*, *16*(5), 299–363. https://doi.org/10.1007/S00572-005-0033-6

Wang, G., Jin, Z., George, T. S., Feng, G., & Zhang, L. (2023). Arbuscular mycorrhizal fungi enhance plant phosphorus uptake through stimulating hyphosphere soil microbiome functional profiles for phosphorus turnover. *New Phytologist*, *238*(6), 2578–2593. https://doi.org/10.1111/NPH.18772

Watts, A., Magkourilou, E., Howard, N., & Field, K. (2023). Can mycorrhizal fungi fix farming? Benefits and limitations of applying them to agroecosystems. *The Biochemist*, *45*(3), 2–7. https://doi.org/10.1042/bio_2023_118

Watts-Williams, S. J., Cavagnaro, T. R., & Tyerman, S. D. (2019). Variable effects of arbuscular mycorrhizal fungal inoculation on physiological and molecular measures of root and stomatal conductance of diverse Medicago truncatula accessions. *Plant, Cell & Environment*, *42*(1), 285–294. https://doi.org/10.1111/PCE.13369

Weiner, J., & Thomas, S. C. (1992). Competition and Allometry in Three Species of Annual Plants. *Ecology*, *73*(2), 648–656. https://doi.org/10.2307/1940771

Wenig, M., Ghirardo, A., Sales, J. H., Pabst, E. S., Breitenbach, H. H., Antritter, F., Weber, B., Lange, B., Lenk, M., Cameron, R. K., Schnitzler, J. P., & Vlot, A. C. (2019). Systemic acquired resistance networks amplify airborne defense cues. *Nature Communications*, *10*(1), 1–14. https://doi.org/10.1038/S41467-019-11798-2

Weremijewicz, J., & Janos, D. P. (2013). Common mycorrhizal networks amplify size inequality in Andropogon gerardii monocultures. *New Phytologist*, *198*(1), 203–213. https://doi.org/10.1111/NPH.12125

Weremijewicz, J., Sternberg, L. da S. L. O. R., & Janos, D. P. (2016). Common mycorrhizal networks amplify competition by preferential mineral nutrient allocation to large host plants. *New Phytologist*, *212*(2), 461–471. https://doi.org/10.1111/NPH.14041

Werner, G. D. A., & Kiers, E. T. (2015). Partner selection in the mycorrhizal mutualism. *New Phytologist*, *205*(4), 1437–1442. https://doi.org/10.1111/NPH.13113

Werner, G. D. A., Strassmann, J. E., Ivens, A. B. F., Engelmoer, D. J. P., Verbruggen, E., Queller, D. C., Noë, R., Johnson, N. C., Hammerstein, P., & Kiers, E. T. (2014). Evolution of microbial markets. *Proceedings of the National Academy of Sciences*, *111*(4), 1237–1244. https://doi.org/10.1073/PNAS.1315980111

Whitehead, A. G., & Turner, S. J. (1998). *Management and regulatory control strategies for potato cyst nematodes (Globodera rostochiensis and Globodera pallida). Potato cyst nematodes, biology, distribution and control.*

Whiteside, M. D., Werner, G. D. A., Caldas, V. E. A., van't Padje, A., Dupin, S. E., Elbers, B., Bakker, M., Wyatt, G. A. K., Klein, M., Hink, M. A., Postma, M., Vaitla, B., Noë, R., Shimizu, T. S., West, S. A., & Kiers, E. T. (2019). Mycorrhizal Fungi Respond to Resource Inequality by Moving Phosphorus from Rich to Poor Patches across Networks. *Current Biology*, *29*(12), 2043-2050.e8. https://doi.org/10.1016/J.CUB.2019.04.061

Wickham, H. (2014). *ggplot2: Elegant Graphics for Data Analysis*. Springer-Verlag New York. https://ggplot2.tidyverse.org

Wilkinson, A., Alexander, I. J., & Johnson, D. (2011). Species richness of ectomycorrhizal hyphal necromass increases soil CO2 efflux under laboratory conditions. *Soil Biology and Biochemistry*, *43*(6), 1350–1355. https://doi.org/10.1016/J.SOILBIO.2011.03.009

Wilschut, R. A., van der Putten, W. H., Garbeva, P., Harkes, P., Konings, W., Kulkarni, P., Martens, H., & Geisen, S. (2019). Root traits and belowground herbivores relate to plant–soil feedback variation among congeners. *Nature Communications*, *10*(1), 1–9. https://doi.org/10.1038

Wipf, D., Krajinski, F., van Tuinen, D., Recorbet, G., & Courty, P. E. (2019). Trading on the arbuscular mycorrhiza market: from arbuscules to common mycorrhizal networks. *New Phytologist*, *223*(3), 1127–1142. https://doi.org/10.1111/NPH.15775

Wondafrash, M., van Dam, N. M., & Tytgat, T. O. G. (2013). Plant systemic induced responses mediate interactions between root parasitic nematodes and aboveground herbivorous insects. *Frontiers in Plant Science*, *4*(APR), 43680. https://doi.org/10.3389

Wurst, S., van Beersum, S., Wagenaar, R., Bakx-Schotman, T., Drigo, B., Janzik, I., Lanoue, A., & van der Putten, W. H. (2009). Plant defence against nematodes is not mediated by changes in the soil microbial community. *Functional Ecology*, *23*(3), 488–495. https://doi.org/10.1111/J.1365-2435.2009.01543.X

Wurzburger, N., Brookshire, E. N. J., McCormack, M. L., & Lankau, R. A. (2017). Mycorrhizal fungi as drivers and modulators of terrestrial ecosystem processes. *New Phytologist*, *213*(3), 996–999. https://doi.org/10.1111/NPH.14409

Wyatt, G. A. K., Toby Kiers, E., Gardner, A., & West, S. A. (2014). A biological market analysis of the plant-mycorrhizal symbiosis. *Evolution*, *68*(9), 2603–2618. https://doi.org/10.1111/EVO.12466

Wyss, U. (2002). Feeding behaviour of plant-parasitic nematodes. In *The biology of nematodes* (pp. 233–260).

Xie, X., Huang, W., Liu, F., Tang, N., Liu, Y., Lin, H., & Zhao, B. (2013). Functional analysis of the novel mycorrhiza-specific phosphate transporter AsPT1 and PHT1 family from Astragalus sinicus during the arbuscular mycorrhizal symbiosis. *New Phytologist*, *198*(3), 836–852. https://doi.org/10.1111/NPH.12188

Xue, C., Hao, Y., Pu, X., Ryan Penton, C., Wang, Q., Zhao, M., Zhang, B., Ran, W., Huang, Q., Shen, Q., & Tiedje, J. M. (2019). Effect of LSU and ITS genetic markers and reference databases on analyses of fungal communities. *Biology and Fertility of Soils*, *55*(1), 79–88. https://doi.org/10.1007/S00374-018-1331-4

Yadav, V., Wang, Z., Guo, Y., & Zhang, X. (2022). Comparative transcriptome profiling reveals the role of phytohormones and phenylpropanoid pathway in early-stage resistance against powdery mildew in watermelon (Citrullus lanatus L.). *Frontiers in Plant Science*, *13*, 1016822. https://doi.org/10.3389/FPLS.2022.1016822

Yadav, V., Wang, Z., Wei, C., Amo, A., Ahmed, B., Yang, X., & Zhang, X. (2020). Phenylpropanoid Pathway Engineering: An Emerging Approach towards Plant Defense. *Pathogens 2020, Vol. 9, Page 312*, *9*(4), 312. https://doi.org/10.3390/PATHOGENS9040312

Yeates, G. W., Saggar, S., Denton, C. S., & Mercer, C. F. (1998). Impact of Clover Cyst Nematode (Heterodera Trifolii) Infection On Soil Microbial Activity in the Rhizosphere of White Clover (Trifolium Repens) - a Pulse-Labelling Experiment. *Nematologica*, *44*(1), 81–90. https://doi.org/10.1163/005225998X00082

Yeates, G. W., Saggar, S., Hedley, C. B., & Mercer, C. F. (1999). Increase in 14C-carbon translocation to the soil microbial biomass when five species of plant-parasitic nematodes infect roots of white clover. *Nematology*, *1*(3), 295–300. https://doi.org/10.1163/156854199508298

Yergaliyev, T. M., Alexander-Shani, R., Dimerets, H., Pivonia, S., Bird, D. McK., Rachmilevitch, S., & Szitenberg, A. (2020). Bacterial Community Structure Dynamics in Meloidogyne incognita -Infected Roots and Its Role in Worm-Microbiome Interactions . *MSphere*, *5*(4). https://doi.org/10.1128/MSPHERE.00306-20

Yuan, Y., van Kleunen, M., & Li, J. (2021). A parasite indirectly affects nutrient distribution by common mycorrhizal networks between host and neighboring plants. *Ecology*, *102*(5), e03339. https://doi.org/10.1002/ECY.3339

Zebelo, S., Piorkowski, J., Disi, J., & Fadamiro, H. (2014). Secretions from the ventral eversible gland of Spodoptera exigua caterpillars activate defense-related genes and induce emission of volatile organic compounds in tomato, Solanum lycopersicum. *BMC Plant Biology*, *14*(1), 1–12. https://doi.org/10.1186/1471-2229-14-140

Zhang, C., van der Heijden, M. G. A., Dodds, B. K., Nguyen, T. B., Spooren, J., Valzano-Held, A., Cosme, M., & Berendsen, R. L. (2024). A tripartite bacterial-fungal-plant symbiosis in the mycorrhiza-shaped microbiome drives plant growth and mycorrhization. *Microbiome 2024 12:1*, *12*(1), 1–21. https://doi.org/10.1186/S40168-023-01726-4

Zhang, L., Chu, Q., Zhou, J., Rengel, Z., & Feng, G. (2021). Soil phosphorus availability determines the preference for direct or mycorrhizal phosphorus uptake pathway in maize. *Geoderma*, *403*, 115261. https://doi.org/10.1016/J.GEODERMA.2021.115261

Zhang, L., Shi, N., Fan, J., Wang, F., George, T. S., & Feng, G. (2018). Arbuscular mycorrhizal fungi stimulate organic phosphate mobilization associated with changing bacterial community structure under field conditions. *Environmental Microbiology*, *20*(7), 2639–2651. https://doi.org/10.1111/1462-2920.14289

Zhang, L., Xu, M., Liu, Y., Zhang, F., Hodge, A., & Feng, G. (2016). Carbon and phosphorus exchange may enable cooperation between an arbuscular mycorrhizal fungus and a phosphate-solubilizing bacterium. *New Phytologist*, *210*(3), 1022–1032. https://doi.org/10.1111/NPH.13838

Zhao, F. jun, Shu, L. fu, Wang, Q. hua, Wang, M. yu, & Tian, X. rui. (2011). Emissions of volatile organic compounds from heated needles and twigs of Pinus pumila. *Journal of Forestry Research*, *22*(2), 243–248. https://doi.org/10.1007/S11676-011-0157-9

Zhao, R., Wang, C., Koorem, K., Song, X., Siemann, E., Ding, J., & Yang, Q. (2024). Aboveground antagonists mitigate belowground plant–antagonist interactions but not affect plant–mutualist interactions. *European Journal of Soil Biology*, *120*, 103577. https://doi.org/10.1016/J.EJSOBI.2023.103577

Zheng, C., Ji, B., Zhang, J., Zhang, F., & Bever, J. D. (2015). Shading decreases plant carbon preferential allocation towards the most beneficial mycorrhizal mutualist. *New Phytologist*, *205*(1), 361–368. https://doi.org/10.1111/NPH.13025

Zhou, D., Feng, H., Schuelke, T., de Santiago, A., Zhang, Q., Zhang, J., Luo, C., & Wei, L. (2019). Rhizosphere Microbiomes from Root Knot Nematode Non-infested Plants Suppress Nematode Infection. *Microbial Ecology*, *78*(2), 470–481. https://doi.org/10.1007/S00248-019-01319-5

Zhou, J., Chai, X., Zhang, L., George, T. S., Wang, F., & Feng, G. (2020). Different Arbuscular Mycorrhizal Fungi Cocolonizing on a Single Plant Root System Recruit Distinct Microbiomes. *MSystems*, *5*(6). https://doi.org/10.1128

Zhu, A., Ibrahim, J. G., & Love, M. I. (2019). Heavy-tailed prior distributions for sequence count data: removing the noise and preserving large differences. *Bioinformatics*, *35*(12), 2084–2092. https://doi.org/10.1093/BIOINFORMATICS/BTY895

Supplementary material

Chapter 2

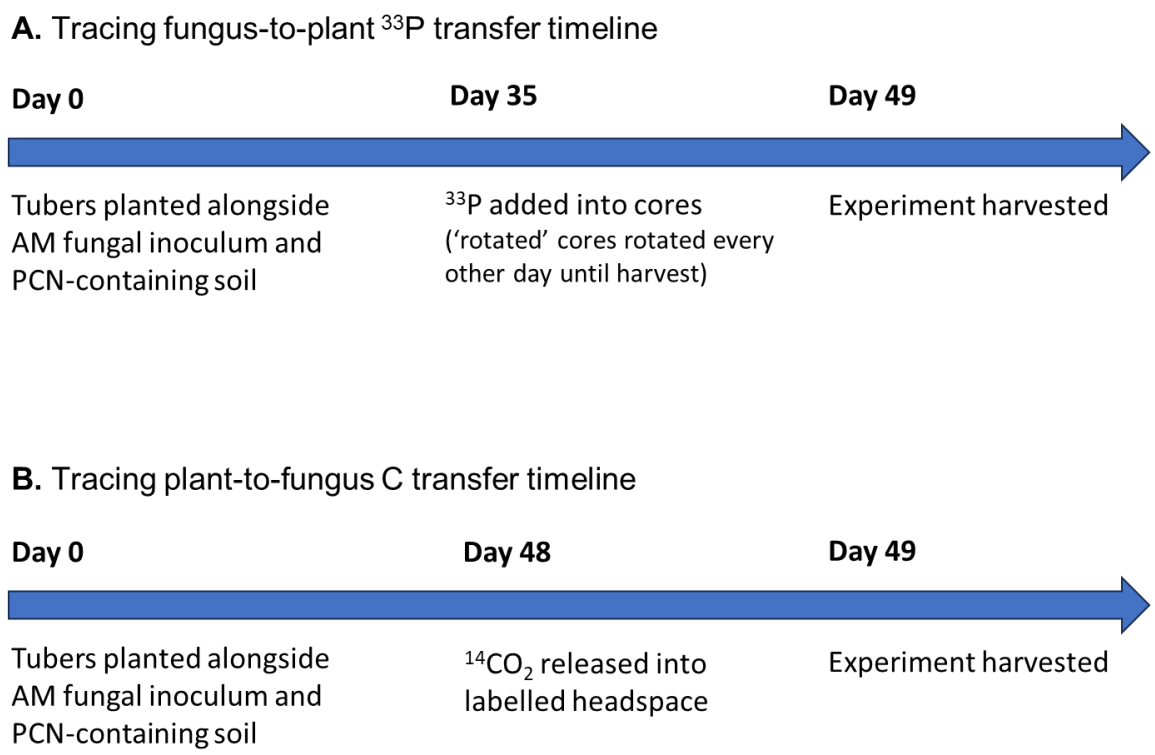

Supplementary Figure 2.1 A simplified experimental timeline for **A.** the tracing of ^{33}P from fungus to plant, and **B.** the tracing of plant C from plant to fungus.

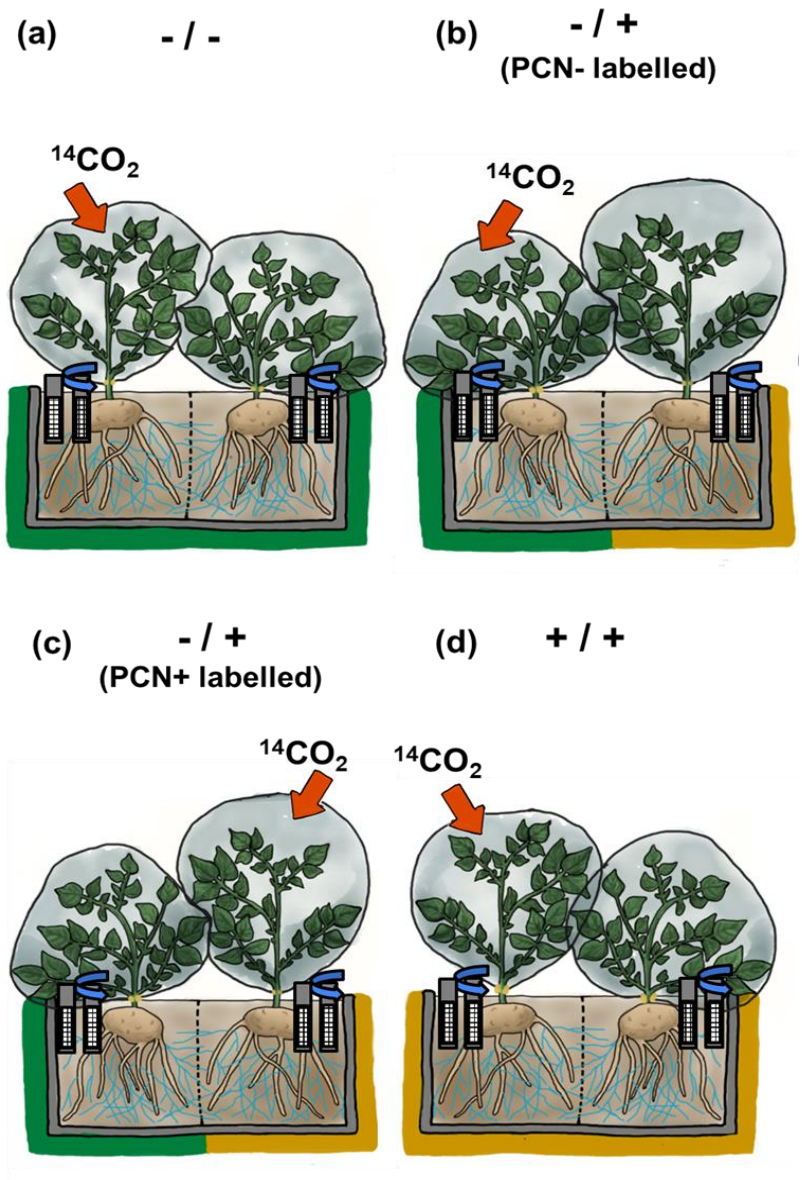

Supplementary Figure 2.2 The experimental design used to test the effect of potato-cyst nematodes on the transfer of recently-fixed plant carbon across the mycorrhizal network. All plants were connected by one or more mycorrhizal networks (illustrated by the blue lines) across a root-excluding 35 µm pore mesh. Plants without PCN are indicated by '–' and a green box, whereas plants with PCN are indicated by '+' a yellow box. Two soil-filled, root-excluding but hyphal-permitting mesh cores were inserted at the extreme boundary of each compartment. At seven weeks of growth and immediately before labelling one plant per mesocosm with $^{14}CO2$ (illustrated by the red arrow), one of the two cores on each compartment was rotated to break hyphal connections whilst the other was left static to maintain hyphal links to the host plants. n = 6 for each mesocosm shown in (a), (b), (c) and (d).

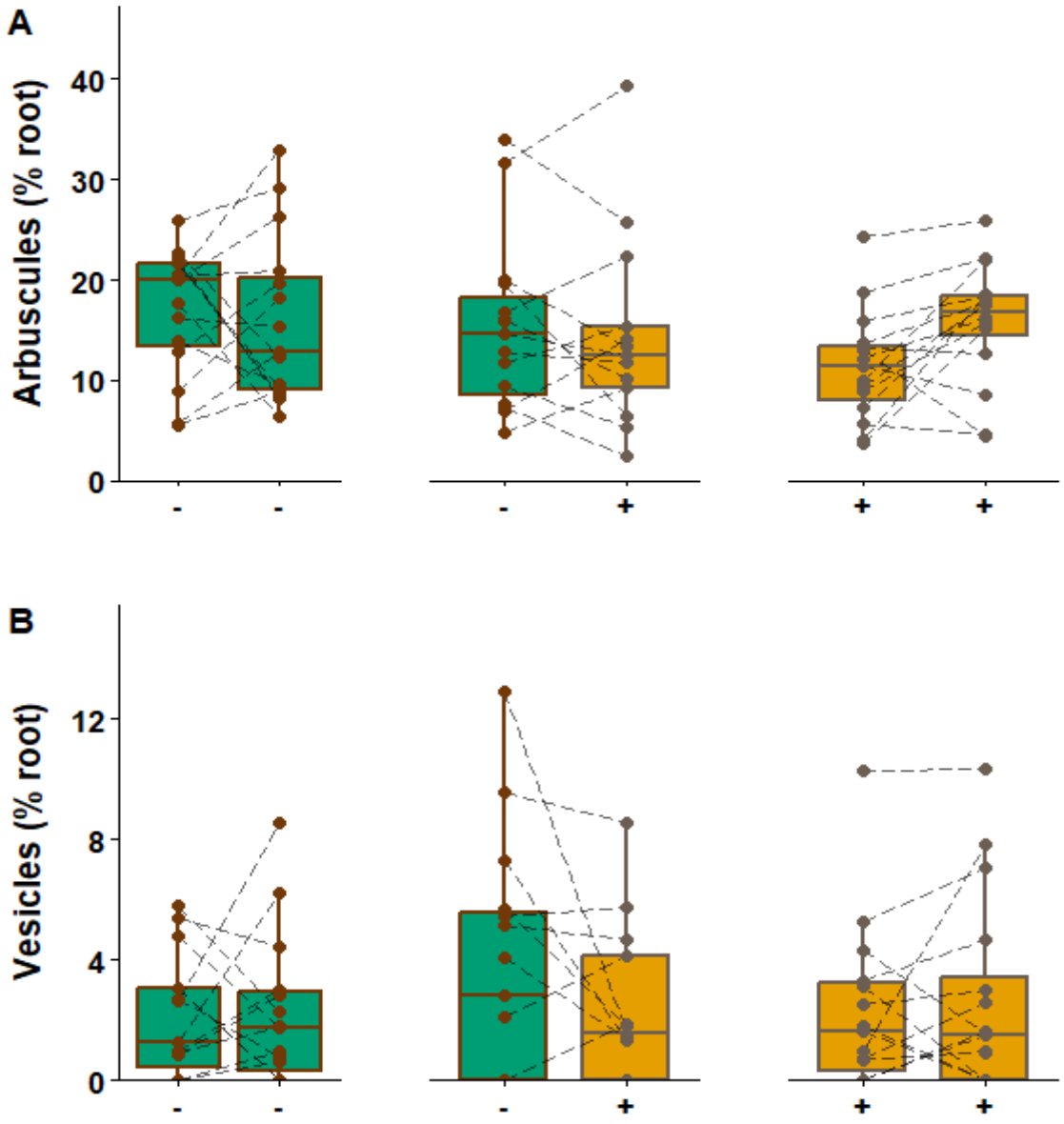

Supplementary Figure 2.3 A. Percentage arbuscular, and **B.** vesicular root colonisation for each PCN treatment. Dashed lines connect paired samples across each side of the same container. The centre line of the boxplot denotes the median, the box the interquartile range and the whiskers show no more than 1.5 times the distance between the 25th and 75th percentile. Data were extracted from a subset of mesocosms across both experiments. Treatments without PCN added to soil are indicated by '-' and green bars, whereas treatments with PCN are indicated by '+' and orange bars.

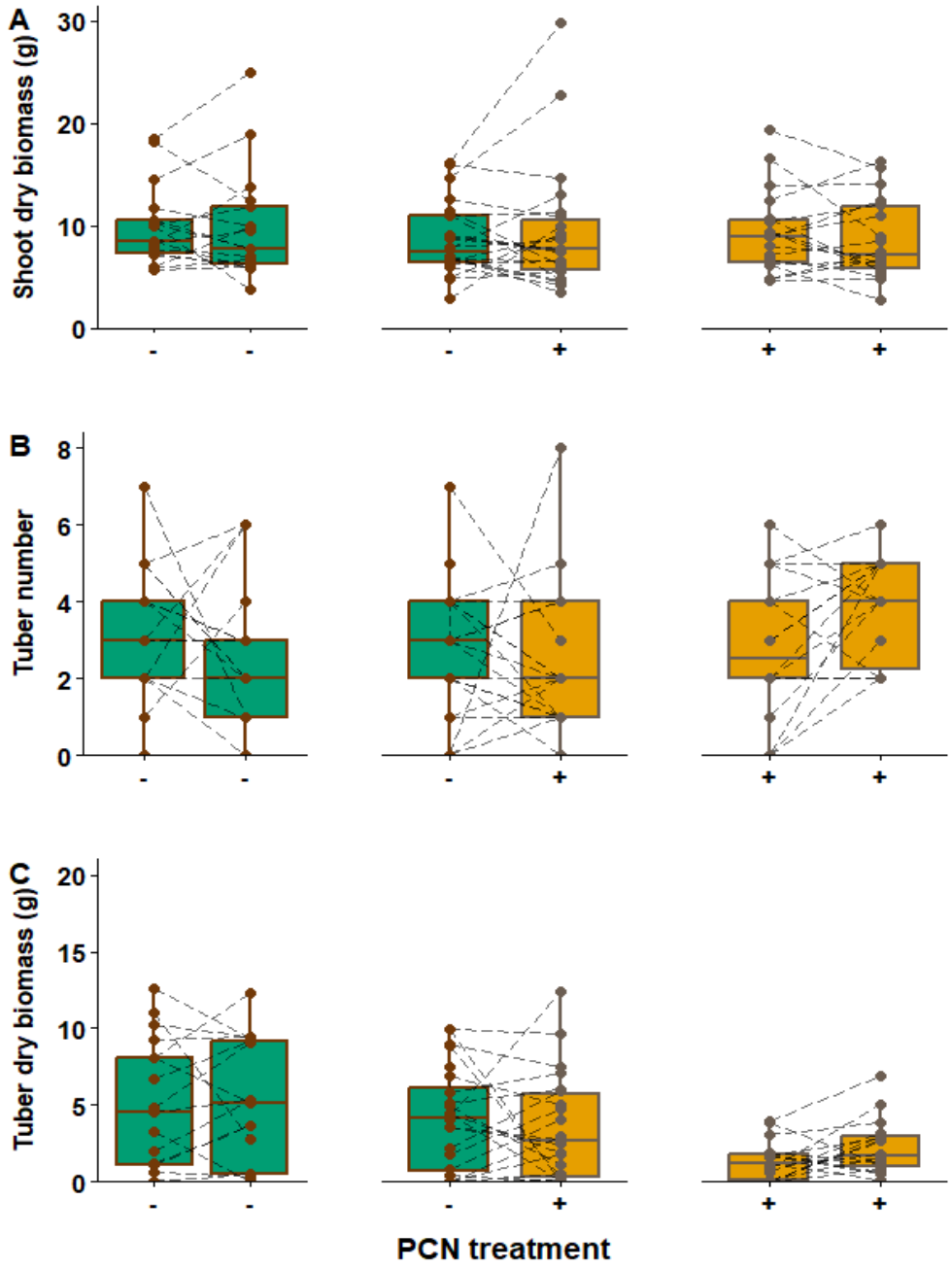

Supplementary Figure 2.4 A. Shoot dry biomass in grams, **B.** Total number of harvested tubers, and **C.** dry tuber yield expressed in grams, for each PCN treatment. Dashed lines connect paired samples across each side of the same container. The centre line of the boxplot denotes the median, the box the interquartile range and the whiskers show no more than 1.5 times the distance between the 25th and 75th percentile. Treatments without PCN added to soil are indicated by '-' and green bars, whereas treatments with PCN are indicated by '+' and orange bars.

Supplementary Table 2.1 Summary of statistical results from linear mixed-effects models showing the effect of the PCN treatment of a plant and/or the effect of the PCN treatment of the neighbouring plants on the PCN reproductive success, root colonisation and plant growth parameters.

	df	F-statistic	p-value
PCN reproductive success			
PCN treatment of neighbour	46	0.99	0.32
AM root colonisation			
PCN treatment	82	0.07	0.79
PCN treatment of neighbour	82	0.04	0.85
Soil hyphal lengths			
PCN treatment	73	0.68	0.41
PCN treatment of neighbour	73	0.07	0.80
Shoot biomass			
PCN treatment	109	0.37	0.55
PCN treatment of neighbour	109	2.94	0.09
FvP/FmP			
PCN treatment	62	0.20	0.65
PCN treatment of neighbour	62	0.00	0.97
SPAD			
PCN treatment	161	0.05	0.82
PCN treatment of neighbour	161	1.29	0.26

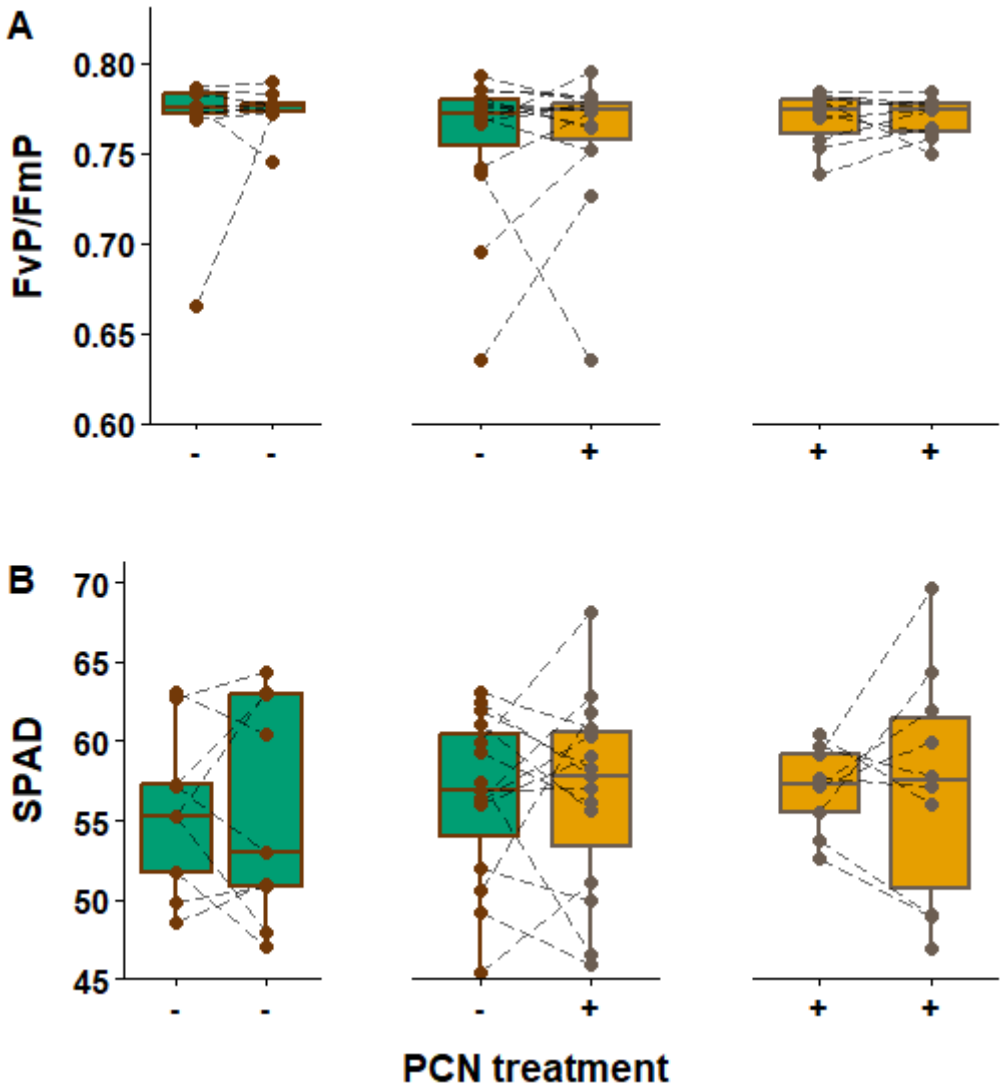

Supplementary Figure 2.5 A. The photochemical activity of photosystem II characterised by the FvP/FmP and **B.** the Relative Chlorophyll Content (SPAD) at the week of harvest for each PCN treatment. Dashed lines connect paired samples across each side of the same container. The centre line of the boxplot denotes the median, the box the interquartile range and the whiskers show no more than 1.5 times the distance between the 25th and 75th percentile. Data were extracted from a subset of mesocosms across both experiments. Plants without PCN are indicated by '-' and green bars, whereas plants with PCN are indicated by '+' and orange bars.

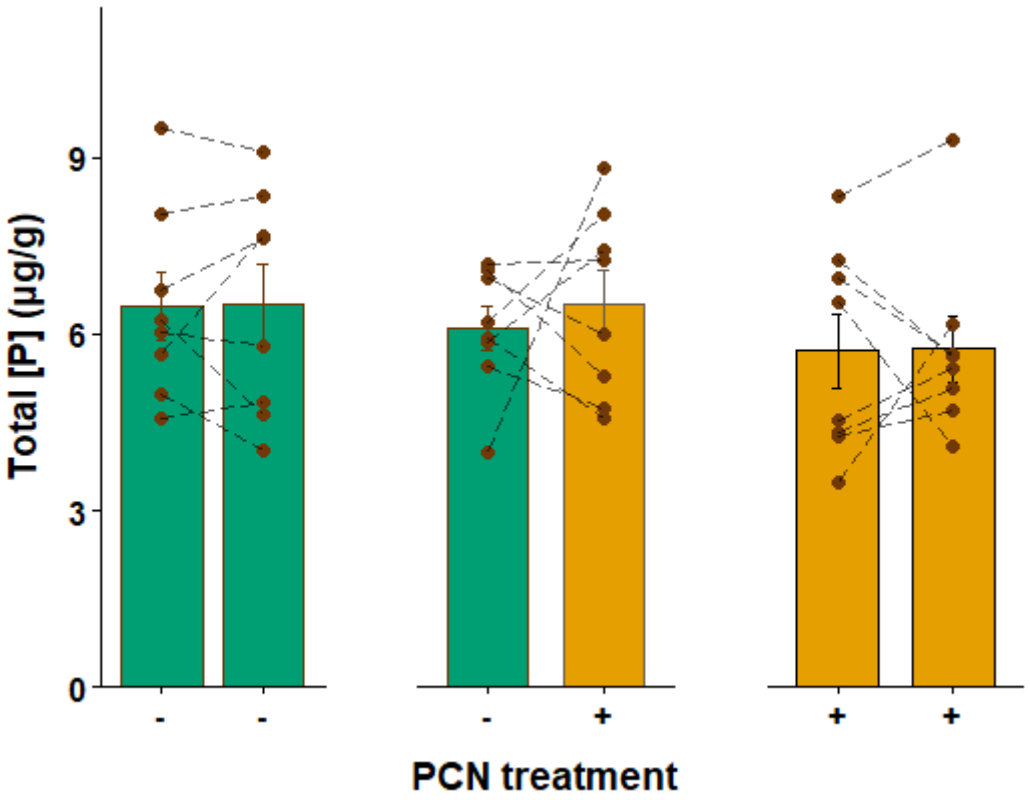

Supplementary Figure 2.6 Concentration of Total P (plant and AM fungal-acquired) in plant shoots for each PCN treatment. Dashed lines connect paired samples across each side of the same container. Barplots denote mean +/- SE. Data were extracted from experimental blocks 1 and 3 of the ^{33}P tracing experiment. Plants without PCN are indicated by '-' and green bars, whereas plants with PCN are indicated by '+' and orange bars.

Chapter 3

Supplementary Table 3.1. Composition of samples used in analysis (i.e., after excluding samples that failed at any step of the cleaning and filtering process)

Experiment	PCN treatment	PCN treatment of neighbour	Roots	Soil	Total
Fungi (ITS)			**42**	**58**	**100**
^{33}P	-	-	6	12	18
^{33}P	-	+	2	6	8
^{33}P	+	-	4	6	10
^{33}P	+	+	6	12	18
^{14}C	-	-	6	5	11
^{14}C	-	+	6	6	12
^{14}C	+	-	6	6	12
^{14}C	+	+	6	5	11
AM fungi (18S)			**40**	**53**	**93**
^{33}P	-	-	4	11	15
^{33}P	-	+	2	5	7
^{33}P	+	-	4	5	9
^{33}P	+	+	6	10	16
^{14}C	-	-	6	5	11
^{14}C	-	+	6	7	13
^{14}C	+	-	6	4	10
^{14}C	+	+	6	6	12
Bacteria			**42**	**18**	**58**
^{33}P	-	-	6	3	9
^{33}P	-	+	3	0	3
^{33}P	+	-	4	1	5
^{33}P	+	+	6	1	7
^{14}C	-	-	6	3	7
^{14}C	-	+	5	3	9
^{14}C	+	-	6	3	8
^{14}C	+	+	6	4	10
			42	18	58

Supplementary Table 3.2 Sequencing primer details and PCR cycle conditions

Target region	Target Group	Oligo name	Primer sequence (with indexes) (5 ->3)	Target size (bases)	Amplification conditions	References
18S of the SSU (RY 115-136) to 5.8S/ITS1 (FE 406-426) of the ITS region	General Fungi, but limiting the ITS bias against Mucoromycota	1624F newITSR	Forward: GTGACTGGAGTTCAGACGTGTGCTCTTCCGATCT-CCTTTGTACACACCGCCCGTCG Reverse: ACACTCTTTCCCTACACGACGCTCTTCCGATCT-CCAAGAGATCCRTTGYTRAAA	~311	35 cycles 95 °C for 15:00 min 94 °C for 00:30 min 55 °C for 01:00 min 72 °C for 00:30 min 72 °C for 10:00 min 10:00 min hold	NA
Variable region V4 of the 18S SSU rRNA gene	Glomeromycota fungi	NS31 AML2	Forward: GTGACTGGAGTTCAGACGTGTGCTCTTCCGATCT-NNNNNNNN-TTGGAGGGCAAGTCTGGTGCC Reverse: ACACTCTTTCCCTACACGACGCTCTTCCGATCT-NNNNNNNN-GAACCCAAACACTTTGGTTTCC	~560	5 cycles 95 °C 15:00 min 94 °C 00:30 min 52 °C 00:30 min 72 °C 01:00 min 30 cycles 94 °C 00:30 min 58 °C 00:30 min 72 °C 01:00 min 72 °C 10:00 min 10:00 min hold	NS31 (Simon et al., 1992) AML2 (Lee et al., 2008) Cycling conditions (Öpik et al., 2013)
Variable region V4 of the 16S SSU rRNA gene	Bacteria	515F (Parada) 806R (Apprill)	Forward: ACACTCTTTCCCTACACGACGCTCTTCCGATCT-NNNNN-GTGYCAGCMGCCGCGGTAA Reverse: GTGACTGGAGTTCAGACGTGTGCTCTTCCGATCT-GGACTACNVGGGTWTCTAAT	~293	30 cycles 95 °C for 15:00 min 94 °C for 00:30 min 51 °C for 01:00 min 72 °C for 00:30 min 72 °C for 10:00 min 10:00 min hold	515F (Parada et al., 2016) SAR11 (806R, Apprill et al., 2015)

Fungi

Supplementary Table 3.3 Statistical results from a negative binomial generalised linear mixed-effects model (GLMM; Observed richness), a linear mixed-effects model with heterogeneous variance structure (LMM; Shannon), and a beta GLMM (Simpson), testing the effects of PCN treatment and sample type (roots vs. soil) on alpha diversity metrics using the **ITS dataset for all fungi**. Type III Wald chi-square (χ^2) tests were used to assess the significance of main effects and interactions.

	df	χ^2	p-value
Observed			
PCN treatment	1	0.20	0.65
Sample type	1	111.09	**<0.01**
Interaction	1	8.55	**<0.01**
Shannon			
PCN treatment	1	0.01	0.94
Sample type	1	94.76	**<0.01**
Interaction	1	14.58	**<0.01**
Simpson			
PCN treatment	1	0.42	0.51
Sample type	1	77.61	**<0.01**
Interaction	1	17.56	**<0.01**

Supplementary Table 3.4 Pairwise comparisons of PCN treatment (PCN– vs. PCN+) within each sample type (roots and soil) for alpha diversity metrics of **fungal** ASVs (**ITS dataset**). Observed richness was analysed using negative binomial GLMMs, Shannon diversity using LMMs, and Simpson diversity using a beta GLMM. Estimated marginal means from each model were used for comparisons, with differences assessed separately for roots and soil using Wald z-tests.

	estimate	SE	df	statistic (t- or z-ratio)	p-value
Observed					
Soil	0.04	0.09	Inf	0.45	0.65
Roots	0.45	0.11	Inf	3.90	**<0.01**
Shannon					
Soil	0.01	0.12	30	0.08	0.94
Roots	0.75	0.16	30	4.62	**<0.01**
Simpson					
Soil	0.03	0.07	Inf	0.35	0.73

	estimate	SE	df	statistic (t- or z-ratio)	p-value
Roots	0.54	0.09	Inf	6.35	**<0.01**

Supplementary Table 3.5 Statistical results from negative binomial GLMMs (Observed richness), LMMs (Shannon), and a beta GLMM (Simpson), testing the effects of PCN treatment and sample type (roots vs. soil) on alpha diversity metrics using the **Glomeromycota** ASVs only extracted from the **ITS and the 18S dataset**, respectively. Type III Wald chi-square (χ^2) tests were used to assess the significance of main effects and interactions.

		df	χ^2	p-value
ITS Glomeromycota	**Observed**			
	PCN treatment	1	0.60	0.44
	Sample type	1	25.10	**<0.01**
	Interaction	1	3.25	0.07
	Shannon			
	PCN treatment	1	0.07	0.80
	Sample type	1	3.23	0.07
	Interaction	1	0.79	0.37
	Simpson			
	PCN treatment	1	0.01	0.93
	Sample type	1	2.96	0.09
	Interaction	1	1.66	0.20
18S Glomeromycota	**Observed**			
	PCN treatment	1	3.70	**0.05**
	Sample type	1	10.52	**<0.01**
	Interaction	1	0.19	0.66
	Shannon			
	PCN treatment	1	2.81	0.09
	Sample type	1	0.01	0.94
	Interaction	1	0.35	0.55
	Simpson			
	PCN treatment	1	2.66	0.10
	Sample type	1	1.38	0.24
	Interaction	1	0.93	0.33

Supplementary Table 3.6 Pairwise comparisons of PCN treatment (PCN– vs. PCN+) within each sample type (roots and soil) for alpha diversity metrics of **Glomeromycota**n ASVs (from the **ITS** and **18S** datasets). Observed richness was analysed using negative binomial GLMMs, Shannon diversity using LMMs, and Simpson diversity using a beta GLMM. Estimated marginal means from each model were used for comparisons, with differences assessed separately for roots and soil using Wald z-tests.

		estimate	SE	df	z-ratio	p-value
ITS Glomeromycota	**Observed**					
	Soil	0.17	0.22	Inf	0.77	0.44
	Roots	0.68	0.22	Inf	3.15	**<0.01**
	Shannon					
	Soil	0.11	0.43	Inf	0.26	0.80
	Roots	0.69	0.50	Inf	1.39	0.17
	Simpson					
	Soil	-0.03	0.32	Inf	-0.08	0.93
	Roots	0.62	0.38	Inf	1.61	0.11
18S Glomeromycota	**Observed**					
	Soil	0.25	0.13	Inf	1.92	**0.05**
	Roots	0.33	0.15	Inf	2.32	**0.02**
	Shannon					
	Soil	0.20	0.12	83.4	1.63	0.11
	Roots	0.10	0.14	87.2	0.71	0.48
	Simpson					
	Soil	0.31	0.19	Inf	1.63	0.10
	Roots	0.07	0.21	Inf	0.31	0.76

Supplementary Table 3.7 Statistical results from binomial GLMMs (logit link) testing the effects of PCN treatment combinations and sample type (roots vs. soil) on the proportion of fungal or **Glomeromycotan** ASVs shared between sides of the container (extracted from the **ITS** and **18S** datasets, respectively). Type III Wald chi-square tests were used to assess the significance of main effects and interactions.

		df	χ^2	p-value
ITS All fungi	Treatment combination	1	7.84	**0.02**
	Sample type	2	1.53	0.22
	Interaction	2	0.32	0.85

18S Glomeromycota	Treatment combination	1	0.26	0.88
	Sample type	2	1.23	0.27
	Interaction	2	1.66	0.44

Supplementary Table 3.8 Pairwise comparisons from binomial GLMMs (logit link) testing the effects of PCN treatment combinations on the proportion of shared fungal or Glomeromycotan between sides of the mesocosm in soil and roots (extracted from the **ITS** and **18S** datasets, respectively). Comparisons were based on estimated marginal means from each model, with differences assessed using Wald z-tests with asymptotic degrees of freedom (df = ∞). All pairwise comparisons were Tukey-adjusted for multiple testing.

			estimate	**SE**	**df**	**statistic**	**p-value**
ITS	**All fungi**	**Soil**					
		–/– vs –/+	0.13	0.09	Inf	1.40	0.34
		–/– vs +/+	-0.13	0.10	Inf	-1.37	0.36
		–/+ vs +/+	-0.26	0.09	Inf	-2.79	**<0.01**
		Roots					
		–/– vs –/+	0.23	0.18	Inf	1.30	0.40
		–/– vs +/+	-0.10	0.20	Inf	-0.47	0.88
		–/+ vs +/+	-0.33	0.20		-1.69	0.21
	18S Glomeromycota	**Soil**					
		–/– vs –/+	0.02	0.21	Inf	0.11	0.99
		–/– vs +/+	-0.08	0.21	Inf	-0.39	0.92
		–/+ vs +/+	-0.11	0.22	Inf	-0.48	0.39
		Roots					
		–/– vs –/+	-0.30	0.23	Inf	-1.30	039
		–/– vs +/+	-0.47	0.26	Inf	-1.86	0.15
		–/+ vs +/+	-0.18	0.23	Inf	-0.79	0.71

Supplementary Table 3.9 Results of PERMANOVA (adonis2) testing the effects of PCN treatment, sample type, and experimental block (strata) on fungal community composition (**ITS dataset**) based on Bray–Curtis dissimilarities. The model included 999 permutations and assessed factors by marginal effects.

Factor	**df**	**Sum of Squares**	**R^2**	**F-statistic**	**p-value**
PCN treatment	1	0.76	0.03	4.70	**<0.01**
Sample type	1	12.22	0.40	75.93	**<0.01**
Experiment (strata)	1	1.48	0.05	9.19	**<0.01**
Residual	96	15.45	0.51		
Total	99	30.28	1.00		

Supplementary Table 3.10 Pairwise PERMANOVA comparisons of the effect of PCN treatment (PC- vs PCN+) on fungal community composition **(ITS dataset)** based on Bray-Curtis dissimilarity. Analyses were performed separately for root and soil samples, with factors assessed by marginal effects and stratified by experiment.

Sample type	**df**	**Sum of Squares**	**R^2**	**F-statistic**	**p-value**
Roots	1	1.64	0.20	9.89	**<0.01**
Soil	1	0.13	0.01	0.79	0.47

Supplementary Table 3.11 Differential abundance of **fungal Phyla (ITS dataset)** comparing soil vs roots, as well as the effect of PCN treatment in soil and roots, analysed using DESeq2. The table reports standard errors, test statistics, p-values, and adjusted p-values for each Phylum. Only Phyla detected in each of the comparisons are included. Taxa present exclusively in one category were assigned a pseudo-log_2 fold change by employing (log_2(mean counts + 1)).

Phylum	baseMean	mean (Roots or PCN-)	mean (Soil or PCN+)	log2Fold_Change	lfcSE	statistic	p_value	p_adjusted	Comparison
Aphelidiomycota	70.13	1.61	119.74	-7.85	0.38	-20.88	<0.01	<0.01	
Ascomycota	11,324.39	11,324.39	11,324.39	0.00	0.00	0.00	1	1	
Basidiobolomycota	0.00	0.00	1.10	-1.07	0.00	0.00	1		
Basidiomycota	1,438.67	236.71	2,309.06	-4.83	0.34	-14.33	<0.01	<0.01	
Blastocladiomycota	0.98	0.00	1.69	-3.12	2.26	-1.38	0.17	0.27	
Chytridiomycota	40.62	11.10	62.01	-4.04	0.66	-6.09	<0.01	<0.01	
Entomophthoromycota	0.07	0.00	0.12	-0.77	3.01	-0.26	0.8	0.93	Roots_vs_Soil
Entorrhizomycota	0.99	0.00	1.71	-2.37	1.92	-1.24	0.22	0.3	
Kickxellomycota	0.09	0.00	0.15	-0.49	3.01	-0.16	0.87	0.94	
Monoblepharomycota	0.13	0.00	0.22	-1.01	3.01	-0.34	0.74	0.93	
Mortierellomycota	1,407.42	194.68	2,285.61	-4.35	0.39	-11.06	<0.01	<0.01	
Mucoromycota	815.85	1,534.09	295.75	2.06	0.33	6.17	<0.01	<0.01	

Phylum	baseMean	mean (Roots or PCN-)	mean (Soil or PCN+)	log2Fold_Change	lfcSE	statistic	p_value	p_adjusted	Comparison
Olpidiomycota	590.30	1,220.31	134.09	2.29	0.39	5.95	<0.01	<0.01	
Rozellomycota	34.90	9.18	150.51	-5.88	0.37	-15.85	<0.01	<0.01	
Sanchytriomycota	0.94	0.00	1.62	-2.56	1.89	-1.35	0.18	0.27	
Aphelidiomycota	70.13	125.30	114.19	0.24	0.36	-0.66	0.51	1	
Ascomycota	11,324.39	11,324.39	11,324.39	0.00	0.01	0.00	1	1	
Basidiobolomycota	0.00	0.00	2.20	-1.68	0.00	0.00	1		
Basidiomycota	1,438.67	2,260.23	2,357.89	0.00	0.43	0.00	1	1	
Blastocladiomycota	0.98	2.24	1.14	0.96	2.87	-0.34	0.74	1	
Chytridiomycota	40.62	65.24	58.77	-1.18	0.81	1.45	0.15	0.95	
Entomophthoromycota	0.07	0.25	0.00	0.94	3.82	-0.25	0.81	1	Soil_PCN-/PCN+
Entorrhizomycota	0.99	0.09	3.33	-3.85	2.42	1.59	0.11	0.95	
Kickxellomycota	0.09	0.00	0.31	-0.66	3.83	0.17	0.86	1	
Monoblepharomycota	0.13	0.44	0.00	1.28	3.82	-0.34	0.74	1	
Mortierellomycota	1,407.42	2,729.10	1,842.13	0.42	0.50	-0.85	0.4	1	
Mucoromycota	815.85	311.90	279.59	0.16	0.42	-0.38	0.7	1	
Olpidiomycota	590.30	160.88	107.31	0.63	0.49	-1.27	0.2	0.95	

Phylum	baseMean	mean (Roots or PCN-)	mean (Soil or PCN+)	log2Fold_Change	lfcSE	statistic	p_value	p_adjusted	Comparison
Rozellomycota	34.90	238.81	62.21	-0.16	0.38	0.43	0.67	1	
Sanchytriomycota	0.94	1.68	1.57	0.16	2.39	-0.07	0.95	1	
Aphelidiomycota	70.13	3.38	0.00	4.16	0.65	-6.44	<0.01	<0.01	
Ascomycota	11,324.39	11,324.39	11,324.39	0.00	0.01	0.00	1	1	
Basidiomycota	1,438.67	466.88	27.46	3.87	0.51	-7.66	<0.01	<0.01	
Chytridiomycota	40.62	21.64	1.51	2.59	1.00	-2.59	<0.01	0.02	Roots_PCN-/PCN+
Mortierellomycota	1,407.42	340.41	62.19	2.10	0.59	-3.56	<0.01	<0.01	
Mucoromycota	815.85	2,587.40	576.54	2.18	0.50	-4.36	<0.01	<0.01	
Olpidiomycota	590.30	2,261.74	273.55	2.78	0.58	-4.83	<0.01	<0.01	
Rozellomycota	34.90	19.10	0.16	4.38	0.63	-7.01	<0.01	<0.01	

Supplementary Table 3.12 Differential abundance of **Mucoromycotan** Classes **(ITS dataset)** comparing soil vs roots, as well as the effect of PCN treatment in soil and roots, analysed using DESeq2. The table reports standard errors, test statistics, p-values, and adjusted p-values for each Class. Only Classes detected in each of the comparisons are included. Taxa present exclusively in one category were assigned a pseudo-$\log_2$ fold change by employing ($\log_2$(mean counts + 1)).

Class	baseMean	mean (Roots or PCN-)	mean (Soil or PCN+)	log2Fold_Change	lfcSE	statistic	p_value	p_adjusted	Comparison
Archaeosporomycetes	7.13	6.79	7.38	-0.26	1.36	-0.19	0.85	0.86	Roots_vs_Soil
Glomeromycetes	642.77	1,260.13	195.72	2.39	0.47	5.09	<0.01	<0.01	
Mucoromycetes	3.23	0.52	5.19	-3.92	0.83	-4.70	<0.01	<0.01	
Paraglomeromycetes	13.50	2.88	21.19	-1.38	1.08	-1.28	0.2	0.32	
Umbelopsidomycetes	58.74	0.00	101.28	-8.24	0.45	-18.46	<0.01	<0.01	
Archaeosporomycetes	7.13	12.76	2.00	3.41	1.73	-1.96	0.05	0.86	Soil_PCN-/PCN+
Glomeromycetes	642.77	207.89	183.55	-0.10	0.60	0.17	0.87	0.96	
Mucoromycetes	3.23	6.08	4.30	0.51	1.02	-0.50	0.62	0.96	
Paraglomeromycetes	13.50	24.28	18.10	1.35	1.36	-0.99	0.32	0.96	
Umbelopsidomycetes	58.74	106.63	95.92	-0.03	0.43	0.08	0.94	0.98	
Archaeosporomycetes	7.13	10.80	3.14	1.64	2.02	-0.81	0.42	0.91	Roots_PCN-/PCN+
Glomeromycetes	642.77	1,905.46	673.47	1.29	0.70	-1.83	0.07	0.19	
Mucoromycetes	3.23	1.09	0.00	2.06	1.29	-1.60	0.11	0.29	
Paraglomeromycetes	13.50	4.69	1.24	5.91	1.62	-3.63	<0.01	<0.01	

Supplementary Table 3.13 Differential abundance of **Mucoromycotan** Families **(ITS dataset)** comparing soil vs roots, as well as the effect of PCN treatment in soil and roots, analysed using DESeq2. The table reports standard errors, test statistics, p-values, and adjusted p-values for each Family. Only Families detected in each of the comparisons are included. Taxa present exclusively in one category were assigned a pseudo-log_2 fold change by employing (log_2(mean counts + 1)).

Family	baseMean	mean (Roots or PCN-)	mean (Soil or PCN+)	log2Fold_Change	lfcSE	statistic	p_value	p_adjusted	Comparison
Acaulosporaceae	0.05	0.00	0.08	-2.34	0.71	-3.31	<0.01	<0.01	Roots_vs_Soil
Ambisporaceae	0.00	0.13	0.00	0.17	0.00	0.00	1		
Archaeosporaceae	1.35	2.03	0.81	0.23	1.47	0.16	0.87	0.91	
Diversisporaceae	1.54	1.40	1.66	0.17	1.62	0.11	0.91	0.91	
Entrophosporaceae	4.84	3.82	5.64	-0.78	0.95	-0.82	0.41	0.66	
Gigasporaceae	1.33	0.96	1.62	-0.82	1.72	-0.47	0.64	0.85	
Glomeraceae	314.34	421.18	230.10	0.88	0.41	2.13	0.03	0.09	
Paraglomeraceae	4.00	1.31	6.12	-1.39	0.88	-1.58	0.11	0.23	
Polonosporaceae	0.21	0.00	2.12	-2.95	1.14	-2.59	<0.01	0.04	
Acaulosporaceae	0.05	0.16	0.00	1.14	0.90	-1.27	0.2	0.56	Soil_PCN-/PCN+
Archaeosporaceae	1.35	0.62	1.00	0.09	1.92	-0.05	0.96	0.96	
Diversisporaceae	1.54	1.11	2.21	-0.82	2.11	0.39	0.7	0.8	

Family	baseMean	mean (Roots or PCN-)	mean (Soil or PCN+)	log2Fold_Change	lfcSE	statistic	p_value	p_adjusted	Comparison
Entrophosporaceae	4.84	1.97	9.31	-1.93	1.25	1.54	0.12	0.56	
Gigasporaceae	1.33	2.96	0.28	1.82	2.24	-0.81	0.42	0.56	
Glomeraceae	314.34	267.35	192.84	0.50	0.54	-0.92	0.36	0.56	
Paraglomeraceae	4.00	8.50	3.74	1.21	1.14	-1.06	0.29	0.56	
Polonosporaceae	0.21	0.62	3.61	1.36	1.46	-0.93	0.35	0.56	
Ambisporaceae	0.00	0.26	0.00	0.33	0.00	0.00	1		Roots_PCN-/PCN+
Archaeosporaceae	1.35	3.05	1.06	1.28	2.14	-0.60	0.55	0.69	
Diversisporaceae	1.54	2.28	0.56	2.75	2.36	-1.16	0.24	0.69	
Entrophosporaceae	4.84	5.91	1.84	1.49	1.38	-1.08	0.28	0.69	
Gigasporaceae	1.33	1.63	0.33	0.26	2.51	-0.10	0.92	0.92	
Glomeraceae	314.34	492.43	353.32	0.47	0.60	-0.78	0.44	0.69	
Paraglomeraceae	4.00	1.59	1.05	2.44	1.30	-1.89	0.06	0.47	

Supplementary Table 3.14 Differential abundance of **Mucoromycotan** Families **(18S dataset)** comparing soil vs roots, as well as the effect of PCN treatment in soil and roots, analysed using DESeq2. The table reports standard errors, test statistics, p-values, and adjusted p-values for each Family. Only Families detected in each of the comparisons are included. Taxa present exclusively in one category were assigned a pseudo-$\log_2$ fold change by employing ($\log_2$(mean counts + 1)).

Family	baseMean	mean (Roots or PCN-)	mean (Soil or PCN+)	log2Fold_Change	lfcSE	statistic	p_value	p_adjusted	Comparison
Archaeosporaceae	90.86	25.21	140.40	-2.16	0.78	-2.78	<0.01	0.01	
Diversisporaceae	315.03	183.06	971.73	-1.55	0.55	-2.82	<0.01	0.01	
Entrophosporaceae	1,182.64	516.74	1,685.21	-1.24	0.50	-2.46	0.01	0.02	
Gigasporaceae	29.33	7.65	418.36	-0.65	1.82	-0.35	0.72	0.81	
Glomeraceae	11,573.23	11,573.23	11,573.23	0.00	0.01	0.00	1	1	Roots_vs_Soil
Pacisporaceae	4.46	0.10	16.78	-3.57	3.00	-1.19	0.23	0.3	
Paraglomeraceae	56.90	1.47	98.73	-6.89	1.22	-5.63	<0.01	<0.01	
Polonosporaceae	15.55	0.48	123.90	-15.76	1.93	-8.15	<0.01	<0.01	
Sacculosporaceae	0.00	0.00	5.70	-2.74	0.00	0.00	1		
Unknown	686.17	486.66	836.75	-0.70	0.54	-1.29	0.2	0.3	
Archaeosporaceae	90.86	54.00	237.18	-2.12	1.00	2.12	0.03	0.1	
Diversisporaceae	315.03	742.04	1,228.97	-0.08	0.71	0.12	0.91	1	
Entrophosporaceae	1,182.64	1,166.19	2,266.52	-0.81	0.65	1.25	0.21	0.38	Soil_PCN-/PCN+
Gigasporaceae	29.33	787.63	4.77	5.48	2.35	-2.33	0.02	0.09	
Glomeraceae	11,573.23	11,573.23	11,573.23	0.00	0.01	0.00	1	1	
Pacisporaceae	4.46	14.68	19.14	5.74	3.85	-1.49	0.14	0.31	

Family	baseMean	mean (Roots or PCN-)	mean (Soil or PCN+)	log2Fold_Change	lfcSE	statistic	p_value	p_adjusted	Comparison
Paraglomeraceae	56.90	155.40	35.25	5.78	1.55	-3.73	<0.01	<0.01	
Polonosporaceae	15.55	182.31	58.47	1.27	2.46	-0.52	0.61	0.78	
Sacculosporaceae	0.00	0.00	12.08	-3.71	0.00	0.00	1		
Unknown	686.17	1,031.09	619.08	0.40	0.70	-0.58	0.56	0.78	
Archaeosporaceae	90.86	29.45	21.74	0.47	1.16	-0.40	0.69	0.93	
Diversisporaceae	315.03	141.04	217.43	-0.69	0.82	0.84	0.4	0.93	
Entrophosporaceae	1,182.64	411.45	602.88	-0.60	0.75	0.80	0.42	0.93	
Gigasporaceae	29.33	7.64	7.65	0.88	2.71	-0.33	0.74	0.93	Roots_PCN-/PCN+
Glomeraceae	11,573.23	11,573.23	11,573.23	0.00	0.01	0.00	1	1	
Pacisporaceae	4.46	0.00	0.17	-1.69	4.48	0.38	0.71	0.93	
Paraglomeraceae	56.90	1.02	1.85	-0.72	1.85	0.39	0.69	0.93	
Polonosporaceae	15.55	0.41	0.54	18.56	2.90	-6.39	<0.01	<0.01	
Unknown	686.17	415.08	545.22	-0.18	0.81	0.22	0.83	0.93	

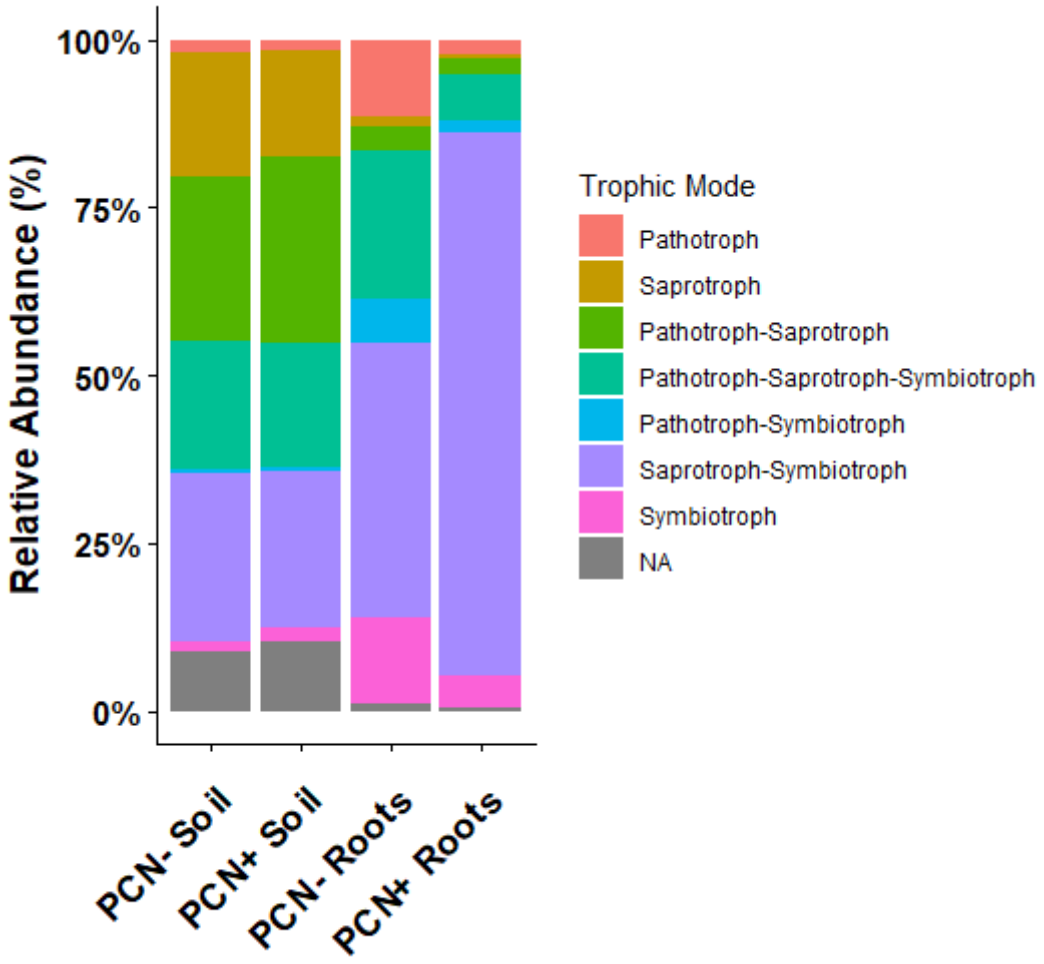

Supplementary Figure 3.1 A. Relative abundance of fungal trophic modes **(ITS dataset)** based on Sample type and PCN treatment. The trophic mode of each ASV was determined using the FUNGuild database (Nguyen et al., 2016).

Bacteria

Supplementary Table 3.15 Statistical results from a negative binomial GLMM (Observed richness), a LMM (Shannon), and a beta GLMM (Simpson), testing the effects of PCN treatment and sample type (roots vs. soil) on alpha diversity metrics using the **16S dataset for all bacteria**. Type III Wald chi-square (χ^2) tests were used to assess the significance of main effects and interactions.

	χ^2	df	p-value
Observed			

	χ^2	df	p-value
PCN treatment	0.85	1	0.36
Sample type	19.18	1	**<0.01**
Interaction	0.68	1	0.41
Shannon			
PCN treatment	0.46	1	0.50
Sample type	64.37	1	**< 0.01**
Interaction	0.60	1	0.44
Simpson			
PCN treatment	0.51	1	0.47
Sample type	93.82	1	**< 0.01**
Interaction	0.50	1	0.48

Supplementary Table 3.16 Pairwise comparisons of PCN treatment (PCN– vs. PCN+) within each sample type (roots and soil) for alpha diversity metrics of **bacterial** ASVs **(16S dataset)**. Observed richness was analysed using negative binomial GLMMs, Shannon diversity using LMMs, and Simpson diversity using a beta GLMM. Estimated marginal means from each model were used for comparisons, with differences assessed separately for roots and soil using Wald z-tests.

	estimate	SE	df	statistic (t- or z-ratio)	P-value
Observed					
Soil	-0.17	0.19	Inf	-0.92	0.36
Roots	0.00	0.14	Inf	-0.03	0.98
Shannon					
Soil	-0.16	0.25	51.4	-0.63	0.53
Roots	0.04	0.16	49.7	0.24	0.81
Simpson					
Soil	-0.02	0.31	54.1	-0.72	0.47
Roots	-0.02	0.18	44.8	-0.09	0.93

Supplementary Table 3.17 Results of PERMANOVA (adonis2) testing the effects of PCN treatment, sample type, and experimental block (strata) on bacterial **(16S dataset)** community composition based on Bray–Curtis dissimilarities. The model included 999 permutations and assessed factors by marginal effects.

Factor	df	Sum of Squares	R^2	F-statistic	p-value
PCN treatment	1	0.24	0.01	1.59	0.14
Sample type	1	7.31	0.44	48.86	**<0.01**
Experiment (strata)	1	0.51	0.03	3.39	**0.01**
Residual	56	8.37	0.50		
Total	59	16.62	1.00		

Supplementary Table 3.18 Pairwise PERMANOVA comparisons of the effect of PCN treatment (PCN– vs PCN+) on the bacterial community composition **(16S dataset)** based on Bray-Curtis dissimilarity, performed separately for roots and soil samples

Sample type	df	Sum of Squares	R^2	F-statistic	p-value
Roots	1	0.22	0.05	2.07	**0.05**
Bulk soil	1	0.22	0.05	0.82	0.63

Supplementary Table 3.19 Bacterial Orders reported to contain taxa with cell-wall degrading enzymes or to be associated with AM fungal hyphae.

Order	Notes	References
Actinomycetales	Cell-wall degrading	Tian et al., 2015
Bacteroidales	Cell-wall degrading	Tian et al., 2015
Betaproteobacteriales	Hyphospheric	Emmet et al., 2021; Wang et al., 2023
Caulobacterales	Cell-wall degrading	Tian et al., 2015
Cellvibrionales	Hyphospheric	Emmet et al., 2021
Chloroflexales	Hyphospheric	Emmet et al., 2021; Wang et al., 2023
Cytophagales	Cell-wall degrading; Hyphospheric	Tian et al., 2015; Emmet et al., 2021; Wang et al., 2023
Enterobacterales	Cell-wall degrading	Tian et al., 2015

Order	Notes	References
Flavobacteriales	Cell-wall degrading	Tian et al., 2015
Fibrobacterales	Hyphospheric	Emmet et al., 2021; Wang et al., 2023
Hyphomicrobiale (previously Rhizobiales)	Hyphospheric	Tian et al., 2015; Wang et al., 2023
Myxococcales	Hyphospheric; Hyphal C-reliant	Emmet et al., 2021; Wang et al., 2023; Kakouridis et al., 2024
Nitrososphaerales	Hyphal C-reliant	Kakouridis et al., 2024
Pseudomonadales (including outdated order Cellvibrionales)	Cell-wall degrading	Tian et al., 2015; Wang et al., 2023
Sphingobacteriales	Cell-wall degrading and hyphal C-reliant	Tian et al., 2015; Kakouridis et al., 2024
Solibacterales	Hyphal C-reliant	Kakouridis et al., 2024
Xanthomonadales	Cell-wall degrading	Tian et al., 2015

Supplementary Table 3.20 Bacterial Genera reported to contain taxa with phosphate-solubilising (PSB) or plant growth–promoting properties (PGPB) across different studies.

Genus	Notes	Reference(s)
Paenibacillus	Hyphospheric, PSB	Duan et al., 2024
Burkholderia	Hyphospheric, PSB	Duan et al., 2024
Stenotrophomonas	Hyphospheric, PSB	Duan et al., 2024
Acinetobacter	PSB	Kumar et al., 2016; Wan et al., 2020
Arthrobacter	Hyphospheric; PSB	Chen et al., 2006; Wan et al., 2020; Duan et al., 2024
Bacillus	Hyphospheric; PSB	Kumar et al., 2016; Wan et al., 2020; Duan et al., 2024
Cupriavidus	PSB; enriched with AMF	Wan et al., 2020; Wang et al., 2023
Massilia	Hyphospheric; PSB	Wan et al., 2020; Duan et al., 2024
Ochrobactrum	PSB	Wan et al., 2020
Pseudomonas	Hyphospheric; PSB	Ordoñez et al., 2016; Kumar et al., 2016; Wan et al., 2020; Duan et al., 2024
Streptomyces	PSB; Enriched with AM fungi	Zhang et al., 2018; Guo et al., 2019; Wang et al., 2023

Genus	Notes	Reference(s)
Gemmatimonas	PSB; Enriched with AM fungi	Zhang et al., 2018; Guo et al., 2019; Wang et al., 2023
Agrobacterium	PGPB	Glick et al., 2012
Rhizobium	PGPB/PSB	Kumar et al., 2016; Tajini et al., 2012; Glick et al., 2012
Azotobacter	PGPB/PSB	Kumar & Singh, 2001; Kumar et al., 2014
Enterobacter	PGPB/PSB	Kumar et al., 2016
Ramlibacter	Enriched with AM fungi	Wang et al., 2023
Aridibacter	Enriched with AM fungi	Wang et al., 2023
Gemmatirosa	Enriched with AM fungi	Wang et al., 2023
Noviherbaspirillum	Enriched with AM fungi, *phod* gene	Wang et al., 2023
Actinomadura	Enriched with AM fungi, *phod* gene	Wang et al., 2023
Rhodococcus	PSB	Chen et al., 2006
Serratia	PSB	Chen et al., 2006; Kumar et al., 2016
Chryseobacterium	PSB	Chen et al., 2006
Gordonia	PSB	Chen et al., 2006
Phyllobacterium	PSB	Chen et al., 2006
Delftia	PSB	Chen et al., 2006

Supplementary Table 3. 21 Differential abundance of **bacterial Orders (16S dataset)** comparing soil vs roots, as well as soil and roots based on PCN treatment (DESeq2). The table reports standard errors, test statistics, p-values, and adjusted p-values for each Phylum. Only Orders detected in each of the comparisons are included. Taxa present exclusively in one category were assigned a pseudo-log_2 fold change by employing (log_2(mean counts + 1)).

Order	baseMean	mean (Roots or PCN-)	mean (Soil or PCN+)	log2Fold_Change	lfcSE	statistic	p_value	p_adjusted	Comparison
Caulobacterales	7.28	1.32	21.18	-4.03	1.21	-3.33	<0.01	<0.01	
Chloroflexales	2.16	0.64	5.70	-2.60	1.99	-1.30	0.19	0.21	
Cytophagales	48.19	16.96	121.08	-2.10	0.58	-3.65	<0.01	<0.01	
Enterobacterales	7.39	0.20	24.15	-18.26	3.22	-5.68			
Flavobacteriales	21.12	26.22	9.20	1.35	0.75	1.80	0.07	0.1	
Hyphomicrobiales	204.10	60.74	538.60	-3.12	0.33	-9.46	<0.01	<0.01	Roots_vs_Soil
Myxococcales	21.29	0.00	70.96	-7.80	1.87	-4.17	<0.01	<0.01	
Nitrososphaerales	49.24	0.00	164.14	-10.06	1.08	-9.32	<0.01	<0.01	
Pseudomonadales	31.24	32.04	29.38	1.46	0.49	2.97	<0.01	<0.01	
Solibacterales	2.85	0.00	9.49	-4.37	3.23	-1.35	0.18	0.21	
Sphingobacteriales	48.01	0.28	159.38	-6.74	2.23	-3.02	<0.01	<0.01	
Caulobacterales	7.28	13.73	28.62	-1.14	1.98	0.58	0.56	0.99	Soil_PCN-/PCN+

Order	baseMean	mean (Roots or PCN-)	mean (Soil or PCN+)	log2Fold_Change	lfcSE	statistic	p_value	p_adjusted	Comparison
Chloroflexales	2.16	7.37	4.04	0.96	3.28	-0.29	0.77	0.99	
Cytophagales	48.19	209.42	32.74	2.06	0.95	-2.18	0.03	0.63	
Enterobacterales	7.39	46.92	1.37	5.08	5.30	-0.96			
Flavobacteriales	21.12	4.64	13.77	-0.53	1.24	0.43	0.67	0.99	
Hyphomicrobiales	204.10	728.33	348.87	0.46	0.54	-0.85	0.39	0.99	
Myxococcales	21.29	10.87	131.05	-3.55	3.05	1.16	0.24	0.99	
Nitrososphaerales	49.24	213.75	114.53	0.67	1.70	-0.40	0.69	0.99	
Pseudomonadales	31.24	54.07	4.68	3.29	0.83	-3.98	<0.01	<0.01	
Solibacterales	2.85	0.00	18.97	-5.07	5.32	0.95	0.34	0.99	
Sphingobacteriales	48.01	7.89	310.87	-3.64	3.66	0.99	0.32	0.99	
Caulobacterales	7.28	1.05	1.56	-0.42	1.33	0.32	0.75	1	
Chloroflexales	2.16	1.00	0.32	0.85	2.17	-0.39	0.7	1	
Cytophagales	48.19	16.57	17.31	0.03	0.62	-0.05	0.96	1	Roots_PCN-/PCN+
Enterobacterales	7.39	0.00	0.39	-16.98	3.50	4.85			
Flavobacteriales	21.12	32.44	20.57	0.65	0.78	-0.83	0.41	1	
Hyphomicrobiales	204.10	57.55	63.64	-0.03	0.36	0.09	0.93	1	

Order	baseMean	mean (Roots or PCN-)	mean (Soil or PCN+)	log2Fold_Change	lfcSE	statistic	p_value	p_adjusted	Comparison
Pseudomonadales	31.24	37.30	27.27	0.09	0.49	-0.18	0.86	1	
Sphingobacteriales	48.01	0.33	0.23	-2.53	2.45	1.03	0.3	1	

Supplementary Table 3.22 Differential abundance of bacterial Genera **(16S dataset)** containing taxa with phosphate-solubilising (PSB) or plant growth–promoting properties (PGPB) in soil and roots based on PCN treatment (DESeq2). The table shows log_2 fold changes, standard errors, test statistics, p-values, and adjusted p-values for each Genus. The table reports standard errors, test statistics, p-values, and adjusted p-values for each Phylum. Only Phyla detected in each of the comparisons are included. Taxa present exclusively in one category were assigned a pseudo-log_2 fold change by employing (log_2(mean counts + 1)).

Genus	baseMean	mean (Roots or PCN-)	mean (Soil or PCN+)	log2Fold_Change	lfcSE	statistic	p_value	p_adjusted	Comparison
Agrobacterium	0.00	0.34	0.00	0.42	0.00	0.00	1		
Bacillus	0.00	0.00	1.50	-1.32	0.00	0.00	1		
Cupriavidus	3.47	0.00	11.56	-4.25	3.23	-1.32			
Flavobacterium	16.79	21.75	5.21	1.93	1.01	1.92	0.06	0.1	Roots_vs_Soil
Gemmatimonas	1.68	0.00	5.61	-4.01	3.23	-1.24	0.21	0.27	
Klebsiella	0.00	0.32	0.00	0.40	0.00	0.00	1		
Massilia	6.64	5.86	8.45	-0.58	1.33	-0.43	0.66	0.73	

Genus	baseMean	mean (Roots or PCN-)	mean (Soil or PCN+)	log2Fold_Change	lfcSE	statistic	p_value	p_adjusted	Comparison
Noviherbaspirillum	13.06	2.66	37.34	-5.14	1.67	-3.08	<0.01	<0.01	
Paenibacillus	10.13	0.19	33.33	-7.34	2.47	-2.97	<0.01	0.01	
Phyllobacterium	0.00	8.99	0.00	3.32	0.00	0.00	1		
Pseudomonas	15.14	0.36	49.64	-5.39	2.84	-1.90	0.06	0.1	
Rhizobium	1.89	2.71	0.00	1.83	3.08	0.59	0.55	0.62	
Streptomyces	111.63	142.39	39.84	1.92	0.65	2.96	<0.01	0.01	
Bacillus	0.00	0.00	3.00	-2.00	0.00	0.00	1		
Cupriavidus	3.47	23.13	0.00	5.96	5.32	-1.12			
Flavobacterium	16.79	4.09	6.33	-0.09	1.68	0.05	0.96	1	
Gemmatimonas	1.68	0.00	11.22	-4.50	5.33	0.84	0.4	1	
Massilia	6.64	6.68	10.23	-0.60	2.20	0.27	0.79	1	Soil_PCN-/PCN+
Noviherbaspirillum	13.06	27.33	47.34	-0.60	2.74	0.22	0.83	1	
Paenibacillus	10.13	48.15	18.51	1.38	4.06	-0.34	0.73	1	
Pseudomonas	15.14	95.46	3.82	4.86	4.68	-1.04	0.3	1	
Streptomyces	111.63	21.25	58.44	-1.41	1.08	1.31	0.19	1	
Agrobacterium	0.00	0.00	0.64	-0.72	0.00	0.00	1		

Genus	baseMean	mean (Roots or PCN-)	mean (Soil or PCN+)	log2Fold_Change	lfcSE	statistic	p_value	p_adjusted	Comparison
Flavobacterium	16.79	29.36	14.83	0.93	1.06	-0.87	0.38	0.98	
Klebsiella	0.00	0.00	0.61	-0.69	0.00	0.00	1		
Massilia	6.64	4.20	7.38	-0.80	1.43	0.56	0.57	0.98	
Noviherbaspirillum	13.06	5.35	0.21	4.38	1.84	-2.38	0.02	0.98	Roots_PCN-/PCN+
Paenibacillus	10.13	0.00	0.37	-1.30	2.72	0.48	0.63	0.98	
Phyllobacterium	0.00	0.00	17.17	-4.18	0.00	0.00	1		
Pseudomonas	15.14	0.27	0.43	-0.69	3.09	0.22	0.82	0.98	
Rhizobium	1.89	3.98	1.55	0.97	3.32	-0.29	0.77	0.98	
Streptomyces	111.63	163.77	122.95	0.43	0.70	-0.62	0.53	0.98	

Both

Supplementary Table 3.23 Fungal and Bacterial genera containing taxa with PPP-antagonistic. properties.

	Genus	Notes	Reference(s)
Fungi	***Dactylellina***	Preying on PPN	Toju and Tanaka, 2019
	Rhizophydium	Preying on PPN	Toju and Tanaka, 2019
	Clonostachys	Preying on PPN	Toju and Tanaka, 2019
	Pochonia	Preying on PPN	Toju and Tanaka, 2019
	Purpureocillium	Preying on PPN; Suppressive soils	Toju and Tanaka, 2019; van Himbeeck et al., 2025
	Trichoderma	Suppressive soils; parasitise PPN	Sikder et al., 2022; van Himbeeck et al., 2025
	Metapochonia	Suppressive soils; parasitise PPN	Sikder et al., 2022; van Himbeeck et al., 2025
	Monocillium	Suppressive soils; parasitise PPN	Sikder et al., 2022
	Exophiala	Suppressive soils; parasitise PPN	Sikder et al., 2022
	Acremonium	Suppressive soils; parasitise PPN	Sikder et al., 2022; van Himbeeck et al., 2025
	Mortierella	Suppressive soils; parasitise PPN	Sikder et al., 2022
	Gibellulopsis	Suppressive soils; parasitise PPN	Sikder et al., 2022
	Metacordyceps	Suppressive soils; parasitise PCN eggs	Manzanilla-López et al. 2017; van Himbeeck et al., 2025
	Arthrobotrys	Suppressive soils	van Himbeeck et al., 2025
Bacteria	**Pseudomonas**	Suppressive soils; reduce PPN juvenile mobility	van Himbeeck et al., 2025
	Rhizobium	Decreased PPN invasion	Sikder et al., 2022
	Adhaeribacter	Decreased PPN invasion	Sikder et al., 2022
	Deinococcus	Decreased PPN invasion	Sikder et al., 2022
	Gemmatimonas	Suppressive soils; Decreased PPN invasion	Adam et al., 2014; Sikder et al., 2022
	Iamia	Decreased PPN invasion	Sikder et al., 2022
	Nocardioides	Decreased PPN invasion	Sikder et al., 2022
	Oceanobacillus	Decreased PPN invasion	Sikder et al., 2022
	Chitinimonas	Decreased PPN invasion	Sikder et al., 2022

Supplementary Table 3.24 Fungal and Bacterial genera containing taxa with PPP-beneficial properties.

	Genus	Notes	Reference(s)
Fungi	***Oidiodendron***	Increased PPN invasion	Sikder et al., 2022
	Metarhizium	Increased PPN invasion	Sikder et al., 2022
Bacteria	***Bacillus***		Sikder et al., 2022
	Castellaniella	Increased PPN invasion	Sikder et al., 2022
	Gemmata		Sikder et al., 2022
	Haliangium	Increased PPN invasion	Sikder et al., 2022

Leptolyngbya		Sikder et al., 2022
Pirellula	Increased PPN invasion	Sikder et al., 2022
Rhodopirellula	Increased PPN invasion	Sikder et al., 2022
Taibaiella	Increased PPN invasion	Sikder et al., 2022

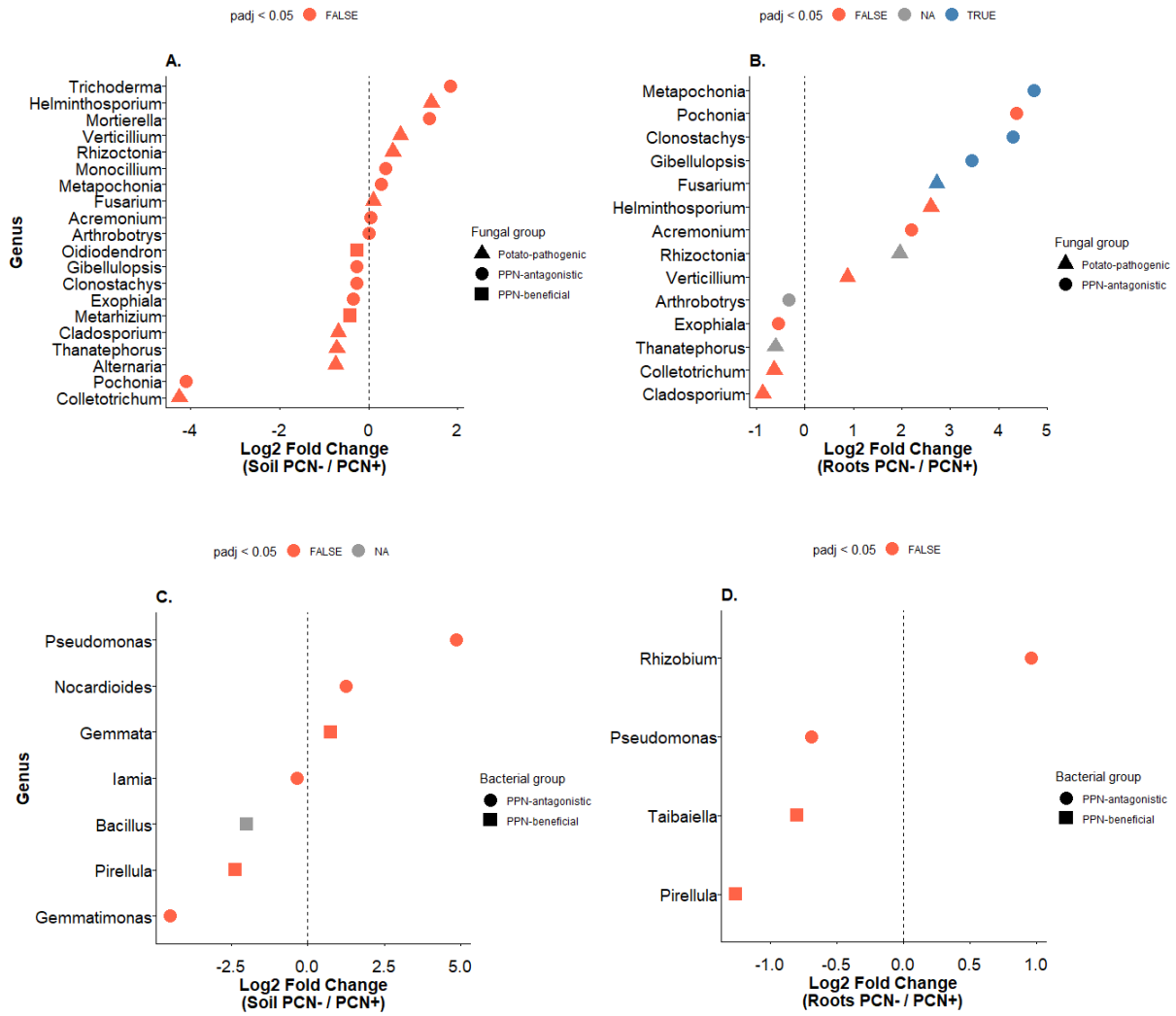

Supplementary Table 3.2 Differential abundance of **fungal (ITS dataset)** and **bacterial (16S dataset) genera** comparing soil vs roots, as well as the effect of PCN treatment in soil and roots, analysed using DESeq2. Only Genera containing taxa with known PPN-antagonistic (circles) or PPN-beneficial (squares) properties (Tables S3.23 and S3.24) are highlighted. Only Genera detected in each of the comparisons are included. Taxa present exclusively in one category were assigned a pseudo-log_2 fold change by employing (log_2(mean counts + 1)).

Chapter 4

Supplementary Table 4.1 MSR medium (Modified Strullu-Romand medium) recipe used for propagating AM fungal inoculum (Rhizophagus irregularis MUCL 41933) on an axenic Ri T-DNA transformed *Daucus carota* root organ culture. The same recipe was also used for filling in the experimental tripartite Petri Dish dishes, except for the addition of Vitamins and Sucrose.

Solution	Component	Concentration / Notes	Amount per 1 L
A: Macrolements	$MgSO_4 \cdot 7H_2O$	73.9 g/L	
	KNO_3	7.60 g/L	10 mL
	KCl	6.50 g/L	
	KH_2PO_4	0.41 g/L	
B: Calcium nitrate	$Ca(NO_3)_2 \cdot 4H_2O$	35.9 g/L	10 mL
C: Vitamins	Pantothenate Ca	0.18 g/L	
	Biotin	0.18 mg/L (from 1 mL stock/500 mL)	
	Niacin	0.20 g/L	5 mL
	Pyridoxine	0.18 g/L	
	Thiamine	0.20 g/L	
	Cyanocobalamine	0.08 g/L	
D: Na Fe EDTA	Na Fe EDTA	1.60 g/L	5 mL
E: Microelements	$MnSO_4 \cdot H_2O$	1.225 g/100 mL stock	
	$ZnSO_4 \cdot 7H_2O$	0.14 g/100 mL stock	
	H_3BO_3	0.925 g/100 mL stock	1 mL
	$CuSO_4 \cdot 5H_2O$	1.1 g/50 mL stock	
	$Na_2MoO_4 \cdot 2H_2O$	0.12 g/100 mL stock	
	$(NH_4)_6Mo_7O_{24} \cdot 4H_2O$	1.7 g/100 mL stock	
Other components	Sucrose		10 g
	Phytagel		5 g
Preparation notes	Adjust pH	5.5-5.8	
	Autoclave	121°C, 15-20 min	

Supplementary Table 4.2 Antimicrobial cocktails are used for the sterilisation of PCN cysts and second-stage juveniles (J2). Concentrations shown are final working concentrations prepared in sterile phosphate-buffered saline.

	Component	Final Concentration
1. Cyst Sterilisation	Penicillin G	100 µg/ml
	Streptomycin	100 µg/ml
	Amphotericin B	0.25 µg/ml
	Polymyxin B	5–10 µg/ml
	Doxycycline	5–10 µg/ml
2. J2 Sterilisation	Streptomycin	100 µg/ml
	Penicillin G	100 µg/ml
	Amphotericin B	25 µg/ml
	Polymyxin B	5–10 µg/ml
	Doxycycline	5 µg/ml
	Tween 20	0.01–0.05%

Chapter 5

Non-volatile metabolites

Supplementary Table 5.1 Candidate potato leaf metabolites corresponding to top MALDI-TOF m/z features. Metabolite IDs are tentative and were annotated by searching the CEU MassBatch database (https://ceumass.eps.uspceu.es/batch_search.xhtml) using a tolerance of 100 mDa against the LipidMaps, Metlin, and KEGG databases, considering positive ion mode and possible adducts [M+H]+, [M+Na]+, and [M+K]+. Full names, adducts, and additional notes (e.g., metabolite class or tentative fragment assignment) are reported. Confirmed identifications are those with exact or highly probable matches in the database.

M/Z	CANDIDATE METABOLITE(S)	NOTES	ADDUCT
256.27	Palmitamide	Fatty acid derivative	M+H
373.08	2-O-Caffeoylglucarate/Capparilosid A	Phenolic acid derivative; plant secondary metabolite	M+H/M+K
455.03	Gangleoidin Acetate	Flavonoid derivative	M+H
606.11	Pelargonidin 3-O-3'',6''-O-dimalonylglucoside	Anthocyanin; flavonoid glycoside	M+H
666.05	Delphinidin 3-O-(6-caffeoyl-beta-D-glucoside)	Anthocyanins	M+K
698.01	Delphinidin 3-O-(2''-O-galloyl-6''-O-acetyl-beta-galactopyranoside)	Anthocyanin; flavonoid glycoside	M+K
757.18	Quercetin 3-(3'',6''-di-p-coumarylglucoside)	Flavonoid glycoside	M+H
771.25	Tamarixetin 3-rutinoside-7-rhamnoside / Kaempferol derivatives	Flavonoid glycosides; secondary metabolites	M+H
877.07	Beta-Alanyl-CoA fragment	Likely glycoalkaloid derivative	M+K
933.31	Torososide B	Steroidal glycoalkaloid/saponin	M+H

Supplementary Table 5.2 Results of PERMANOVA (adonis2) testing the effects of PCN treatment and growth week on leaf non-volatile metabolites based on Bray–Curtis dissimilarities.

Factor	df	Sum of Squares	R^2	F-statistic	p-value
PCN treatment	1	0.05	0.00	1.18	0.33
Growth week	1	10.53	0.84	238.67	**<0.01**
Residual	43	1.90	0.15		
Total	45	12.48	1.00		

Supplementary Table 5.3. Pairwise PERMANOVA comparisons of the effect of PCN treatment (PCN– vs PCN+) on leaf non-volatile metabolites based on Bray-Curtis dissimilarity, performed separately for each growth week. The model included 999 permutations and assessed factors by marginal effects.

	df	Sum of Squares	R^2	F-statistic	p-value
Growth Week 5	1	0.01	0.06	1.31	0.25
Growth Week 7	1	0.01	0.05	1.23	0.28

Supplementary Table 5.4 Statistical results from linear mixed-effects models, showing the effects of PCN treatment and growth week on leaf non-volatile metabolite intensity. Type III Wald chi-square tests were used to assess the significance of main effects and interactions.

Effect	χ^2	df	p-value
PCN treatment	0.45	1	0.50
Growth Week	11.47	1	**<0.01**
Interaction	0.31	1	0.58

Supplementary Table 5.5 Pairwise comparisons from linear mixed-effects models testing the effect of PCN treatment (PCN– vs PCN+) on leaf non-volatile metabolite intensity within each sampling week (Growth Week 5 and 7). Comparisons are estimated marginal means (emmeans) contrasts, Tukey-adjusted, with Kenward–Roger degrees of freedom.

	Estimate	SE	df	t-ratio	p-value
Growth Week 5	-0.01	0.01	41.10	-0.89	0.38
Growth Week 7	-0.00	0.01	39.70	-0.15	0.88

Supplementary Table 5.6 Candidate potato leaf defence-related or secondary metabolites. Metabolites and their respective molecular weights (MW) were confirmed as plant metabolites using the BioSino Plant Metabolite Database (https://www.biosino.org/). Protonated molecular ions ([M+H]+), sodium adduct ions ([M+Na]+), and potassium adduct ions ([M+K]+) were calculated, as commonly detected in positive ion MALDI-TOF MS. These adduct-adjusted ions were then matched against the peaks observed in the experimental data.

METABOLITE	MW (DA)	[M+H]+ (M/Z)	[M+NA]+ (M/Z)	[M+K]+ (M/Z)
ACC	101.10	102.11	124.09	140.06
GABA	103.12	104.13	126.11	142.08
PROLINE	115.13	116.14	138.12	154.09
PIPECOLIC ACID	129.16	130.17	152.15	168.12
SALICYLIC ACID	138.12	139.13	161.11	177.08
COUMARIC ACID	164.16	165.17	187.15	203.12
PHENYLALANINE	165.19	166.20	188.18	204.15
4-FORMYLSALICYLIC ACID	166.13	167.14	189.12	205.09
CAFFEIC ACID	180.16	181.17	203.15	219.12
GLUCOSE	180.16	181.17	203.15	219.12
FERULIC ACID	194.18	195.19	217.17	233.14
TRYPTOPHAN	204.22	205.23	227.21	243.18
JASMONIC ACID	210.27	211.28	233.26	249.23
TRAUMATIN (OPDA)	212.28	213.29	235.27	251.24
METHYL JASMONATE	224.30	225.31	247.29	263.26
12-HYDROXYJASMONIC ACID	226.27	227.28	249.26	265.23
ABA	264.32	265.33	287.31	303.28
LINOLEIC ACID	280.40	281.41	303.39	319.36
SUCROSE	342.30	343.31	365.29	381.26
CHLOROGENIC ACID	354.31	355.32	377.30	393.27
CHLOROGENIC ACID METHYL ESTER	368.30	369.31	391.29	407.26
SOLANIDINE	397.64	398.65	420.63	436.60
A-CHACONINE	852.06	853.07	875.05	891.03
A-SOLANINE	868.10	869.11	891.09	907.06

Supplementary Table 5.7 Statistical comparisons of log_2 fold change of candidate defence-related metabolites in potato leaves based on PCN treatment. (t-test, FDR-adjusted)

mz peak	target_mz	mean_PCN-	mean_PCN+	log2FC	p-value	p-adj
116.05	116.14	0.00	0.00	-0.05	0.56	0.63
195.10	195.10	0.01	0.01	-0.31	0.45	0.63
211.10	211.28	0.00	0.00	-0.19	0.58	0.63
227.10	227.21	0.00	0.00	-0.15	0.43	0.63
265.25	265.23	0.00	0.00	-0.10	0.58	0.63

287.08	287.31	0.00	0.00	0.02	0.79	0.79
393.11	393.27	0.00	0.00	-0.05	0.47	0.63
398.36	398.65	0.01	0.01	0.14	0.19	0.63
852.54	853.07	0.09	0.09	0.13	0.19	0.63
868.54	868.11	0.07	0.07	0.13	0.25	0.63
874.56	875.05	0.01	0.01	0.14	0.28	0.63
890.52	891.03	0.01	0.01	0.14	0.16	0.63
906.50	907.06	0.00	0.00	0.14	0.35	0.63

Supplementary Table 5.8 Statistical results from a linear mixed-effects model testing the effects of PCN treatment and growth week on the total emission of defence-related metabolites. Type III Wald chi-square (χ^2) tests were used to assess the significance of main effects and interactions.

	df	**χ^2**	**p-value**
PCN treatment	1	0.06	0.81
Growth Week	1	28.17	**<0.01**
Interaction	1	0.00	1.00

Supplementary Table 5.9 Pairwise comparisons of PCN treatment (PCN– vs. PCN+) within each growth week on the emission of defence-related metabolites. Estimated marginal means from each model were used for comparisons, with differences assessed separately for roots and soil using Wald z-tests.

	estimate	**SE**	**df**	**statistic (t- or z-ratio)**	**p-value**
Growth Week 5	-0.02	0.02	41.1	-0.98	0.33
Growth Week 7	-0.02	0.02	39.7	-1.02	0.32

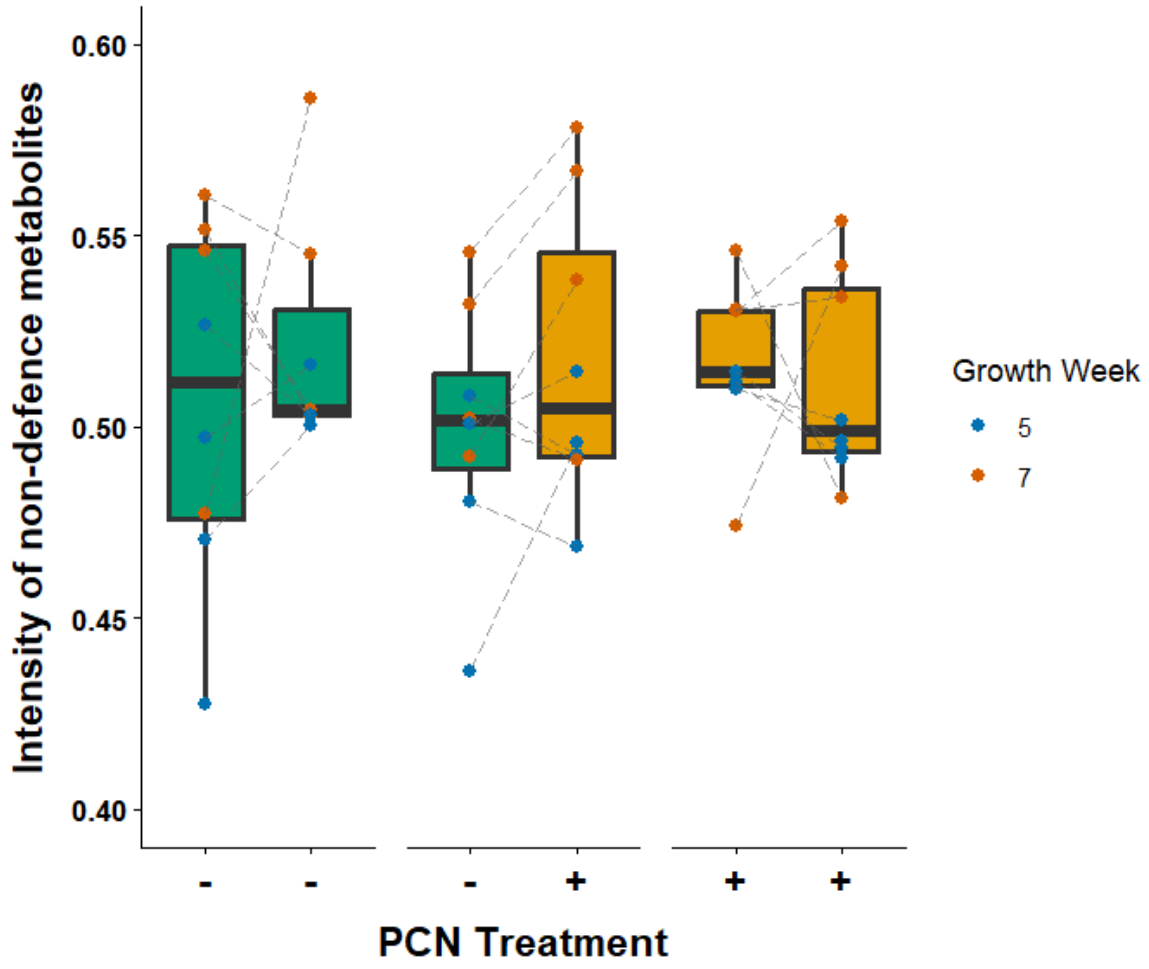

Supplementary Figure 5.1 Total intensity values of non-defence-related m/z peaks detected in potato leaves across both sampling timepoints (weeks 5 and 7), split per mesocosm. Boxplots span the interquartile range (IQR), the line inside marks the median, and whiskers extend to 1.5 × IQR; points outside are potential outliers. Plants without PCN are indicated by '–' and green boxplots, while plants with PCN are indicated by '+' and orange boxplots. Individual points represent biological replicates, with colours denoting the sampling timepoint (Growth Week 5 in blue, Week 7 in reddish-brown). Dashed lines connect paired m/z peaks across each side of the same mesocosm for a given timepoint. Intensities were calculated as the summed abundance per sample excluding defence-related metabolites (Table S4.x), measured by MALDI-TOF MS in positive ion mode.

VOCs

Supplementary Table 5.10 Results of PERMANOVA (adonis2) testing the effects of PCN treatment and PCN treatment of the neighbour on leaf volatile metabolites based on Bray–Curtis dissimilarities.

Factor	df	Sum of Squares	R^2	F-statistic	p-value
PCN treatment	1	0.10	0.02	0.37	0.87
PCN treatment neighbour	1	0.83	0.19	2.98	**0.04**
Residual	12	3.33	0.78		
Total	14	4.25	1.00		

Supplementary Table 5.11 List of volatile organic compounds (VOCs) detected in potato leaf samples, with retention time (RT, in minutes) and major mass spectral peaks (Peak.1 and Peak.2, m/z). Compound IDs are tentative and were assigned using the NIST mass spectral library (version 2.2) and classified into chemical classes: aldehydes, monoterpene hydrocarbons, oxygenated monoterpenes (alcohols, aldehydes, ketones), sesquiterpene hydrocarbons, aromatic hydrocarbons, and alkanes. Defence-related VOCs include oxygenated monoterpenes and selected sesquiterpenes. The 'Passed Filtering' column indicates whether a compound was retained in the analysis based on its peak area being greater than zero relative to the blank and present in >15% of samples.

Common Name	Class	RT	Peak 1	Peak 2	Passed Filtering
Toluene	Benzenoid	5.39	92	91	YES
Octane	Alkane	6.09	56	57	NO
Hexanal	Aldehyde (C6)	6.62	56	57	NO
Xylene	Benzenoid	8.34	91	106	YES
Heptanal	Aldehyde (C7)	9.36	70	55	NO
Tricyclene	Monoterpene hydrocarbon	9.6	93	136	YES
α-Pinene	Monoterpene hydrocarbon	9.91	93	91	NO
Camphene	Monoterpene hydrocarbon	10.32	93	121	NO
α-Phellandrene	Monoterpene hydrocarbon	10.49	91	92	NO
β-Phellandrene	Monoterpene hydrocarbon	11.02	93	91	YES

Sulcatone	Monoterpenoid ketone	11.52	108	55	NO
Octanal	Aldehyde (C8)	11.75	84	55	NO
p-Mentha-1,3,8-triene	Monoterpene hydrocarbon	12.19	119	91	NO
4-Acetyl-1-methylcyclohexene	Oxygenated monoterpene	12.37	95	123	NO
α-carene	Monoterpene hydrocarbon	12.9	93	91	NO
Campholenal derivative	Oxygenated monoterpene (aldehyde)	13.64	95	108	NO
Nonanal	Aldehyde (C9)	13.85	57	70	NO
cis-p-Mentha-2,8-dien-1-ol	Oxygenated monoterpene (alcohol)	14.08	91	119	NO
Campholenal	Oxygenated monoterpene (aldehyde)	14.38	108	93	NO
Unknown_14.51	Unknown	14.51	73	267	YES
Pinocarveol	Oxygenated monoterpene	14.7	92	91	NO
Verbenol	Oxygenated monoterpene (alcohol)	14.82	91	109	NO
Tetralin	Aromatic hydrocarbon (Internal standard)	15.12	104	91	NA
Pinocarvone	Oxygenated monoterpene (ketone)	15.18	81	53	NO
Decanal	Aldehyde (C10)	15.76	56	57	YES
α-Thujenal	Oxygenated monoterpene (aldehyde)	15.85	79	91	NO
Verbenone	Monoterpenoid ketone	16.11	107	135	NO
Pinanediol	Monoterpenoid	17.26	83	69	NO
Campholenal	Oxygenated monoterpene (aldehyde)	18.54	108	93	NO

β-Caryophyllene	Sesquiterpene hydrocarbon	19.5	91	93	NO
α-Bergamotene	Sesquiterpene hydrocarbon	19.64	93	119	YES
β-Sesquiphellandrene	Monoterpene hydrocarbon	19.75	91	69	YES
Geranylacetone	Sesquiterpene ketone	19.92	69	151	NO
β-Farnesene	Sesquiterpene hydrocarbon	20.45	69	93	YES
β-Sesquiphellandrene derivative	Monoterpene hydrocarbon	20.98	69	93	YES
Unknown_22.94	Unknown	22.94	173	55	YES
Benzoic acid	Benzenoid ester	23.5	105	70	YES
Unknown_24.90	Unknown	24.9	100	207	NO
Unknown_25.44	Unknown	25.44	73	207	YES

Supplementary Table 5.12 Statistical comparisons of log_2 fold change of candidate defence-related VOCs emitted from potato leaves based on PCN treatment and the PCN treatment of the neighbouring plant (Wilcoxon rank-sum test-adjusted).

comparison	VOC	PCN-	PCN+	log2FC	p-value
PCN treatment	Benzoic acid	0.01	0.00	9.88	0.30
	Decanal	0.01	0.01	-0.99	1.00
	Geranylacetone	0.01	0.00	6.49	0.53
	Toluene	0.02	0.04	-0.57	0.65
	Tricyclene	5.74	12.68	-1.14	0.71
	Unknown.25_44	0.00	0.00	8.08	0.30
	Unknown_14.51	0.04	0.09	-1.31	0.47
	Unknown_22.94	0.00	0.09	-4.29	0.08
	Xylene	0.01	0.01	-0.14	0.64
	α-Bergamotene	0.03	0.04	-0.77	0.61
	β-Caryophyllene	0.02	0.05	-1.05	0.83
	β-Farnesene	0.01	0.00	1.08	0.64
	β-Sesquiphellandrene	0.30	0.30	0.03	0.65
	β-Sesquiphellandrene derivative	0.01	0.00	2.14	0.53
PCN treatment of neighbour	Benzoic acid	0.01	0.00	0.87	0.85
	Decanal	0.01	0.00	2.24	0.64
	Geranylacetone	0.00	0.01	-1.62	1.00
	Toluene	0.03	0.02	0.60	0.56

Tricyclene	6.01	11.94	-0.99	0.12
Unknown.25_44	0.00	0.00	-1.00	0.16
Unknown_14.51	0.06	0.02	1.88	0.10
Unknown_22.94	0.03	0.01	1.37	1.00
Xylene	0.01	0.01	0.89	0.32
α-Bergamotene	0.04	0.01	1.92	0.51
β-Caryophyllene	0.03	0.03	-0.06	0.71
β-Farnesene	0.01	0.01	-0.72	1.00
β-Sesquiphellandrene	0.33	0.23	0.53	0.17
β-Sesquiphellandrene derivative	0.01	0.02	-1.59	1.00

Supplementary Table 5.13 Statistical results from linear models assessing the effect of neighbouring plant treatment on the emission of VOCs from PCN-free plants using Type III ANOVA. Log-transformed emission values were used with a small pseudocount added to account for zeros where necessary.

VOC Class	**Source**	**Sum Sq**	**df**	**F value / LR χ^2**	**p-value**
Total emission	(Intercept)	0.07	1	0.01	0.92
	PCN treatment of neighbour	3.71	1	0.60	0.46
	Residuals	55.34	9		
Unknown	(Intercept)	73.35	1	130.53	<0.01
	PCN treatment of neighbour	0.28	1	0.50	0.50
	Residuals	5.06	9		
Aldehydes	PCN treatment of neighbour	0.76	1		0.38
Benzenoids	(Intercept)	80.04	1	53.30	<0.01
	PCN treatment of neighbour	1.43	1	0.95	0.36
	Residuals	13.52	9		
Monoterpenoids	(Intercept)	1.00	1	0.11	0.75
	PCN treatment of neighbour	4.82	1	0.54	0.48
	Residuals	81.04	9		
Sesquiterpenoids	(Intercept)	238.64	1	7.25	0.02
	PCN treatment of neighbour	60.57	1	1.84	0.21
	Residuals	296.26	9		